School of Doctoral Studies in Biological Sciences
University of South Bohemia in České Budějovice
Faculty of Science

Role of Psb28 proteins in the biogenesis of the Photosystem II complex in the cyanobacterium *Synechocystis* sp. PCC 6803

Ph.D. Thesis

Mgr. Bečková Martina

Supervisor: **Prof. RNDr. Komenda Josef, DSc.**
Institute of Microbiology, Academy of Sciences of the Czech Republic
University of South Bohemia, České Budějovice

České Budějovice 2016

This thesis should be cited as:

Bečková, M., 2016: Role of the Psb28 proteins in the biogenesis of the Photosystem II complex in the cyanobacterium *Synechocystis* sp. PCC 6803. Ph.D. Thesis. University of South Bohemia, Faculty of Science, School of Doctoral Studies in Biological Sciences, České Budějovice, Czech Republic, 124 p.

▪ Annotation

The thesis focuses on the role of Psb28 proteins, namely the Psb28-1 and its homolog Psb28-2, in the biogenesis of the Photosystem II complex (PSII) in the cyanobacterium *Synechocystis* PCC 6803. The aims of this work were to localize the proteins within the cells, and to determine their function. A fraction of both Psb28 proteins was identified in the monomeric PSII core complexes but most proteins were found in the unassembled protein fraction associated with thylakoid membranes. Psb28-1 was mostly detected as a dimer while Psb28-2 as a monomer. Psb28-1 also differed from Psb28-2 by its higher affinity to the PSII core complex lacking CP43 antenna. Characterization of Psb28-less mutants suggested regulatory function of the proteins in PSII biogenesis in connection with chlorophyll biosynthetic pathway. Analysis of preparations isolated using FLAG-tagged versions of Psb28 proteins showed their association with Photosystem II - Photosystem I supercomplexes, especially under increased irradiance, and supported a role of Photosystem I in the PSII biogenesis.

▪ Declaration [in Czech]

Prohlašuji, že svoji disertační práci jsem vypracovala samostatně pouze s použitím pramenů a literatury uvedených v seznamu citované literatury.

Prohlašuji, že v souladu s § 47b zákona č. 111/1998 Sb. v platném znění souhlasím se zveřejněním své disertační práce, a to v úpravě vzniklé vypuštěním vyznačených částí archivovaných Přírodovědeckou fakultou elektronickou cestou ve veřejně přístupné části databáze STAG provozované Jihočeskou univerzitou v Českých Budějovicích na jejích internetových stránkách, a to se zachováním mého autorského práva k odevzdanému textu této kvalifikační práce. Souhlasím dále s tím, aby toutéž elektronickou cestou byly v souladu s uvedeným ustanovením zákona č. 111/1998 Sb. zveřejněny posudky školitele a oponentů práce i záznam o průběhu a výsledku obhajoby kvalifikační práce. Rovněž souhlasím s porovnáním textu mé kvalifikační práce s databází kvalifikačních prací Theses.cz provozovanou Národním registrem vysokoškolských kvalifikačních prací a systémem na odhalování plagiátů.

České Budějovice, MH. 10. 2016 ……

Martina Bečková

This thesis originated from a partnership of Faculty of Science, University of South Bohemia, and Algatech Centre, Institute of Microbiology, Academy of Sciences of the Czech Republic.

Financial support

This work was supported by the Grant Agency of the Czech Republic (projects P501/11/0377 and P501/12/G055), by the Academy of Sciences (RVO61388971) and by Algatech (CZ.1.05/2.1.00/03.0110) and National Program of Sustainability (LO1416).

Acknowledgements

I am very grateful to my supervisor professor Josef Komenda for giving me the opportunity to join his research team and to work on this interesting topic. I appreciate his never-ending enthusiasm for science, useful ideas, great discussions, and willingness to listen and help whenever was needed. My special thanks belong to Vendula Krynická, Jana Knoppová and Markéta Linhartová for teaching me all the methods, for their kindness, patience and help. Many thanks also belong to Roman Sobotka and Martin Tichý for their valuable advice, discussions and overall help. Of course, my special thanks belongs to my family and friends, who always supported me.

"I know I can be difficult sometimes" but I am very happy I could work with such amazing colleagues who provided a perfect atmosphere in our institute/labs and worked as very good teams. YOU CHANGED AND BRIGHTENED MY LIFE, THANK YOU FOR THAT!

List of papers and author's contribution

The thesis is based on the following papers and manuscript (listed chronologically):

I. **Boehm, M., Yu, J., Reisinger, V., Beckova, M., Eichacker, L.A., Schlodder, E., Komenda, J., and Nixon, P.J. (2012). Subunit composition of CP43-less photosystem II complex of *Synechocystis* sp. PCC 6803: implications for the assembly and repair of photosystem II. Phil. Trans. R. Soc. B 36, 3444-3454.**
Martina Bečková constructed, cultivated and characterized a strain expressing the FLAG-Psb28-2 protein, purified it using affinity chromatography and analyzed the obtained preparation by 2D electrophoresis in combination with immunodetection. She also analyzed wild type and CP43-less strains grown under different light conditions.

II. **Bialek, W., Wen, S., Michoux, F., Beckova, M., Komenda, J., Murray, J.W., and Nixon, P.J. (2013). Crystal structure of the Psb28 accessory factor of *Thermosynechococcus elongatus* photosystem II at 2.3 Å. Photosynth Res, 117:375-383.**
Martina Bečková constructed, cultivated and characterized a strain expressing Psb28-FLAG, purified the Psb28-FLAG protein using affinity chromatography and analyzed the obtained preparation by 2D electrophoresis in combination with immunodetection. She also analyzed PSI-less strains for the presence of Psb28-1.

III. **Tichý, M., Bečková, M., Kopečná, J., Noda, J., Sobotka, R., and Komenda, J. (2016). Strain of *Synechocystis* PCC 6803 with aberrant assembly of Photosystem II contains tandem duplication of a large chromosomal region. Front. Plant Sci. 7:648. doi: 10.3389/fpls.2016.00648.**
Martina Bečková cultivated and spectroscopically characterized both wild type strains and the revertant, she analyzed their membranes by 2D electrophoresis in combination with immunodetection.

IV. **Bečková, M., Gardian, Z., Yu, J., Nixon, P.J., and Komenda, J. (2016). Association of Psb28 and Psb27 proteins with PSII-PSI supercomplexes upon exposure of *Synechocystis* sp. PCC 6803 to high light. Molecular Plant, S1674-2052(16)30161-7. doi: 10.1016/j.molp.2016.08.001.**
Martina Bečková constructed all strains expressing FLAG-Psb28 proteins, performed most of biochemical experiments and contributed to writing the manuscript.

Josef Komenda and Peter Nixon, the corresponding authors of the manuscripts, confirm the contribution of Martina Bečková in these publications as described above.

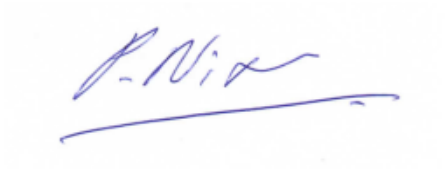

…… ……..

Prof. RNDr. Josef Komenda, DSc. Prof. Peter Nixon

Contents

List of abbreviations

A. thaliana	*Arabidopsis thaliana*
ATP	Adenosine triphosphate
CM	Cytoplasmic membrane
CtpA	C-terminal processing protease involved in D1 maturation
Chl	Chlorophyll
CP43, CP47	PS II core antenna protein (PsbC and PsbB, respectively)
Cyt b-559	Cytochrome b_{559}
GT	Glucose-tolerant
Hlips/HLIPs	High-light-inducible proteins (HliA-D)
iD1	Intermediate precursor form of D1 after removal of part of the C-terminal extension
LHCII	Light harvesting complexes of Photosystem II
mD1	Mature form of D1
$NADP^+$	Nicotinamide adenine dinucleotide phosphate
NADPH	Reduced form of $NADP^+$
OEC	Oxygen evolving complex
OM	Outer membrane
PCC	Pasteur Culture Collection
pD1	Precursor form of D1 with complete C-terminal extension
PSI	Photosystem I
PSII	Photosystem II
Psa	Subunit of Photosystem I
Psb	Subunit of Photosystem II
RCII	PSII reaction center
RC47	PSII core complex lacking CP43
RCC1*	PSII monomer lacking oxygen evolving complex
RCC1	Monomeric PSII core complex
RCC2	Dimeric PSII core complex
SCPs	Small CAB (chlorophyll a/b binding)-like proteins
TEM	Transmission electron microscopy
TM	Thylakoid membrane
TRP	Tetratricopeptide repeat
WT	Wild type
Ycf	Hypothetical chloroplast open reading frame

1 Introduction

1.1 Preface

Cyanobacteria are the only known prokaryotes capable of plant-like oxygenic photosynthesis. Their ancestors began to oxygenate our atmosphere 2,400 million years ago and today they play an important role in a global CO_2 assimilation and oxygen recycling. Using photosynthesis, organisms such as cyanobacteria, algae and plants convert solar energy into chemical energy that they use as a fuel for their biochemical and metabolic activities and produce oxygen as a by-product. Since we consume oxygen and produce carbon dioxide, photosynthesis is the only way to balance this system. It is not only a process indispensable for the existence of life on Earth but it could also represent an elegant, natural and in fact inexhaustible source of energy for mankind. Development of new techniques in molecular biology, genetic engineering, and microscopy provides us an opportunity to better understand this energy converting system that could bring new ideas on how to use photosynthesis for our own needs.

1.1.1 Oxygenic photosynthesis

Oxygenic photosynthesis is a process during which the absorbed light energy is converted into chemical energy, water splits into oxygen and carbon dioxide is fixed and reduced to form sugars. It represents a complex set of reactions which may be divided into light and dark phases. Photosynthetic light energy conversion occurs on the multi-subunit pigment protein complexes, Photosystem II (PSII) and Photosystem I (PSI). Both are embedded in thylakoid membranes, inner membranes of cyanobacteria or chloroplasts, and electron flow between them is connected by the complex of cytochromes b6 and f (cyt b_6-f) and mobile electron transporters. PSII works as a light-driven water:plastoquinone oxidoreductase, that removes electrons from water to feed the electron transport chain reducing $NADP^+$ and catalyzing formation of the transmembrane proton gradient used for ATP synthesis, forming molecular oxygen as a by-product. The electron transfer goes from PSII through cytochrome b_6-f to PSI that mediates (with additional input of light energy) electron transfer from plastocyanin or cytochrome c553 to ferredoxin and reduces $NADP^+$ to NADPH. The subsequent biochemical reactions use energy and reducing equivalents generated in the light phase to fix carbon dioxide into carbohydrates in the so called Calvin-Benson cycle.

1.1.2 Cyanobacteria versus plants

According to the Endosymbiotic theory, chloroplasts are evolutionarily descendants of cyanobacteria that were taken inside another cell (first postulated by Lynn Margulis in 1967). During evolution the engulfed unicellular cyanobacterium developed into a eukaryotic

chloroplast from which a number of genes moved to the nucleus, and so the cell took over part of the regulation of the chloroplast (Martin and Herrmann, 1998).

We find differences in cyanobacterial and chloroplast thylakoid membrane organization and architecture and the type of light harvesting antennae. The protein composition of the photosystems is, however, conserved across the photosynthetic organisms. The only substantial difference is in the set of the proteins of the oxygen evolving complex (OEC) of the PSII (reviewed in Ifuku, 2015).

In cyanobacteria and red algae the peripheral antenna system that directs the energy to reaction center (RC) of photosystems, is provided by the phycobilisomes located on the cytosolic or stromal surface of the membrane (reviewed in Mullineaux, 2008; Watanabe and Ikeuchi, 2013). In plants and most other algae the peripheral antennae are composed of membrane-spanning Chl-binding proteins, so called light harvesting complexes (LHC) (Van Amerongen and Croce, 2013).

The plant LHC together with specific lipids largely assist with the formation of special thylakoid structures, the stacked grana regions that are connected by stromal lamellae (Gounaris and Barber, 1983). The PSII and LHCII antenna system are preferentially located in grana region whereas PSI and ATP synthase in the lamellae. Moreover, this architecture is also forced by a novel class of thylakoid-shaping proteins, which were found in high amount in curved shaped grana margins, named curvature thylakoid1A-D (CURT1A-D) (Armbruster et al., 2013; Pribil et al., 2014).

1.1.3 Model organism - cyanobacterium *Synechocystis* sp. PCC 6803

Although there is a certain divergence in the structure and composition of photosynthetic complexes among plants, algae and cyanobacteria, they can be studied using a suitable model organisms and the obtained knowledge can be used as a background for other systems. The freshwater cyanobacterium *Synechocystis* that was deposited in the Pasteur Culture Collection (PCC) in 1968 (*Synechocystis* sp. PCC 6803, hereafter *Synechocystis* 6803; https://research.pasteur.fr/en/team/biological-resources-center), is such an excellent model organism for the analysis of photosynthetic processes including PSII assembly. It displays a unique combination of physiological, morphological and molecular genetic characteristics. Moreover, this cyanobacterium was among the first organisms with a fully sequenced genome (Kaneko et al., 1996).

Tree-dimensional structure of *Synechocystis* 6803 cytoplasm organization was investigated using high-resolution bio-imaging techniques (for instance van de Meene et al., 2006). The cells of this unicellular cyanobacterium have a spherical shape and are about 1.5-2 μm in diameter

(Fig. 1). They are gram-negative bacteria with a cell envelope consisting of an outer membrane separated from plasma membrane by a peptido-glycan layer. The cell interior harbors the thylakoid membranes, which form layered sheets that mostly follow the periphery of the cell. Thylakoid membranes surround a central cytoplasm that contains inclusions, such as carboxysomes, lipid bodies, ribosomes, fibrils of circular DNA and less often, cyanophycin granules (van de Meene et al., 2006). The thylakoid membrane system forms a base not only for photosynthetic reactions but also for respiration, making the coordination of the biochemical reactions even more complex (Peschek et al., 2004; Vermaas, 1994).

Photosynthesis research on *Synechocystis* 6803 is mostly performed using a glucose-tolerant substrain (GT) derived from the original motile and glucose-sensitive Pasteur Culture Collection (PCC) wild-type (WT) strain. GT is widely used for its easy cultivation under a wide range of physiological conditions in both liquid and solid media, its spontaneous natural transformation, DNA homologous recombination ability, loss of motility allowing better manipulation with single colonies and the biggest advantage, the possibility to study mutants with disrupted photosynthesis (Williams, 1988). This substrain has been spread into many laboratories in the world but it became evident that during prolonged cultivation under specific laboratory conditions the substrain diversified and individual substrains in various laboratories became phenotypically different. Re-sequencing of genomes of several GT substrains from different laboratories revealed unique mutations in each of them (Kanesaki et al., 2012; Morris et al., 2014). Consequently it became obvious that these genotypic differences may also underlie the observed variability in phenotypes of particular mutants containing the same mutated genes but constructed in different laboratories and described in different studies (for instance, Dobáková et al., 2009; Sakata et al., 2013). This finding emphasizes the crucial importance of the background WT strain used for the mutant construction.

The genome of *Synechocystis* 6803 contains up to twelve copies of a single 3.57 mega bases chromosome that codes for 3.317 genes, and seven plasmids. Introducing new methods into molecular biology and genetic engineering allows now to create *Synechocystis* 6803 mutant strains with missing, so called “knock out”, inserted, or differently modified genes. The cells easily accept foreign genetic information in the form of linear or circular DNA and introduce it into their genomes by double-homologous recombination. Interestingly, the natural transformation of *Synechocystis* 6803 cells has been shown to be the most efficient way to generate mutants (Zang et al., 2007). Therefore, sonication or other methods used to disrupt the cell membranes are usually not necessary. To transform all cyanobacterial chromosomes, the antibiotic resistance cassettes are usually inserted in the vicinity of a modified gene. Then an increasing concentration of antibiotics is used for the segregation process to obtain mutant cells having all genomic copies with the desired mutation.

Since the prokaryotic cyanobacterium doesn't have any other membrane organelles, the vast majority of membranes comprise the thylakoid membranes. Using a mechanical breakage and differential centrifugation it is relatively easy to isolate the thylakoid membranes (with a small fraction of plasmatic and outer membranes) and separate them from a soluble fraction. Isolated membrane or soluble fractions may be used for a range of protein analyses.

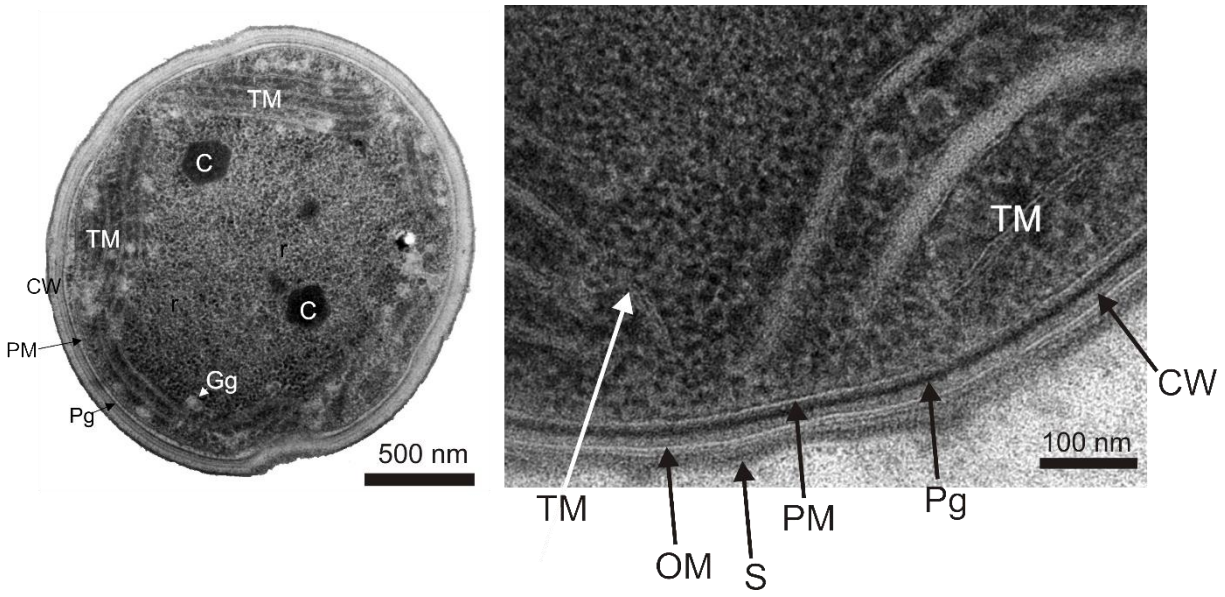

Figure 1. Transmission electron microscope image of *Synechocystis* PCC 6803. Magnified section shows membrane composition of the cell. C, carboxysomes; CW, cell wall; Gg, glycogen granules; OM, outer membrane; Pg, peptido-glycan layer in periplasmic space; PM, plasma membrane; S, surface layer; TM, thylakoid membrane (Image made by Mgr. Lenka Bučinská).

1.2 Photosystem II

Photosystem II is embedded in thylakoid membranes of photosynthetic organisms and is the first pigment-protein complex in the light dependent redox reactions of oxygenic photosynthesis. The structure and assembly of this sophisticated complex has been a subject of research for many years.

1.2.1 Structure of the Photosystem II complex

The structural framework of the PSII complex was established at 3.5 Å, 2.9 Å and 1.9 Å (Fig. 2) resolution using complexes isolated from the thermophilic cyanobacteria of the genus *Thermosynechococcus* sp. (Ferreira et al., 2004; Guskov et al., 2009; Umena et al., 2011, respectively). Although the crystal structure of PSII from higher plants has not been solved, photosystems of cyanobacteria and plants are largely conserved regarding basic structural

features and protein composition. This was very recently confirmed by 3.2 Å resolution structure of the plant PSII supercomplex solved by cryoelectron microscopy (Wei et al., 2016). The prevailing fully functional form of this multi-subunit pigment protein complex is a dimer. One monomeric PSII complex from *T. elongatus* consists of 17 transmembrane protein subunits, 3 peripheral proteins of oxygen evolving complex, and about 80 cofactors (35 chlorophyll a molecules, 12 carotenoid molecules, 2 pheophytin a molecules, 3 plastoquinones, 25 integral lipids, 1 chloride ion, 1 non-haem iron, 2 haem iron and Mn4CaO5 metal cluster; Guskov et al., 2009; Suga et al., 2015; Umena et al., 2011). The heart of the monomer complex presents two reaction complex subunits D1 and D2 each with 5 transmembrane α helices, which bind cofactors (Chl *a*, pheophytin, and β-carotene) involved in the primary charge separation (Nanba and Satoh, 1987). On either side are inner antennae CP43 and CP47 each with 6 transmembrane α helices and cofactors (Chl *a* and β-carotene). CP43 also participates (together with D1) in ligation ions of the oxygen evolving Mn_4CaO_5 cluster. On the periphery of these large subunits there are 13 small (PsbI, H, J, Z, E, F, K, L, M, T, X, 30, Y), mostly single helix, subunits and the lumenal part of the complex is shielded by three extrinsic subunits PsbO, PsbU and PsbV which stabilize the Mn_4CaO_5 cluster and form with it oxygen evolving complex (OEC) (reviewed by Nixon et al., 2010). Recently, CyanoQ, the homolog of plant extrinsic protein PsbQ that has not been found in the crystal structure of the PSII, has been proposed, based on the crosslinking experiments, to be part of the cyanobacterial OEC (Liu et al., 2014).

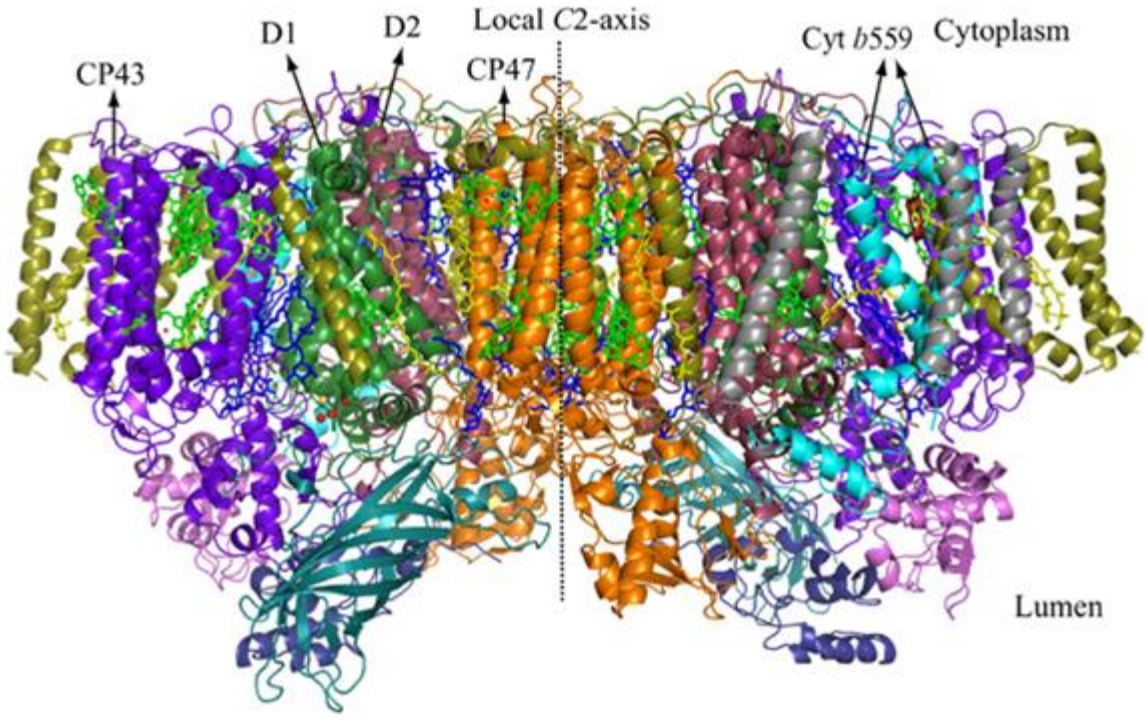

Figure 2. Crystal structure of the Photosystem II complex from *Thermosynechococcus vulcanus* at resolution 1.9 Å (borrowed from Umena et al., 2011).

The stability and activity of photosynthetic complexes is also supported by a unique lipid composition of thylakoid membranes, where the PSII is embedded (Boudière et al., 2014). As deduced from X-ray crystallographic analysis, glycolipids (which comprise 70% of thylakoid lipids) have been shown to interact closely with PSII and so might play the critical roles for the structure and function of the protein complexes (Mizusawa and Wada, 2012; Umena et al., 2011). The glycolipids DGDG (digalactosyldiacylglycerol) and PG (phosphatidylglycerol) were shown to be important for the function of PSII in particular (Boudière et al., 2014; Hagio et al., 2002; Sakurai et al., 2007).

1.2.2 Overview of Photosystem II biogenesis

Photosystem II is a multi-subunit pigment protein complex with a specific protein organization. The assembly of its components was proposed to be a stepwise process and requires the association of several pigment-protein intermediate complexes (modules; Fig. 3) in a specific order (reviewed by Komenda et al., 2012b; Nixon et al., 2010). Where the steps of PSII assembly take place, has not yet been completely clarified. In earlier studies, the location of early assembly steps in the plasma membrane (Zak et al., 2001) and later steps in the thylakoid membrane, led to conclusion that at least temporary connections between the two membrane systems are required (Nevo et al., 2007; Nickelsen et al., 2011; Pisareva et al., 2011; van de Meene et al., 2006). In *Synechocystis* 6803, the existence of such convergence sites (so-called thylakoid centers) was proposed (Rast et al., 2015; Schottkowski et al., 2009; Stengel et al., 2012) as outlined below but their existence is still highly controversial. Moreover, the recently published study of Selão et al. (2016) brought evidence that the initial steps of PSII assembly most probably occurs in the TM or in specific thylakoid-derived membrane sections.

1.2.2.1 PSII assembly - *de novo*

The early steps of PSII assembly comprise synthesis of reaction centre subunits, the D1 precursor (pD1) and D2, formation of the D1 and D2 modules and their binding to yield a PSII reaction centre complex (RCII). The later steps represent the attachment of the inner antennae modules CP47 and CP43 to RCII to form PSII monomer and dimer (Fig. 3).

During the initial phase of the assembly process in *Synechocystis* 6803, the pair of the PsbE and PsbF subunits of cytochrome-b_{559} (hereafter Cyt b-559) was proposed to act as a nucleation factor of PSII assembly (Komenda et al., 2004). The accumulation of Cyt b-559 is prerequisite for efficient synthesis and accumulation of the D2 reaction center subunit. The binding of D2 to Cyt b-559 results in the formation of the D2 assembly module (Komenda et al., 2004). The D1 protein, another key reaction center subunit of PSII, is synthesized as a precursor (pD1) with a cleavable 16 amino acid C-terminal extension (Nixon et al., 1992), and together with PsbI forms the D1 module (Dobakova et al., 2007). Mutual binding of the D1 and D2 modules results

in formation of the reaction center complex (Komenda et al., 2004). Interestingly, the above mentioned C-terminal extension of the pD1 is cleaved in two steps with the first cleavage after residue Ala352 (Komenda et al., 2007a) by CtpA protease (Anbudurai et al., 1994) yielding the intermediate form of D1 (iD1) that is found mostly in RCII complexes (Komenda et al., 2007a). The location of the above mentioned early steps of the assembly is still under debate. According to the latest study of Selão et al. (2016), the pD1 insertion and maturation into mD1 under various light conditions as well as the formation of the RC complex occur only in the thylakoid membranes. Moreover, unlike the previous study (Zak et al., 2001) the CtpA protease was found in thylakoid membranes (Selão et al., 2016) and all these data support the idea of the initial steps occurring in the TM or in specific thylakoid-derived membrane sections (Selão et al., 2016). Specific thylakoid membrane parts called T-zones were also proposed to encompass the initial steps of PSII assembly in the chloroplast of *Chlamydomonas reinhradtii* (Uniacke and Zerges, 2007). These specific regions are located at the periphery of pyrenoid where ribosomes and chloroplast mRNA coding for subunits of PSII were detected. Whether this model works in other organisms needs to be clarified.

In the later stage of PSII assembly, CP47 module containing the CP47 inner antenna and small subunits PsbH, PsbL and PsbT (Boehm et al., 2012; Komenda et al., 2005; Promnares et al., 2006) is attached to the RCII complex forming the PSII core complex lacking CP43 frequently designated RC47. This attachment also promotes the second cleavage of the remaining eight amino acids of iD1 yielding the mature D1 protein (Komenda et al., 2007a). Subsequent attachment of the CP43 module consisting of CP43, PsbK, Psb30 and PsbZ (Komenda et al., 2008) allows formation of the monomeric PSII core complex, RCC1. RCC1 is the starting point for light-driven assembly of the Mn_4CaO_5 cluster and attachment of the lumenal extrinsic subunits (PsbO, PsbU, PsbV, CyanoQ) which act as a “cap” to shield the cluster (reviewed by Roose et al., 2007). Since the carboxyl terminus of D1 is a ligand to a manganese atom in the Mn_4CaO_5 cluster, the removal of C-terminal extension of pD1 is important for its correct assembly and function (Nixon et al., 1992; Umena et al., 2011). The final step of the PSII assembly is a dimerization of the monomers to form the RCC2 dimer.

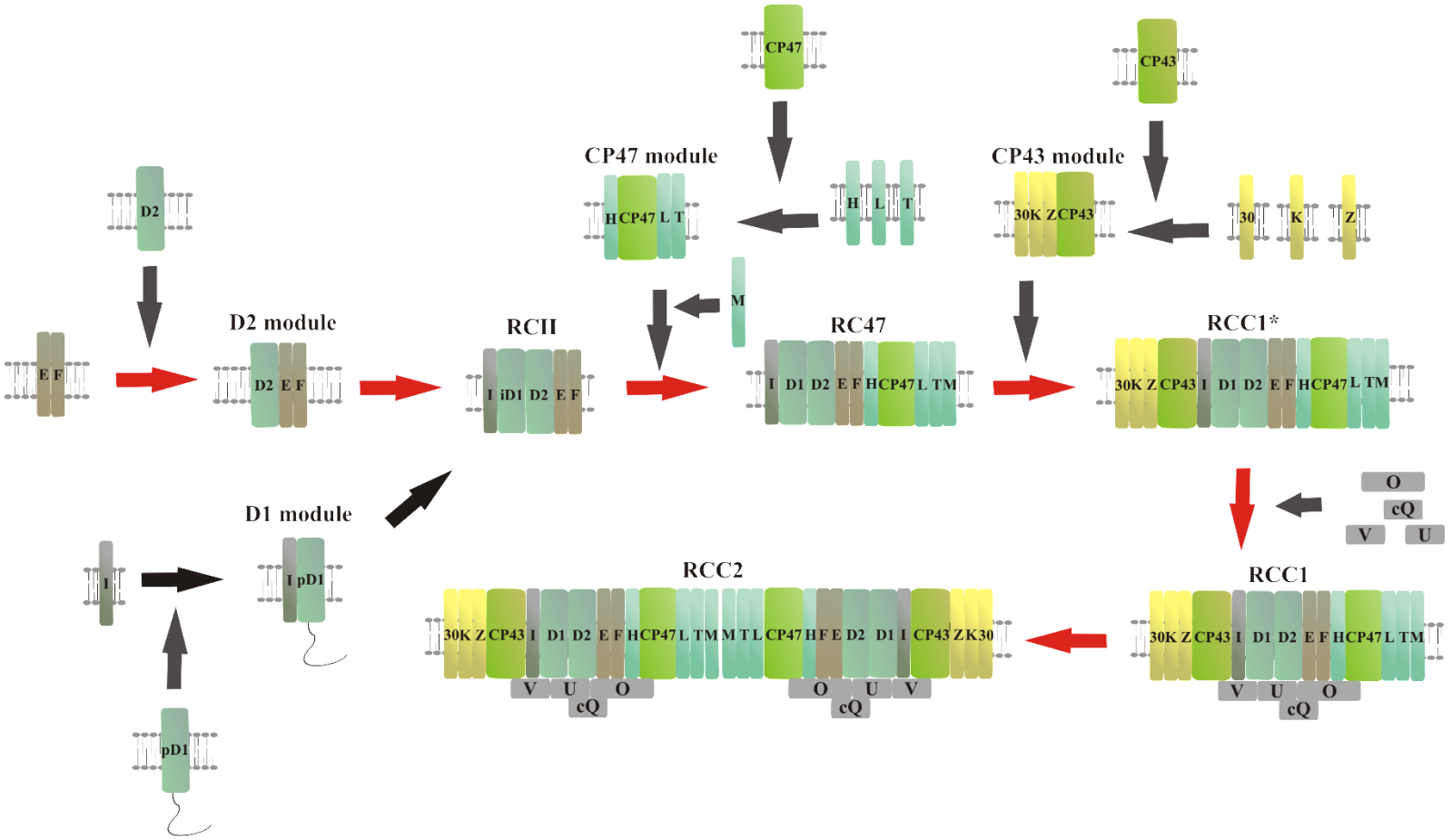

Figure 3. Simplified model of Photosystem II assembly steps. The assembly process occurs through several pigment-protein intermediate complexes (modules). In the first step the D2 module (Cyt b-559-D2) and the D1 module (PsbI-pD1) form a reaction center complex (RCII complex) to which the CP47 module (CP47 inner antenna with PsbH, L and T subunits) are attached to form RC47 assembly complex. The subsequent attachment of the CP43 module (the second inner antenna in complex with Psb30, K, and Z) leads to formation of PSII monomer (RCC1*). The attachment and assembly of Mn_4CaO_5 cluster together with extrinsic subunits PsbO, U, V and CyanoQ results in the fully functional PSII monomer (RCC1) and the assembly is finished with PSII dimerization (RCC2).

1.2.3 PSII repair cycle

PSII is a place of charge separation, a specific redox reaction due to which it is prone to a light induced irreversible damage. The most sensitive protein to photodamage is the D1 subunit. It is assumed that when it is damaged it must be replaced by a newly synthesized copy during the so called PSII repair cycle (reviewed by Nixon et al., 2010). Its current model involves partial disassembly of PSII, degradation of the damaged D1 subunit and incorporation of a newly synthesized one.

In the first step the PSII dimer dissociates to PSII monomers and proteins of oxygen evolving complex also leave. Since D1 is shielded by the CP43 inner antennae, the CP43 module is detached to form the RC47 complex. In this complex the damaged D1 is accessible for membrane-bound FtsH2/FtsH3 protease complex that degrades the protein from its N-terminus (Boehm et al., 2012). The newly synthesized pD1 subunit is incorporated back into the CP47-D2-Cyt b559 complex and PSII re-assembles by attachment of CP43 module (Komenda et al., 2007b). How the FtsH complexes differentiate between damaged and undamaged D1 subunits is unclear (Nagarajan and Burnap, 2014). However, authors of recently published work (Krynická et al., 2015) propose that the protease accessibility induced by PSII disassembly could be important determinant in the selection of the D1 and D2 subunits for degradation by FtsH proteases. It seems that at least partial disassembly of PSII, not necessarily triggered by photodamage, could facilitate the contact between the degraded subunit and the FtsH protease (Krynická et al., 2015).

1.3 Overview of PSII auxiliary protein factors

Over the years, a number of proteins participating in the assembly and repair of PSII have been found. They were mostly identified in specific mutants lacking a component essential for the next assembly/repair step (Komenda et al., 2008; Komenda et al., 2004). Since these proteins were not found in the crystal structure of PSII (Umena et al., 2011), they are, most probably, not components of the final functional PSII complex, the PSII dimer. They are involved in distinct steps of PSII assembly/repair and so control and optimize these processes (Fig. 4). Some of the proteins are conserved in both cyanobacteria and plants, and even retained their function during evolution. Most of the auxiliary factors from *Synechocystis* 6803 were nicely described in several reviews (Mabbitt et al., 2014; Nixon et al., 2010; Pagliano et al., 2013; Shi et al., 2012). Not all auxiliary factors from *Synechocystis* 6803 are known but compared to number of factors known from plants they are just few (Lu, 2016).

The *Synechocystis* 6803 factors PratA, Ycf39, HliC, HliD, Ycf48, Slr0151 and CyanoP (encoded by genes *slr2048*, *slr0399, ssl1633*, *ssr1789*, *slr2034*, *slr0151*, *and sll1418*, respectively) assist the early PSII assembly steps (Komenda and Sobotka, 2016; Rast et al., 2016; Stengel et al.,

2012). Another set of protein factors, the HliA/B/C, PAM68, Psb27, Psb28, and Psb29 (encoded by the *ssl2542/ssr2595/ssl1633, sll0933*, *slr1645*, *sll1398* and *sll1414* genes, respectively) mostly identified as components of His-tagged PSII preparations isolated from *Synechocystis* 6803 (Boehm et al., 2011; Kashino et al., 2002) were proposed to function in later stages of the PSII assembly.

1.3.1 Auxiliary factors of early PSII assembly stage

One of the factors participating in the early stage of PSII assembly is PratA, the Mn^{2+}-binding protein that also interacts with the C-terminal part of the D1 subunit. The protein was mostly found in the periplasm but its small population was proposed to define a specific membrane sub-fraction (the so-called thylakoid centres) (Nickelsen and Rengstl, 2013) containing substantial amounts of pD1, which is there processed by CtpA protease and loaded by manganese (Nickelsen and Rengstl, 2013; Rast et al., 2015; Schottkowski et al., 2009; Stengel et al., 2012).

Another PSII auxiliary factor designated Ycf48 was identified in *Synechocystis* 6803 as a homolog of a HCF136 factor from *Arabidopsis thaliana* (Meurer et al., 1998). It binds to the lumenal side of D1 subunit where it plays a role in stabilization of the newly synthesized pD1 and its subsequent binding to the D2 assembly module (Komenda et al., 2008; Plucken et al., 2002). Moreover, this protein was shown to be important for the efficient incorporation of newly synthesized D1 into the partially disassembled PSII complexes during the PSII repair (Komenda et al., 2008).

An interesting, yet not well described factor is the Slr0151, a tetratricopeptide repeat (TRP) protein from *Synechocystis* 6803. By yeast two-hybrid and pull-down analysis the Slr0151 protein was shown to interact with CP43 and D1, and was proposed to participate in the PSII repair under high light conditions (Yang et al., 2014). Recently, it was shown that inactivation of Slr0151 affects thylakoid ultrastructure even in cells grown under standard light conditions (Rast et al., 2016). Moreover, a close functional relationship of Slr0151 with Ycf48 was proposed (Rast et al., 2016).

Ycf39 was localized at cytoplasmic side of the membrane in *Synechocystis* 6803 (Knoppová et al., 2014) and it was predicted to belong to a short-chain alcohol dehydrogenase/reductase superfamily containing NAD(P)H binding domain (Ermakova-Gerdes and Vermaas, 1999). Recently, the protein has been shown to be important for efficient chlorophyll delivery to the newly synthesized D1 subunit and for photoprotection of the D1 module and RCII assembly complex as it associate with HliC and HliD proteins, members of high-light inducible protein family homologous to plant LHC complexes (Knoppová et al., 2014).

On the lumenal side of the RCII assembly complex the lipoprotein CyanoP has recently been localized (Knoppová et al., 2016). Unlike its plant homologue PsbP, which is a constitutive lumenal subunit of PSII (Bricker et al., 2012), CyanoP has been found to interact with the D2 assembly module and seems to stabilize it against premature proteolysis by lumenal proteases (Knoppová et al., 2016).

1.3.2 Auxiliary factors of later PSII assembly stage

The later assembly stage includes the formation of the RC47 complex, PSII monomer lacking CP43 inner antennae, onto which the Psb28-1 protein factor was shown to bind (Dobáková et al., 2009). Since this thesis is focused on the Psb28-1 protein from cyanobacterium *Synechocystis* 6803 and its homolog Psb28-2 (encoded by gene *slr1739*), the proteins are described in more detail below (section 1.3.2.1 Psb28 proteins).

Sll0933, an orthologue of PAM68 protein in *A. thaliana*, was shown to interact with Ycf48 (Rengstl et al., 2011) and via their interaction the inner antenna protein CP47 attaches to the RCII complex, forming RC47 (Rengstl et al., 2013). Recently, it was shown to be a membrane protein bound to CP47 in the stage before PsbH subunit is attached, and it seems to interact with ribosomes while CP47 is synthesized (Bučinská L. and Sobotka R., unpublished data).

Under high irradiance CP47 module can also bind HliA/B/C members of Hlip family, which most probably protect this module against photodamage (Promnares et al., 2006).

Psb27 is a 12 kDa protein (Kashino et al., 2002) extrinsically associated with the lumenal side of the PSII core complex and containing a lipidic moiety (Nowaczyk et al., 2006). It does not contain any transmembrane domain (Chen et al., 2006). The protein was found to transiently associate with the CP43 assembly module (Komenda et al., 2012a; Liu et al., 2011a), where it protects CP43 against proteolysis (Komenda et al., 2012a). Furthermore, the Psb27 is supposed to prevent the premature binding of extrinsic OEC subunits to the PSII center core (Roose and Pakrasi, 2008). Psb27 was also detected in dimeric PSII (Grasse et al., 2011), in PSI and PSII-PSI supercomplexes (Komenda et al., 2012a). The protein was proposed to affect interaction between CP43 and PSI which led to hypothesis that PSI might have some particular role in the biogenesis/repair of PSII (Komenda et al., 2012a). Similar, nuclear-encoded Psb27 Arabidopsis orthologues Psb27-H1 and Psb27-H2 (also known as LPA19) were found to participate in the repair of PSII (Chen et al., 2006) and in processing of the D1 precursor under high light (Wei et al., 2010), respectively.

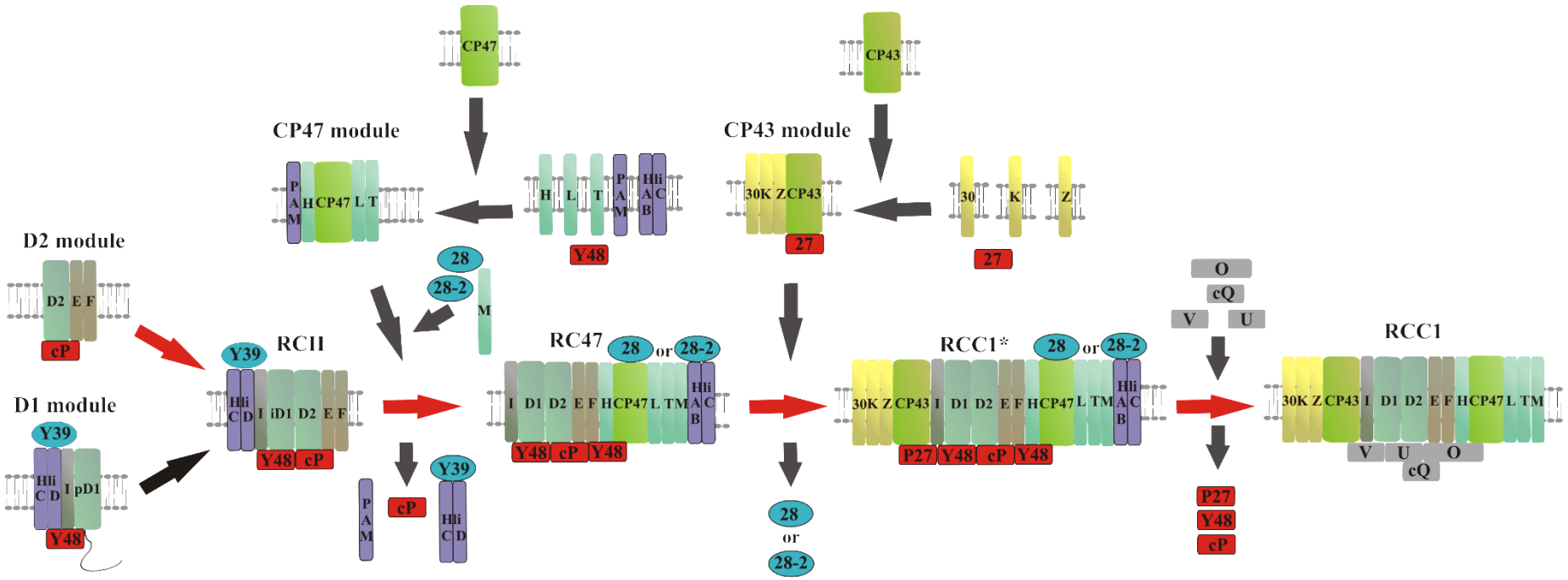

Figure 4. Model of the Photosystem II assembly showing some of the assembly factors. Stromal factors are in light blue: Ycf39 (Y39), Psb28-1 (28), Psb28-2 (28-2); lumenal factors are in red: Ycf48 (Y48), Cyano P (cP), Psb27 (P27); membrane factors are in violet: high light inducible proteins (HliA/B/C/D), Sll0933-homolog of *Arabidopsis* PAM (PAM). Proteins of oxygen evolving complex are in grey: PsbO (O), CyanoQ (cQ), PsbU (U), PsbV (V).

1.3.2.1 Psb28 proteins - Psb28(-1) and Psb28-2

Psb28 proteins (also known as Psb13 or Ycf79) form a protein family (Interpro Photosystem II Psb28, class 1, IPR005610), members of which are widely distributed in oxygenic photosynthetic organisms from cyanobacteria to higher plants. In *Synechocystis* 6803 it is encoded by *sll1398* gene. The protein was initially identified as a 13 kDa sub-stoichiometric component of PSII in a His-tagged CP47 preparation isolated from *Synechocystis* 6803 (Kashino et al., 2002). Psb28 was also detected as a component of PSII complexes in *Synechocystis* 6803 depleted of phosphatidylglycerol (Sakurai et al., 2007) and its regulatory function during the PSII assembly was proposed. Later, Dobáková et al. (2009) detected the protein not bound to fully assembled PSII complexes but preferentially to the RC47 assembly intermediate complex. Their results supported the role of the protein in PSII biogenesis as outlined below (see Phenotype section).

In eukaryotes Psb28 can be either plastid- (Ycf79) or nuclear- encoded (Oudot-Le Secq et al., 2007). Interestingly, in *Thalassiosira pseudonana*, a centric diatom, there are two similar Psb28 genes. One gene is located in the nucleus, the other in the plastid (Armbrust et al., 2004). It was shown that both genes in *T. pseudonana* are transcribed and the nuclear gene product fused to the yellow fluorescent protein is indeed targeted into the plastids directed by the N-terminal bipartite presequence containing signal peptide and transit peptide (Jiroutová et al., 2010). In contrast, there is only one *psb28* gene in the plastid genome of another diatom *Phaeodactylum tricornutum* (Oudot-Le Secq et al., 2007). The authors propose that copying of the plastid *psb28* gene into the *T. pseudonana* nuclear genome may be a recent event giving an example that the gene transfer from the endosymbiont's genome to its host nuclear genome is still an ongoing process (Jiroutová et al., 2010; Oudot-Le Secq et al., 2007). Regarding higher plants, in *Arabidopsis thaliana*, Psb28 is the product of a single nuclear gene (*At4g28660*) with a molecular weights 15.1 kDa. In *Oryza sativa*, the transcription of *psb28* (*Os01g71190*) was found to be induced by high irradiance and inactivation of this gene by T-DNA insertion resulted in a pale-green phenotype (Jung et al., 2008).

As it was mentioned above, apart from gene encoding Psb28 protein (hereafter Psb28-1), the genome of *Synechocystis* 6803 (and some other cyanobacteria) also contains a second Psb28-like gene *slr1739* that encodes a homolog of Psb28-1 protein designated Psb28-2. It is a 14 kDa protein with 23.8 % identity and 36.1 % similarity in their amino acid sequences (Sakata et al., 2013).

1.3.2.1.1 Psb28-1 vs PsbW – confusion in nomenclature

PsbW is sometimes incorrectly used as a synonym of Psb28(-1) protein in databases and some articles. It is important to note that they are two completely different proteins.

PsbW is a PSII transmembrane protein located in chloroplast thylakoid membranes of several plants. It was first described as a 6.1 kDa polypeptide associated with the reaction centre core complex of the photosystem II from spinach (*Spinacia oleracea*). As a eukaryotic protein encoded by a nuclear gene, carries a bipartite transit peptide which directs the mature protein into the chloroplast lumen (Irrgang et al., 1995; Lorkovic et al., 1995). Cross-linking experiments indicated association of PsbW with D1, D2 and Cyt b-559 in the isolated RCII complex (Irrgang et al., 1995; Lorkovic et al., 1995). *Arabidopsis thaliana* transformants lacking PsbW showed decreased levels of PSII dimers and PSII-LHCII supercomplexes (Garcia-Cerdan et al., 2011; Shi et al., 2000). Therefore, it was suggested that PsbW could work as a linker for LHCII binding to PSII complex and/or stabilize the PSII dimer (Shi et al., 2000; Thidholm et al., 2002). Recently, the protein has been found in the structure of spinach PSII obtained by single-particle cryoelectron microscopy confirming that the association of the LHCII trimer with the core complex is mediated by PsbW (Wei et al., 2016). LHCII trimer binds to PsbW on its lumenal and stromal side and the transmembrane helix of PsbW interacts with PsbI located on the side opposite to the LHCII binding site. Simultaneously PsbI interacts with the first transmembrane helix of the D1 subunit and PsbW. In addition, the N-terminal region of PsbW extends to the lumenal surface and interacts with PsbO and D1, while its C-terminal region is located on the stromal surface and binds to the loop region between the fourth and fifth transmembrane helices of CP43 (Wei et al., 2016).

A corresponding gene to PsbW that belongs to PsbW protein family (Pham ID: PF07123) has not been found in cyanobacteria and it seems not to be related to Psb28 protein family (Pfam ID: PF03912) that currently comprise 152 protein sequences. The name PsbW should be used only for a 6 kDa hydrophobic protein that is always nuclear-encoded (Shi and Schröder, 2004). Therefore, the gene annotated as *psbW* in the *Synechocystis* 6803 genome and the plastid genomes of *Ophiocordyceps sinensis*, *Guillardia theta* and several red algae (e.g. *Galdieria sulphuraria*; Thangaraj et al., 2010) encodes a hydrophilic 13 kDa protein and should be called Psb28 (Psb28-1) (Kashino et al., 2002).

1.3.2.1.2 Localization

For the first time, a small amount of Psb28-1 was identified in the nickel affinity purified PSII complexes containing His-tagged CP47 (Kashino et al., 2002). Based on its amino acid sequence, it was proposed to be a hydrophilic protein lacking transmembrane helices (Dobáková et al., 2009). Dobáková and coworkers showed that it can be easily removed from membranes using $CaCl_2$, completely washed off by 0.1 M sodium carbonate and sodium hydroxide, and digested by trypsin, confirming its peripheral location on the cytoplasmic side of thylakoid membranes (Dobáková et al., 2009). Two dimensional electrophoretic analysis

detected the native Psb28-1 protein mostly in unassembled protein fraction and only a portion of the Psb28-1 was localized in the RC47 assembly complex (Boehm et al., 2012; Dobáková et al., 2009; Sakata et al., 2013). This result was confirmed by affinity purification of N-terminally His-tagged protein (Psb28-1-6xHis) that copurified mostly with RC47 complex but also with a small amount of the PSII monomer and unassembled CP47 (Dobáková et al., 2009). However, the authors speculated that Psb28-1 probably remains attached to the PSII monomer only for a limited time after binding of CP43 to RC47. This was supported by detection of Psb28-1 in isolated PSII core complex containing His-tagged Psb27 subunit (Liu et al., 2011b) that is supposed to bind onto the PSII monomer before the proteins of oxygen evolving complex are attached (Komenda et al., 2012a; Roose and Pakrasi, 2008).

Dobáková et al. (2009) also showed that the abundance of the protein was greatly reduced in PsbH-less strain and almost completely missing in the CP47-less strain. Since PsbH is protein component of the CP47 assembly module, they proposed location of the Psb28-1 binding site on the CP47 inner antenna in the vicinity of the PsbH subunit. Interestingly, the same location was also proposed for the HliA and HliB proteins (also named ScpC and ScpD, i.e. small CAB-like proteins, respectively) that could photoprotect the CP47 assembly module (Promnares et al., 2006). Later, Yao and co-workers proposed that Psb28-1 could stabilize interaction between CP47 and HliB (Yao et al., 2007).

The Psb28-2 protein was found among thylakoid proteins of *Synechocystis* 6803 in the proteomic study of Pisareva et al. (2011) but so far the protein has not been localized within the particular membrane protein complexes.

1.3.2.1.3 Phenotypes of the Psb28-null mutants and possible function of the proteins

During a last few years several studies have been done on Psb28-1 deletion mutants. Interestingly, the observed phenotypes of knockout mutants (including our result presented in the thesis) exhibited a noteworthy variability. The first report on knockout ΔPsb28-1 mutant published by Dobáková et al. (2009), described several effects of Psb28-1 deletion on the photosynthetic apparatus. Their ΔPsb28-1 mutant exhibited a slower autotrophic growth than the wild type, and contained a lower cellular content of chlorophyll. 77K fluorescence emission spectra of cells showed that the decrease in chlorophyll content is due to the lower level of PSI. They also showed that the deletion of this protein did not affect the function of the fully assembled photochemically active PSII complex, but resulted in slightly accelerated turnover of D1 subunit and more efficient PSII repair. Since the selective replacement of D1 subunit most probably occurs in the RC47 complex (Komenda et al., 2006) where the Psb28-1 was localized, it confirmed the regulatory function of the protein in PSII assembly/repair.

Pulse chase radioactive labelling of mutant and wild type strain combined with two-dimensional blue-native/SDS-PAGE analysis demonstrated that in the mutant RC47 complex and unassembled CP47 were missing, and RCa and unassembled D1 accumulated. Since the presence of RCa indicates a limited availability of CP47 (Dobakova et al., 2007; Komenda et al., 2004) authors came to conclusion that PSII assembly in Psb28-1 deletion mutant is limited by availability of CP47. Furthermore, the absence of Psb28-1 also negatively affected the synthesis of PsaA/B heterodimer of PSI. In other words, their results suggest that the decreased synthesis of the CP47 inner antenna in mutant leads to a lower level of RC47 complex, and lower cellular level of chlorophyll in the mutant is related to the decreased synthesis of PsaA/PsaB heterodimer of PSI (Dobáková et al., 2009).

The relation of Psb28-1 and CP47 was further verified in two Psb28-1 double deletion mutant strains lacking either CP43 or *psbEFLJ* operon. In the ΔCP43 mutant (accumulating the RC47 complex) the Psb28-1 deletion led to a 50% decrease in the RC47 level and the unassembled CP47 was almost undetectable, confirming a lower availability of the newly synthesized CP47. In the ΔpsbEFLJ mutant that accumulates unassembled CP47 but no other CP47 containing complexes (Komenda et al., 2004) the additional deletion of Psb28-1 led to substantial decrease in the steady state level of the unassembled CP47, whereas the accumulation of the unassembled D1 was increased.

Dobáková et al. (2009b) observed changes in levels of chlorophyll precursors, namely an increased level of Mg protoporhyrin IX monomethyl ester and a decreased level of protochlorophylide, indicating inhibition of chlorophyll biosynthesis at the step of isocyclic ring E formation mediated by AcsF cyclase (encoded by gene *sll1214*). Moreover, AcsF was co-purified with the His-tagged Psb28-1 protein indicating the Psb28-1 may stimulate AcsF activity and therefore, de novo synthesis of chlorophyll *a.*

The independent study of Sakata et al. (2013) showed a different phenotype of the ΔPsb28-1 deletion mutant. It exhibited growth retardation only under high light treatment combined with high temperature and the growth defect was further enhanced in the ΔPsb28-1/ΔdgdA double mutant additionally defective in biosynthesis of digalactosyldiacylglycerol (DGDG). Interestingly, the single ΔdgdA mutant accumulated an increased level of Psb28-1 most of which was bound to monomeric PSII complexes or to RC47. Accordingly, the authors suggested that this protein is important during PSII repair, especially under high temperatures.

The first study dealing with the function of Psb28-2 was done by Jonathan Moore in his Master thesis (Moore, 2011). His Psb28-2 null mutant exhibited slightly slower growth and deficient energy transfer between the phycobilisomes and the photosystems. This was in contrast with a later study of Sakata et al. (2013), in which a knock out mutant didn't exhibit any difference

in photosynthetic growth compared to wild type. Whether this protein plays a role in PSII biogenesis remained unknown.

The diverse phenotypes of independent studies were suggested to be caused by different cultivation conditions (Mabbitt et al., 2014). Another explanation is that wild type background used for generation of the mutants could also influence the mutant phenotypes. However, this possibility has never been tested.

1.3.2.1.4 Expression of *Psb28* genes

CyanoEXpress, a web database for exploration and visualization of the integrated transcriptome of cyanobacterium *Synechocystis* 6803 (Hernandez-Prieto and Futschik, 2012), can be used as a guide to design experiments while study proteins with unknown function. Expression of *psb28-1* and *psb28-2* genes shows differences under variety of environmental conditions, indicating a distinct functional role for each protein.

Most divergence of their expression was found under the dark conditions, where the transcription of *psb28-1* is decreased whereas that of *psb28-2* is increased. Consistent with this, the *psb28-2* gene was shown to increase expression, whenever overall expression of PSII genes is decreased (Hernández-Prieto et al., 2016).

1.3.2.1.5 Proteins structures

Psb28-1 NMR structure

Psb28-1 was proposed to be a hydrophilic protein without transmembrane helices (Dobáková et al., 2009) which was confirmed by the solution NMR structure of the C-terminally His-tagged Psb28-1 protein from *Synechocystis* 6803 (120 aa; PDB: 2KVO; Yang et al., 2011). The structure features seven β strands arranged into two anti-parallel β sheets, one long α helix, two short helices, and nine loop regions connecting these elements (Fig. 5). In the surface area, nine solvent accessible cavities were defined, ranging from 418.1 $Å^2$ to 35.5 $Å^2$. ConSurf analysis conducted for the Psb28 protein family (that time composed of 47 sequences in total using PSI-BLAST) showed that the cavities four and nine using their nomenclature occur on the same side of the protein surface and has the highest conserved residues percentages (with 5/7 and 4/6, respectively) and therefore seems to be evolutionary significant. Their conserved surface residues (C4: Ile4, Glu12, Pro16, Phe35 and Tyr100; C9: Ala2, Asp56, Arg95 and Phe96) are mostly found in the loop regions L1 (between beta1 and beta2), L2, L6 (between beta4 and beta5) and at the C-terminus (alfa helix). According to Yang et al. (2011), these cavities might play an important role in PSII-related function of the protein.

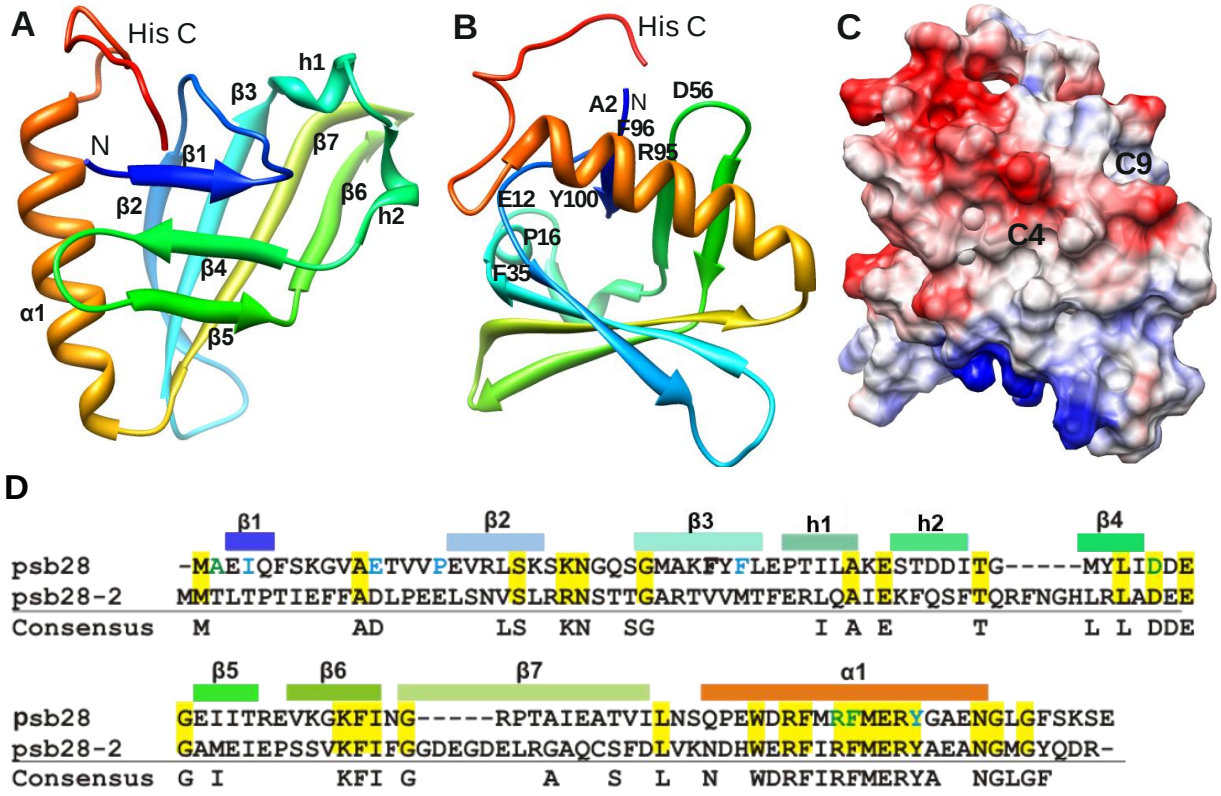

Figure 5. Structural models of Psb28-1 from *Synechocystis* 6803. A. Solution NMR structure of Psb28-1 (PDB: 2KVO; Yang et al., 2010); **B**. Different orientation of A. Eight highly conserved residues of C4 and C9 are highlighted; **C**. Electrostatic potential surface diagram in same orientation as B., C4 and C9 cavities are labelled; **D.** Alignment of Psb28(-1) and Psb28-2 amino acid sequence from *Synechocystis* 6803. Highly conserved residues in C4 and C9 cavity of Psb28(-1) were labeled in blue and green letters, respectively (Pictures were adapted from Yang et al., 2011).

Psb28-1 crystallography

The recently published crystallography of Psb28 from *T. elongatus* (encoded by gene *tlr0493*) provided an evidence that Psb28-1 protein exists in an oligomeric form, most probably a dimer in vivo (PDB: 3ZPN; Bialek et al., 2013). Comparison of amino acid sequences between Psb28 from *T. elongatus* and Psb28-1 and Psb28-2 from *Synechocystis* 6803 showed 59% identity (78% similarity) and 33% identity (57% similarity), respectively (Bialek et al., 2013). Compared to the solution NMR structure, this crystal structure lacks the short helices between beta-strands 3 and 4 in 2KVO structure but includes a five residue long alfa-helix in this region incorporating Lys42-Glu46. Although the structures share significant similarities, they did not bring an insight into the function of the protein in the PSII assembly.

Psb28-2 predicted model

The relatively high amino acid sequence similarity between Psb28-1 and Psb28-2 (Fig. 5D) indicates a possible resemblance of their secondary and tertiary structure. Mabbitt et al. (2014) constructed models of the Psb28-2 protein from *Synechocystis* 6803 using the PHYRE (version 2) web server (Kelley and Sternberg, 2009) based on the solution NMR structure (PDB: 2KVO; Fig. 6) and crystallography (PDB: 3ZPN) of Psb28-1 protein from *Synechocystis* 6803 and *Thermosynechococcus elongatus*, respectively. The model structures features considerable similarities with Psb28-1. However, real structure of Psb28-2 remains unsolved.

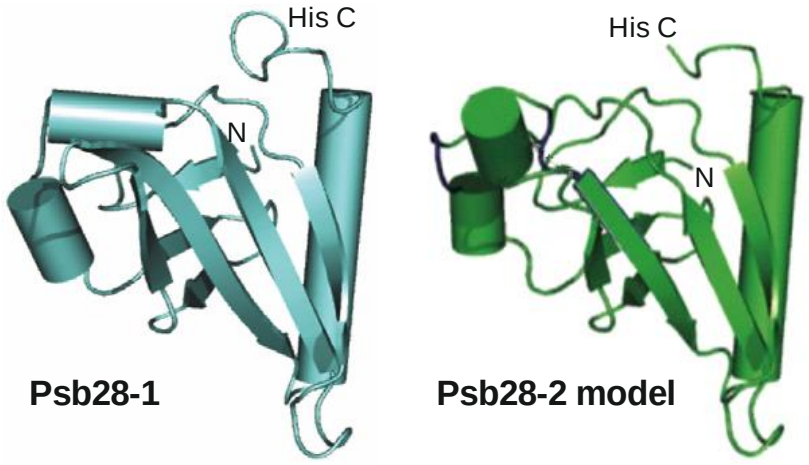

Figure 6. Predicted model of Psb28-2 from *Synechocystis* 6803. Ribbon diagram of Psb28-1 (PDB: 2KVO) in different orientation (left); Ribbon diagram of Psb28-2 model created by PHYRE (version 2) web server (Kelley and Sternberg, 2009) based on the NMR model of Psb28-1 (right). (Pictures were adapted from Mabbitt et al., 2014).

2 Aim of the thesis

Photosystem II is a multi-subunit pigment protein complex and a key component of the photosynthetic machinery of cyanobacteria, algae and plants. Its assembly has turned out to be a highly complex process which occurs in a sequential order that requires many auxiliary protein factors. Although the cyanobacterial PSII structure was solved and the main steps of its assembly defined, there are still a number of unexplored genes which code for proteins that may play some role in PSII assembly. My thesis is dedicated to two homologs of Psb28 proteins, the Psb28-1 encoded by the *sll1398* gene and Psb28-2 encoded by the *slr1739* gene that were proposed to be regulatory or auxiliary factors during the PSII assembly. This work is continuation of the research done by Dobáková and coworkers who co-localized Psb28-1 with the with the RC47 assembly complex (Dobáková et al., 2009). They proposed the protein to be important for synthesis of chlorophyll and/or apoproteins of chlorophyll-binding proteins CP47 and PsaA/PsaB from PSI (Dobáková et al., 2009b). Although other studies on Psb28 proteins have been done, their precise location and function remained unclear (Dobáková et al., 2009; Sakata et al., 2013).

The main aims of my work were:

1. Localization of both proteins within photosynthetic membrane complexes.
2. Comparative study of Psb28 mutants constructed in wild-type strains with different genetic background.
3. Establishing the mutual functional relationship between both proteins.

3 Summary

The results included in the thesis are published in the four peer-reviewed articles. The first publication focuses on the subunit composition and importance of the RC47 assembly complex *in vivo*. RC47 complex is the assembly intermediate of PSII lacking CP43 (PsbC) and the complex where Psb28-1 protein has previously been localized. Due to the low abundance of RC47 complex in wild type thylakoid membranes, the CP43 (PsbC) null mutant of the cyanobacterium *Synechocystis* 6803 that accumulates RC47 complexes was used for the study. The two-dimensional analysis of its thylakoid membranes detected RC47 in complex with both Psb28 proteins and with photoprotective HliA and HliB proteins (also called ScpC and ScpD). The location of Psb28-1 and Psb28-2 in RC47 was further confirmed by analysis of His-tagged Psb28-1 and FLAG-tagged Psb28-2 preparations, respectively. Our results lead to conclusion that Psb28-1 and Psb28-2 may share the same binding site on the RC47 complex and consequently do not bind to the same monomeric RC47 complex, assuming only one binding site. Moreover, they may also compete for the same or overlapping binding site with Hlips (Scps). Our results showed that RC47 is photochemically active and proposed RC47 as a complex in which D1 is being replaced during the D1 turnover.

The second publication presents the crystal structure of the Psb28 protein (Tlr0493) from the thermophilic cyanobacterium *Thermosynechococcus elongatus* at a resolution of 2.3 Å. The *T. elongatus* Psb28 protein is the closest homolog to *Synechocystis* 6803 Psb28-1 protein and it is shown that the crystal structure of the Psb28 monomer is similar to the solution structures of C-terminally His-tagged Psb28-1 from *Synechocystis* 6803 obtained previously by nuclear magnetic resonance spectroscopy. One new aspect is that *Escherichia coli*-expressed *T. elongatus* Psb28 is able to form dimers in solution and packs as a dimer of dimers in the crystal. Analysis of thylakoid membranes from wild type and mutant strains of *Synechocystis* 6803 by blue native-polyacrylamide gel electrophoresis suggested that Psb28-1 in this strain also exists as an oligomer *in vivo*, most likely a dimer. On the other hand, the Psb28-2 homolog was detected *in vivo* only as a monomer. Overall we concluded that Psb28 proteins exist in different oligomeric states and that the dimer interface in the Psb28-1 crystal might be physiologically relevant.

The third publication calls attention to a spectrum of *Synechocystis* 6803 'wild-type' substrains with apparently different phenotypes used in photosynthetic studies in our laboratory as well as abroad. We analyzed organization of photosynthetic membrane complexes in standard motile Pasteur collection strain termed PCC and two non-motile glucose-tolerant substrains (named here GT-P and GT-W) previously used as genetic backgrounds for construction of many photosynthetic site directed mutants. The genome re-sequencing revealed tandem duplication

of a large region of the chromosome in GT-W substrain that contains 100 genes including ones encoding D1, Psb28 and other PSII-related proteins. The phenotype variability of wild types is described and discussed as well as genome mutations. We also constructed new Psb28-1-less mutants in the background of both glucose-tolerant substrains and demonstrated the difference in their chlorophyll content explaining phenotypic variability obtained for Psb28 mutant strains described in previous publications. In conclusion, our study emphasizes the crucial importance of the proper control strain for evaluating *Synechocystis* 6803 mutants.

The last article is focused on localization and function of both Psb28-1 and Psb28-2 proteins in cyanobacterium *Synechocystis* 6803. Using FLAG-tagged Psb28-2 we detected the protein in both monomeric PSII core complexes and RC47. Overall our results lead to conclusion that Psb28-2 preferentially binds to PSII monomer whereas Psb28-1 binds to RC47 complex. We also showed that exposure of cells to increased irradiance results in association of both tagged Psb28 proteins with oligomeric forms of PSII and with PSII-PSI supercomplexes that seems to be composed of trimeric Photosystem I (PSI) and two PSII monomers. The missing fluorescence of these supercomplexes, which also contain Psb27 factor, indicates not fully functional PSII accomplishing their maturation and functional activation under protection of PSI, an efficient quencher. Thus, the formation of PSII-PSI supercomplexes may be important step in the PSII biogenesis especially under high irradiance. The additional analysis of newly constructed Psb28 deletion mutants confirmed absence of the RC47 complex in the Psb28-deletion mutant and its increased level in the Psb28-2 deletion mutant. We also confirmed decreased synthesis of CP47 and PSI subunits in Psb28-1 mutant previously observed by Dobáková and coworkers (Dobáková et al., 2009). Moreover, the ΔPsb28-1/ΔPsb28-2 double mutant showed identical phenotype to the Psb28-1-less mutant suggesting the antagonistic regulatory function of both Psb28 proteins where Psb28-1 binding to RC47 could stimulate synthesis of CP47 and PSI whereas binding of Psb28-2 could outcompete Psb28-1 from the binding site limiting CP47 and PSI synthesis. This could be relevant, for instance, in the dark when expression of *psb28-1* is suppressed while that of *psb28-2* induced. We also showed that mutants lacking the Psb27 and Psb28-1, but not Psb28-2, are affected in growth under conditions of continuous and especially intermittent high light.

4 Results

Published results

4.1 Subunit composition of CP43-less photosystem II complex of *Synechocystis* sp. PCC 6803: implications for the assembly and repair of photosystem II.

Reprint of: Boehm, M., Yu, J., Reisinger, V., Beckova, M., Eichacker, L.A., Schlodder, E., Komenda, J., and Nixon, P.J., (2012). Phil. Trans. R. Soc. B 36, 3444-3454

PHILOSOPHICAL TRANSACTIONS OF THE ROYAL SOCIETY B

CrossMark click for updates

Phil. Trans. R. Soc. B (2012) **367**, 3444–3454
doi:10.1098/rstb.2012.0066

Research

Subunit composition of CP43-less photosystem II complexes of *Synechocystis* sp. PCC 6803: implications for the assembly and repair of photosystem II

M. Boehm[1], J. Yu[1], V. Reisinger[2], M. Beckova[3,4], L. A. Eichacker[2], E. Schlodder[5], J. Komenda[3,4] and P. J. Nixon[1,*]

[1]*Division of Molecular Biosciences, Imperial College London, South Kensington Campus, London SW7 2AZ, UK*
[2]*Center for Organelle Research (CORE), University of Stavanger, Kristine Bonnevis vei 22, 4036 Stavanger, Norway*
[3]*Department of Phototrophic Microorganisms, Institute of Microbiology, Academy of Sciences, 37981 Třeboň, Czech Republic*
[4]*Faculty of Science, University of South Bohemia, Branisovska 31, Ceske Budejovice, Czech Republic*
[5]*Max-Volmer Laboratory for Biophysical Chemistry, Technical University Berlin, 10623 Berlin, Germany*

Photosystem II (PSII) mutants are useful experimental tools to trap potential intermediates involved in the assembly of the oxygen-evolving PSII complex. Here, we focus on the subunit composition of the RC47 assembly complex that accumulates in a *psbC* null mutant of the cyanobacterium *Synechocystis* sp. PCC 6803 unable to make the CP43 apopolypeptide. By using native gel electrophoresis, we showed that RC47 is heterogeneous and mainly found as a monomer of 220 kDa. RC47 complexes co-purify with small Cab-like proteins (ScpC and/or ScpD) and with Psb28 and its homologue Psb28-2. Analysis of isolated His-tagged RC47 indicated the presence of D1, D2, the CP47 apopolypeptide, plus nine of the 13 low-molecular-mass (LMM) subunits found in the PSII holoenzyme, including PsbL, PsbM and PsbT, which lie at the interface between the two momomers in the dimeric holoenzyme. Not detected were the LMM subunits (PsbK, PsbZ, Psb30 and PsbJ) located in the vicinity of CP43 in the holoenzyme. The photochemical activity of isolated RC47-His complexes, including the rate of reduction of $P680^+$, was similar to that of PSII complexes lacking the Mn_4CaO_5 cluster. The implications of our results for the assembly and repair of PSII *in vivo* are discussed.

Keywords: RC47; *Synechocystis*; low-molecular-mass subunit; accessory factor; Psb28; ScpC

1. INTRODUCTION

The photosystem II (PSII) complex is the light-driven water : plastoquinone oxidoreductase of oxygenic photosynthesis, located in the thylakoid membranes of cyanobacteria and chloroplasts [1]. The recent X-ray crystal structures of dimeric PSII complexes isolated from thermophilic cyanobacteria, at resolutions of 3.5 Å [2], 3.0 Å [3], 2.9 Å [4] and 1.9 Å [5], have provided remarkable insights into the organization of the proteins and cofactors within the oxygen-evolving holoenzyme. However, the molecular details of PSII assembly remain largely unknown. Recent work has led to the proposal that PSII is assembled in a stepwise manner from smaller sub-complexes or modules consisting of a large chlorophyll (Chl)-binding protein (D1, D2, CP43 or CP47) and one or more low-molecular-mass (LMM) subunits plus bound pigment [6]. According to this model, a PSII reaction centre (RC) complex is assembled from PsbI/precursor D1 [7] and cytochrome (cyt) *b*-559/D2 [8] sub-complexes. Attachment of the CP47 sub-complex [9] results in formation of an assembly intermediate called the RC47 assembly complex [8], which then binds the CP43 sub-complex [9] to form the monomeric PSII core complex. At this stage, the oxygen-evolving Mn_4CaO_5 cluster is able to assemble in a light-driven process, the lumenal extrinsic proteins (PsbO, PsbU and PsbV) are attached and PSII can dimerize. A number of auxiliary factors have also been identified that are important for assisting/regulating assembly [10–12].

PSII is also a weak link in photosynthesis and is vulnerable to irreversible damage by visible light *in vivo*, leading to so-called chronic photoinhibition [13]. Damaged PSII can, however, be repaired through the

* Author for correspondence (p.nixon@imperial.ac.uk).

Electronic supplementary material is available at http://dx.doi.org/10.1098/rstb.2012.0066 or via http://rstb.royalsocietypublishing.org.

One contribution of 16 to a Theo Murphy Meeting Issue 'The plant thylakoid membrane: structure, organization, assembly and dynamic response to the environment'.

operation of a 'PSII repair cycle' in which the damaged protein subunit, mainly the D1 subunit, is selectively replaced by a newly synthesized subunit and PSII reactivated [12]. Current models suggest that following damage, dimeric PSII partially disassembles and damaged D1 is removed from a monomeric PSII sub-complex lacking the lumenal extrinsic proteins and the CP43 complex [14–16]. Once damaged D1 has been replaced, active dimeric PSII complexes are reassembled following reattachment of CP43 and the extrinsic subunits.

A PSII core complex lacking CP43, often referred to as the RC47 complex in cyanobacteria [8], or sometimes the CP43-less core monomer in chloroplasts [17], can be detected in mildly solubilized thylakoid membrane extracts by blue native–polyacrylamide gel electrophoresis (BN–PAGE). Increased amounts of RC47 are found in mutants with impaired binding of CP43, such as ΔPsbI [18] and ΔPsbK [10], and in strains with impaired PSII repair [19,20]. The 'RC47 complex' detected in thylakoid membranes by BN–PAGE is, however, potentially heterogeneous, as CP43-less PSII core complexes are formed in both the PSII repair cycle and during de novo assembly.

A major impediment to isolation and detailed characterization of the RC47 assembly complex is its low abundance in the thylakoid membrane and potential contamination by RC47 complexes generated from disassembly of PSII during repair or during sample preparation. It is, however, likely that the RC47 assembly complex is very similar in composition to the non-oxygen-evolving PSII sub-complex that accumulates in mutant strains unable to synthesize the CP43 subunit [21]. Despite only being expressed at 10 per cent of wild-type (WT) levels, Rögner *et al.* [22] were able to purify CP43-less PSII complexes from a *psbC* deletion mutant of *Synechocystis* 6803, using first an anion exchange and then a hydroxyapatite chromatography step. They showed that the isolated complex was monomeric and was inactive in oxygen evolution, but was still able to catalyse light-driven electron transfer from tyrosine Y_z to the primary quinone electron acceptor, Q_A [22].

Here, we have extended the pioneering studies of Rögner *et al.* [22] to include a detailed assessment of the oligomerization state and subunit composition of the RC47 assembly complex *in vivo*. In addition, we have used a His-tagging approach to isolate the RC47 assembly complex to permit analysis of its subunit composition and photochemical activity. The implications of our results for the assembly and repair of PSII *in vivo* are discussed in light of the recent advances in our understanding of the structure of the cyanobacterial PSII holoenzyme.

2. MATERIAL AND METHODS

(a) *Cyanobacterial strains and growth conditions*

The glucose-tolerant strain of *Synechocystis* sp. PCC 6803 [23] and the previously constructed ΔCP43 [21] and His-tagged CP47 (PSII-His) strains [9] were used in this work. Strains were grown in liquid BG-11 mineral medium and maintained on solid BG-11 plates containing 1.5 per cent (w/v) agar, both containing 5 mM *N*-tris (hydroxymethyl)methyl-2-aminoethanesulfonic acid–KOH, pH 8.2, at a light intensity of 40 or 5 $\mu E\ m^{-2}\ s^{-1}$ of white fluorescent light, respectively and at 29°C. The medium was supplemented with 5 mM glucose and where applicable, kanamycin (50 $\mu g\ ml^{-1}$) or erythromycin (10 $\mu g\ ml^{-1}$) was added.

(b) *Construction of mutants*

To generate a *Synechocystis* sp. PCC 6803 mutant strain that contained His-tagged PSII lacking CP43 (strain ΔCP43/CP47-His), the CP47 protein was His-tagged, and the CP43 protein was inactivated by partial deletion of the *psbC* gene and replacement by a kanamycin-resistance cassette. To His-tag the CP47 protein, the gentamycin-resistance cassette of the pCP47His-tagGm^R plasmid [24] was removed by *Bam*HI digestion and, after blunting the ends, an erythromycin-resistance cassette was introduced to generate pCP47His-Ery^R. This plasmid was transformed into the *Synechocystis* sp. PCC 6803 glucose-tolerant strain to generate the PSII-His mutant. To inactivate the CP43 protein, the *psbC* gene was amplified by PCR with the following primers: CP43 + 1000-Fw, 5′-ATATTTTCCCCTTCTTCGTAGGGGTGC-3′ and CP43 + 1000-Rev, 5′-CTGCCATTAAAGAAT TGGCTAAAGAAGCAGGTC-3′. After ligation into the pGEMTeasy vector (Promega, UK), a kanamycin-resistance cassette was introduced between the *Hin*dIII and *Sma*I sites located between 767 bp and 1228 bp, respectively, downstream of the start codon annotated in CyanoBase. This plasmid was transformed into the CP47His mutant to yield the CP47-His/ΔPsbC strain. The genotypes of the mutants were verified by PCR analysis, using gene-specific primers.

Plasmid pPsbAIpetJ-FLAG was used for construction of the strain expressing FLAG-tagged Psb28-2 under the control of the copper-regulated *petJ* promoter at the *psbAI* locus. It was constructed as follows: a 600-bp *Xba*I-*Cfr*9I fragment upstream and a 600-bp *Bgl*II–*Xma*jI fragment downstream of the *psbAI* gene were amplified by PCR and cloned into pETBlue-2 plasmid (Novagen). The *petJ* promoter from *Synechocystis* sp. PCC 6803 (positions 846 614–846 331 according to CyanoBase) and 3xFLAG sequence (Sigma) were amplified by PCR, ligated and again amplified by PCR for cloning between the *psbAI* fragments. Finally, the kanamycin-resistance gene (*aphX*) from pUC4K, amplified as a *Bam*HI-*Bgl*II fragment, was cloned into the *Bgl*II site upstream of the second *psbAI* fragment leaving a single *Bgl*II site for cloning of *psb28-2*.

To clone FLAG-tagged Psb28-2 into the integration plasmid, the *psb28-2* (*slr1739*) gene was amplified by PCR using the following primers: *Not*I + *slr1739*-Fw, 5′-CCGGTGGCGGCCGCAATGACCCTCACTC CC-3′ and *slr1739* + *Bgl*II-Rev, 5′-AACTTTAGATC TCTAACGATCTTGGTAG-3′. After *Not*I and *Bgl*II digestion and ligation into the plasmid, the construct was transferred into the ΔPsb28-2 deletion mutant. This mutant was previously constructed by replacement of the *psb28-2* gene by a chloramphenicol-resistance cassette. Segregation in the *psbAI* locus was confirmed by PCR analysis, using gene-specific primers. To induce expression of the FLAG-tagged Psb28-2

protein, the strain was cultivated in BG-11 medium with 5 mM glucose lacking $CuSO_4$.

(c) *Isolation of protein complexes*

The RC47-His protein complex was purified by Ni^{2+}-affinity chromatography as described for the CP43-His and CP47-His proteins [9]. However, the fractions eluted with 50 and 100 mM imidazole were concentrated using 100 kDa molecular weight cut-off (MWCO) protein concentrators (Sartorius, UK). As a second purification step, the concentrated affinity-purified sample was diluted 10 times with KPN buffer (40 mM K-phosphate, pH 8.0, 100 mM NaCl) containing 0.04 per cent (w/v) *n*-dodecyl-β-D-maltoside (β-DM) and loaded onto a column packed with Toyopearl 650S DEAE anion-exchange chromatography resin (Anachem, UK). Chromatography was performed at a flow rate of 0.5 ml min^{-1} and with KPN buffer containing 0.04 per cent (w/v) β-DM as the running buffer. Initially, for the first 10 min, the running buffer also contained 5 mM $MgSO_4$ and over the next 50 min, the concentration of $MgSO_4$ was raised linearly to 200 mM. The run was monitored at 280 nm using a Jasco MD-2015 plus diode array detector (Jasco, UK) and 0.5-ml fractions were collected by a Frac-920 fraction collector (GE Healthcare, UK). Selected fractions were pooled, supplemented with 10 per cent (v/v) glycerol and concentrated using 100-kDa MWCO protein concentrators (Sartorius, UK).

His-tagged oxygen-evolving and non-oxygen-evolving PSII complexes were isolated from the PSII-His strain, using the methods described by Service *et al.* [25] and Boehm *et al.* [9], respectively.

For isolation of Flag-tagged Psb28-2, membranes were solubilized in KPN buffer containing 1 per cent β-DM, and the supernatant was loaded onto a column containing 300 µl of anti-FLAG M2 affinity gel (Sigma, USA), pre-equilibrated with KPN buffer containing 0.04 per cent β-DM (KPN–DDM). To remove any loosely bound contaminants, the column was first washed with 5 ml of KPN–DDM and then the FLAG-Psb28-2 was eluted by a 30 min incubation of resin in 200 µl of KPN-DDM containing 20 per cent glycerol and 150 µl ml^{-1} 3xFLAG peptide (Sigma, USA). Resin was removed by centrifugation at 500*g* for 5 min. His-tagged Psb28 was isolated as described in Dobakova *et al.* [26].

(d) *Protein analysis*

The Chl *a* content of samples was determined by extraction into methanol and absorption measurements at 666 and 750 nm [16]. Protein samples were analysed by BN– and SDS–PAGE, according to Boehm *et al.* [27]. Unless stated otherwise, 6–12% (w/v) polyacrylamide (PAA) BN–PAGE and 18% (w/v) PAA SDS–PAGE gels containing 6 M urea were used. Alternatively, a combination of 4–14% (w/v) PAA clear native (CN) and 12–20% (w/v) PAA SDS–PAGE containing 7 M urea was used for analysis of membrane protein complexes, as described in Komenda *et al.* [10]. The resulting gels were stained with either Coomassie blue or silver or Sypro Orange or electro-blotted onto PVDF membrane using the iBlot system (Invitrogen, UK), according to the manufacturer's instructions. Immunoblotting analyses were conducted using specific primary antibodies and a horseradish peroxidase-conjugated secondary antibody (GE Healthcare). Signals were visualized using a chemiluminescent kit (SuperSignal West Pico, Pierce, USA). Primary antibodies used in this study were: (i) αD1, αD2, αCP43 and αCP47 [9]; (ii) αHis-tag (Invitrogen); (iii) αPsbH (raised against the whole PsbH protein from *Synechocystis* 6803); (iv) αPsb28 [26]; (v) αPsb28-2 (raised against peptide 40–53 of the Psb28-2 protein from *Synechocystis* 6803); (vi) αPsb28 (raised against Psb28 of *Thermosynechococcus elongatus*); and (vii) αScpC/D [28]. Cells were pulse-labelled for 20 min at 29°C and at a light intensity of 500 µE m^{-2} s^{-1} as described in Komenda *et al.* [10].

(e) *Low-temperature absorption spectroscopy*

Spectra were recorded at a resolution of 0.5 or 1 nm in a Cary-1E-UV/vis spectrophotometer (Varian) equipped with a liquid nitrogen bath cryostat (DN 1704 from Oxford). The purified protein complexes were diluted to an optical density (OD) of approximately 1 at the maximum in the Q_Y-region in buffer (10 mM MES pH 6.5, 10 mM $CaCl_2$, 10 mM $MgCl_2$, 0.02% β-DM and 60–65% glycerol).

(f) *Detection of cyt* b*-559*

Isolated RC47-His complexes containing 10 µg of Chl *a* were diluted into 500 µl of KPN buffer containing 1 µM potassium ferricyanide, and a baseline was run for the sample between 520 and 600 nm (UV-1601, Shimadzu, UK). After the addition of a few grains of sodium dithionite to the sample, the reduced-minus-oxidized absorbance spectrum was recorded.

(g) *Transient absorbance spectroscopy*

Laser-flash-induced absorbance changes (ΔA) at 830 nm owing to the formation of the Chl radical cation $P680^+$ were measured as described previously [29], using a continuous wave laser diode (Hitachi HL 8318G) as the measuring light source. The samples were excited by non-saturating laser flashes at 532 nm with a pulse duration of 3 ns (Nd-YAG laser YG411 from Quantel). For measurements in the nanosecond range, the detection system (photodiode FND-100 from EG and G; amplifier IV86 from HMI; transient recorder Tektronix TDS 540B, sampling rate 2 GS s^{-1}) had an electrical bandwidth of 500 Hz–200 MHz. In the micro- and millisecond range, a HVA-10M-60-F amplifier from FEMTO was used. The decay kinetics were analysed by a sum of exponential decay components minimizing the sum of squares of the weighted residuals.

(h) *Mass spectrometry*

Mass spectrometry of LMM proteins was performed as described by Granvogl *et al.* [30]. For offline electrospray ionization mass spectrometry (ESI-MS), 20 µl of anion-exchange-purified RC47-His protein complex was precipitated in 80 per cent (v/v) acetone at −20°C overnight. After centrifugation for 20 min at

13 000*g* in a microfuge, the supernatant was discarded and the air-dried pellet dissolved in a solution containing 70 per cent (v/v) acetone, 10 per cent (v/v) 2-propanol and 1 per cent (v/v) formic acid. The sample was then directly applied to a nano spray emitter and mass spectra were obtained using a Waters Q-TOF premier equipped with a nanoESI source. For scanning the LMM proteins, MS spectra at the mass range of 800–2500 *m*/*z* were acquired, and data were recorded at a capillary voltage of 0.8 kV and a cone voltage of 37 V. After MS data collection at a rate of 1 s per scan, 30 scans were averaged. The acquisition of fragment ion spectra was performed at a collision energy between 26 and 40 eV, and data were analysed by the MassLynx/BioLynx v. 4.1 software. Sequence tags obtained from the fragment spectra were used for similarity search (www.ebi.ac.uk/Tools/fasta33), and the sample was analysed in several repetitions.

3. RESULTS

(a) *Characterization of the RC47 assembly complex in a* Synechocystis *strain lacking CP43*

To assess the oligomeric status of the RC47 assembly complex *in vivo*, we carried out a two-dimensional protein gel analysis of solubilized thylakoids isolated from radiolabelled cells of a *psbC* deletion mutant, ΔCP43, unable to synthesize CP43 [8,22]. Protein complexes were resolved by clear-native gel electrophoresis in the first dimension, then by denaturing gel electrophoresis in the second dimension (figure 1). Immunochemical detection of PSII subunits indicated that the RC47 assembly complex was present mainly as the monomer (of size approx. 220 kDa), but that trace amounts of a larger complex, most probably the dimer, were also present (figure 1; RC47(2)). Smearing of the monomeric RC47 band suggested some heterogeneity in composition. Some unassembled CP47 was also observed in the LMM region. Newly synthesized, radiolabelled D1 protein was exclusively detected in the RC47 complex (figure 1, autoradiogram). The high degree of labelling of D1 in comparison with other PSII proteins is consistent with extremely fast turnover of D1 in the RC47 complex (see also Komenda *et al.* [19]).

Dobakova *et al.* [26] have previously shown that Psb28 (Sll1398), an accessory protein of PSII not found in the crystallized holoenzyme, is able to associate with the RC47 complex *in vivo*. In line with this conclusion, we were also able to detect Psb28 in the RC47 assembly complex in the ΔCP43 mutant, although most Psb28 was found unassembled (figure 1). The genome of *Synechocystis* also contains a gene coding for a second Psb28 homologue termed Psb28-2 (Slr1739). Using specific anti-peptide antibodies, we detected a small amount of Psb28-2 protein co-migrating with the RC47 complex (figure 1, lower panel, blots). To obtain stronger support for a specific association between Psb28-2 and RC47, we conducted pull-down experiments using a strain of WT *Synechocystis* 6803 expressing FLAG-tagged Psb28-2 and were able to affinity-purify RC47 complexes (figure 2). The two RC47 bands separated by native PAGE reflect release of FLAG-tagged Psb28-2 either during electrophoresis or during the isolation procedure (data not shown). Using

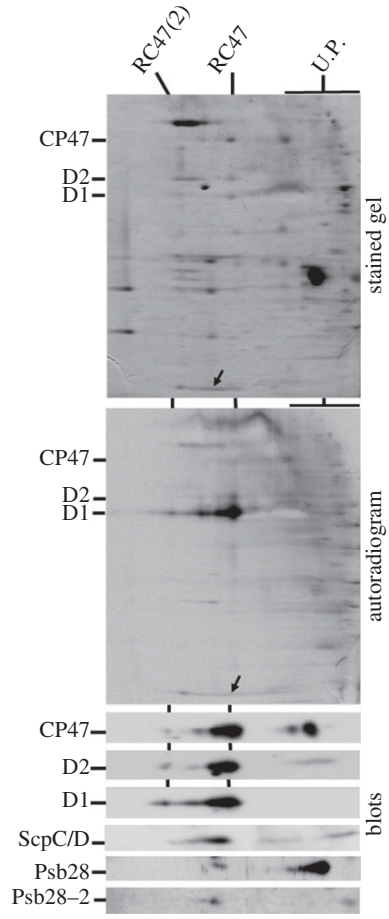

Figure 1. Two-dimensional analysis of thylakoid membranes isolated from the radioactively labelled ΔCP43 *Synechocystis* strain. Thylakoid membranes corresponding to an amount of 4 μg Chl *a* were separated on a 4–14% (w/v) polyacrylamide (PAA) CN-PAGE linear gradient gel, and another 12–20% (w/v) PAA SDS–PAGE gel was used for the second dimension. The gels were stained with Sypro Orange (stained gel), then blotted onto PVDF membrane and sequentially probed with antibodies against indicated proteins (blots). Dried membrane was then used for autoradiography (autoradiogram). The positions of monomeric RC47 and dimeric RC47 (RC47(2)) are indicated. U.P. are unassembled proteins; arrows indicate location of the ScpC/D proteins on the gel and autoradiogram.

a similar approach, RC47 complexes could also be affinity-purified using His-tagged Psb28 (figure 2; see also [26]). In this case, the three bands observed by native electrophoresis appear to reflect the presence or absence of His-tagged Psb28 (data not shown).

Upon exposure to high irradiances (500 μE m^{-2} s^{-1}), the ScpC/D subunits, which are small Cab-like proteins possibly involved in transient binding of pigments [31], have also been detected in the RC47 complex found in WT samples, both by radioactive labelling and by immunodetection [28,32]. Interestingly, in contrast to WT [32], there was no detectable radioactive labelling of these bands in the ΔCP43 mutant (figure 1, upper and middle panels, arrows), indicating that the ScpC/D proteins were either not synthesized under the radiolabelling conditions used or had already preaccumulated in the complex even at a low irradiance of

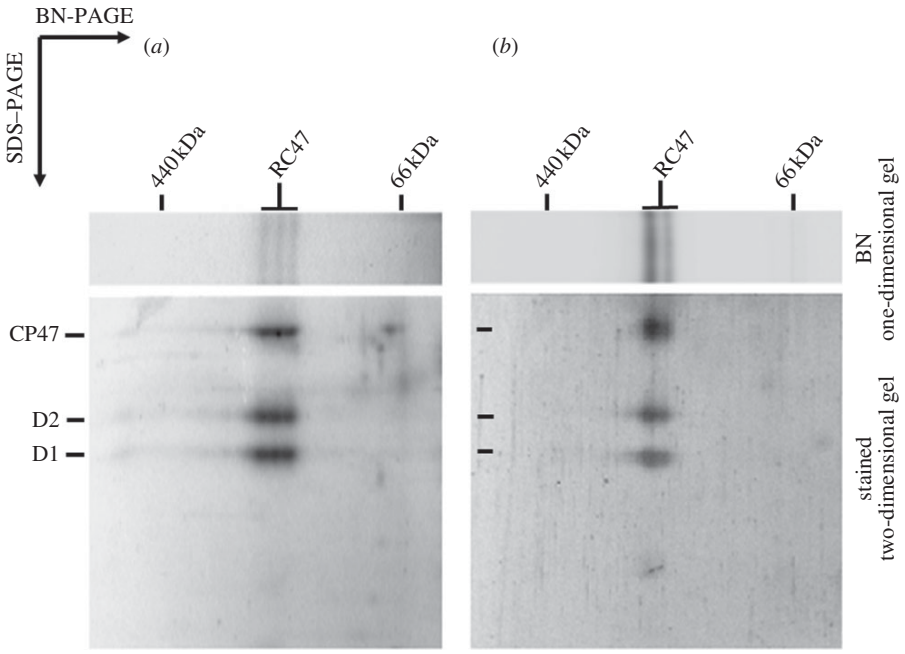

Figure 2. Two-dimensional analysis of RC47 complexes isolated from thylakoid membranes of *Synechocystis* strains expressing (*a*) His-tagged Psb28 or (*b*) FLAG-tagged Psb28-2. Complexes corresponding to an amount of 1 µg Chl *a* were separated on a 4–14% (w/v) polyacrylamide (PAA) CN–PAGE linear gradient gel, and another 12–20% (w/v) PAA SDS–PAGE gel was used for the second dimension. The gels were stained with Sypro Orange. The position of the monomeric RC47 is indicated.

40 µE m^{-2} s^{-1}. The latter alternative was supported by immunoblot analysis using an antibody specific for SpcC/D (figure 1, blots) and further confirmed by detection of ScpC/D in the same cells that were not radioactively labelled and thus not treated for short times at high irradiance (data not shown).

Rögner *et al.* [22] have estimated that the RC47 complex in ΔCP43 accumulates to about 10 per cent of the level of PSII core complexes found in WT. However, when we grew the ΔCP43 strain at low irradiance (5 µE m^{-2} s^{-1}), the cellular content of the RC47 complex strongly decreased, reaching a level hardly detectable by protein staining (see the electronic supplementary material, figure S1). Semi-quantitative immunoblotting, using antibodies against D1, suggested that the amount of RC47 was less than 10 per cent of the level found in the strain grown under our standard growth conditions (40 µE m^{-2} s^{-1}; electronic supplementary material, figure S1). These data showed that the accumulation of the RC47 complex in the ΔCP43 strain was strongly irradiance-dependent. This effect was specific for the RC47 complex as the amount of PSII core complexes in WT cells cultivated under identical conditions did not change significantly with varying irradiance (see the electronic supplementary material, figure S1). In addition, there was a noticeable decrease in phycobilin content in low-light-grown cells of ΔCP43 in comparison with cells grown under standard conditions (see the electronic supplementary material, figure S2).

(b) *Isolation of the RC47-His complex from* Synechocystis *sp. PCC 6803*

To perform a more detailed characterization of the RC47 assembly complex, we isolated a His-tagged RC47 complex from a strain of *Synechocystis* 6803 (ΔCP43/CP47-His) in which a His_6-tag was added to the C-terminus of CP47 and the *psbC* gene encoding CP43 was inactivated (see §2). Previous work has shown that a C-terminal His-tag on CP47 does not prevent assembly of a functional PSII complex [33,34]. In agreement with results obtained with the non-tagged strain under standard growth conditions, the level of expression of the RC47-His complex was approximately 10 per cent of the levels of PSII in WT as deduced by two-dimensional BN–PAGE and was mainly present as a monomer of size approximately 220 kDa (data not shown). Despite the relatively low levels of expression, the RC47-His complex could be purified from detergent-solubilized thylakoid membranes by immobilized Ni-affinity chromatography (see the electronic supplementary material, figure S3*a*). Some residual contaminating proteins were removed by a subsequent anion-exchange chromatography step (see the electronic supplementary material, figure S3*b*). BN–PAGE revealed that the final RC47-His complex was largely monodisperse with a size of 220 kDa (see the electronic supplementary material, figure S3*c*).

The 77K absorption spectra of the RC47-His complex and a control non-oxygen-evolving His-tagged PSII complex (PSII-His) are shown in figure 3. The main qualitative difference between the two spectra is a relative reduction in the RC47-His complex of the intensity of the absorption band at 435 nm (Soret transition of Chl *a*) indicative of the presence of less Chl *a* in the complex, as observed previously [22].

(c) *Subunit composition*

Analysis of the RC47-His complex and control oxygen-evolving (active) and non-oxygen-evolving (inactive)

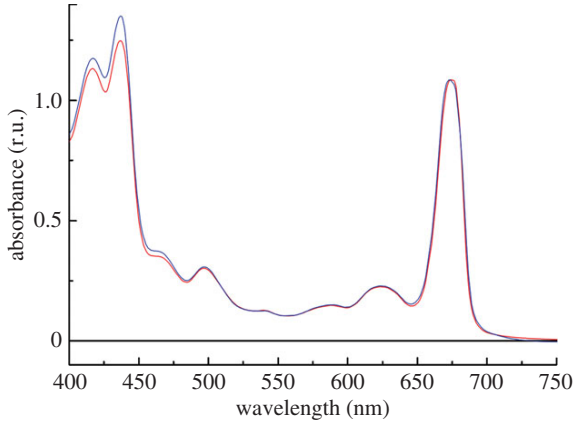

Figure 3. 77K absorption spectra of the RC47-His and PSII-His protein complexes isolated from *Synechocystis* sp. PCC 6803. Red, RC47-His; blue, PSII-His.

PSII-His complexes by SDS–PAGE is shown in figure 4*a*. The presence of the CP47, D1, D2 and PsbH subunits in the RC47-His complex and the absence of CP43 and PsbO was confirmed by immunoblotting (figure 4*b*). Immunoblotting using antibodies raised to Psb28 from *T. elongatus* indicated that the major 13-kDa Coomassie-blue-stained band present in RC47-His contained Psb28 (figure 4*b*). Mass spectrometry confirmed the presence of both Psb28 and Psb28-2 in this band in line with the results presented in figure 1 (data not shown). The presence of low amounts of Psb28 in the inactive PSII-His complexes might reflect some contamination by RC47-His which co-purifies.

Each cyanobacterial PSII monomer in the crystallized PSII dimeric complex contains 12–13 LMM subunits, depending on the preparation. Two of these subunits, PsbE and PsbF, are the apopolypeptides of cyt *b*-559, which we could detect in the RC47-His complex by reduced-minus-oxidized difference spectroscopy (see the electronic supplementary material, figure S3*d*). Mass spectrometry unambiguously identified a further 7 LMM subunits in the isolated RC47-His complex (see the electronic supplementary material, figure S4 and table 1), including PsbT, PsbM and PsbL, which in the dimeric complex lie at the interface between the two monomeric complexes.

(d) *Electron transfer in the RC47-His complex*

Although oxidation of tyrosine, Yz, has been demonstrated in the RC47 complex [22], the kinetics of electron transfer on the donor side of the complex have not been examined. The rate of reduction of $P680^+$ was followed by measuring the change in absorbance at 830 nm following flash excitation (figure 5). In the case of oxygen-evolving PSII-His, the rate of $P680^+$ reduction occurred with multi-exponential kinetics (data not shown) with the fastest phase occurring on the nano-second timescale, in line with results in the literature [35]. Both the RC47-His and the non-oxygen-evolving PSII-His complexes displayed similar but much slower rates of $P680^+$ reduction, on the microsecond time-scale, with time constants as previously reported for non-oxygen-evolving PSII [36].

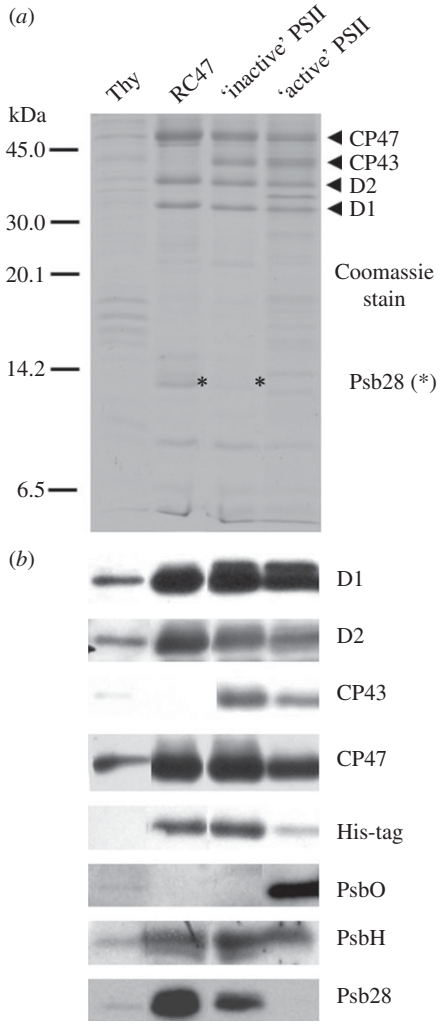

Figure 4. SDS–PAGE and immunoblotting analysis of the RC47-His and PSII-His complexes isolated from *Synechocystis* sp. PCC 6803. (*a*) Coomassie-stained 18% (w/v) PAA SDS–PAGE gel and (*b*) immunoblotting analyses with indicated antibodies. Thylakoid membranes (0.5 µg Chl *a*), the RC47-His protein complex (1 µg Chl *a*) and non-oxygen-evolving (inactive) as well as oxygen-evolving (active) PSII core complexes (1 µg Chl *a* each) were loaded on the gels.

The $P680^+Q_A^-$–$P680Q_A$ difference spectra of RC47-His and PSII-His complexes were also recorded at 77 K (data not shown). They did not show significant differences, indicating the intactness of the reaction centre in the RC47-His complex. When normalized on an equal RC basis, assuming 35 Chl/PSII-His and 22 Chl/RC47-His, the amount of $P680^+$ formed following flash excitation was within 15 per cent of each other, indicative of similar charge separation activity. As expected from previous studies, there was no evidence for retention of a functional Mn_4CaO_5 cluster or the secondary quinone electron acceptor, Q_B, in the RC47-His complex [22].

Light-minus-dark difference spectra were determined in RC47-His and PSII-His at 77 K to analyse the oxidation of secondary, side-path electron donors (cyt *b*-559, chlorophyll Z and β-carotene) that function in PSII at a low temperature (figure 6). The difference spectra were obtained by subtracting the

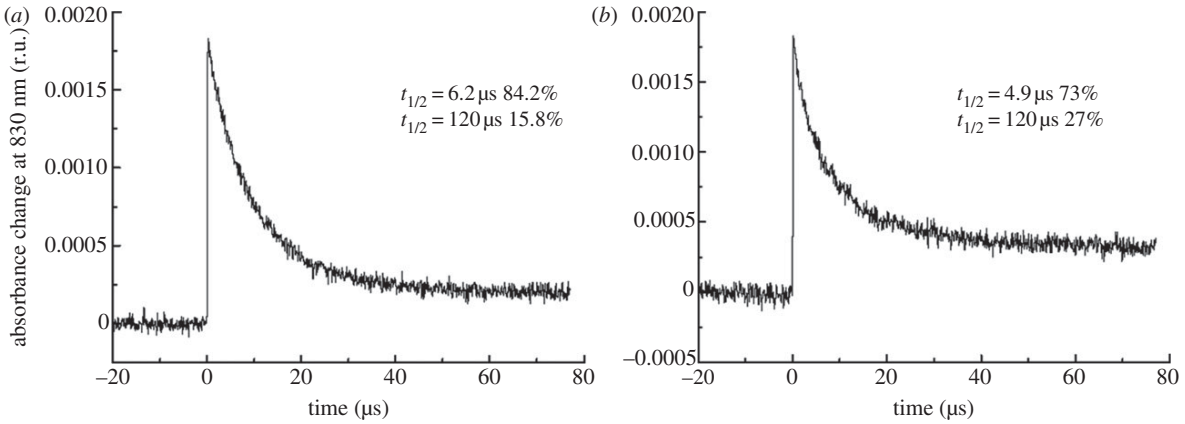

Figure 5. Kinetics of $P680^+$ reduction. Laser-flash-induced absorbance changes (ΔA) at 830 nm due to the formation of the Chl radical cation $P680^+$ in (*a*) RC47-His and (*b*) non-oxygen-evolving PSII-His complexes were monitored. The decay kinetics were fitted to a sum of exponential decay components minimizing the sum of squares of the weighted residuals.

Table 1. Detection of low-molecular-mass proteins in the RC47-His complex by mass spectrometry. SU, subunit. Accession number according to the UniProt database (http://www.uniprot.org/).

PSII SU	accession no.	detected signals (charge state)	de novo sequenced protein fragment	sequence coverage (%)
PsbF	P09191	1200.67 $[M + 4H]^{4+}$	VFFVGAIAAMQFIQR	34
PsbH	P14835	1168.22 $[M + 6H]^{6+}$	PVMGVFMALFL	17
PsbI	Q54697	867.41 $[M + 5H]^{5+}$	FISLFIFGFLS	66
		874.99 $[M + 5H]^{5+}$	YVVGLFISLFIFGFLSSD	
		1083.76 $[M + 4H]^{4+}$	TLKIAVYIVVGLFISLFIFGFLS	
		1087.77 $[M + 4H]^{4+}$	YIVVGLFISL	
		1093.25 $[M + 4H]^{4+}$	LKIAVYIVVGLFISLFIFG	
PsbL	Q55354	1118.61 $[M + 4H]^{4+}$	YLGLLLVAVLGILFSSYF	46
		1122.52 $[M + 4H]^{4+}$	YLGLLLVAVLGILF	
		1124.01 $[M + 4H]^{4+}$	LLVAVLGIL	
		1128.03 $[M + 4H]^{4+}$	LLVAVLGIL	
PsbM	P72701	1310.68 $[M + 3H]^{3+}$	VNNLGFIASIL	46
		1316.31 $[M + 3H]^{3+}$	VNNLGFIASILFVLVP	
PsbT	P74787	892.43 $[M + 4H]^{4+}$	LVLTMALAVL	68
		897.88 $[M + 4H]^{4+}$	SVAYILVLTMALAVLFFAI	
		899.41 $[M + 5H]^{5+}$	LVLTMALAVL	
		902.17 $[M + 4H]^{4+}$	ALAVLFFAI	
		1189.42 $[M + 3H]^{3+}$	MESVAYILVLTMALAVLF	
		1194.92 $[M + 3H]^{3+}$	MESVAYILVLTMALA	
PsbX	P72575	1053.87 $[M + 4H]^{4+}$	LGAAIVLIPAT	72
		1059.19 $[M + 4H]^{4+}$	LWSLVLGAAIVLIPATVGLIFISQKDKI	
		1063.27 $[M + 4H]^{4+}$	SLVLGAAIVLIPAT	
		1067.26 $[M + 4H]^{4+}$	LGAAIVLI	
PsbY	P73676	1057.82 $[M + 4H]^{4+}$	RVIVVVSPLLIAATWAAINIG	54

absorbance spectrum in the dark-adapted state from that after illumination with continuous white light for about 60 s. The difference spectra exhibit the characteristic band shift centred at 543 nm (C550) owing to the reduction of Q_A. An absorbance decrease at 557 nm due to light-induced oxidation of cyt *b*-559 at low temperature was not observed. Most likely cyt *b*-559 is already in the oxidized state before freezing. The remaining absorbance changes are consistent with the oxidation of chlorophyll Z (Chl_Z) and/or β-carotene (Car). The observed band shift in the Q_Y-region can be assigned to a blue shift of the site energy of the accessory Chl coordinated by D1 (Chl_{D1}) caused by Car^+ and Chl_Z^+ on the D2 side [37]. The additional bleaching band around 668 nm has been attributed to the oxidation of Chl_Z [37]. The features in the wavelength region between 460 and 510 nm indicate most likely the oxidation of Car that is oxidized directly by $P680^+$. Subsequently, Car^+ oxidizes cyt *b*-559 or Chl_Z if the cytochrome is preoxidized [38].

4. DISCUSSION

We describe here further characterization of the RC47 assembly complex found in a ΔCP43 mutant blocked at a late stage in PSII assembly. Early work showed that the ΔCP43 mutant is unable to evolve oxygen in cells [21,22]. With hindsight, this effect is most likely due to the important role that CP43 plays in providing

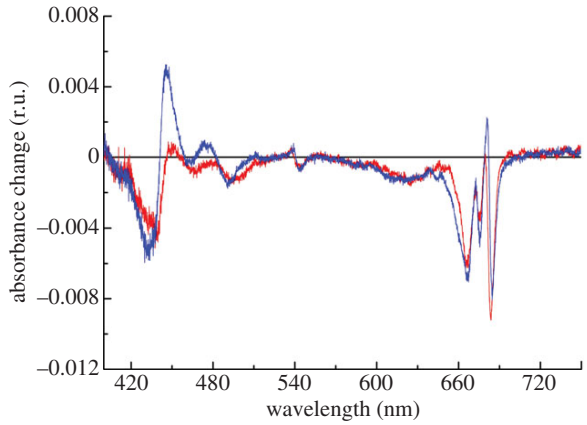

Figure 6. Light-minus-dark absorption spectrum at 78K induced by illumination of RC47-His and non-oxygen-evolving PSII-His complexes. The purified protein complexes were diluted to an OD of approximately 1 at the maximum in the Q_Y-region and illuminated for approximately 1 min. Red, RC47-His; blue, PSII-His.

one of the amino-acid ligands to the Mn_4CaO_5 cluster [2] and the general destabilization of the cluster and the lumenal side of the complex that results in the absence of CP43. In addition, loss of CP43 also seems to impair electron transfer on the acceptor side of the PSII complex in cells [22], possibly by perturbing the conformation of the Q_B-binding pocket [39].

Although incapable of oxidizing water, the isolated RC47 complex is able to photoreduce Q_A and photo-oxidize tyrosine Yz [22]. The kinetic experiments reported here on a His-tagged RC47 complex indicate that the rate of oxidation of Yz is equivalent to that seen in non-oxygen-evolving core complexes lacking the Mn_4CaO_5 cluster (figure 5), which suggests that the additional removal of CP43 has little impact on the local structure of PSII around $P680^+$ and Yz. Consistent with this, previous measurements of the rate of charge recombination in isolated complexes suggested that loss of CP43 had only minor effects on the free energy difference between the Q_A/Q_A^- and $Y_Z^\bullet/Y_Z$ redox couples [22].

Many early attempts to isolate the RC47 complex for spectroscopic studies have relied on the stripping of CP43 from larger PSII core complexes, using chaotropic salts or detergents. However, the harsh extraction conditions used sometimes led to loss of Q_A [40–45] as well as removal of some pigment and LMM subunits [45]. Isolating the RC47 complex from mutants lacking CP43 helps overcome these potential problems [22].

By isolating the RC47-His assembly complex, we have been able to examine by mass spectrometry which of the LMM subunits of PSII are able to bind to the RC47 complex in the absence of CP43. As anticipated, the PsbZ, PsbK and Psb30 subunits, which bind to CP43 in the crystal structures and which are found in CP43 assembly sub-complexes [9,10], were not detected in RC47-His. The PsbJ subunit, which is located close to PsbK and Psb30 in the holoenzyme but not yet found in the CP43 sub-complex, was also not detected in RC47. These data are consistent with weaker binding of PsbJ to PSII in the absence of the CP43 sub-complex. As expected, all the LMM subunits intimately associated with the D1, D2 and CP47 subunits in the crystal structures (i.e. PsbI, PsbX, PsbE, PsbF, PsbY and PsbH) were identified. Interestingly all three LMM subunits—PsbT, PsbM and PsbL—that lie at the interface between the two monomeric complexes in the dimer were also present, despite the fact that the RC47-His was predominantly found in a monomeric form. These three subunits are considered important but not crucial for formation and stabilization of the dimeric form of the complex [46]. Presumably, additional monomer–monomer interactions, possibly involving lipid molecules [47] and the luminal extrinsic proteins [48], contribute strongly to stabilization of the dimer.

Our results therefore suggest that during disassembly of damaged PSII to form the damaged RC47 complex, CP43 might be detached in the form of a CP43 sub-complex consisting of CP43 and the LMM subunits PsbK, PsbZ and Psb30 [9,10]. The Psb27 subunit might also bind to the lumenally exposed region of disassembled CP43 [10]. All the remaining LMM subunits, apart from possibly PsbJ, may remain tightly bound to the damaged RC47 complex stabilizing bound pigment in those subunits that are undamaged and to be recycled.

The isolated RC47-His complex also contained the Psb28 accessory factor in agreement with earlier conclusions [26]. A binding site for Psb28 on the cytoplasmic side of CP47 close to PsbH has been suggested based on the ability of His-tagged Psb28 to pull-down unassembled CP47 and the reduction in Psb28 levels in a mutant lacking PsbH [26]. Although Psb28 is mainly associated with the RC47 complex in *Synechocystis* 6803, Psb28 can interact with larger monomeric WT complexes [26] and has recently been found in isolated core complexes containing Psb27 but lacking a fully functional Mn_4CaO_5 cluster [49,50]. The role of Psb28 is currently unknown, but on the basis of phenotype of a null mutant of *Synechocystis* 6803, it might regulate chlorophyll availability during the biogenesis of PSI and PSII [26]. We show here that a second Psb28 homologue, Psb28-2, also associates with RC47 (figure 2). Our current model is that Psb28 and Psb28-2 compete for the same binding site on RC47 and consequently do not bind to the same monomeric RC47 complex, assuming only one binding site. The reason for two Psb28 homologues in *Synechocystis* is unclear especially when many cyanobacteria have just one.

We have also detected the presence of ScpC and/or ScpD in the RC47 complex in accord with previous studies on high-light-treated WT cells [28,32]. Recent work has shown that binding of Scps to PSII is important for preventing the production of singlet oxygen most probably generated by chlorophyll molecules that are accidentally released either during PSII repair or during extensive PSII damage [51]. By taking into account the extremely fast turnover of the D1 protein in the ΔCP43 strain (figure 1 and [19]), we assume that even at standard growth irradiances, the probability of chlorophyll release is high and therefore the Scps are associated with RC47 even under these conditions.

We noticed that accumulation of the RC47 complex in cells of ΔCP43 was strongly dependent on the light conditions during growth. Upon lowering the irradiance from 40 to 5 $\mu E\ m^{-2}\ s^{-1}$, the level of the RC47 complex dropped significantly (see the electronic supplementary material, figure S1). A similar decrease was reported by Shimada *et al.* [52] for ΔCP43 grown under light-activated heterotrophic growth conditions (growth in darkness with daily 15 min light exposure). Cellular chlorophyll levels were moderately reduced in ΔCP43 to approximately 70 per cent of WT levels, but this effect was observed at both light conditions (see the electronic supplementary material, figure S2). On the other hand, there was a strong decrease in phycobilin content in low-light-grown cells of the mutant in comparison with cells grown under standard conditions (see the electronic supplementary material, figure S2). This behaviour is reminiscent of the ΔPsbO mutant, which, like the ΔCP43 mutant, also exhibits an extremely fast turnover of the D1 protein [16,53].

We speculate that D1 turnover in these mutants might not be tightly coupled to light damage so that undamaged D1 is targeted for degradation at low light. In the case of RC47, the lack of CP43 might destabilize the N-terminal region of D1 and increase accessibility of the FtsH protease complex, which is involved is degrading photodamaged D1 during PSII repair [12], to the undamaged but destabilized D1 subunit. The lower levels of RC47 observed at low irradiance would reflect the inability of D1 synthesis and the light-driven biosynthesis of Chl to match this enhanced rate of D1 degradation [54]. Loss of chlorophyll induced by aberrantly high D1 turnover at low irradiance may lead to phycobilin deficiency [53,54]. For the PsbO-less mutant, fast turnover of D1 might be triggered at low light by spontaneous disassembly of the Mn_4CaO_5 cluster [53].

Because the RC47 complex is incapable of oxidizing water but is able to perform charge separation, it is potentially highly vulnerable to both donor-side and acceptor-side photoinhibition. Our analysis of the isolated RC47-His complex indicates that the vast majority of the complexes are photochemically active consistent with the operation of effective photoprotection/repair processes. The photoprotective mechanisms might include changes to the redox potential of Q_A so that singlet oxygen production following charge recombination is reduced [55], which to some extent might explain the observed impaired electron transfer on the acceptor side of the complex, between Q_A and Q_B, in whole cells of ΔCP43 [22]; the operation of side-path electron donors Chl_Z and cyt *b*-559 in PSII [38] (figure 6); and impaired transfer of excitation energy from the phycobilisome to help 'switch off' the RC47 complex [52]. In addition, D1 is rapidly and preferentially labelled in the RC47 complex (figure 1; [19]) consistent with the view that RC47 complexes are excellent substrates for selective D1 replacement. Together, these features help ensure that only active RC47 complexes are available for assembling oxygen-evolving PSII.

We thank the UK Biotechnology and Biological Sciences Research Council (grant no. BB/F020554/1) and Engineering and Physical Science Research Council (grant no. EP/F002070X/1) for financial support. J.K. and M. Beckova were supported by projects Algatech (CZ.1.05/2.1.00/03.0110), RVO61388971 and P501/11/0377 of the Grant Agency of the Czech Republic. We are also grateful to Michael Hippler (Department of Biology, University of Münster, Germany) for confirming the presence of Psb28 and Psb28-2 in the RC47-His complex by mass spectrometry.

REFERENCES

1 Wydrzynski, T. J. & Satoh, K. 2005 *Photosystem II: the light-driven water:plastoquinone oxidoreductase*. Dordrecht, The Netherlands: Springer.
2 Ferreira, K. N., Iverson, T. M., Maghlaoui, K., Barber, J. & Iwata, S. 2004 Architecture of the photosynthetic oxygen-evolving center. *Science* **303**, 1831–1838. (doi:10.1126/science.1093087)
3 Loll, B., Kern, J., Saenger, W., Zouni, A. & Biesiadka, J. 2005 Towards complete cofactor arrangement in the 3.0 Å resolution structure of photosystem II. *Nature* **438**, 1040–1044. (doi:10.1038/nature04224)
4 Guskov, A., Kern, J., Gabdulkhakov, A., Broser, M., Zouni, A. & Saenger, W. 2009 Cyanobacterial photosystem II at 2.9-Å resolution and the role of quinones, lipids, channels and chloride. *Nat. Struct. Mol. Biol.* **16**, 334–342. (doi:10.1038/nsmb.1559)
5 Umena, Y., Kawakami, K., Shen, J. R. & Kamiya, N. 2011 Crystal structure of oxygen-evolving photosystem II at a resolution of 1.9 Å. *Nature* **473**, 55–60. (doi:10.1038/nature09913)
6 Komenda, J., Sobotka, R. & Nixon, P. J. 2012 Assembling and maintaining the photosystem II complex in chloroplasts and cyanobacteria. *Curr. Opin. Plant Biol.* **15**, 245–251. (doi:10.1016/j.pbi.2012.01.017)
7 Komenda, J., Nickelsen, J., Tichy, M., Prasil, O., Eichacker, L. A. & Nixon, P. J. 2008 The cyanobacterial homologue of HCF136/YCF48 is a component of an early photosystem II assembly complex and is important for both the efficient assembly and repair of photosystem II in *Synechocystis* sp. PCC 6803. *J. Biol. Chem.* **283**, 22 390–22 399. (doi:10.1074/jbc.M801917200)
8 Komenda, J., Reisinger, V., Müller, B. C., Dobakova, M., Granvogl, B. & Eichacker, L. A. 2004 Accumulation of the D2 protein is a key regulatory step for assembly of the photosystem II reaction center complex in *Synechocystis* PCC 6803. *J. Biol. Chem.* **279**, 48 620–48 629. (doi:10.1074/jbc.M405725200)
9 Boehm, M., Romero, E., Reisinger, V., Yu, J., Komenda, J., Eichacker, L. A., Dekker, J. P. & Nixon, P. J. 2011 Investigating the early stages of photosystem II assembly in *Synechocystis* sp. PCC 6803: isolation of CP47 and CP43 complexes. *J. Biol. Chem.* **286**, 14 812–14 819. (doi:10.1074/jbc.M110.207944)
10 Komenda, J., Knoppova, J., Kopecna, J., Sobotka, R., Halada, P., Yu, J. F., Nickelsen, J., Boehm, M. & Nixon, P. J. 2012 The Psb27 assembly factor binds to the CP43 complex of photosystem II in the cyanobacterium *Synechocystis* sp PCC 6803. *Plant Physiol.* **158**, 476–486. (doi:10.1104/pp.111.184184)
11 Mulo, P., Sirpio, S., Suorsa, M. & Aro, E. M. 2008 Auxiliary proteins involved in the assembly and sustenance of photosystem II. *Photosynth. Res.* **98**, 489–501. (doi:10.1007/s11120-008-9320-3)
12 Nixon, P. J., Michoux, F., Yu, J., Boehm, M. & Komenda, J. 2010 Recent advances in understanding the assembly and repair of photosystem II. *Ann. Bot.* **106**, 1–16. (doi:10.1093/aob/mcq059)

13 Takahashi, S. & Badger, M. R. 2011 Photoprotection in plants: a new light on photosystem II damage. *Trends Plant Sci.* **16**, 53–60. (doi:10.1016/j.tplants.2010.10.001)
14 Adir, N., Shochat, S. & Ohad, I. 1990 Light-dependent D1 protein-synthesis and translocation is regulated by reaction center II. Reaction center II serves as an acceptor for the D1 precursor. *J. Biol. Chem.* **265**, 12 563–12 568.
15 Barbato, R., Friso, G., Rigoni, F., Vecchia, F. D. & Giacometti, G. M. 1992 Structural-changes and lateral redistribution of photosystem-II during donor side photoinhibition of thylakoids. *J. Cell Biol.* **119**, 325–335. (doi:10.1083/jcb.119.2.325)
16 Komenda, J. & Barber, J. 1995 Comparison of *psbO* and *psbH* deletion mutants of *Synechocystis* PCC 6803 indicates that degradation of D1 protein is regulated by the Q_B site and dependent on protein synthesis. *Biochemistry* **34**, 9625–9631. (doi:10.1021/bi00029a040)
17 Rokka, A., Suorsa, M., Saleem, A., Battchikova, N. & Aro, E. M. 2005 Synthesis and assembly of thylakoid protein complexes: multiple assembly steps of photosystem II. *Biochem. J.* **388**, 159–168. (doi:10.1042/BJ20042098)
18 Dobakova, M., Tichy, M. & Komenda, J. 2007 Role of the PsbI protein in photosystem II assembly and repair in the cyanobacterium *Synechocystis* sp. PCC 6803. *Plant Physiol.* **145**, 1681–1691. (doi:10.1104/pp.107.107805)
19 Komenda, J., Barker, M., Kuvikova, S., de Vries, R., Mullineaux, C. W., Tichy, M. & Nixon, P. J. 2006 The FtsH protease slr0228 is important for quality control of photosystem II in the thylakoid membrane of *Synechocystis* sp. PCC 6803. *J. Biol. Chem.* **281**, 1145–1151. (doi:10.1074/jbc.M503852200)
20 Komenda, J., Tichy, M., Prasil, O., Knoppova, J., Kuvikova, S., de Vries, R. & Nixon, P. J. 2007 The exposed N-terminal tail of the D1 subunit is required for rapid D1 degradation during photosystem II repair in *Synechocystis* sp PCC 6803. *Plant Cell* **19**, 2839–2854. (doi:10.1105/tpc.107.053868)
21 Vermaas, W. F. J., Ikeuchi, M. & Inoue, Y. 1988 Protein-composition of the photosystem-II core complex in genetically engineered mutants of the cyanobacterium *Synechocystis* sp Pcc-6803. *Photosynth. Res.* **17**, 97–113. (doi:10.1007/BF00047683)
22 Rögner, M., Chisholm, D. A. & Diner, B. A. 1991 Site-directed mutagenesis of the *psbC* gene of photosystem II: isolation and functional characterization of CP43-less photosystem II core complexes. *Biochemistry* **30**, 5387–5395. (doi:10.1021/bi00236a009)
23 Williams, J. G. K. 1988 Construction of specific mutations in photosystem II photosynthetic reaction center by genetic engineering methods in *Synechocystis* 6803. *Methods Enzymol.* **167**, 766–778. (doi:10.1016/0076-6879(88)67088-1)
24 Debus, R. J., Campbell, K. A., Gregor, W., Li, Z. L., Burnap, R. L. & Britt, R. D. 2001 Does histidine 332 of the D1 polypeptide ligate the manganese cluster in photosystem II? An electron spin echo envelope modulation study. *Biochemistry* **40**, 3690–3699. (doi:10.1021/bi002394c)
25 Service, R. J. *et al.* 2011 Participation of glutamate-354 of the CP43 polypeptide in the ligation of manganese and the binding of substrate water in photosystem II. *Biochemistry* **50**, 63–81. (doi:10.1021/bi1015937)
26 Dobakova, M., Sobotka, R., Tichy, M. & Komenda, J. 2009 Psb28 protein is involved in the biogenesis of the photosystem II inner antenna CP47 (PsbB) in the cyanobacterium *Synechocystis* sp. PCC 6803. *Plant Physiol.* **149**, 1076–1086. (doi:10.1104/pp.108.130039)
27 Boehm, M., Nield, J., Zhang, P., Aro, E. M., Komenda, J. & Nixon, P. J. 2009 Structural and mutational analysis of band 7 proteins in the cyanobacterium *Synechocystis* sp. strain PCC 6803. *J. Bacteriol.* **191**, 6425–6435. (doi:10.1128/JB.00644-09)
28 Yao, D., Kieselbach, T., Komenda, J., Promnares, K., Prieto, M. A., Tichy, M., Vermaas, W. & Funk, C. 2007 Localization of the small CAB-like proteins in photosystem II. *J. Biol. Chem.* **282**, 267–276. (doi:10.1074/jbc.M605463200)
29 Hillmann, B. & Schlodder, E. 1995 Electron-transfer reactions in photosystem-II core complexes from *Synechococcus* at low-temperature: difference spectrum of $P680^+Q_A^-/P680Q_A$ at 77 K. *BBA Bioenergetics* **1231**, 76–88. (doi:10.1016/0005-2728(95)00068-T)
30 Granvogl, B., Zoryan, M., Ploscher, M. & Eichacker, L. A. 2008 Localization of 13 one-helix integral membrane proteins in photosystem II subcomplexes. *Anal. Biochem.* **383**, 279–288. (doi:10.1016/j.ab.2008.08.038)
31 Funk, C. & Vermaas, W. 1999 A cyanobacterial gene family coding for single-helix proteins resembling part of the light-harvesting proteins from higher plants. *Biochemistry* **38**, 9397–9404. (doi:10.1021/bi990545)
32 Promnares, K., Komenda, J., Bumba, L., Nebesarova, J., Vacha, F. & Tichy, M. 2006 Cyanobacterial small chlorophyll-binding protein ScpD (HliB) is located on the periphery of photosystem II in the vicinity of PsbH and CP47 subunits. *J. Biol. Chem.* **281**, 32 705–32 713. (doi:10.1074/jbc.M606360200)
33 Bricker, T. M., Young, A., Frankel, L. K. & Putnam-Evans, C. 2002 Introduction of the 305Arg → 305Ser mutation in the large extrinsic loop E of the CP43 protein of *Synechocystis* sp. PCC 6803 leads to the loss of cytochrome c550 binding to photosystem II. *BBA Bioenergetics* **1556**, 92–96. (doi:10.1016/S0005-2728(02)00367-5)
34 Li, Z. L., Bricker, T. M. & Burnap, R. 2000 Kinetic characterization of his-tagged CP47 Photosystem II in *Synechocystis* sp PCC6803. *BBA Bioenergetics* **1460**, 384–389. (doi:10.1016/S0005-2728(00)00207-3)
35 Schlodder, E., Brettel, K., Schatz, G. H. & Witt, H. T. 1984 Analysis of the Chl-a_{II}^+ reduction kinetics with nanosecond time resolution in oxygen-evolving photosystem-II particles from *Synechococcus* at 680 and 824 nm. *Biochim. Biophys. Acta* **765**, 178–185. (doi:10.1016/0005-2728(84)90012-4)
36 Conjeaud, H. & Mathis, P. 1980 The effect of Ph on the reduction kinetics of P-680 in tris-treated chloroplasts. *Biochim. Biophys. Acta* **590**, 353–359. (doi:10.1016/0005-2728(80)90206-6)
37 Schlodder, E., Renger, T., Raszewski, G., Coleman, W. J., Nixon, P. J., Cohen, R. O. & Diner, B. A. 2008 Site-directed mutations at D1-Thr179 of photosystem II in *Synechocystis* sp PCC 6803 modify the spectroscopic properties of the accessory chlorophyll in the D1-branch of the reaction center. *Biochemistry* **47**, 3143–3154. (doi:10.1021/bi702059f)
38 Faller, P., Fufezan, C. & Rutherford, A. W. 2005 Side-path electron donors: cytochrome b559, chlorophyll Z and β-carotene in photosystem II. In *Photosystem II: the light-driven water: plastoquinone oxidoreductase* (eds K. Wydrzynski & K. Satoh), pp. 347–365. Dordrecht, The Netherlands: Springer.
39 Carpenter, S. D., Charite, J., Eggers, B. & Vermaas, W. 1990 Characterization of site-directed and hybrid psbc mutants of *Synechocystis* 6803. In *Current research in photosynthesis*, vol. I (ed. M. Baltcheffsky), pp. 359–362. Dordrecht, The Netherlands: Kluwer Academic Publishers.

40 Akabori, K., Tsukamoto, H., Tsukihara, J., Nagatsuka, T., Motokawa, O. & Toyoshima, Y. 1988 Disintegration and reconstitution of photosystem-II reaction center core complex. I. Preparation and characterization of 3 different types of subcomplex. *Biochim. Biophys. Acta* **932**, 345–357. (doi:10.1016/0005-2728(88)90170-3)

41 Petersen, J., Dekker, J. P., Bowlby, N. R., Ghanotakis, D. F., Yocum, C. F. & Babcock, G. T. 1990 EPR Characterization of the CP47-D1-D2-cytochrome-b-559 complex of photosystem-II. *Biochemistry* **29**, 3226–3231. (doi:10.1021/bi00465a012)

42 Szabo, I., Rigoni, F., Bianchetti, M., Carbonera, D., Pierantoni, F., Seraglia, R., Segalla, A. & Giacometti, G. M. 2001 Isolation and characterization of photosystem II subcomplexes from cyanobacteria lacking photosystem I. *Eur. J. Biochem.* **268**, 5129–5134. (doi:10.1046/j.0014-2956.2001.02441.x)

43 Yamagishi, A. & Katoh, S. 1985 Further characterization of the 2 photosystem-II reaction center complex preparations from the thermophilic cyanobacterium *Synechococcus* sp. *Biochim. Biophys. Acta* **807**, 74–80. (doi:10.1016/0005-2728(85)90054-4)

44 Yamaguchi, N., Takahashi, Y. & Satoh, K. 1988 Isolation and characterization of a photosystem-II core complex depleted in the 43-kDa-chlorophyll-binding subunit. *Plant Cell Physiol.* **29**, 123–129.

45 Zheleva, D., Sharma, J., Panico, M., Morris, H. R. & Barber, J. 1998 Isolation and characterization of monomeric and dimeric CP47-reaction center photosystem II complexes. *J. Biol. Chem.* **273**, 16 122–16 127. (doi:10.1074/jbc.273.26.16122)

46 Kawakami, K., Umena, Y., Iwai, M., Kawabata, Y., Ikeuchi, M., Kamiya, N. & Shen, J. R. 2011 Roles of PsbI and PsbM in photosystem II dimer formation and stability studied by deletion mutagenesis and X-ray crystallography. *BBA Bioenergetics* **1807**, 319–325. (doi:10.1016/j.bbabio.2010.12.013)

47 Broser, M., Gabdulkhakov, A., Kern, J., Guskov, A., Muh, F., Saenger, W. & Zouni, A. 2010 Crystal structure of monomeric photosystem II from *Thermosynechococcus elongatus* at 3.6 Å resolution. *J. Biol. Chem.* **285**, 26 255–26 262. (doi:10.1074/jbc.M110.127589)

48 Enami, I., Okumura, A., Nagao, R., Suzuki, T., Iwai, M. & Shen, J. R. 2008 Structures and functions of the extrinsic proteins of photosystem II from different species. *Photosynth. Res.* **98**, 349–363. (doi:10.1007/s11120-008-9343-9)

49 Liu, H. J., Roose, J. L., Cameron, J. C. & Pakrasi, H. B. 2011 A genetically tagged Psb27 protein allows purification of two consecutive photosystem II (PSII) assembly intermediates in *Synechocystis* 6803, a cyanobacterium. *J. Biol. Chem.* **286**, 24 865–24 871. (doi:10.1074/jbc.M111.246231)

50 Nowaczyk, M. M., Krause, K., Mieseler, M., Sczibilanski, A., Ikeuchi, M. & Rögner, M. 2012 Deletion of *psbJ* leads to accumulation of Psb27-Psb28 photosystem II complexes in *Thermosynechococcus elongatus*. *Biochim. Biophys. Acta* **1817**, 1339–1345. (doi:10.1016/j.bbabio.2012.02.017)

51 Sinha, R. K., Komenda, J., Knoppova, J., Sedlarova, M. & Pospisil, P. 2012 Small CAB-like proteins prevent formation of singlet oxygen in the damaged photosystem II complex of the cyanobacterium *Synechocystis* sp PCC 6803. *Plant Cell Environ.* **35**, 806–818. (doi:10.1111/j.1365-3040.2011.02454.x)

52 Shimada, Y., Tsuchiya, T., Akimoto, S., Tomo, T., Fukuya, M., Tanaka, K. & Mimuro, M. 2008 Spectral properties of the CP43-deletion mutant of *Synechocystis* sp PCC 6803. *Photosynth. Res.* **98**, 303–314. (doi:10.1007/s11120-008-9350-x)

53 Komenda, J., Knoppova, J., Krynicka, V., Nixon, P. J. & Tichy, M. 2010 Role of FtsH2 in the repair of photosystem II in mutants of the cyanobacterium *Synechocystis* PCC 6803 with impaired assembly or stability of the CaMn(4) cluster. *Biochim. Biophys. Acta* **1797**, 566–575. (doi:10.1016/j.bbabio.2010.02.006)

54 Hernandez-Prieto, M. A., Tibiletti, T., Abasova, L., Kirilovsky, D., Vass, I. & Funk, C. 2011 The small CAB-like proteins of the cyanobacterium *Synechocystis* sp. PCC 6803: their involvement in chlorophyll biogenesis for photosystem II. *Biochim. Biophys. Acta* **1807**, 1143–1151. (doi:10.1016/j.bbabio.2011.05.002)

55 Vass, I. & Cser, K. 2009 Janus-faced charge recombinations in photosystem II photoinhibition. *Trends Plant Sci.* **14**, 200–205. (doi:10.1016/j.tplants.2009.01.009)

4.1.1 Supplemental information

Supplementary Figures

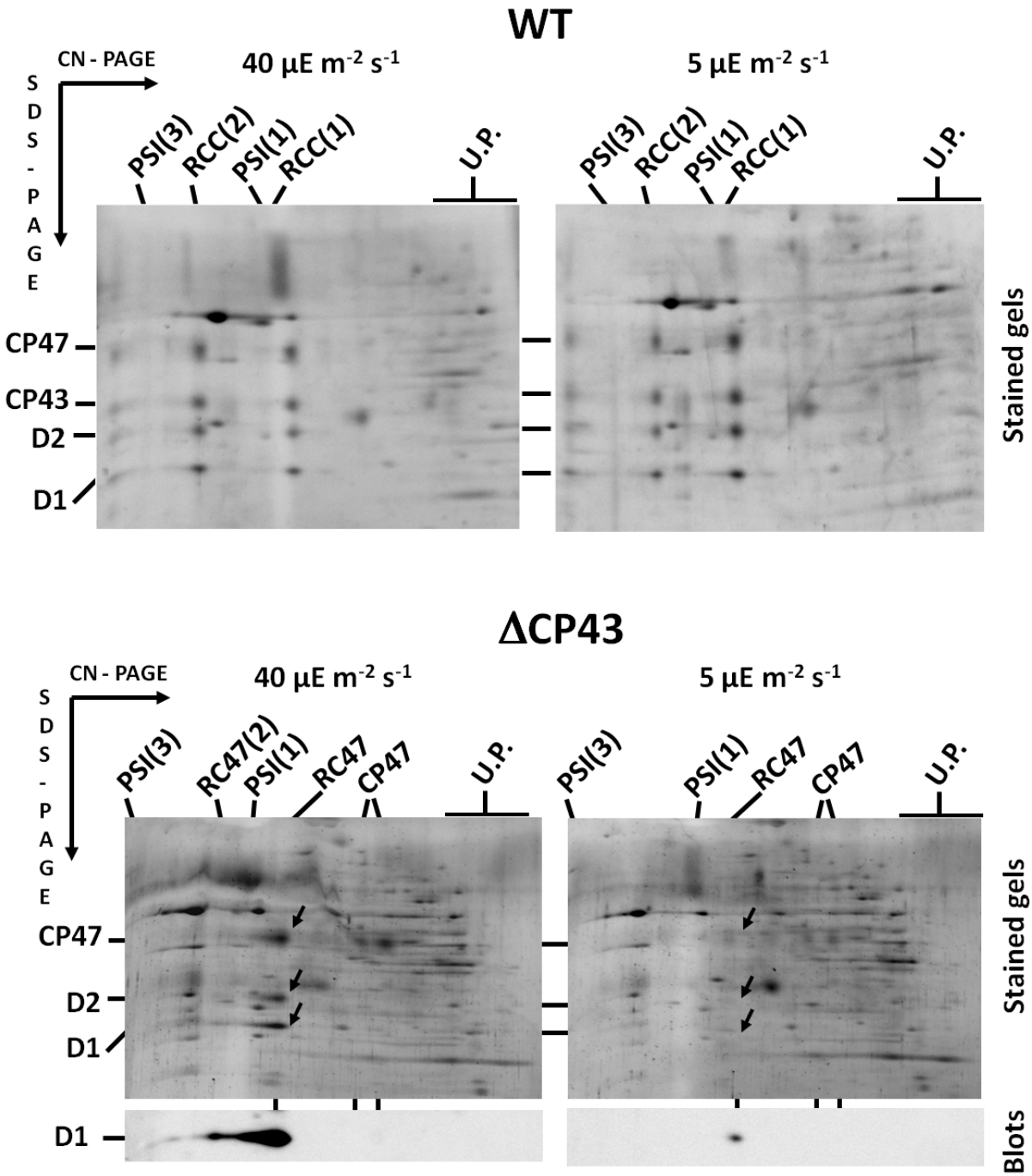

Figure S1: Comparative two-dimensional analysis of thylakoid membranes isolated from the WT *Synechocystis* 6803 and ΔCP43 strains grown at irradiance of either 40 (left panels) or 5 (right panels) µE m^{-2} s^{-1}. Thylakoid membranes corresponding to an amount of 4 µg Chl *a* were separated on 4 to 14 % (w/v) polyacrylamide (PAA) CN-PAGE linear gradient gel and another 12-20 % (w/v) PAA SDS-PAGE gel was used for the second dimension. The gels were

stained with Sypro Orange (Stained gel), then blotted onto PVDF membrane and sequentially probed with antibodies against the D1 protein (Blots). The positions of the trimeric (PSI(3) and monomeric (PSI(1)) PSI complexes, dimeric (RCC(2)) and monomeric (RCC(1)) PSII core complexes, putative dimeric (RC47(2)) and monomeric RC47 and unassembled CP47 complexes are indicated.

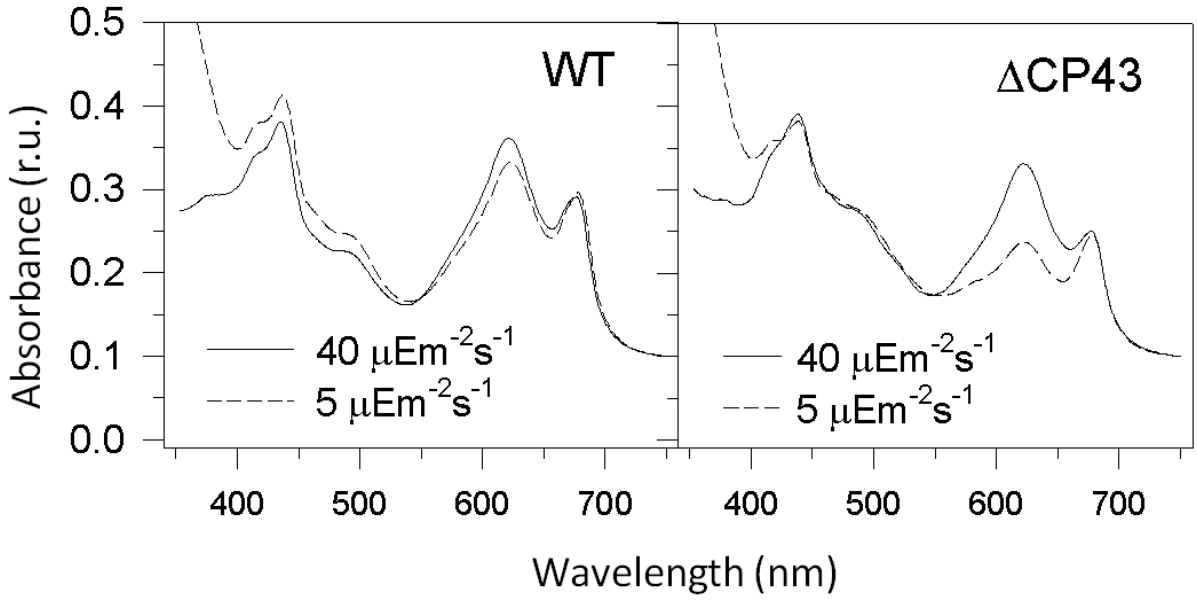

Figure S2: Absorption spectra of cells of the WT and ΔCP43 strains cultivated at an irradiance of 40 or 5 µE m^{-2} s^{-1} and then transferred to 100 µE m^{-2} s^{-1}. All spectra were measured using a Shimadzu UV3000 spectrophotometer using cultures with an identical OD_{750nm}.

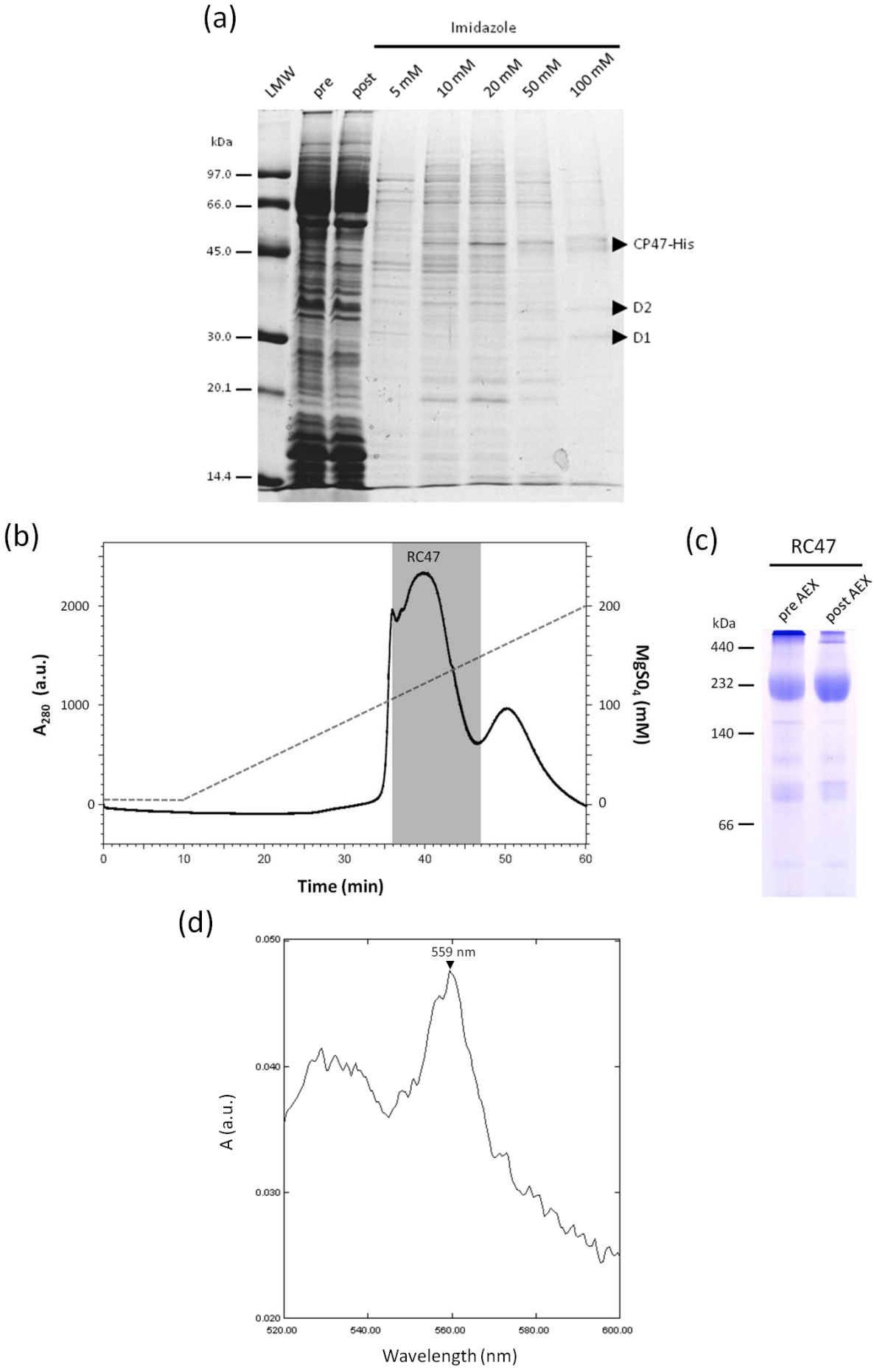
(a)
Imidazole
LMW
pre
post
5 mM
10 mM
20 mM
50 mM
100 mM
kDa
97.0
66.0
45.0
30.0
20.1
14.4
CP47-His
D2
D1
(b)
RC47
2000
1000
0
200
100
0
A280 (a.u.)
MgSO4 (mM)
0
10
20
30
40
50
60
Time (min)
(c)
RC47
pre AEX
post AEX
kDa
440
232
140
66
(d)
559 nm
0.050
0.040
0.030
0.020
A (a.u.)
520.00
540.00
560.00
580.00
600.00
Wavelength (nm)

Fig S3: Isolation and analysis of the RC47-His protein complex of *Synechocystis* sp. PCC 6803. (A) The fractions collected during the Ni^{2+}-affinity purification of the RC47-His protein complex from *Synechocystis* sp. PCC 6803 were analysed by SDS-PAGE. Pre and Post incubation samples (corresponding to an amount of 1 µg of Chl *a*) as well as equal amounts of samples taken from the various washes (5, 10 and 20 mM imidazole) and elutions (50 and 100 mM imidazole) were analysed on a 12.5 % (w/v) PAA SDS PAGE gel that was subsequently silver-stained. The positions of the D1, D2 and CP47-His proteins are indicated. (B) After the Ni^{2+}-affinity purification, the RC47-His complex was further purified by anion-exchange chromatography. The elution profile of the anion exchange chromatography run was monitored at 280 nm with the fractions that were later pooled marked by the gray area. The profile of the $MgSO_4$ linear gradient from 5 to 200 mM is indicated by the dashed line. (C) RC47-His protein complex samples (pre and post anion-exchange chromatography, Pre AEX and Post AEX, respectively) were analysed on an 8 to 12 % (w/v) PAA BN-PAGE linear gradient gel that was subsequently Coomassie-stained. Samples corresponding to an amount of 0.5 µg of Chl *a* were loaded per lane. High molecular weight (HMW) marker was obtained from GE Healthcare, UK. (D) Reduced-minus-oxidized difference spectrum of RC47-His complexes showing presence of the typical absorption peak for Cyt *b*-559 at 559 nm (indicated by an arrowhead).

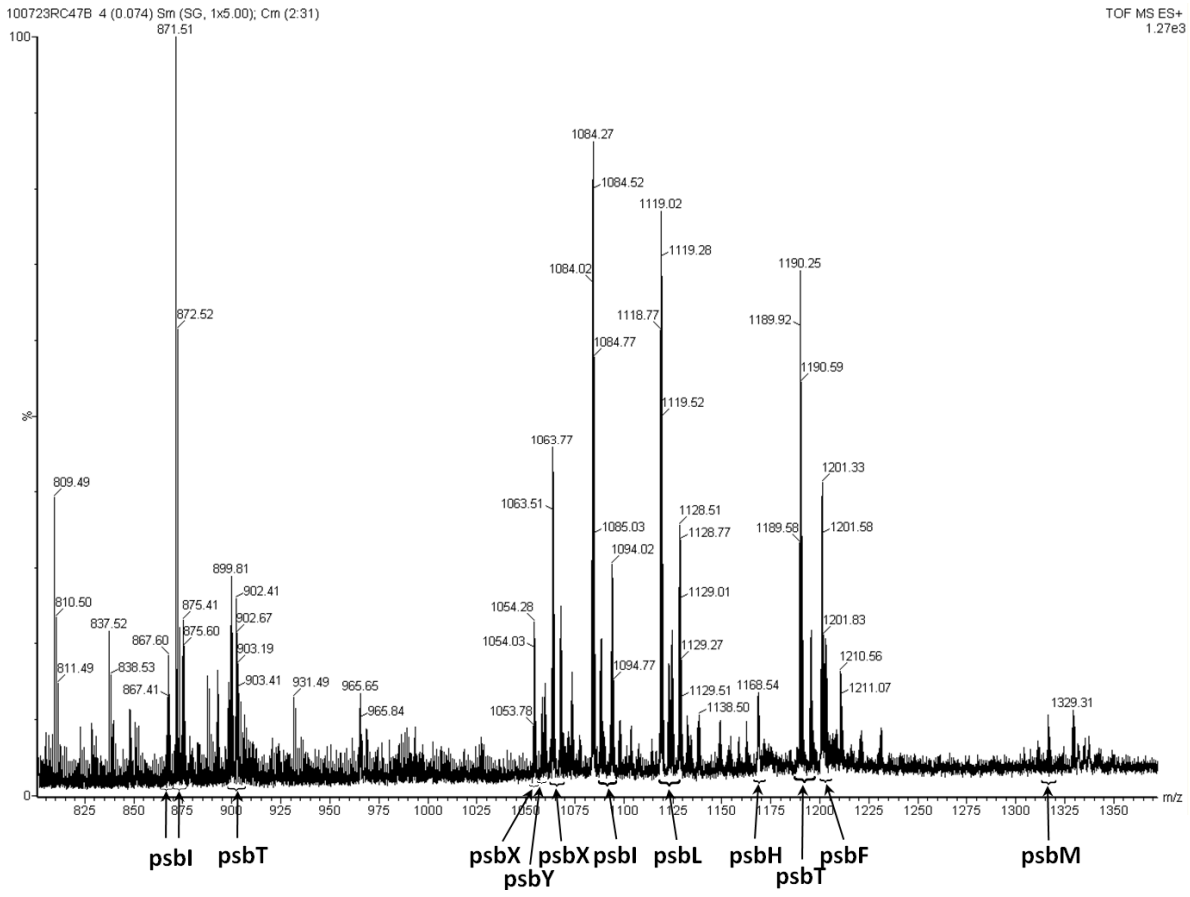

Figure S4: ESI-MS spectrum of the low-molecular-mass (LMM) proteins present in the RC47-His complex isolated from *Synechocystis* sp. PCC 6803. LMM proteins were precipitated in 80 % (v/v) acetone and dissolved in 70 % (v/v) acetone, 10 % (v/v) propan-2-ol and 1 % (v/v) formic acid for analysis by static nanoESI-MS. The following PSII subunits were detected: PsbF, -H, -I, -L, -M, -T, -X and -Y. Multiple signals for the same protein, represent different charge states or modifications.

4.2 Crystal structure of the Psb28 accessory factor of *Thermosynechococcus elongatus* photosystem II at 2.3 Å.

Reprint of: Bialek, W., Wen, S., Michoux, F., Beckova, M., Komenda, J., Murray, J.W., and Nixon, P.J. (2013). Photosynth Res 117:375-383

Photosynth Res (2013) 117:375–383
DOI 10.1007/s11120-013-9939-6

REGULAR PAPER

Crystal structure of the Psb28 accessory factor of *Thermosynechococcus elongatus* photosystem II at 2.3 Å

Wojciech Bialek · Songjia Wen · Franck Michoux · Martina Beckova · Josef Komenda · James W. Murray · Peter J. Nixon

Received: 6 June 2013 / Accepted: 2 October 2013 / Published online: 15 October 2013

Abstract Members of the Psb28 family of proteins are accessory factors implicated in the assembly and repair of the photosystem II complex. We present here the crystal structure of the Psb28 protein (Tlr0493) found in the thermophilic cyanobacterium *Thermosynechococcus elongatus* at a resolution of 2.3 Å. Overall the crystal structure of the Psb28 monomer is similar to the solution structures of C-terminally His-tagged Psb28-1 from *Synechocystis* sp. PCC 6803 obtained previously by nuclear magnetic resonance spectroscopy. One new aspect is that *Escherichia coli*-expressed *T. elongatus* Psb28 is able to form dimers in solution and packs as a dimer of dimers in the crystal. Analysis of wild type and mutant strains of *Synechocystis* 6803 by blue native-polyacrylamide gel electrophoresis suggests that Psb28-1, the closest homologue to *T. elongatus* Psb28 in this organism, also exists as an oligomer in vivo, most likely a dimer. In line with the prediction based on the crystal structure of *T. elongatus* Psb28, the addition of a 3× Flag-tag to the C-terminus of *Synechocystis* 6803 Psb28-1 interferes with the accumulation of the Psb28-1 oligomer in vivo. In contrast, the more distantly related Psb28-2 protein found in *Synechocystis* 6803 lacks the residues that stabilize dimer formation in the *T. elongatus* Psb28 crystal and is detected as a monomer in vivo. Overall our data suggest that the dimer interface in the Psb28 crystal might be physiologically relevant.

Keywords Assembly factor · Psb28 · Psb28-2 · X-ray crystallography · Photosystem II · Cyanobacteria

Abbreviations

D1	Photosystem II reaction center subunit encoded by *psbA*
D2	Photosystem II reaction center subunit encoded by *psbD*
CP43 and CP47	Photosystem II proximal light-harvesting subunits encoded by *psbC* and *psbB*, respectively
RC47	Photosystem II complex lacking CP43
RCC1	Monomeric photosystem II
RCC2	Dimeric photosystem II
RMSD	Root mean square deviation

Introduction

The Photosystem II (PSII) complex, which functions as the light-driven water: plastoquinone oxidoreductase of oxygenic

Electronic supplementary material The online version of this article (doi:10.1007/s11120-013-9939-6) contains supplementary material, which is available to authorized users.

W. Bialek · S. Wen · F. Michoux · J. W. Murray · P. J. Nixon (✉)
Sir Ernst Chain Building–Wolfson Laboratories, Department of Life Sciences, Imperial College London, South Kensington Campus, London SW7 2AZ, UK
e-mail: p.nixon@imperial.ac.uk

Present Address:
S. Wen
Department of Biochemistry, LKS Faculty of Medicine, The University of Hong Kong, Pokfulam, Hong Kong, China

Present Address:
F. Michoux
Alkion Biopharma, 4 Rue Pierre Fontaine, 91058 Evry, France

M. Beckova
Faculty of Science, University of South Bohemia, Branisovska 31, Ceske Budejovice, Czech Republic

J. Komenda
Institute of Microbiology, Academy of Sciences, 379 81 Trebon, Czech Republic

photosynthesis, is found in the thylakoid membrane system of cyanobacteria and chloroplasts. Crystal structures of isolated dimeric oxygen-evolving PSII complexes have been determined for the cyanobacteria *Thermosynechococcus elongatus* and *Thermosynechococcus vulcanus* (Kamiya and Shen 2003; Ferreira et al. 2004; Loll et al. 2005; Guskov et al. 2009; Umena et al. 2011). In the case of *T. elongatus*, each monomer is composed of 17 intrinsic and 3 extrinsic subunits and a variety of cofactors (Guskov et al. 2009). Recent studies have begun to reveal how PSII is assembled from its component parts. Current evidence suggests a modular assembly of PSII (Nixon et al. 2010; Boehm et al. 2011). First, a PSII reaction centre (PSII RC) complex is formed from PsbI-precursor D1 (Dobakova et al. 2007) and cytochrome b_{559}-D2 (Komenda et al. 2004) sub-complexes. Then a CP47 module (Boehm et al. 2011) is attached to create the RC47 complex, after which a CP43 module (Boehm et al. 2011) is added to form the non-oxygen-evolving monomeric PSII complex. At this stage, the oxygen-evolving Mn_4CaO_5 cluster is assembled; the PsbO, PsbU and PsbV lumenal extrinsic proteins are attached and PSII can dimerise (reviewed by Komenda et al. 2012a). Removal of the C-terminal extension of the precursor D1 subunit (Komenda et al. 2007), which is required for assembly of the Mn_4CaO_5 cluster (Nixon et al. 1992), is initiated in vivo after formation of the PSII RC (Komenda et al. 2004).

The PSII complex is susceptible to light-induced damage, which can lead to chronic photoinhibition (Adir et al. 2003). Damaged subunits, predominantly the D1 subunit, are replaced during the so-called 'PSII repair cycle'. Current models suggest that the damaged PSII complex partially disassembles to form the monomeric RC47 complex (Komenda et al. 2004); the damaged D1 protein is degraded by a hetero-oligomeric FtsH protease complex (Boehm et al. 2012a) and replaced by a newly synthesised copy of D1. Oxygen-evolving monomeric and dimeric complexes are then reformed as in PSII assembly (Komenda et al. 2012a).

A number of accessory factors have been identified in various types of PSII complex that are absent in the crystallised dimeric PSII complex (Nixon et al. 2010; Chi et al. 2012). Their functions are still unclear, but current evidence suggests roles in the assembly and repair of PSII or the optimisation of water oxidation. One of these, Psb28-1, encoded by sll1398 in *Synechocystis* sp. PCC 6803 (hereafter *Synechocystis* 6803), is known to bind to the cytoplasmic surface of PSII close to CP47 and PsbH (Dobakova et al. 2009) and in the vicinity of the HliB and HliC subunits that can attach to PSII in vivo (Promnares et al. 2006; Yao et al. 2007). Psb28-1 is mainly found in RC47 complexes in WT (Dobakova et al. 2009) and has been recently detected in isolated PSII core complexes containing the His-tagged Psb27 subunit (Liu et al. 2011). Analysis of a *psb28-1* null mutant of *Synechocystis* 6803 has led to the hypothesis that Psb28-1 might be involved in the synthesis of chlorophylls and/or the apopolypeptides of the chlorophyll-binding proteins CP47 and PsaA/PsaB (Dobakova et al. 2009) although this phenotype appears to be dependent on the particular WT strain used (Sakata et al. 2013). In addition, Psb28-1 is involved in maintaining PSII activity during heat stress possibly at the level of repair (Sakata et al. 2013). *Synechocystis* 6803, like certain other cyanobacteria, also encodes a second Psb28 homologue, designated Psb28-2, encoded by slr1739, which has also been detected in RC47 complexes (Boehm et al. 2012b).

The structure of a C-terminally His-tagged derivative of Psb28-1 encoded by *Synechocystis* 6803 has been determined by nuclear magnetic resonance spectroscopy (NMR) (Yang et al. 2011). Here, we present the crystal structure of the single Psb28 homologue found in the thermophilic cyanobacterium *T. elongatus* which has also been reported to associate with PSII (Nowaczyk et al. 2012). As anticipated, the overall fold of Psb28 is conserved between the two species. However, our results suggest that Psb28-1 might actually exist as a dimer in vivo and that dimerization is impaired by addition of protein tags at the C-terminus.

Materials and methods

Cloning, expression and purification of Psb28

A PCR fragment containing the Psb28 gene of *T. elongatus* (*tlr0493*) was amplified from genomic DNA using Phusion polymerase (NEB, UK) and primers Psb28-BamHI-F (5′-TATATAGGATCCGGTGCAATGGCAGAAATT-3′) and Psb28-EcoRI-R (5′-TATATA GAATTCTTATCAAGAGT TCTCAGACTTCTGAAAGCCA-3′), purified, digested by BamHI/EcoRI and ligated (Quick Ligation Kit, New England Biolabs, UK) into a modified version of pRSET-A that directs the expression of a target protein with a thrombin-cleavable N-terminal His_6-tag (Michoux et al. 2010). Soluble His_6-tagged Psb28 was expressed in the KRX strain of *Escherichia coli*, purified using immobilised Ni^{2+}-affinity chromatography and the His-tag removed by thrombin cleavage as described by Michoux et al. (2012). Size-exclusion chromatography was performed on a Superdex75 10/300 GL column (GE Healthcare) equilibrated with 50 mM Tris pH 8.0, 150 mM NaCl or 50 mM MES pH 6.5, 5 mM $MgCl_2$, 5 mM $CaCl_2$. The column was calibrated for each buffer with molecular weight markers for gel filtration chromatography from Sigma (BSA, carbonic anhydrase, cytochrome *c* and aprotinin).

Crystallization and structure solution

The protein lacking the hexahistidine tag was concentrated to 32 mg/ml and crystallisation screens were set up at 19 °C

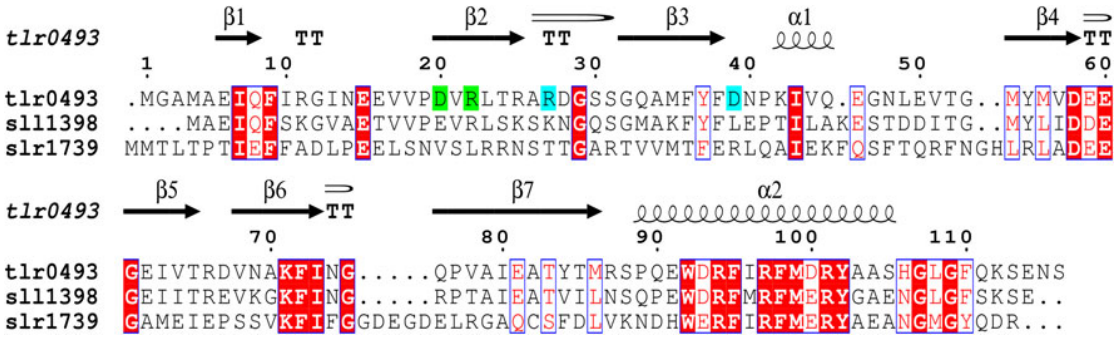

Fig. 1 Sequence alignment of Psb28 from *T. elongatus* (*tlr0493*) and Psb28-1 (*sll1398*) and Psb28-2 (*slr1739*) from *Synechocystis* 6803. Residues involved in salt bridges between different chains in putative dimer are highlighted in green and cyan. The picture was created by ESPript server (Gouet et al. 1999) and β-hairpins (⊃) were detected by ProMotif (Hutchinson and Thornton 1996)

using a Mosquito® robot (TTP LabTech, UK). Rod-shaped Psb28 crystals appeared in sitting drops with the protein solution mixed with an equal volume of 20 % (v/v) PEG200, 20 % (w/v) PEG4000, 10 % (v/v) 2-propanol buffer and 100 mM HEPES sodium salt pH 7.5. A crystal was mounted in a loop and plunged into liquid nitrogen with no further cryoprotection. Data were collected on beamline I04-1 at Diamond Light Source on a Pilatus 6 M detector.

The structure was solved by molecular replacement in PHASER (McCoy et al. 2007). The NMR structure of Psb28-1 from *Synechocystis* (PDB code 2KVO) was truncated to match the *T. elongatus* sequence by CHAINSAW and the first model used as a search model. A partial solution with three copies showed a clear Psb28 dimer. A search with this dimer yielded a clear solution with two dimers in the asymmetric unit. The structure was completed and edited in Coot (Emsley et al. 2010), with cycles of refinement in REFMAC5 (Murshudov et al. 2011) and finally with Phenix (Adams et al. 2010). Non-crystallographic symmetry restraints were applied. The atomic model and structure factors have been deposited in the PDB under accession number 3ZPN.

Growth of *Synechocystis* strains and protein analysis

The glucose-tolerant wild type strain (WT-G) of *Synechocystis* 6803 (Williams 1988) and the previously constructed ΔCP43 (Vermaas et al. 1988), ΔCP43/CP47-His (Boehm et al. 2012b), ΔPSI (Shen et al. 1993), ΔPSI/ΔHliABCD (Vavilin et al. 2007) strains were used in this study. The Hlip- and Psb28-lacking derivatives of the ΔCP43 strain were obtained by the transformation of the ΔCP43 strain using genomic DNA isolated from previously described insertion mutants lacking HliA, HliB (Xu et al., 2002) and Psb28 (Dobakova et al. 2009). Similarly, the PSI-less strain lacking PsbH was obtained by transformation of the ΔPSI strain using genomic DNA isolated from the *psbH* deletion strain (Mayes et al. 1993). The C-terminally flagged strain was constructed by transformation of the WT-G strain by a synthetic construct bearing the nucleotide sequence of *psb28-1* gene fused to a sequence encoding a 3 × *flag* sequence at the C-terminus followed by a zeocine-resistance cassette together with 300-bp upstream and 200-bp downstream region of the original *psb28-1* gene. Strains were grown in liquid BG-11 mineral medium and maintained on solid BG-11 plates containing 1.5 % (w/v) agar, both containing 5 mM *N*-tris (hydroxymethyl)methyl-2-aminoethanesulfonic acid–KOH, pH 8.2, at a light intensity of 40 (for WT-G strains) or 5 (for PSI-less strains) $\mu E\ m^2\ s^{-1}$ of white fluorescent light at 29 °C. The medium was supplemented with 5 mM glucose.

Two-dimensional protein analyses were performed by a combination of blue native and SDS-PAGE as described in Komenda et al. (2012b). 2D gels were stained by Sypro Orange, blotted onto PVDF membranes and probed with specific antibodies against D1, Psb28-1 and Psb28-2 of *Synechocystis* 6803 (Komenda et al. 2012b; Boehm et al. 2012b).

Results and discussion

Sequence alignment

In contrast to *Synechocystis* 6803 which contains two Psb28 homologues, there is only one Psb28 homologue encoded in the *T. elongatus* genome (Fig. S1). Sequence comparisons revealed 59 % identity (78 % similarity) and 33 % identity (57 % similarity) between Psb28 from *T. elongatus* and Psb28-1 and Psb28-2 from *Synechocystis* 6803, respectively (Fig. 1). The full length gene *tlr0493* encoding Psb28 was expressed in *E. coli* as an N-terminal His-tagged derivative (Fig. S2a). After removal of the His-tag by thrombin cleavage (Fig. S2b), to leave two additional Gly-Ser residues at the N-terminus, and concentrating to 32 mg/ml, the protein was crystallised in two crystal forms only one of which

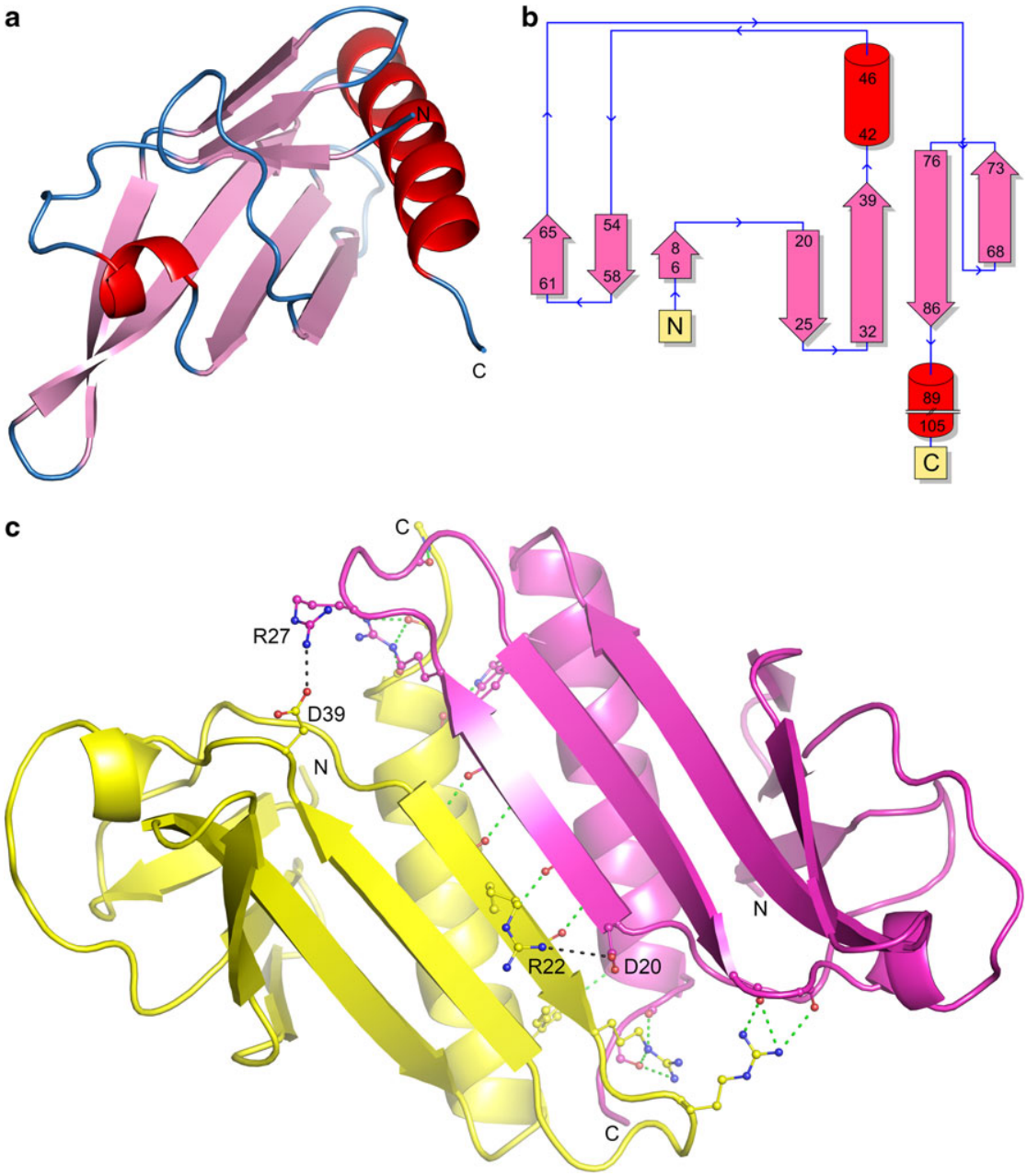

Fig. 2 Structural features of Psb28 from *T. elongatus*. **a** 3D fold of protein **b** its topological cartoon representation and c protein–protein interactions in dimeric Psb28 from *T. elongatus*. Salt bridges and hydrogen bonds are shown as *black* and *green dashed lines*, respectively. For full list of residues involved in H-bonds refer to Table S1

was suitable for structure determination. Size-exclusion chromatography indicated that the *E. coli*-expressed Psb28 used for crystallisation could exist as monomers or dimers depending on the buffer (Fig. S2c and d).

Structure description

The best X-ray diffraction data sets were collected for crystals obtained in 20 % (v/v) PEG200, 20 % (w/v) PEG4000, 10 % (v/v) 2-propanol buffer and 100 mM HEPES sodium salt pH 7.5 (Fig. S3a) and the structure was solved by molecular replacement using the NMR structure of Psb28-1 from *Synechocystis* 6803 (PDB: 2KVO); Table 1 shows the data collection and refinement statistics. The structure reveals that β-strands and α-helices account for 44 and 20 % of Psb28, respectively (Fig. 2). Two antiparallel β-sheets (A and B) are composed of β-strands, β1-4-5 and β2-3-6-7, with β-hairpins connecting β2 and β3, β4 and β5 and β6 and β7. One inverse

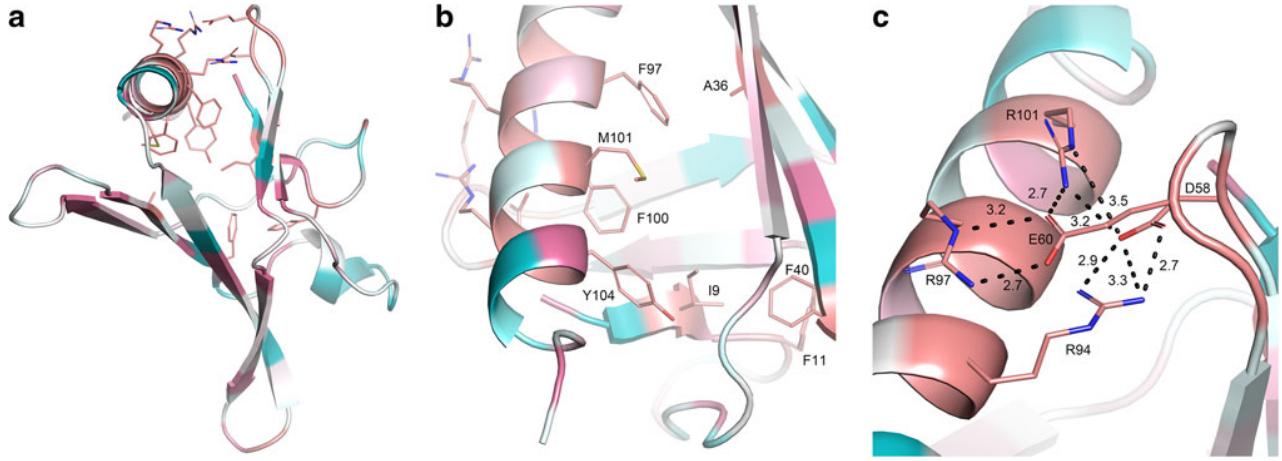

Fig. 3 Analysis of conserved residues distribution between cyanobacterial, algal and plant Psb28-1 and cyanobacterial Psb28-2 as calculated by Consurf (Ashkenazy et al. 2010). **a** Side chains of the most conserved residues are shown as sticks. **b** Side chains (shown as *sticks*) of conserved residues lining the hydrophobic core of the protein. **c** Interactions between the two absolutely conserved regions found in both the Psb28-1 and Psb28-2 with lengths given in Å. The conservation colouring scale spans from teal for variable to salmon for the most conserved residues. Compare with sequence alignment from Fig. 1

γ-turn is present ($Arg_{66}Asp_{67}Val_{68}$) between β5 and β6 (Fig. 1). Two α-helices are present, one short consisting of five residues (Lys_{42}-Glu_{46}) and one longer of 17 residues (Pro_{89}-Ser_{105}). The former is located between β3 and β4 and the latter is close to the C-terminus. The first 2 and last 6 residues are missing from electron density so that only residues 3–110 were modelled.

Comparison with the solution structure of *Synechocystis* Psb28-1

Structural comparison between the Psb28 crystal structure presented here, and Psb28-1 revealed a high overall similarity with a pairwise C_α RMSD of 1.6 Å as calculated by SSM (Krissinel and Henrick 2004). As shown in Fig. S4, the most significant difference between both the proteins lies in the loop between β-strands 3 and 4 (see below). In addition, Psb28 from *T. elongatus* lacks a 3_{10} helix composed of residues 39–41 (2KVO original numbering) and the second 3_{10} helix of Psb28-1 is replaced by a five-residue long α-helix (Lys_{42}-Glu_{46}). Only one significant hit, Psb28-1, with a Z score of 13.8, was detected by DALI analysis (Holm and Rosenstrom 2010).

In the crystal structure, four molecules are present in the asymmetric unit (Fig. S3b). As suggested by PISA (Krissinel and Henrick 2007), and in contrast to the solution structure of His-tagged Psb28-1 from *Synechocystis* 6803, Psb28 from *T. elongatus* forms two dimers composed of chains A–B and C–D. The interface is created between long C-terminal α-helices and β-strands 2 with numerous hydrogen bonds between chains (Table S1). Two salt bridges (Asp_{20}-Arg_{22} and Arg_{27}-Asp_{39}) further stabilize the dimer (Fig. 2c).

Table 1 Data collection and refinement statistics for the Psb28 crystal structure

Crystal parameters	
Space group	$P\ 4_3$
Cell dimensions	$a = b = 57.06$ Å $c = 183.32$ Å $\alpha = \beta = \gamma = 90^\circ$
Data collection	
Beamline	Diamond Light Source I04–1
Wavelength (Å)	0.92000
Resolution (Å)	2.36–57.06 (2.42–2.36)
Unique observations	23633 (1702)
R_{merge}	0.05 (0.55)
Mean ($< I>/\sigma I$)	13.2 (1.75)
Completeness (%)	98.7 (97.6)
Multiplicity	3.1 (2.9)
Refinement	
R_{work}/R_{free} (%)	19.45/23.42
Number of protein residues	427
RMSD stereochemistry	
Bond lengths (Å)	0.009
Bond angles (°)	1.339
Ramachandran analysis (%)	
Residues in outlier regions	0.48
Residues in favoured regions	98.3
Residues in allowed regions	99.5

Numbers in parentheses refer to the outermost resolution shell

$R_{merge} = \Sigma\ |I - < I>|/\Sigma\ I$ where I is the integrated intensity of a given reflection and $< I >$ is the mean intensity of multiple corresponding symmetry-related reflections

$R_{work} = \Sigma\ ||F_o| - |F_c||/\Sigma\ F_o$ where F_o and F_c are the observed and calculated structure factors respectively

$R_{free} = R_{work}$ calculated using ~5 % random data excluded from the refinement

RMSD stereochemistry is the deviation from ideal values

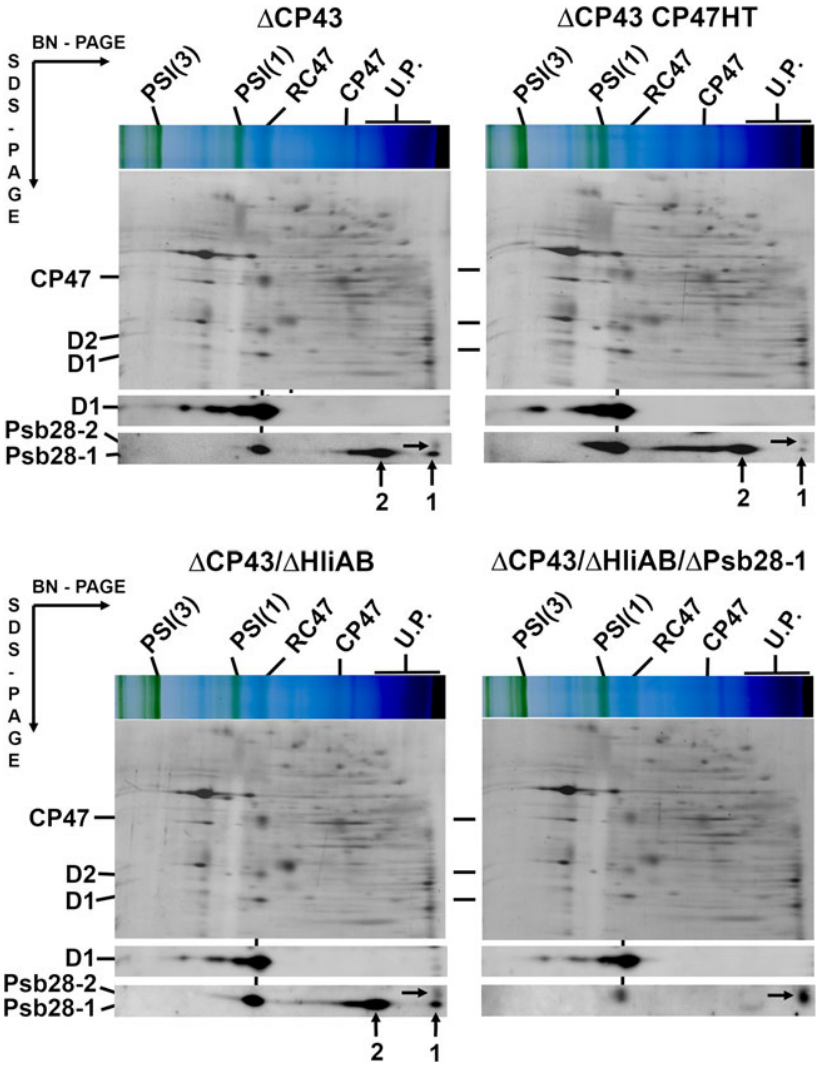

Fig. 4 The occurrence of the monomeric and dimeric forms of Psb28-1 protein in various CP43-less strains. Membranes isolated from the strains cultivated under 10 μmol photons m^{-2} s^{-1} in the presence of 5 mM glucose were analysed by 2D CN/SDS-PAGE. The gel was stained by Sypro Orange and then blotted to PVDF membrane which was probed by antibodies specific to D1, D2 and Psb28-1. The dimeric (2) and monomeric (1) forms of Psb28 are designated by *vertical arrows*. For comparison, signals of Psb28-2 protein corresponding to the monomer obtained using a specific antibody are also shown and designated by *horizontal arrows*. The loaded samples contained 5 μg of Chl

Sequence alignments suggest that a salt bridge may also be present between Glu_{17} and Arg_{19} of Psb28-1 from *Synechocystis* 6803. Our structural analysis also suggests that a second salt bridge might form between Lys_{24} and Glu_{37} of Psb28-1 despite the fact that the loop with Lys_{24} adopts different conformations to the corresponding region in the protein from the thermophilic cyanobacterium. In fact, the flexibility of this region may result from the lack of the stabilizing effect of an intradimeric salt bridge. Based on a structural alignment of the C-terminally tagged Psb28-1 monomer and the Psb28 dimer described here, we speculate that the presence of the His-tag at the C-terminus of Psb28 might impede dimerization (Fig. S5).

Analysis of conserved residues and implications for the structure of Psb28-2

Using the crystal structure of Psb28 from *T. elongatus* described here and sequences of cyanobacterial, algal and plant Psb28-1 and cyanobacterial Psb28-2, we mapped conserved residues on the protein structure using a Consurf analysis (Fig. 3a). This analysis revealed that the conserved hydrophobic residues shown in Fig. 3b create a hydrophobic core inside Psb28 and that most conserved residues are located in two clusters of charged residues. One of them, a patch of acidic residues, forms a β-turn between β4 and β5, whereas the other, composed of basic residues, is found in the middle part of the long C-terminal α-helix. Interestingly, these two clusters interact with each other by means of intramolecular hydrogen bonds and salt bridges (Fig. 3c). By bridging two distant parts of the protein. these interactions seem to enable the formation of the hydrophobic core and probably stabilize the protein structure. Given the relatively high sequence similarity between Psb28-1 and Psb28-2 and that sequences of both the protein sub-families were taken into consideration, this analysis supports the idea that Psb28-2 adopts a very similar 3D fold to Psb28-1.

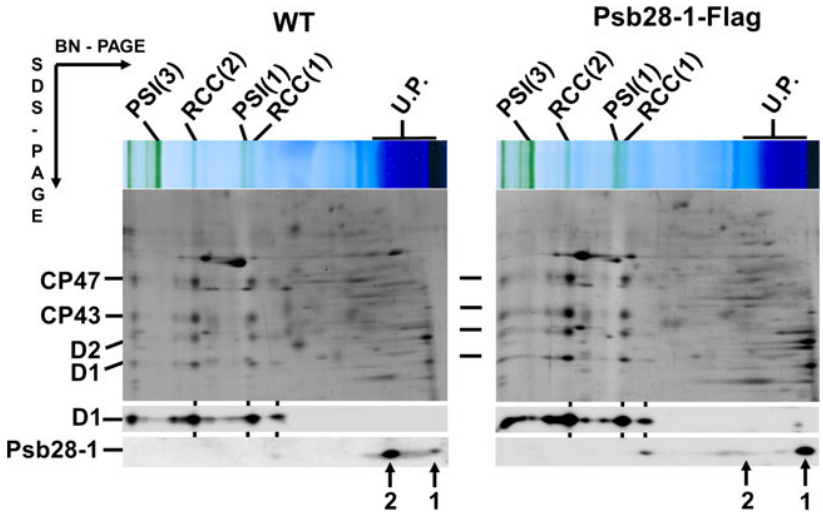

Fig. 5 The occurrence of the monomeric form of Psb28-1 in the strain expressing the C-terminally Flagged Psb28-1 protein. Membranes isolated from both the strains were analysed by 2D BN/SDS-PAGE. The gel was stained by Sypro Orange and then blotted to PVDF membrane which was probed by antibodies specific to D1 and Psb28-1. The dimeric (*2*) and monomeric (*1*) forms of Psb28-1 are designated by *vertical arrows*. The loaded samples contained 5 μg of Chl

Analysis of Psb28-1 and Psb28-2 in *Synechocystis* 6803

To explore the possibility that Psb28-1 and Psb28-2 of *Synechocystis* 6803 might exist in different oligomeric states in vivo, we separated detergent-solubilised membrane protein extracts by BN-PAGE in the first dimension and by SDS-PAGE in the second dimension, followed by immunoblotting using antibodies specific for Psb28-1 and Psb28-2 (Fig. 4). Using this technique, three distinct populations of Psb28-1 were detected. As reported previously some of the Psb28-1 co-migrated with the RC47 complex that accumulates in ΔCP43 mutants (Dobakova et al. 2009; Boehm et al. 2012b), but most (band 2 in Fig. 4) migrated with an apparent molecular mass distinctly larger than that of 'unassembled' Psb28-2 present in all strains but most abundant in the ΔPsb28-1 strain (Fig. 4). Some Psb28-1 did co-migrate with Psb28-2 (band 1 in Fig. 4), but its abundance was variable between samples and sometimes not detected (Boehm et al. 2012b). Control immunoblots confirmed that band 2 of Psb28-1 did not co-migrate with the CP47 subunit (data not shown), and its migration was unaffected in strains lacking either PsbH or four members of the Hli protein family (HliA-D), two of which are known to attach to RC47 under high-light conditions (Fig. S6) (Yao et al. 2007). Together these data suggest that band 2 is probably an oligomer. According to the crystal structure (Fig. S5), dimerisation of Psb28-1 is potentially impaired by addition of a tag at the C-terminus of Psb28-1. Consistent with this hypothesis, a C-terminal 3xFlag-tag derivative of Psb28-1 expressed in *Synechocystis* 6803 now migrated mainly as a monomer (band 1) in the same region of the BN gel as Psb28-2 (Fig. 5).

Conclusion

In summary, we have determined the crystal structure of Psb28 from *T. elongatus* and have provided evidence that Psb28-1, but not Psb28-2, of *Synechocystis* 6803 forms a higher order structure, most likely a dimer, in vivo. The physiological importance of Psb28-1 dimerisation is currently unknown. Our data provide a structural model for how Psb28-1 might oligomerise in vivo which can be tested in the future by mutagenesis. The crystal structure determined here might prove to be useful in determining the site of attachment of Psb28 to PSII determined through cross-linking experiments.

Acknowledgments The authors would like to thank the Biotechnology and Biological Sciences Research Council (BBSRC) for financial support (Grant BB/I00937X/1). JWM holds a BBSRC David Phillips Fellowship (BB/F023308/1). JK and MB were supported by projects Algatech (CZ.1.05/2.1.00/03.0110), RVO61388971 and P501/11/0377 of the Grant Agency of the Czech Republic. The authors wish to thank the staff of the Diamond Light Source for their assistance.

References

Adams PD, Afonine PV, Bunkoczi G, Chen VB, Davis IW, Echols N, Headd JJ, Hung LW, Kapral GJ, Grosse-Kunstleve RW, McCoy AJ, Moriarty NW, Oeffner R, Read RJ, Richardson DC, Richardson JS, Terwilliger TC, Zwart PH (2010) PHENIX: a comprehensive Python-based system for macromolecular structure solution. Acta Crystallogr D 66:213–221

Adir N, Zer H, Shochat S, Ohad I (2003) Photoinhibition—a historical perspective. Photosynth Res 76:343–370

Ashkenazy H, Erez E, Martz E, Pupko T, Ben-Tal N (2010) ConSurf 2010: calculating evolutionary conservation in sequence and structure of proteins and nucleic acids. Nucleic Acids Res 38:W529–W533

Boehm M, Romero E, Reisinger V, Yu J, Komenda J, Eichacker LA, Dekker JP, Nixon PJ (2011) Investigating the early stages of photosystem II assembly in *Synechocystis* sp. PCC 6803: isolation of CP47 and CP43 complexes. J Biol Chem 286:14812–14819

Boehm M, Yu J, Krynicka V, Barker M, Tichy M, Komenda J, Nixon PJ, Nield J (2012a) Subunit organization of a *Synechocystis* hetero-oligomeric thylakoid FtsH complex involved in photosystem II repair. Plant Cell 24:3669–3683

Boehm M, Yu J, Reisinger V, Beckova M, Eichacker LA, Schlodder E, Komenda J, Nixon PJ (2012b) Subunit composition of CP43-less photosystem II complexes of *Synechocystis* sp. PCC 6803: implications for the assembly and repair of photosystem II. Philos Trans R Soc Lond B Biol 367:3444–3454

Chi W, Ma J, Zhang L (2012) Regulatory factors for the assembly of thylakoid membrane protein complexes. Philos Trans R Soc Lond B Biol 367:3420–3429

Dobakova M, Tichy M, Komenda J (2007) Role of the PsbI protein in photosystem II assembly and repair in the cyanobacterium *Synechocystis* sp. PCC 6803. Plant Physiol 145:1681–1691

Dobakova M, Sobotka R, Tichy M, Komenda J (2009) Psb28 protein is involved in the biogenesis of the photosystem II inner antenna CP47 (PsbB) in the cyanobacterium *Synechocystis* sp. PCC 6803. Plant Physiol 149:1076–1086

Emsley P, Lohkamp B, Scott WG, Cowtan K (2010) Features and development of Coot. Acta Crystallogr D 66:486–501

Ferreira KN, Iverson TM, Maghlaoui K, Barber J, Iwata S (2004) Architecture of the photosynthetic oxygen-evolving center. Science 303:1831–1838

Gouet P, Courcelle E, Stuart DI, Metoz F (1999) ESPript: analysis of multiple sequence alignments in postscript. Bioinformatics 15:305–308

Guskov A, Kern J, Gabdulkhakov A, Broser M, Zouni A, Saenger W (2009) Cyanobacterial photosystem II at 2.9-Å resolution and the role of quinones, lipids, channels and chloride. Nat Struct Mol Biol 16:334–342

Holm L, Rosenstrom P (2010) Dali server: conservation mapping in 3D. Nucl Acids Res 38:W545–W549

Hutchinson EG, Thornton JM (1996) PROMOTIF–a program to identify and analyze structural motifs in proteins. Protein Sci 5:212–220

Kamiya N, Shen JR (2003) Crystal structure of oxygen-evolving photosystem II from *Thermosynechococcus vulcanus* at 3.7-Å resolution. Proc Natl Acad Sci USA 100:98–103

Komenda J, Reisinger V, Muller BC, Dobakova M, Granvogl B, Eichacker LA (2004) Accumulation of the D2 protein is a key regulatory step for assembly of the photosystem II reaction center complex in *Synechocystis* PCC 6803. J Biol Chem 279:48620–48629

Komenda J, Kuvikova S, Granvogl B, Eichacker LA, Diner BA, Nixon PJ (2007) Cleavage after residue Ala352 in the C-terminal extension is an early step in the maturation of the D1 subunit of Photosystem II in *Synechocystis* PCC 6803. Biochim Biophys Acta 1767:829–837

Komenda J, Sobotka R, Nixon PJ (2012a) Assembling and maintaining the Photosystem II complex in chloroplasts and cyanobacteria. Curr Opin Plant Biol 15:245–251

Komenda J, Knoppova J, Kopecna J, Sobotka R, Halada P, Yu J, Nickelsen J, Boehm M, Nixon PJ (2012b) The Psb27 assembly factor binds to the CP43 complex of photosystem II in the cyanobacterium *Synechocystis* sp. PCC 6803. Plant Physiol 158:476–486

Krissinel E, Henrick K (2004) Secondary-structure matching (SSM), a new tool for fast protein structure alignment in three dimensions. Acta Crystallogr D 60:2256–2268

Krissinel E, Henrick K (2007) Inference of macromolecular assemblies from crystalline state. J Mol Biol 372:774–797

Liu H, Roose JL, Cameron JC, Pakrasi HB (2011) A genetically tagged Psb27 protein allows purification of two consecutive photosystem II (PSII) assembly intermediates in *Synechocystis* 6803, a cyanobacterium. J Biol Chem 286:24865–24871

Loll B, Kern J, Saenger W, Zouni A, Biesiadka J (2005) Towards complete cofactor arrangement in the 3.0 Å resolution structure of photosystem II. Nature 438:1040–1044

Mayes SR, Dubbs JM, Vass I, Hideg E, Nagy L, Barber J (1993) Further characterization of the *psbH* locus of *Synechocystis* sp. PCC 6803: inactivation of *psbH* impairs Q_A to Q_B electron transport in photosystem 2. Biochemistry 32:1454–1465

McCoy AJ, Grosse-Kunstleve RW, Adams PD, Winn MD, Storoni LC, Read RJ (2007) Phaser crystallographic software. J Appl Crystalogr 40:658–674

Michoux F, Takasaka K, Boehm M, Nixon PJ, Murray JW (2010) Structure of CyanoP at 2.8 Å: implications for the evolution and function of the PsbP subunit of photosystem II. Biochemistry 49:7411–7413

Michoux F, Takasaka K, Boehm M, Komenda J, Nixon PJ, Murray JW (2012) Crystal structure of the Psb27 assembly factor at 1.6 Å: implications for binding to Photosystem II. Photosynth Res 110:169–175

Murshudov GN, Skubak P, Lebedev AA, Pannu NS, Steiner RA, Nicholls RA, Winn MD, Long F, Vagin AA (2011) REFMAC5 for the refinement of macromolecular crystal structures. Acta Crystallogr D 67:355–367

Nixon PJ, Trost JT, Diner BA (1992) Role of the carboxy terminus of polypeptide D1 in the assembly of a functional water-oxidizing manganese cluster in photosystem II of the cyanobacterium *Synechocystis* sp. PCC 6803: assembly requires a free carboxyl group at C-terminal position 344. Biochemistry 31:10859–10871

Nixon PJ, Michoux F, Yu J, Boehm M, Komenda J (2010) Recent advances in understanding the assembly and repair of photosystem II. Ann Bot 106:1–16

Nowaczyk MM, Krause K, Mieseler M, Sczibilanski A, Ikeuchi M, Rogner M (2012) Deletion of *psbJ* leads to accumulation of Psb27-Psb28 photosystem II complexes in *Thermosynechococcus elongatus*. Biochim Biophys Acta 1817:1339–1345

Promnares K, Komenda J, Bumba L, Nebesarova J, Vacha F, Tichy M (2006) Cyanobacterial small chlorophyll-binding protein ScpD (HliB) is located on the periphery of photosystem II in the vicinity of PsbH and CP47 subunits. J Biol Chem 281:32705–32713

Sakata S, Mizusawa N, Kubota-Kawai H, Sakurai I, Wada H (2013) Psb28 is involved in recovery of photosystem II at high temperature in *Synechocystis* sp. PCC 6803. Biochim Biophys Acta 1827:50–59

Shen G, Boussiba S, Vermaas WFJ (1993) *Synechocystis* sp. PCC 6803 strains lacking photosystem I and phycobilisome function. Plant Cell 5:1856–1863

Umena Y, Kawakami K, Shen JR, Kamiya N (2011) Crystal structure of oxygen-evolving photosystem II at a resolution of 1.9 Å. Nature 473:55–60

Vavilin D, Yao D, Vermaas W (2007) Small Cab-like proteins retard degradation of photosystem II-associated chlorophyll in *Synechocystis* sp. PCC 6803: kinetic analysis of pigment labeling with ^{15}N and ^{13}C. J Biol Chem 282:37660–37668

Vermaas WFJ, Ikeuchi M, Inoue Y (1988) Protein composition of the photosystem II core complex in genetically engineered mutants of the cyanobacterium *Synechocystis* sp. PCC 6803. Photosynth Res 17:97–113

Williams JGK (1988) Construction of specific mutations in PSII photosynthetic reaction center by genetic engineering methods in *Synechocystis* 6803. Methods Enzymol 167:766–778

Xu H, Vavilin D, Funk C, Vermaas W (2002) Small Cab-like proteins regulating tetrapyrrole biosynthesis in the cyanobacterium *Synechocystis* sp. PCC 6803. Plant Mol Biol 49:149–160

Yang Y, Ramelot TA, Cort JR, Wang D, Ciccosanti C, Hamilton K, Nair R, Rost B, Acton TB, Xiao R, Everett JK, Montelione GT, Kennedy MA (2011) Solution NMR structure of photosystem II reaction center protein Psb28 from *Synechocystis* sp. Strain PCC 6803. Proteins 79:340–344

Yao D, Kieselbach T, Komenda J, Promnares K, Prieto MA, Tichy M, Vermaas W, Funk C (2007) Localization of the small CAB-like proteins in photosystem II. J Biol Chem 282:267–276

4.2.1 Supplemental information

Table S1 Hydrogen bonds between dimer partners in dimeric Psb28 from *T. elongatus*

#	Chain	Dist. [Å]	Chain
1	B:LEU$_{23}$[N]	2.86	A:VAL$_{21}$[O]
2	B:VAL$_{21}$[N]	2.99	A:LEU$_{23}$[O]
3	B:GLY$_{109}$[N]	2.84	A:GLY$_{29}$[O]
4	B:ARG $_{27}$[N$^{\eta 2}$]	2.72	A:ASP$_{39}$[O$^{\delta 2}$]
5	B:TRP$_{92}$[N$^{\varepsilon 1}$]	2.95	A:ALA$_{103}$[O]
6	B:ARG$_{25}$[N$^{\varepsilon}$]	2.85	A:HIS$_{106}$[O]
7	B:ARG$_{25}$[N$^{\varepsilon}$]	3.17	A:GLY$_{107}$[O]
8	B:ARG$_{25}$[N$^{\eta 2}$]	2.90	A:GLY$_{107}$[O]
9	B:GLU$_{16}$[O]	3.77	A: ARG$_{27}$[N$^{\eta 1}$]
10	B:ASP$_{20}$[O$^{\delta 2}$]	3.71	A:ARG$_{22}$[N$^{\eta 1}$]
11	B:VAL$_{21}$[O]	2.77	A:LEU$_{23}$[N]
12	B:LEU$_{23}$[O]	3.04	A:VAL$_{21}$[N]
13	B:GLY$_{29}$[O]	2.85	A:GLY$_{109}$[N]
14	B:ALA$_{103}$[O]	2.82	A:TRP$_{92}$[N$^{\varepsilon 1}$]
15	B:HIS$_{106}$[O]	2.92	A:ARG$_{25}$[N$^{\varepsilon}$]
16	B:GLY$_{107}$[O]	3.10	A:ARG$_{25}$[N$^{\varepsilon}$]
17	B:GLY$_{107}$[O]	2.96	A:ARG$_{25}$[N$^{\eta 2}$]

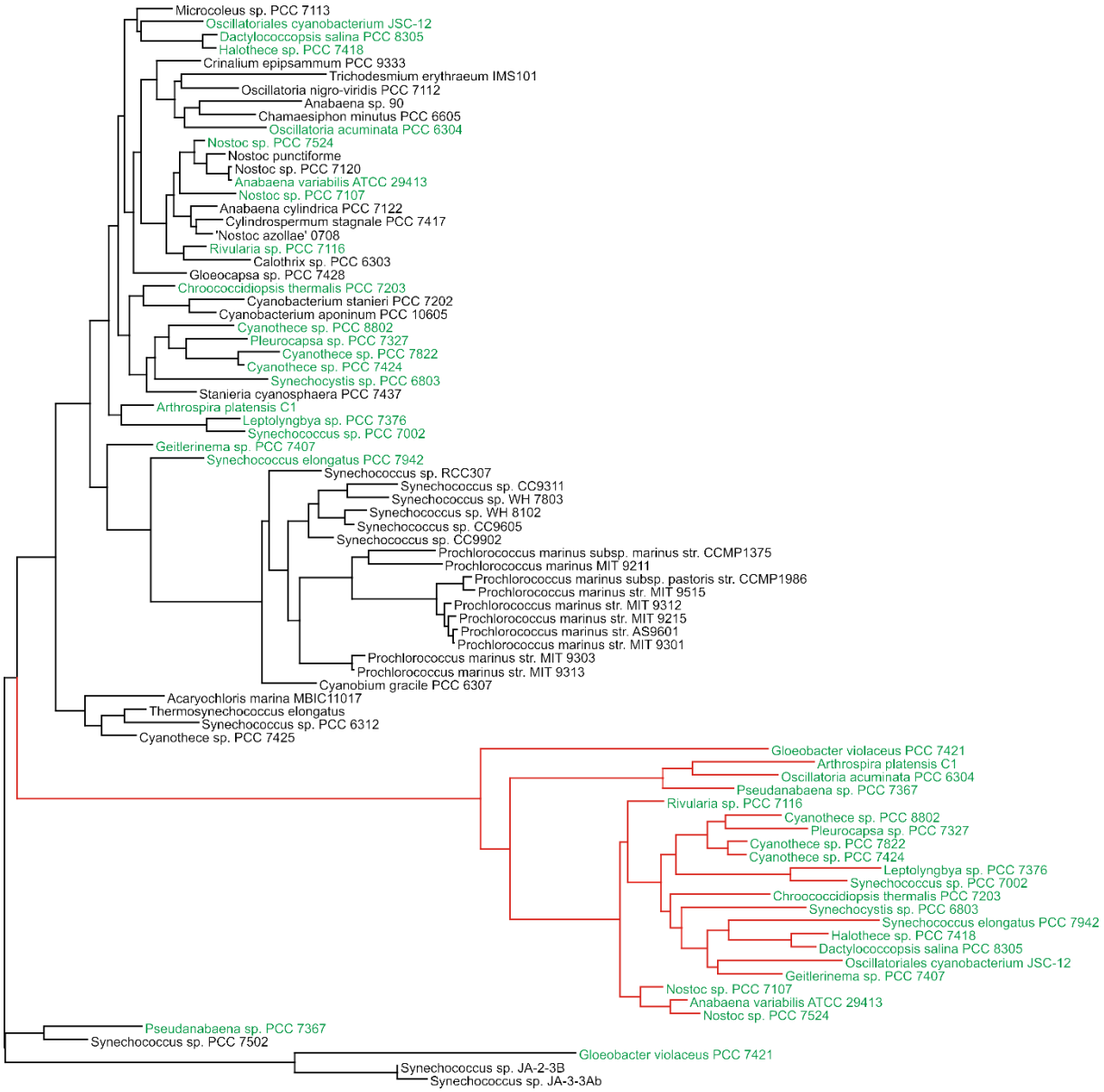

Figure S1 Phylogenetic analysis of Psb28-1 and 28-2 in completely sequenced cyanobacterial genomes (as of November 2012). Cyanobacterial species harboring genes for both Psb28-1 (black lines) and Psb28-2 (red lines) are highlighted in green.

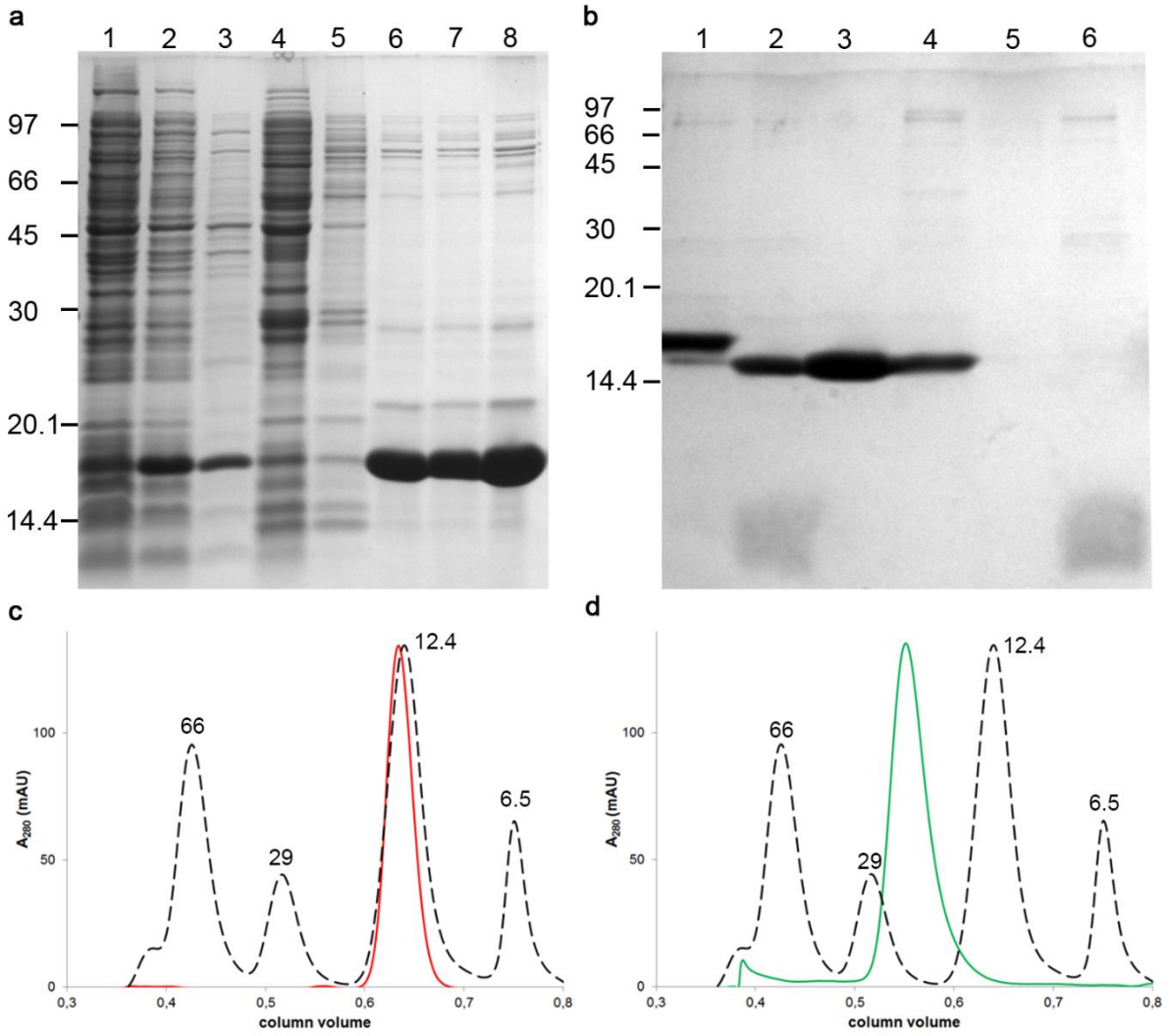

Figure S2 Over-expression and isolation of *T. elongatus* Psb28 from *E. coli.* **a** Coomassie blue-stained SDS-PAGE gel of *E. coli* fractions isolated by immobilized nickel-affinity chromatography. *E. coli* cells before induction (lane 1); soluble fraction after induction loaded onto Ni^{2+}-column (lane 2); unbound fraction (lane 3); wash 1 and 2 with 50 mM imidazole (lanes 4 and 5); eluted fractions obtained with 300 mM imidazole (lanes 6-8). Molecular masses of the protein ladder are given in kDa. **b** Coomassie blue-stained SDS-PAGE gel of samples isolated after thrombin cleavage. His-tagged Psb28 before tag removal (lane 1); sample after overnight digestion with thrombin (lane 2); Ni^{2+}-column flow-through (lane 3); Ni^{2+}-column washes with 50 mM imidazole (lane 4); 50 mM imidazole (lane 5) and 300 mM imidazole (lane 6). **c** and **d** Size-exclusion analysis of Psb28 after removal of His-tag. The normalized chromatograms show that the protein elutes mainly in the form of a monomer with calculated mass of ~13 kDa or a dimer (~26 kDa) when the column was equilibrated with 50 mM Tris pH 8.0, 0.15 M NaCl (**c**) or 50 mM MES pH 6.5, 5 mM $MgCl_2$, 5 mM $CaCl_2$ (**d**), respectively. Dashed line represents a calibration run of protein standards given in kDa.

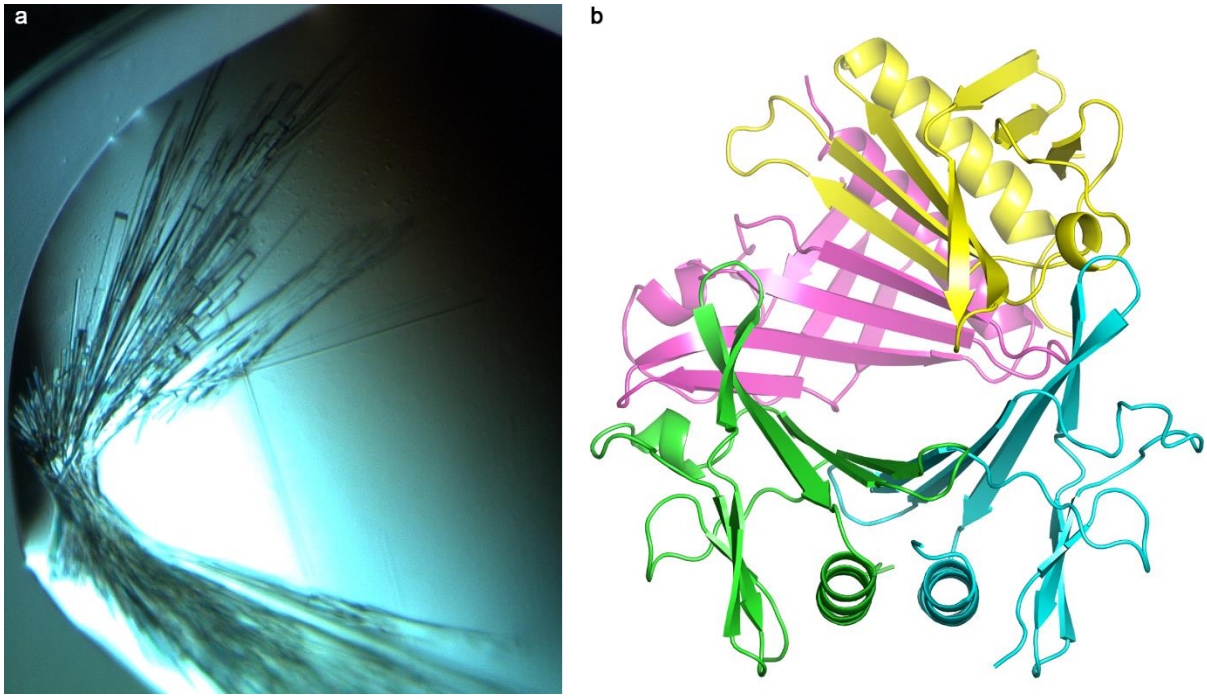

Figure S3 a Crystals of Psb28 from *T. elongatus* in 100 mM HEPES sodium salt pH 7.5, 20% (v/v) PEG200, 20% (w/v) PEG 4000, 10% (v/v) 2-propanol. **b** Cartoon representation of the 4 Psb28 molecules in the asymmetric unit.

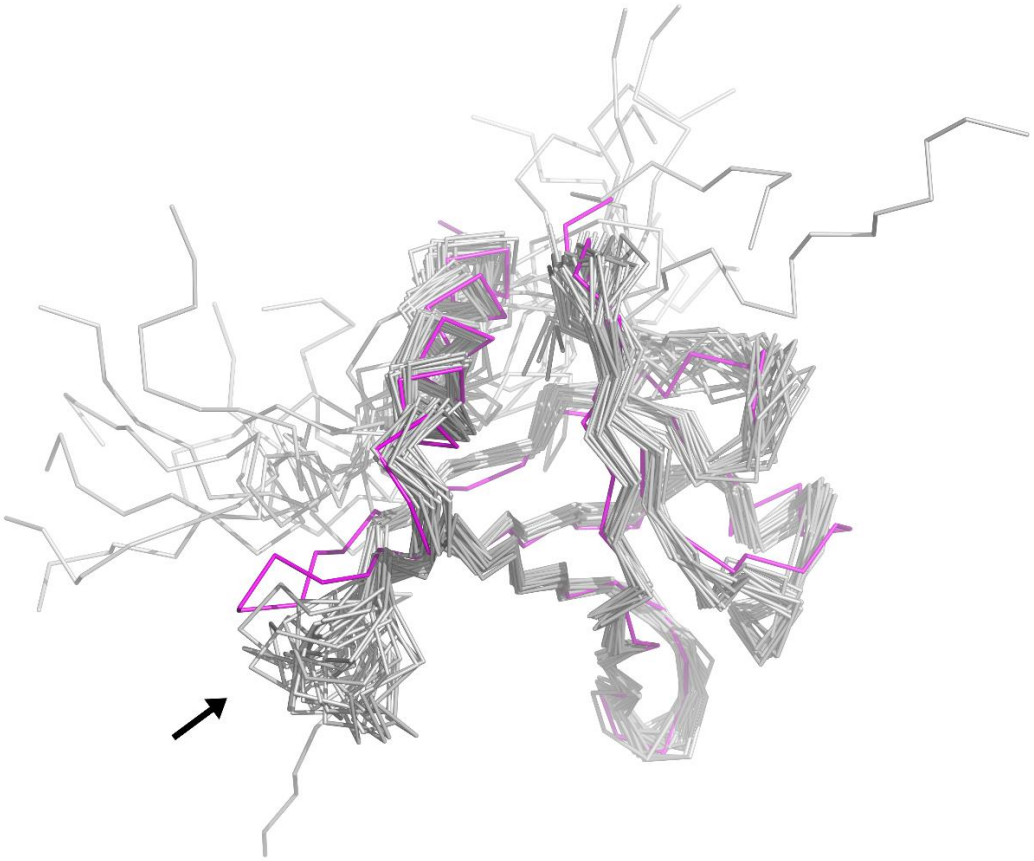

Figure S4 Comparison of structure of Psb28 from *T. elongatus* (magenta) with solution structure of Psb28-1 from *Synechocystis* 6803 (gray). The former was solved by X-ray crystallography and the latter by NMR and all the models in the ensemble are depicted here. The arrow shows the least similar region in both structures.

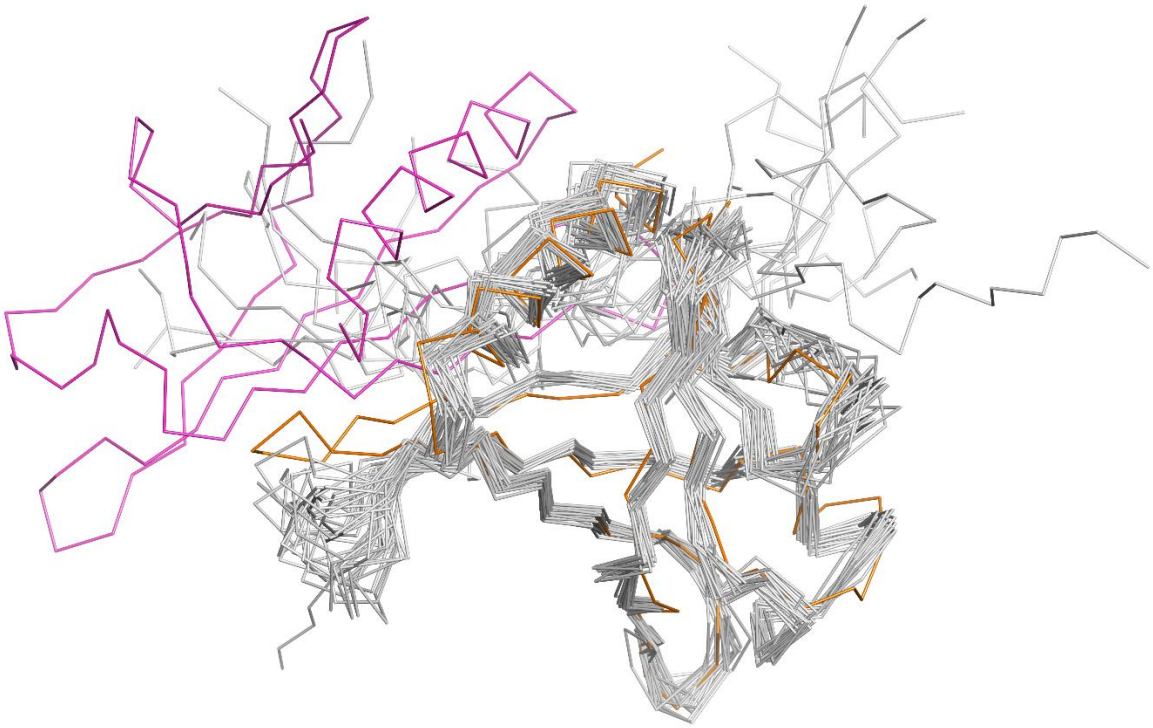

Figure S5 Dimeric Psb28 from *T. elongatus* (magenta and orange) superimposed onto Psb28-1 from *Synechocystis* 6803 (gray). The protein from *T. elongatus* was crystallized in a dimeric form without the fusion tag, whereas the NMR ensemble shows a monomeric Psb28 from *Synechocystis* 6803 with C-terminal His-tag. N and C-termini are color-coded as protein molecules.

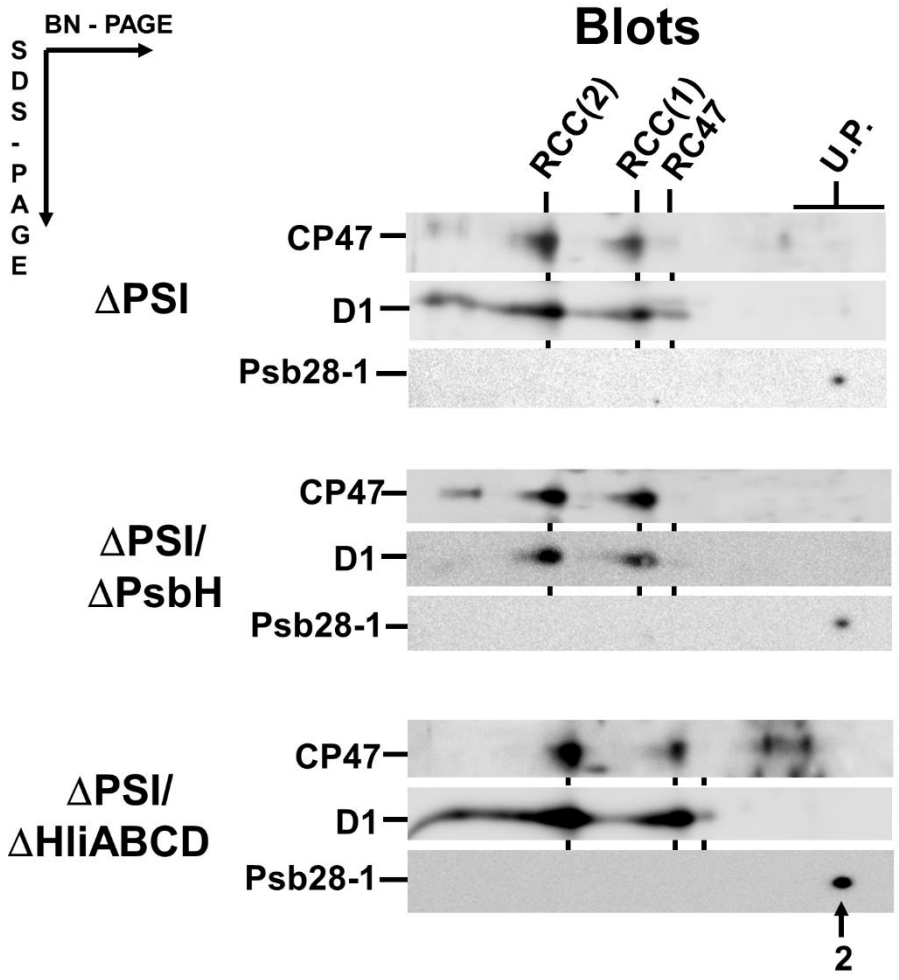

Figure S6 The electrophoretic mobility of the putative dimeric form of Psb28 remains the same in strain lacking a small PSII subunit PsbH or small Hli proteins. Membranes isolated from all three PSI-less strains grown in the presence of glucose were analyzed by 2D electrophoresis. The gel was blotted to PVDF membrane which was probed by antibodies specific to CP47, D1 and Psb28-1. The dimeric (2) form of Psb28 is designated by the vertical arrow. The loaded sample contained 1 μg of Chl.

4.3 Strain of *Synechocystis* PCC 6803 with aberrant assembly of Photosystem II contains tandem duplication of a large chromosomal region.

Reprint of: Tichý, M., Bečková, M., Kopečná, J., Noda, J., Sobotka, R., and Komenda, J. (2016). Front. Plant Sci. 7:648. doi: 10.3389/fpls.2016.00648.

frontiers in Plant Science

ORIGINAL RESEARCH
published: 12 May 2016
doi: 10.3389/fpls.2016.00648

Strain of Synechocystis PCC 6803 with Aberrant Assembly of Photosystem II Contains Tandem Duplication of a Large Chromosomal Region

Martin Tichý[1,2], *Martina Bečková*[1,2], *Jana Kopečná*[1], *Judith Noda*[1], *Roman Sobotka*[1,2] *and Josef Komenda*[1,2]*

[1] Laboratory of Photosynthesis, Institute of Microbiology, Academy of Sciences of the Czech Republic, Center Algatech, Třeboň, Czech Republic, [2] Faculty of Science, University of South Bohemia, České Budějovice, Czech Republic

Cyanobacterium *Synechocystis* PCC 6803 represents a favored model organism for photosynthetic studies. Its easy transformability allowed construction of a vast number of *Synechocystis* mutants including many photosynthetically incompetent ones. However, it became clear that there is already a spectrum of *Synechocystis* "wild-type" substrains with apparently different phenotypes. Here, we analyzed organization of photosynthetic membrane complexes in a standard motile Pasteur collection strain termed PCC and two non-motile glucose-tolerant substrains (named here GT-P and GT-W) previously used as genetic backgrounds for construction of many photosynthetic site directed mutants. Although, both the GT-P and GT-W strains were derived from the same strain constructed and described by Williams in 1988, only GT-P was similar in pigmentation and in the compositions of Photosystem II (PSII) and Photosystem I (PSI) complexes to PCC. In contrast, GT-W contained much more carotenoids but significantly less chlorophyll (Chl), which was reflected by lower level of dimeric PSII and especially trimeric PSI. We found that GT-W was deficient in Chl biosynthesis and contained unusually high level of unassembled D1-D2 reaction center, CP47 and especially CP43. Another specific feature of GT-W was a several fold increase in the level of the Ycf39-Hlip complex previously postulated to participate in the recycling of Chl molecules. Genome re-sequencing revealed that the phenotype of GT-W is related to the tandem duplication of a large region of the chromosome that contains 100 genes including ones encoding D1, Psb28, and other PSII-related proteins as well as Mg-protoporphyrin methylester cyclase (Cycl). Interestingly, the duplication was completely eliminated after keeping GT-W cells on agar plates under photoautotrophic conditions for several months. The GT-W strain without a duplication showed no obvious defects in PSII assembly and resembled the GT-P substrain. Although, we do not exactly know how the duplication affected the GT-W phenotype, we hypothesize that changed stoichiometry of protein components of PSII and Chl biosynthetic machinery encoded by the duplicated region impaired properassembly and functioning of these multi-subunit complexes. The study also emphasizes the crucial importance of a proper control strain for evaluating *Synechocystis* mutants.

Keywords: ***Synechocystis*** **6803, chlorophyll, photosystem I, photosystem II assembly, large tandem duplication**

OPEN ACCESS

Edited by:
John Love,
University of Exeter, UK

Reviewed by:
Alessandro Vitale,
CNR–National Research Council of Italy, Italy
Ben Matthew Abell,
Sheffield Hallam University, UK

***Correspondence:**
Josef Komenda
komenda@alga.cz

Specialty section:
This article was submitted to Plant Cell Biology, a section of the journal Frontiers in Plant Science

Received: *14 December 2015*
Accepted: *28 April 2016*
Published: *12 May 2016*

Citation:
Tichý M, Bečková M, Kopečná J, Noda J, Sobotka R and Komenda J (2016) Strain of Synechocystis PCC 6803 with Aberrant Assembly of Photosystem II Contains Tandem Duplication of a Large Chromosomal Region. Front. Plant Sci. 7:648. doi: 10.3389/fpls.2016.00648

INTRODUCTION

Cyanobacteria represent excellent model organisms for photosynthesis research as they perform oxygenic photosynthesis similar to that in algae and plants while having much simpler cellular organization. Unlike the other photosynthetic bacteria they possess both types of reaction center and oxidize water to molecular oxygen by Photosystem II (PSII) and reduce NADP by Photosystem I (PSI). For both pigment-protein complexes the high resolution crystal structures are available, mostly thanks to thermophilic cyanobacteria with very stable complexes ideal for crystallographic analysis (Jordan et al., 2001; Ferreira et al., 2004; Umena et al., 2011).

PSII is the multi-subunit membrane complex that utilizes light energy to catalyze oxidation of water. For this process to occur the inner symmetrically located antennae CP47 and CP43 containing chlorophyll (Chl) and β-carotene deliver absorbed light energy to a pair of reaction center (RCII) subunits called D1 and D2, which bind the cofactors involved in primary charge separation. There are also around 13 small, mostly single helix trans-membrane subunits mostly bound at the periphery of D1, D2, CP47, and CP43 (Ferreira et al., 2004; Guskov et al., 2009; Umena et al., 2011). The lumenal part of the complex is the binding site for the PsbO, PsbU, and PsbV extrinsic subunits (reviewed in Roose et al., 2007) which optimize the environment for the $CaMn_4O_5$ cluster extracting electrons from water (Ferreira et al., 2004; Guskov et al., 2009; Umena et al., 2011).

Information on the biogenesis of cyanobacterial PSII is less complete and mostly comes from characterization of this process in the cyanobacterium *Synechocystis* PCC 6803 (hereafter *Synechocystis*). This cyanobacterial strain is able to grow in the presence of glucose even without functional PSII and is therefore appropriate for constructing site-directed mutants affected in its assembly (Williams, 1988). Existing data indicate that each large Chl-protein initially forms a pre-complex (module) containing neighboring low-molecular-mass polypeptides plus pigments and cofactors. These modules are afterwards combined in a step-wise fashion initially into the PSII reaction center (RCII) complex consisting of D1 and D2 modules, then CP47 module is attached forming a complex called RC47 (Boehm et al., 2011, 2012). Finally the PSII core complex is completed after binding of the CP43 module (Boehm et al., 2011). The light-driven assembly of the oxygen-evolving $CaMn_4O_5$ cluster occurs afterwards and is assisted by the lumenal extrinsic proteins (Nixon et al., 2010). Accessory factors, such as Ycf39, Ycf48, Psb27, Psb28, and others, associate transiently with PSII at specific stages of assembly but their functions remain unclear (Komenda et al., 2012b).

Availability of high-throughput sequencing techniques allowed genomic sequence comparison among various WT-variants (substrains) of *Synechocystis* used in many laboratories and revealed inherent sequence variability among them. The history of the *Synechocystis* WT-variants has been described recently (Morris et al., 2014). The original motile Pasteur Culture Collection 6803 strain has been used to generate a non-motile, glucose tolerant strain (Williams, 1988). This strain has been disseminated to several laboratories around the world, resulting in many "wild-type" substrains.

In the present study we compared organization of photosynthetic membrane complexes with emphasis on PSII assembly in three *Synechocystis* substrains, two of them variants of the Williams glucose-tolerant strain. The comparison showed that the level and assembly state of PSII (and PSI) in the glucose-tolerant strain obtained from the laboratory at Imperial College London was similar to that in the standard motile Pasteur Culture collection strain (PCC). In contrast, the glucose tolerant strain originating from the strain used in the Arizona lab of Wim Vermaas showed aberrant assembly of PSII, much lower level of PSI related to the decreased synthesis of Chl and high content of carotenoids. Sequencing of the latter strain showed that its genome contains a tandem duplication of a large chromosomal region, most probably responsible for the observed phenotype.

EXPERIMENTAL PROCEDURES

Strains, Their Origin, Construction, and Cultivation

The strains used in this study were the motile, glucose sensitive strain of *Synechocystis* sp. PCC 6803 from the Pasteur collection, and two glucose-tolerant strains (Williams, 1988): GT-P obtained from the laboratory of Prof. Peter Nixon at Imperial College London and GT-W obtained from the laboratory of Prof. Wim Vermaas at Arizona State University. Frozen stocks of GT-P from 2002 and GT-W from 1999 were used for characterization and sequencing. The Psb28-lacking strains were transformed using genomic DNAs isolated from a previously constructed Psb28-less strain (Dobáková et al., 2009). *Synechocystis* strains were grown autotrophically in a rotary shaker under irradiance of 40 μmol photons m^{-2} s^{-1} at 30°C in liquid BG11 medium (Rippka et al., 1979). All experiments and measurements with cells were performed at least in triplicate and typical results are shown in figures.

Cell Absorption Spectra and Determination of Chl Content

Absorption spectra of whole cells were measured at room temperature using a Shimadzu UV-3000 spectrophotometer (Kyoto, Japan). To determine Chl levels, pigments were extracted from cell pellets with 100% methanol and the Chl concentration was determined spectroscopically (Porra et al., 1989).

Determination of Chromosomes Number by Flow Cytometry

Single colonies of GT-P and GT-W strains were inoculated in 50 ml of BG11 medium and grown under standard conditions until they reached a final $OD_{730\,nm}$ value 0.3–0.5. Two milliliters of cells were collected by centrifugation at 8000 × g for 5 min and washed once with fresh media. Collected cells were fixed with 1 ml of 70% ethanol and incubated for 1 h at room temperature. In order to remove residual fixation solution, cells

were washed twice with PBS buffer and resuspended in 100 µl of the same buffer. One microliter of RNAase A was added and samples were incubated for 1 h at 37°C. After enzymatic degradation of RNA, 900 µl of PBS were added, and cells were stained for 20 min in darkness with the cell permeant fluorochrome SYBR Safe (Life Technologies), used in a 1:10,000 dilution of commercial stock. To prepare the reference, with one chromosome per cell a single colony of *Escherichia coli (E. coli)* strain BL-21 was inoculated in 2 ml of M9 minimal media. The culture was grown overnight at 37°C and then supplemented with 20 µg ml^{-1} of chloramphenicol. After 1.5 h of growth in the presence of antibiotic, cells were harvested by centrifugation at 8000 × g for 5 min and fixed and stained by the same method used for *Synechocystis* cells. *Synechocystis* and *E. coli* stained cells were loaded on an APOGEE cytometer (Apogee Flow Systems), and at least 20,000 events were recorded. Samples were excited using a 488 nm laser and the fluorescence emission was collected by a detector with a 530/30 nm filter. The chromosome copy number of *Synechocystis* strains was estimated using the chloramphenicol-treated *E. coli* culture as a standard.

Analysis of Pigments by HPLC

For quantitative determination of Chl precursors, three milliliters of culture at $OD_{750\,nm}$ = 0.5–0.6 was spun down and resuspended in 20 µL of water. Pigments were extracted with an excess of 70% methanol/30% water, filtrated and immediately analyzed via HPLC (Agilent-1200). Separation was carried out on a reverse phase column (ReproSil pur 100, C8, 3 µm particle size, 4 × 150 mm, Watrex) with 35% methanol and 15% acetonitrile in 0.25 M pyridine (solvent A) and 50% methanol in acetonitrile as solvents B. Pigments were eluted with a gradient of solvent B (40%–52% in 5 min) followed by 52–55% of solvent B in 30 min at a flow rate of 0.8 ml min^{-1} at 40°C. Eluted pigments were detected by two fluorescence detectors set at several different wavelengths to detect all Chl precursors from coproporphyrin(ogen) III (Copro III) to monovinyl-chlorophyllide (Chlide); for details see Kopečná et al. (2015)

2D Electrophoresis, Immunodetection, and Protein Radiolabeling

Membrane and soluble protein fractions were isolated from 50 ml of cells at $OD_{750\,nm}$ ∼0.4 according to Dobáková et al. (2009) using buffer A (25 mM MES/NaOH, pH 6.5, 5 mM $CaCl_2$, 10 mM $MgCl_2$, 25% glycerol). Isolated membrane complexes (0.25 mg ml^{-1} Chl) were solubilized in buffer A containing 1% n-dodecyl-β-D-maltoside and analyzed either by blue-native (BN) or by clear-native (CN) PAGE at 4°C in a 4–14% gradient polyacrylamide as described in Komenda et al. (2012a). The protein composition of the complexes were analyzed by electrophoresis in a denaturing 12–20% linear gradient polyacrylamide gel containing 7 M urea (Komenda et al., 2012a). Proteins separated in the gel were stained by SYPRO Orange and the gel was either dried and exposed on a Phosphorimager plate or blotted onto a PVDF membrane. Membranes were incubated with specific primary antibodies and then with secondary antibody-horseradish peroxidase conjugate (Sigma, St. Louis, USA). The primary antibodies used in this study were raised in rabbits against: (i) residues 58–86 of the spinach D1 polypeptide; (ii) residues 311-322 of Ycf39 (Knoppová et al., 2014); and (iii) the last 15 residues of *Synechocystis* Psb28 (Dobáková et al., 2009). Antibody against *Synechocystis* ferrochelatase was kindly provided by Prof. Annegret Wilde (Albert Ludwigs Universität, Freiburg) and antibody against barley Mg-protoporphyrin methyl ester oxidative cyclase was kindly provided by Prof. Poul Erik Jensen (University of Copenhagen).

For protein and Chl labeling, the cells were incubated with [^{14}C]glutamate for 30 min as described in Kopečná et al. (2012). After separation of labeled proteins by CN PAGE in the first dimension and by SDS PAGE in the second dimension the 2D 18% polyacrylamide gel was stained by SYPRO Orange, scanned for fluorescence and dried. The gel was exposed on a Phosphorimager plate overnight, scanned by Storm and, for evaluation of Chl labeling, the image was quantified by ImageQuant 5.2 software (all from GE Healthcare, Vienna, Austria).

Genome Re-Sequencing and Mapping

Synechocystis re-sequencing was performed commercially at the Gene Profiling Facility, Princess Margaret Hospital, Toronto. One hundred base paired-end sequencing was performed on a Illumina HiSeq 2000 system (12 samples per lane). Raw paired reads were mapped to the GT-Kazusa sequence using Geneious 7.0 software (http://www.geneious.com; Kearse et al., 2012). Only variants with a higher than 60% frequency were considered. Alternatively, read sequences were assembled *de novo* with the Geneious 7.0 software before mapping to the reference.

RESULTS

Three Variants of the *Synechocystis* Wild Type Strain: Their History and Organization of Photosynthetic Complexes

We compared three *Synechocystis* strains that are used in our laboratory for construction of various, mostly photosynthetic mutants. While the glucose sensitive motile strain, designated here PCC, was directly obtained from Pasteur Culture Collection, the other two strains originated from the glucose-tolerant Williams strain (Williams, 1988). The first one, which we named GT-P, was first grown in the Dupont laboratory of Bruce Diner from which it was transferred to Imperial College (London) and later to our laboratory in Třeboň (Institute of Microbiology, Czech Academy of Sciences). The second one, named GT-W, came from the laboratory of Wim Vermaas (Arizona State University).

Comparison of absorption spectra of the three strains grown autotrophically showed a large similarity between the PCC and GT-P, with the only apparent difference being a higher

phycobilisome content (maximum at 625 nm) in PCC (**Figure 1**). On the other hand, the GT-W strain contained much more carotenoids and less Chl than both previously mentioned strains. Interestingly, when both strains were grown in the presence of 5 mM glucose, in both strains the amount of carotenoids decreased but the level of Chl decreased only in GT-P while in GT-W it increased (Figure S1).

The differences in cellular absorption spectra of autotrophic cultures were also reflected by differences in the content of photosynthetic membrane complexes assessed by 2D blue-native/SDS-PAGE (**Figure 2**). In this respect PCC and GT-P were very similar containing the majority of PSI and PSII as trimers and dimers, respectively, and relatively low levels of the monomeric PSII core complex and CP43-less PSII (RC47). The strains also contained only very low amounts of unassembled CP47 and CP43 and no detectable antenna-less RCII complexes. In contrast, unusually high amounts of unassembled CP47 and especially CP43 were detected in the GT-W strain. Immunoblotting also revealed accumulation of RCII complexes and a concomitant several fold increase in the amount of Ycf39 detected as a component of a larger of two RCII complexes (RCII*) and especially as the unassembled complex with Hlips (Knoppová et al., 2014). Moreover, the levels of PSI trimer and PSII dimers were similar to the levels of their monomeric forms. Finally, cytochrome b_6f complex was present in PCC and GT-P almost exclusively as a monomer while almost equal amounts of dimer and monomer was detected in GT-W. In summary, the strain GT-W showed unusual pigment-protein composition different from the other two strains suggesting aberrant assembly of photosynthetic complexes, namely PSII, and their lower cellular content.

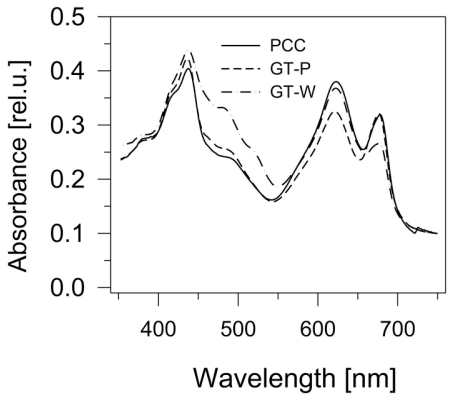

FIGURE 1 | Whole cell absorption spectra of three *Synechocystis* strains PCC, GT-P, and GT-W. The spectra were measured by Shimadzu UV3000 spectrophotometer and were normalized for absorbance of 0.1 at 750 nm.

Chlorophyll Biosynthesis is Strongly Affected in GT-W

As the trimeric PSI complex is the main sink for newly produced Chl molecules in *Synechocystis* (Kopečná et al., 2012), the low PSI level in cells of GT-W should be reflected by changes in Chl metabolism. To assess the rate of *de novo* Chl formation we labeled cells of both GT strains using [^{14}C]glutamate and analyzed Ch-binding membrane complexes using 2D clear-native/SDS-PAGE. In order to separate free pigments from

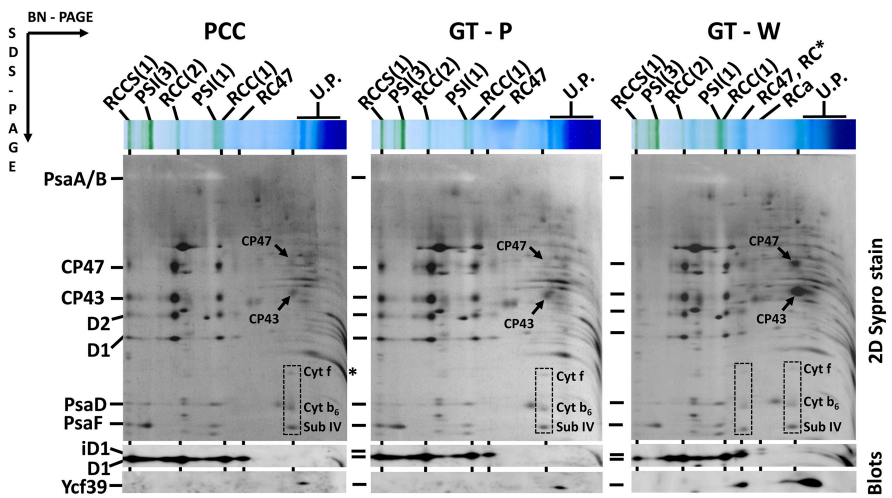

FIGURE 2 | Organization of photosynthetic membrane complexes in PCC, GT-P, and GT-W strains assessed by 2D blue-native/SDS-PAGE in combination with immunoblotting. Membrane proteins of thylakoids isolated from each strain were separated by 4–14% blue-native PAGE, and then in the second dimension by 12–20% SDS-PAGE. The 2D gel was stained by SYPRO Orange and then blotted to a PVDF membrane. The D1 and Ycf39 proteins were detected by specific antibodies (Blots). Unassembled CP47 and CP43 are designated by arrows and subunits of cyt b_6–f complex (Cyt f, cyt b_6, and subunit IV in order from top to bottom) are boxed. Other designations: RCCS1, PSI–PSII supercomplex; RCC(2), and RCC(1), dimeric, and monomeric PSII core complexes; PSI(3) and PSI(1), trimeric and monomeric PSI; RC47, PSII core complex lacking CP43; RC* and RCa, PSII reaction center complexes lacking CP47 and CP43; U.P., unassembled proteins. Arrows indicate unassembled forms of CP47 and CP43 very abundant in GT-W. Each loaded sample contained 5 μg of Chl.

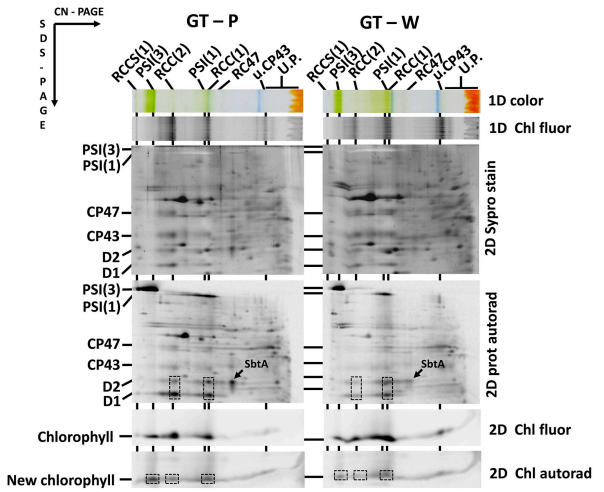

FIGURE 3 | Radiolabeling of membrane proteins and chlorophyll in the GT-P and GT-W strains. Cells of each strain were radiolabeled by [^{14}C]glutamate. Membrane proteins and pigments were then separated by 2D clear-native/SDS-PAGE. Pigment-protein complexes were separated by 2D CN/SDS-PAGE. The first dimension 4-14% native gel was photographed (1D color) and scanned for fluorescence by LAS 4000 (1D Chl fluor). The second dimension 18% SDS PAGE gel was stained with SYPRO (2D SYPRO stain) and scanned for Chl fluorescence (2D Chl fluor). Radioactivity in proteins (2D prot autorad) and in released Chl (2D Chl Autorad) in dried gels was detected by Phosphoimager. The overall signal of the labeled Chl in GT-W quantified by Image Quant software was 37 ± 9% of that in GT-P. The value represents a mean ± SD from three independent measurements. The most important differences between the strains in the amounts of labeled protein (monomeric and dimeric PSII complexes) and Chl (PSI trimer and monomer and PSII dimer) are emphasized by boxes. The labeling of SbtA is also designated by an arrow. Each loaded sample contained 5 µg of Chl. All designations used are described in **Figure 2**.

proteins, we performed 2D protein analysis in the 18% gel, which was briefly stained by SYPRO Orange, scanned for Chl and SYPRO fluorescence and then immediately dried up to retain maximal amounts of free pigments in the gel. In agreement with work of Kopečná et al. (2012) most of the labeled Chl in GT-P was bound to trimeric PSI. However, in GT-W the signals of labeled Chl incorporated into the PSI trimer and PSII dimer were much weaker (**Figure 3**, lower boxes). Labeling in the abundant PSI monomer was also lower in GT-W. Overall, the total signal of labeled Chl in GT-W was <40% of that in GT-P, which demonstrated a significantly reduced rate of *de novo* Chl formation in the GT-W substrain. Since [^{14}C]glutamate also labeled proteins, autoradiogram of the whole gel provided information about synthesis of membrane proteins. GT-W showed a typical protein labeling pattern with intensive labeling of D1 and much lower labeling of D2, CP43, and CP47 in both PSII core monomers and dimers. In contrast, the intensity of D1 and D2 labeling in the PSII core complexes of GT-W was similar but labeling of both proteins in the PSII dimer was much lower than in the monomer and in GT-P (**Figure 3**, middle boxes). Interestingly, the labeling of SbtA, a bicarbonate transporter, was also much lower in GT-W indicating an inability of the strain to actively induce import of anorganic carbon for CO_2 fixation (**Figure 3**, arrows).

To further support the conclusion about inhibition of Chl biosynthesis in GT-W, we compared levels of later Chl biosynthesis precursors in GT-P and GT-W (**Figure 4**). HPLC analysis confirmed that in GT-W the levels of most intermediates were strongly decreased. Only the level of coproporhyrin(ogen) III (copro III) in GT-W was rather similar to that in GT-P suggesting either a block in the subsequent formation of protoporphyrinogen IX and protoporphyrin IX (PP_{IX}) or, alternatively, a fast consumption of PP_{IX} by the heme branch of the tetrapyrrole biosynthesis pathway.

Genomic Sequencing Revealed Duplication of a Large Part of GT-W Chromosome

To explore the genetic basis for the observed aberrant assembly of photosynthetic complexes and decreased Chl biosynthesis, we performed whole genome re-sequencing of both GT strains on a commercial basis, using the Illumina HiSeq platform. Although, the sequence of the original Williams strain is not available, it can be interpolated from the published sequences of the GT strains. Our sequencing supports a common origin of both GT-P and GT-W strains from the Williams GT strain. The GT-P and GT-W strains shared one mutation while containing one and four additional specific mutations respectively (**Table 1**). In addition to the point mutations detected directly by mapping of the reads to the reference sequence, we observed that one part of the GT-W chromosome exhibited approximately twofold coverage of reads. Interestingly, this large 110 kbp region was bordered by ISY100 transposases, sll0431 and sll1397, sharing 100% identity at the DNA level (**Figure 5**, Table S1). It indicates that this part of the genome was duplicated, possibly in the form of a tandem repeat. Indeed, the presence of such tandem duplication was confirmed by PCR with outbound primers from the beginning and end of the duplication (Figure S2). The duplicated region contained 100 genes (Table S1) including those encoding PSII components (D1 protein) and its assembly factors (e.g., Psb28), which could possibly be related to the aberrant PSII assembly observed in the GT-W strain.

Interestingly, the characteristics of the GT-W strain spontaneously changed when repeatedly restreaked on plates without glucose and under moderate light conditions (30 µmol photons s^{-1} m^{-2}) for several months. The strain gradually attained a pigment composition similar to GT-P (**Figure 6**) and also the pattern of membrane protein complexes became similar to that in GT-P with disappearance of most of the unassembled CP43, CP47, and RCII∗ and an increase in the level of PSI trimer (**Figure 7**). This strain also contained lower levels of Ycf39, Psb28, HemH, and Cycl in comparison with GT-W (**Figure 7**). PCR analysis showed that this revertant strain, designated GT-Wrev, lost the duplication (Figure S2) indicating that it is responsible for most of the Chl-deficient phenotype of GT-W.

Since the observed duplication of part of the genome could be a compensatory mechanism for a lower number of genome copies in the GT-W strain, we also compared the number

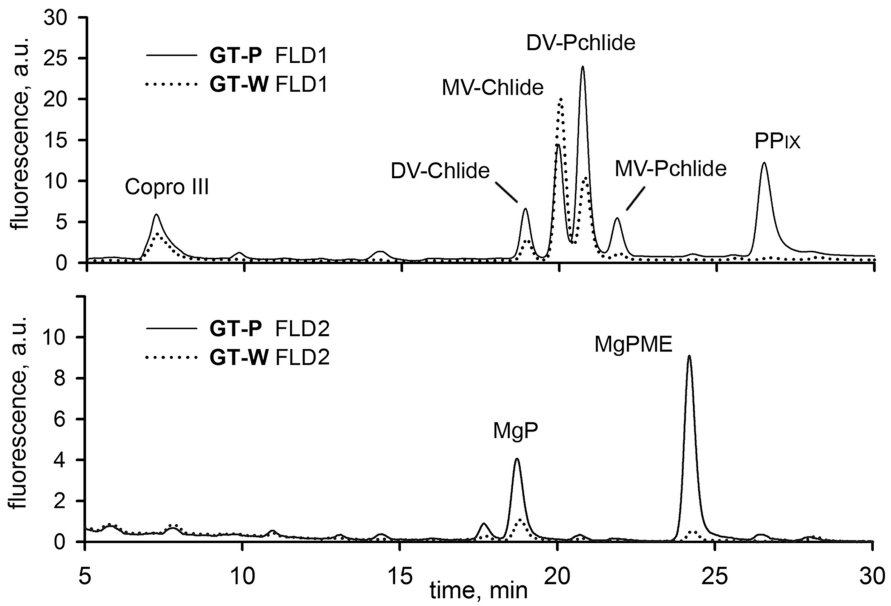

FIGURE 4 | HPLC chromatograms of chlorophyll biosynthesis precursors in GT-P and GT-W strains. Cells of both strains were extracted with 70% methanol and Chl precursors were quantified by HPLC equipped with two fluorescence detectors (FLD1 and FLD2). Each detector was set to wavelengths selected to detect indicated Chl precursors (see Experimental Procedures). Copro III, coproporhyrin(ogen) III; DV-Chlide, divinyl chlorophyllide; DV-Pchlide, divinyl protochlorophyllide; PP_{IX}, protoporphyrin IX; MgP, Mg-protoporphyrin IX; MgPME, Mg-protoporphyrin methylester; MV-Chlide, monovinyl chlorophyllide; MV-Pchlide, monovinyl protochlorophyllide.

TABLE 1 | List of specific mutations in GT-P and GT-W strains.

Base position	Type	Mutated nucleotide	Amino acid change	Gene ID	Annotation	Gene product
GT-P						
488230	SNP	T→G	F255C	*slr1609*	*fadD*	long-fatty-acid CoA ligase
842060	SNP	C→T	R186Q	*sll1799*	*rpl3*	50S ribosomal protein L3
GT-W						
488268	SNP	G→A	V268I	*slr1609*	*fadD*	long-fatty-acid CoA ligase
842060	SNP	G→T	R186Q	*sll1799*	*rpl3*	50S ribosomal protein L3
2354038	Del	5326 bp del	E283Q	*slr0364*	*swmB*	cell surface protein
2780356	SNP	G→C	E283Q	*slr0906*	*psbB*	CP47 protein of PSII
3297450	SNP	C→T	L216 silent	*sll1367*	–	hypothetical protein

Base position refers to the GT-Kazusa sequence.

of chromosomes in both strains. DNA content was assessed using flow cytometry after staining by SYBR Safe and the copy-number calibrated using *E. coli* cells (see Experimental Procedures). **Figure 8** shows that both strains similarly contain 7–11 chromosome copies per cell.

Psb28 Deletion Mutant Constructed in the GT-W Background Shows More Pronounced Phenotype

Previously, Dobáková et al. (2009) has shown a partial Chl deficiency in the Psb28-less strain, causing inhibition of CP47 and PSI synthesis. This strain was constructed in the GT-W background. In contrast, a subsequent study of Sakata et al. (2013) has not confirmed this phenotypic manifestation and the Psb28-less mutant, which has been constructed in WT background closely related to our GT-P strain and has not exhibited lower cellular Chl level. Since the different phenotypes of the mutants could be caused by a different genetic background of the mutants, we tested this possibility by deleting the *psb28* gene in both the GT-P and GT-W strains. *In vivo* absorption spectra of both mutants were then compared with the original control strains (**Figure 9**). The spectrum of the mutant constructed in the GT-P background was indistinguishable from the control, while the GT-W-based mutant showed a lower Chl level as well as much more carotenoids than the control. We also compared the composition of the membrane protein complexes of GT-W and the derived Psb28-less mutant (**Figure 10**). The

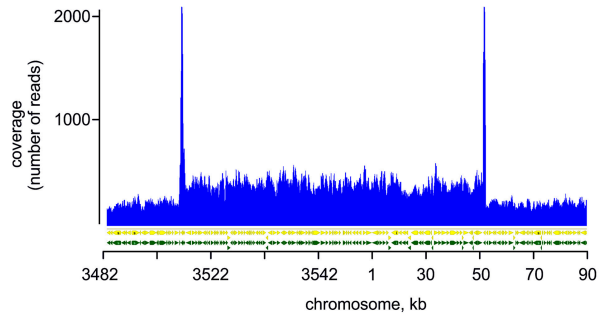

FIGURE 5 | Mapping of reads on the duplicated region of GT-W chromosome. Paired-end reads from Illumina sequencing of the GT-W genome mapped on the reference *Synechocystis* genome (see Experimental Procedures). The read coverage is roughly doubled in the chromosomal region 3520 kb–50 kb; peaks at the border of this region are an artifact of the mapping of reads originating probably from transponase genes located on plasmids.

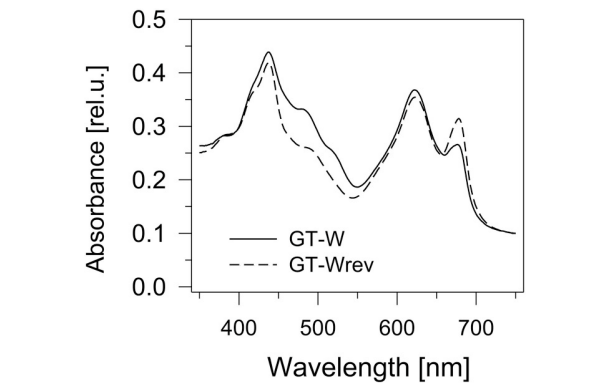

FIGURE 6 | Whole cell absorption spectra of the GT-W strain and its revertant GT-Wrev. The spectra were measured by Shimadzu UV3000 spectrophotometer and normalized for absorbance of 0.1 at 750 nm.

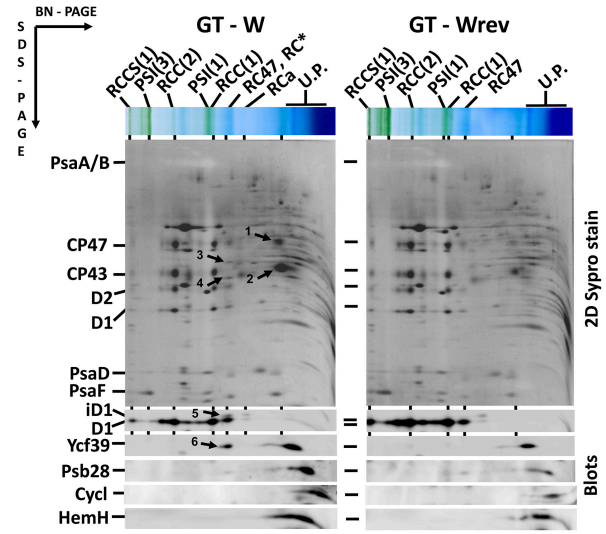

FIGURE 7 | Organization of photosynthetic membrane complexes in the GT-W strain and its revertant GT-Wrev assessed by 2D blue-native/SDS-PAGE in combination with immunoblotting. Membrane proteins of thylakoids isolated from each strain were separated by 4–14% blue-native PAGE, and then in the second dimension by 12–20% SDS-PAGE. The 2D gel was stained by SYPRO Orange and then blotted to a PVDF membrane. The D1, Ycf39, Psb28, Cycl, and HemH proteins were detected by specific antibodies (Blots). Designations as in **Figure 2**. Arrows indicate unassembled forms of CP47(1) and CP43(2), the Ycf48 (3), and Ycf39 (4, 6) assembly factors, and an intermediate form of D1 (5) in RCII* complex, which are all much more abundant than in GT-Wrev. Each loaded sample contained 5 μg of Chl.

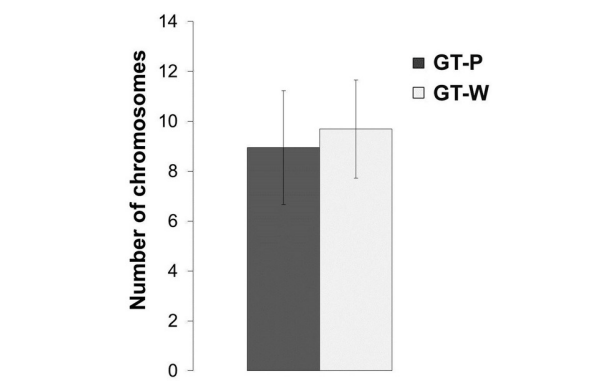

FIGURE 8 | Number of chromosomes detected in the strains GT-P and GT-W. Calculation was done by comparison of the SYBR Safe fluorescence detected by flow cytometry in the both *Synechocystis* strains, using chloramphenicol-treated *E. coli* BL-21 culture as a reference.

mutant contained higher levels of the RCII complexes and Ycf39, the PSII assembly factor protein which has been proposed to participate in the Chl recycling (Knoppová et al., 2014). The data supported the idea that the differences observed in the two above mentioned studies (Dobáková et al., 2009; Sakata et al., 2013) were caused by the different WT background in which the mutants were constructed.

DISCUSSION

During our previous studies dealing with the biogenesis of photosynthetic membrane complexes in *Synechocystis* we characterized dozens of mutants constructed in different background strains originating from various laboratories. We noticed that mutants constructed in background strains coming from the London laboratory of Peter Nixon and the Arizona laboratory of Wim Vermaas had quite different phenotypes although they both originated from the glucose-tolerant Williams substrain (Williams, 1988; Morris et al., 2014). Under photoautotrophic conditions GT-W grew much slower than GT-P (not shown) and the cultures appeared quite different with regard to their cellular spectra, pigment content, and composition of membrane protein complexes. GT-P was in this respect very similar to the glucose sensitive motile PCC strain with minimal amount of unassembled or partially assembled

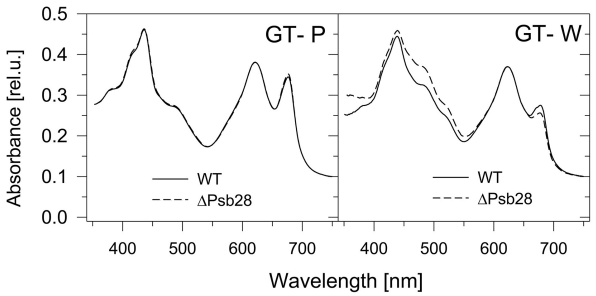

FIGURE 9 | Whole cell absorption spectra of the Psb28-deletion mutants in comparison with their background strains GT-P and GT-W used for their construction. The spectra were measured by Shimadzu UV3000 spectrophotometer and normalized for absorbance of 0.1 at 750 nm.

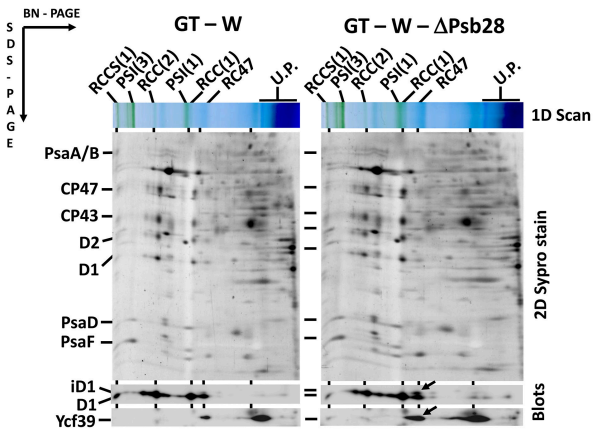

FIGURE 10 | Organization of photosynthetic membrane complexes in the GT-W strain and Psb28-less mutant constructed in this background. Thylakoid proteins isolated from each strain were separated by 4–14% blue-native-PAGE, and then in the second dimension by 12–20% SDS-PAGE. The 2D gel was stained by SYPRO Orange and then blotted to a PVDF membrane. The D1 and Ycf39 proteins were detected by specific antibodies (Blots). Designations as in **Figure 2**. Arrows indicate intermediate forms of the D1 protein and the Yc39 assembly factor present in the RCII* complex, which is more abundant in the Psb28-less strain. Each loaded sample contained 5 μg of Chl.

PSII components. GT-W was much more yellowish and this also corresponded to higher carotenoid and lower Chl levels (**Figure 1**). Moreover, this was also accompanied by aberrant composition of Chl-binding complexes. The strain accumulated a significant level of RCII complexes on the one side and unassembled CP47 and CP43 on the other side indicating that the binding of both PSII antennae to RCII is impaired.

Re-sequencing of the GT-W and GT-P genome revealed one common mutation in a 50S ribosomal protein L3 in comparison with the inferred chromosome sequence of the glucose-tolerant Williams strain. GT-W contained four specific mutations: one silent in the hypothetical protein Sll1367, the second in the PSII protein CP47, the third in the 500 kDa protein Slr0364, and the fourth in the long chain fatty acid coenzyme A-ligase (Slr1609; **Table 1**). The mutation in CP47 was a conservative amino acid change E283Q in the region of a large lumenal loop of the protein important for the assembly of PSII (Haag et al., 1993). A large deletion was found in the huge Slr0364 protein homologous to a protein involved in swimming motility (McCarren and Brahamsha, 2007).

Unexpectedly, no common mutations were found between the GT-W strain and the GT-O strains (Morris et al., 2014) also originating from the Vermaas lab. Although, there is a 5-year difference between the times the strains left the lab, this does not explain why there is no overlap in mutations and why GT-W and GT-P share the *rpl3* mutation while it is absent in GT-O.

The GT-P strain also contained a mutation in the *slr1609* gene. Interestingly, *slr1609* is the most frequently mutated gene—six independent (different) mutations can be found in *Synechocystis* strains sequenced by us and others (Tichý, unpublished data). The reason for this variability is unknown as is the effect of mutations on the activity of the enzyme, which is needed for reuse of fatty acids released from lipids after the action of lipases (Kaczmarzyk and Fulda, 2010). We checked the composition of pigment protein complexes in the *slr1609* deletion mutant but there was no apparent effect of the missing enzyme (Komenda and Tichý, unpublished data).

Apart from the point mutations, the specific feature of the GT-W chromosome was the presence of the large tandem duplication. Genome analysis of eukaryotes revealed that a tandemly arrayed duplicates account for significant proportion of genes and that duplication events are expected to play an important role in evolution of eukaryotes (Rizzon et al., 2006). Although, it is not clear whether gene duplication is a major evolutionary driving force also in prokaryotes compared to horizontal gene transfer, small tandem duplications on a single gene level have been shown previously to complement a non-photosynthetic phenotype of a PSII mutant (Tichy and Vermaas, 2000). In the current experiment we have sequenced 12 *Synechocystis* strains, among them several mutants and their revertants, and we have found one more example of another duplication between two transposases responsible for complementation of a *Synechocystis* mutant (Tichý, unpublished data). It suggests that such genome rearrangements are happening regularly and that under favorable conditions they may get easily selected for.

We have shown that loss of the duplication is accompanied by an increase in the level of PSI and by restoration of proper assembly of PSII (**Figure 7**). This indicates that the impaired autotrophic phenotype of the GT-W strain is related to the duplication and not to the observed specific mutations. We do not know whether the duplication in the GT-W strain is actually segregated or if there are still chromosomes present without the duplication as there is no simple check to confirm the non-duplicated variant. However, from the fact that the growth of GT-W in the absence of glucose easily led to the loss of the duplication it seems that the GT-W strain contains chromosomes both with and without the duplication. We think that the duplication got selected for during prolonged growth on glucose and that the lower level of PSI and impaired assembly of PSII are advantageous under glucose-induced stress. When the

conditions change to photoautotrophy, the ratio of chromosomes with and without the duplication in cells can gradually change, finally leading to complete loss of the duplication.

We do not know how the duplication resulted in low levels of Chl and the inability of CP47 and CP43 to bind to RC in GT-W. Most of the genes present in the duplication code for proteins with unknown function, however, the presence of the gene coding for the PSII structural protein D1 is striking. We believe that the presence of an extra copy of this highly expressed gene could change the stoichiometry of subunits in this multi-subunit complex leading to the observed lower accumulation of PSII and higher accumulation of PSII intermediates. Such gene imbalances and their consequences caused by partial genome duplications have been extensively studied in eukaryotes (Birchler and Veitia, 2012). It has been shown that both under-expression and over-expression of protein complex subunits could lead to similar deleterious effects (Papp et al., 2003). Interestingly, in plants, genes coding for PSII subunits were mostly eliminated from chromosome regions produced by partial genome duplications as opposed to whole-genome duplications (Coate et al., 2011). This is explained by PSII being particularly gene-dosage sensitive (Coate et al., 2011), as incompletely assembled PSII not only impairs photosynthesis but also increase photo-oxidative damage in the cell (Komenda and Masojídek, 1995).

An extra gene copy of Psb28, which has been proposed to affect Chl biosynthesis (Dobáková et al., 2009), and Cycl (Slr1214), cyclase involved in the formation of the fifth ring of Chl, resulted in increased expression and accumulation of these proteins (**Figure 7**). However, this also could lead to an imbalance between individual enzymes of the Chl biosynthesis pathway envisioned to form a multi-enzymatic complex (Sobotka, 2014) Also there was more HemH, which might at least partly explain the low level of PP_{IX} detected in GT-W. Indeed, after the loss of duplication, the GT-Wrev showed a lower level of all of these proteins.

Specifically for prokaryotic cyanobacteria, where transcription is spatially connected to translation, it is also possible that the duplication disturbed the local arrangement in the PSII biogenesis centers further impairing correct and prompt PSII assembly and/or proper interaction with Chl biosynthetic machinery.

It is interesting that the GT-W background is appropriate for complete segregation of mutants in the Chl biosynthesis pathway which cannot segregate in the GT-P background. As an example we can mention the mutant lacking Ycf54, a protein factor needed for the efficient formation of the fifth ring during Chl biosynthesis (this volume of the journal). As mentioned above, the duplication limits the stress imposed on the mutant cells during segregation on glucose media and this helps them to survive mutations, which would be lethal in the other WT variants. On the other hand, rather small phenotypic changes in Chl biosynthesis caused by mutagenesis of GT-P can be enhanced by construction of the mutants in GT-W with already impaired Chl biosynthesis as demonstrated for the Psb28-less strain. As a consequence, the mutants show better detectable phenotypic differences which helps identify the function of proteins encoded by the mutated genes. In conclusion, this study shows that the choice of the proper background strain is not only essential for correct evaluation of mutant phenotypic characteristics but also for successful construction of severely affected mutants that might not survive when made in the inappropriate WT variant.

AUTHOR CONTRIBUTIONS

MT performed experiments, evaluated and interpreted data, wrote the manuscript, MB performed experiments and evaluated data, JKop performed experiments, JN performed experiments, evaluated and interpreted data, wrote the manuscript, RS performed experiments, evaluated, and interpreted data, wrote the manuscript, JK performed experiments, evaluated, and interpreted data, wrote the manuscript.

FUNDING

The work was supported by National Programme of Sustainability I of The Ministry of Education, Youth and Sports, ID: LO1416.

ACKNOWLEDGMENTS

Authors are grateful to Jan Pilný and Lenka Moravcová for excellent technical assistance during protein and pigment analyses.

SUPPLEMENTARY MATERIAL

The Supplementary Material for this article can be found online at: http://journal.frontiersin.org/article/10.3389/fpls.2016.00648

REFERENCES

Birchler, J. A., and Veitia, R. A. (2012). Gene balance hypothesis: connecting issues of dosage sensitivity across biological disciplines. *Proc. Natl. Acad. Sci. U.S.A.* 109, 14746–14753. doi: 10.1073/pnas.1207726109

Boehm, M., Romero, E., Reisinger, V., Yu, J., Komenda, J., Eichacker, L. A., et al. (2011). Investigating the early stages of photosystem II assembly in *Synechocystis* sp. PCC 6803: isolation of CP47 and CP43 complexes. *J. Biol. Chem.* 286, 14812–14819. doi: 10.1074/jbc.M110.207944

Boehm, M., Yu, J., Reisinger, V., Beckova, M., Eichacker, L. A., Schlodder, E., et al. (2012). Subunit composition of CP43-less photosystem II complexes of *Synechocystis* sp PCC 6803: implications for the assembly and repair of photosystem II. *Philos. Trans. R. Soc. Lond. B Biol. Sci.* 367, 3444–3454. doi: 10.1098/rstb.2012.0066

Coate, J. E., Schlueter, J. A., Whaley, A. M., and Doyle, J. J. (2011). Comparative evolution of photosynthetic genes in response to polyploid and nonpolyploid duplication. *Plant Physiol.* 155, 2081–2095. doi: 10.1104/pp.110.169599

Dobáková, M., Sobotka, R., Tichý, M., and Komenda, J. (2009). Psb28 protein is involved in the biogenesis of the Photosystem II Inner Antenna CP47 (PsbB) in the Cyanobacterium *Synechocystis* sp PCC 6803. *Plant Physiol.* 149, 1076–1086. doi: 10.1104/pp.108.130039

Ferreira, K. N., Iverson, T. M., Maghlaoui, K., Barber, J., and Iwata, S. (2004). Architecture of the photosynthetic oxygen-evolving center. *Science* 303, 1831–1838. doi: 10.1126/science.1093087

Guskov, A., Kern, J., Gabdulkhakov, A., Broser, M., Zouni, A., and Saenger, W. (2009). Cyanobacterial photosystem II at 2.9-angstrom resolution and the role of quinones, lipids, channels and chloride. *Nat. Struct. Mol. Biol.* 16, 334–342. doi: 10.1038/nsmb.1559

Haag, E., Eaton-Rye, J. J., Renger, G., and Vermaas, W. F. J. (1993). Functionally important domains of the large hydrophilic loop of CP47 as probed by oligonucleotide-directed mutagenesis in Synechocystis sp. PCC 6803. *Biochemistry* 32, 4444–4454. doi: 10.1021/bi00067a037

Jordan, P., Fromme, P., Witt, H. T., Klukas, O., Saenger, W., and Krauss, N. (2001). Three-dimensional structure of cyanobacterial photosystem I at 2.5 A resolution. *Nature* 411, 909–917. doi: 10.1038/35082000

Kaczmarzyk, D., and Fulda, M. (2010). Fatty acid activation in cyanobacteria mediated by acyl-acyl carrier protein synthetase enables fatty acid recycling. *Plant Physiol.* 152, 1598–1610. doi: 10.1104/pp.109.148007

Kearse, M., Moir, R., Wilson, A., Stones-Havas, S., Cheung, M., Sturrock, S., et al. (2012). Geneious Basic: an integrated and extendable desktop software platform for the organization and analysis of sequence data. *Bioinformatics* 28, 1647–1649. doi: 10.1093/bioinformatics/bts199

Knoppová, J., Sobotka, R., Tichý, M., Yu, J., Konik, P., Halada, P., et al. (2014). Discovery of a chlorophyll binding protein complex involved in the early steps of photosystem II assembly in Synechocystis. *Plant Cell* 26, 1200–1212. doi: 10.1105/tpc.114.123919

Komenda, J., Knoppová, J., Kopečná, J., Sobotka, R., Halada, P., Yu, J. F., et al. (2012a). The Psb27 assembly factor binds to the CP43 complex of photosystem II in the Cyanobacterium *Synechocystis* sp PCC 6803. *Plant Physiol.* 158, 476–486. doi: 10.1104/pp.111.184184

Komenda, J., and Masojídek, J. (1995). Structural changes of Photosystem II complex induced by high irradiance in cyanobacterial cells. *Eur. J. Biochem.* 233, 677–682. doi: 10.1111/j.1432-1033.1995.677_2.x

Komenda, J., Sobotka, R., and Nixon, P. J. (2012b). Assembling and maintaining the Photosystem II complex in chloroplasts and cyanobacteria. *Curr. Opin. Plant Biol.* 15, 245–251. doi: 10.1016/j.pbi.2012.01.017

Kopečná, J., Komenda, J., Bučínská, L., and Sobotka, R. (2012). Long-Term acclimation of the cyanobacterium *Synechocystis* sp PCC 6803 to high light is accompanied by an enhanced production of chlorophyll that is preferentially channeled to trimeric Photosystem I. *Plant Physiol.* 160, 2239–2250. doi: 10.1104/pp.112.207274

Kopečná, J., Pilný, J., Krynická, V., Tomčala, A., Kis, M., Gombos, Z., et al. (2015). Lack of phosphatidylglycerol inhibits chlorophyll biosynthesis at multiple sites and limits chlorophyllide reutilization in *Synechocystis* sp. strain PCC 6803. *Plant Physiol.* 169, 1307–1317. doi: 10.1104/pp.15.01150

McCarren, J., and Brahamsha, B. (2007). SwmB, a 1.12-megadalton protein that is required for nonflagellar swimming motility in Synechococcus. *J. Bacteriol.* 189, 1158–1162. doi: 10.1128/JB.01500-06

Morris, J., Crawford, T., Jeffs, A., Stockwell, P., Eaton-Rye, J., and Summerfield, T. (2014). Whole genome re-sequencing of two 'wild-type'strains of the model cyanobacterium *Synechocystis* sp. PCC 6803. *New Zeal. J. Bot.* 52, 36–47. doi: 10.1080/0028825X.2013.846267

Nixon, P. J., Michoux, F., Yu, J. F., Boehm, M., and Komenda, J. (2010). Recent advances in understanding the assembly and repair of photosystem II. *Ann. Bot.* 106, 1–16. doi: 10.1093/aob/mcq059

Papp, B., Pál, C., and Hurst, L. D. (2003). Dosage sensitivity and the evolution of gene families in yeast. *Nature* 424, 194–197. doi: 10.1038/nature01771

Porra, R. J., Thompson, W. A., and Kriedemann, P. E. (1989). Determination of accurate extinction coefficients and simultaneous equations for assaying chlorophylls *a* and *b* extracted with four different solvents: verification of the concentration of chlorophyll standards by atomic absorption spectroscopy. *BBA-Bioenergetics* 975, 384–394. doi: 10.1016/S0005-2728(89)80347-0

Rippka, R., Deruelles, J., Waterbury, J. B., Herdman, M., and Stanier, R. Y. (1979). Generic assignments, strain histories and properties of pure cultures of cyanobacteria. *J. Gen. Microbiol.* 111, 1–61. doi: 10.1099/00221287-111-1-1

Rizzon, C., Ponger, L., and Gaut, B. S. (2006). Striking similarities in the genomic distribution of tandemly arrayed genes in *Arabidopsis* and rice. *PLoS Comp. Biol.* 2:e115. doi: 10.1371/journal.pcbi.0020115

Roose, J. L., Wegener, K. M., and Pakrasi, H. B. (2007). The extrinsic proteins of photosystem II. *Photosynth. Res.* 92, 369–387. doi: 10.1007/s11120-006-9117-1

Sakata, S., Mizusawa, N., Kubota-Kawai, H., Sakurai, I., and Wada, H. (2013). Psb28 is involved in recovery of photosystem II at high temperature in *Synechocystis* sp. PCC 6803. *BBA-Bioenergetics* 1827, 50–59. doi: 10.1016/j.bbabio.2012.10.004

Sobotka, R. (2014). Making proteins green; biosynthesis of chlorophyll-binding proteins in cyanobacteria. *Photosynth. Res.* 119, 223–232. doi: 10.1007/s11120-013-9797-2

Tichy, M., and Vermaas, W. (2000). Combinatorial mutagenesis and pseudorevertant analysis to characterize regions in loop E of the CP47 protein in *Synechocystis* sp. PCC 6803. *Eur. J. Biochem.* 267, 6296–6301. doi: 10.1046/j.1432-1327.2000.01718.x

Umena, Y., Kawakami, K., Shen, J. R., and Kamiya, N. (2011). Crystal structure of oxygen-evolving photosystem II at a resolution of 1.9 A. *Nature* 473, 55–60. doi: 10.1038/nature09913

Williams, J. G. K. (1988). Construction of specific mutations in Photosystem-II photosynthetic reaction center by genetic-engineering methods in *Synechocystis*-6803. *Method. Enzymol.* 167, 766–778. doi: 10.1016/0076-6879(88)67088-1

Conflict of Interest Statement: The authors declare that the research was conducted in the absence of any commercial or financial relationships that could be construed as a potential conflict of interest.

4.3.1 Supplemental information

Supplemental Table S1. List of all genes located in the duplicated chromosomal segment in the WT-W strain. The order of genes reflects that in the chromosome.

Gene	Product
sll0431	transposase
ssr0817	transposase
slr0462	transposase
sll0430	heatshock protein
slr1176	glucose-1-phosphateadenylyl transferase
slr1177	hypothetical protein
slr1178	hypothetical protein
slr1179	anhydro-N-acetylmuramic acid kinase
sll1110	peptide chain release factor
sll1109	hypothetical protein
sll1108	stationary-phase survival protein SurE homolog
slr1181	photosystem II D1 protein
slr1182	hypothetical protein
slr1183	hypothetical protein
slr1184	hypothetical protein
slr1185	cytochrome b6/f-complex iron-sulfur protein
slr1186	hypothetical protein
slr1187	hypothetical protein
slr1188	chloroplast membrane-associated 30 kD protein
slr1189	hypothetical protein
sll1107	hypothetical protein
sll1106	hypothetical protein
slr1192	zinc-containing alkohol dehydrogenase family
slr0585	argininosuccinate synthetase
slr0586	hypothetical protein
slr0587	hypothetical protein
sll0578	Phosphoribosylaminoimidazole carboxylase
sll0577	hypothetical protein
slr0588	hypothetical protein
slr0589	hypothetical protein
slr0590	hypothetical protein
sll0576	putative sugar-nucleotide epimerase/dehydratase
sll0575	ATP-binding protein
sll0574	probable lipopolysaccharide ABC transporter permease protein
slr0591	hypothetical protein
sll0573	carbamate kinase
sll0572	hypothetical protein
slr0592	hypothetical protein
slr0593	cAMP protein kinase regulatory chain
sll0569	recombinase A

slr0594	hypothetical protein
sll0567	Ferric uptake regulation protein
slr0597	Inosinemonophosphate cyclohydrolase
sll0565	hypothetical protein
sll0564	hypothetical protein
slr0598	hypothetical protein
slr0599	serine/threonine kinase
slr0600	hypothetical protein
slr0601	hypothetical protein
slr0602	hypothetical protein
sll0563	hypothetical protein
slr0603	DNA polymerase III alpha subunit
slr0604	LepA gene product
slr0605	hypothetical protein
slr0606	hypothetical protein
slr0607	hypothetical protein
slr0608	phosphoribosyl-ATP pyrophosphohydrolase
slr0609	cobalamin synthesis protein P47K/CobW
slr0610	hypothetical protein
slr0611	solanesyldiphosphate synthase
slr0612	hypothetical protein
slr0613	hypothetical protein
sll0558	hypothetical protein
sll1214	magnesium-protoporphyrin IX monomethyl ester cyclase
sll1213	hypothetical protein
sll1212	GDP-D-mannose dehydratase
slr1311	photosystem II D1 protein
slr1312	arginine decarboxylase
sll1209	NAD-dependent DNA ligaseLigA
slr1315	hypothetical protein
slr1316	iron(III) dicitrate transport system permease protein
slr1317	iron(III) dicitrate transport system permease protein
slr1318	iron(III) dicitrate transport system permease protein
slr1319	iron(III) dicitrate transport system permease protein
sll1206	ferric aerobactin receptor
sll1205	regulatory protein PchR
sll1204	hypothetical protein
sll1203	hypothetical protein
sll1202	hypothetical protein
sll1409	ferrichrome-iron receptor
sll1408	regulatory protein PcrR
sll1407	hypothetical protein
sll1406	ferrichrome-iron receptor
sll1405	biopolymer transport ExbD protein homologue
sll1404	biopolymer transport ExbB protein homologue
slr1484	hypothetical protein
slr1488	ABC transporter
slr1489	regulatory protein PchR

slr1490	ferrichrome-iron receptor
slr1491	iron(III) dicitrate-binding periplasmic protein
slr1492	iron(III) dicitrate-binding periplasmic protein
slr1493	hypothetical protein
slr1494	ABC transporter
sll1401	hypothetical protein
sll1400	hypothetical protein
ssl2733	hypothetical protein
sll1399	hypothetical protein
sll1398	photosystem II 13 kD protein Psb28
slr1495	hypothetical protein
sll1397	transposase

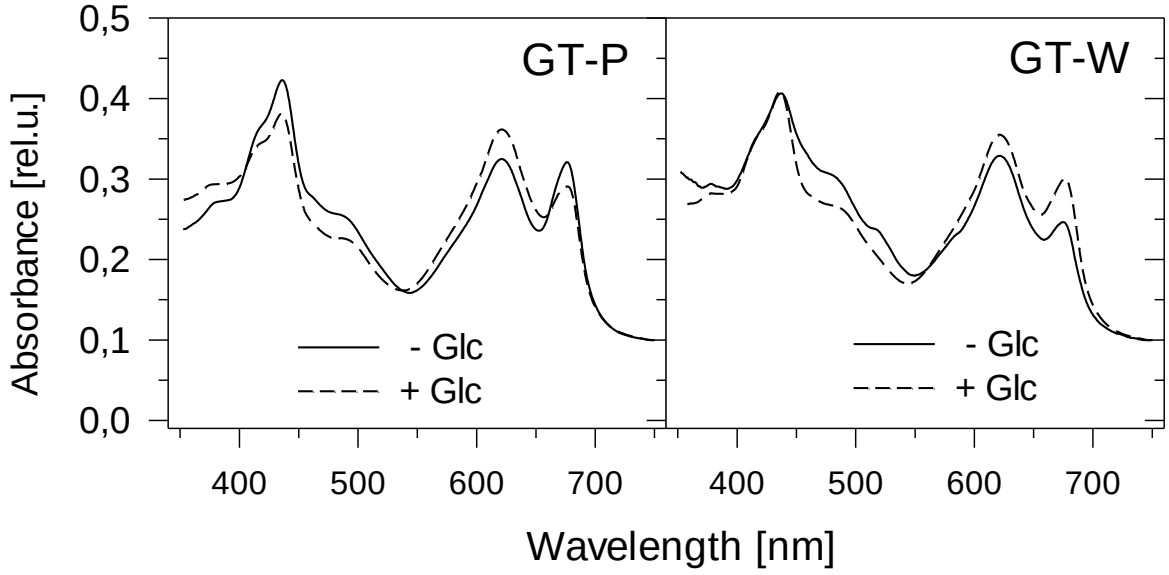

Figure S1. Whole cell absorption spectra of the GT-P and GT-W strains grown in the absence and presence of 5 mM glucose. The spectra were measured by spectrophotometer Shimadzu UV3000 and were normalized for absorbance of 0.1 at 750 nm.

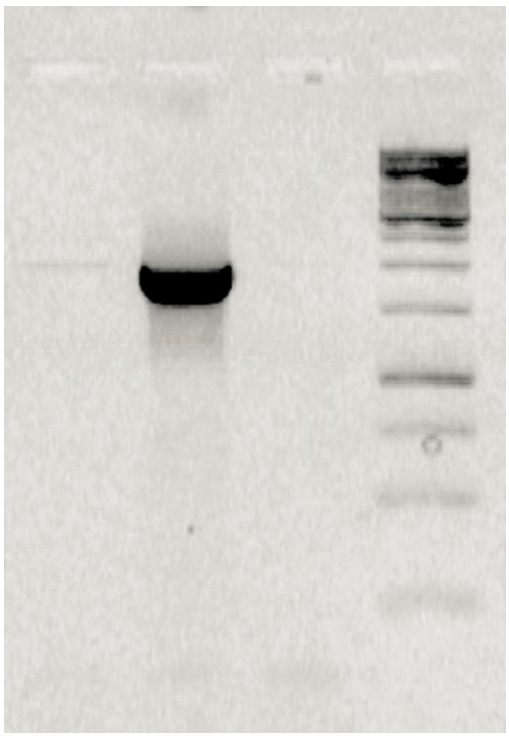

Figure S2. PCR detection of the 110 kbp duplication using outbound primers from the beginning and from the end of duplication. The expected size of the PCR product is 1690 bp. The size of the closest bands on the DNA is 1.5 and 2 kbp.

4.4 Association of Psb28 and Psb27 proteins with PSII-PSI supercomplexes upon exposure of *Synechocystis* sp. PCC 6803 to high light.

Accepted manuscript: Bečková, M., Gardian, Z., Yu, J., Konik, P., Nixon, P.J., and Komenda, J. (2016). Molecular Plant, pii: S1674-2052(16)30161-7. doi: 10.1016/j.molp.2016.08.001.

Association of Psb28 and Psb27 Proteins with PSII-PSI Supercomplexes Upon Exposure of *Synechocystis* sp. PCC 6803 to High Light

Martina Bečková[1,2], Zdenko Gardian[2,3], Jianfeng Yu[4], Peter Koník[1,2], Peter J. Nixon[4] and Josef Komenda[1,2*]

[1]Institute of Microbiology, Center Algatech, Opatovický mlýn, 37981 Třeboň, Czech Republic
[2]Faculty of Science, University of South Bohemia, Branišovská 1760, 37005 České Budějovice, Czech Republic
[3]Institute of Plant Molecular Biology, Biology Centre Academy of Sciences, Branišovská 31, 37005 České Budějovice, Czech Republic
[4]Sir Ernst Chain Building-Wolfson Laboratories, Department of Life Sciences, Imperial College London, South Kensington Campus, London, SW7 2AZ UK

***Correspondence: Josef Komenda (komenda@alga.cz)**

Running title: Function of Psb28 proteins in *Synechocystis*

Short summary:

PSII assembly factors Psb28-1 and Psb28-2 from the cyanobacterium *Synechocystis* sp. PCC 6803 bind to the PSII complexes containing CP47 and under increased irradiance they also associate with Psb27-containing PSII-PSI supercomplexes. Data suggest the involvement of PSI in PSII biogenesis, possibly by photoprotecting PSII through energy spillover. Absence of Psb28-1 but not Psb28-2 leads to the intermittent-high-light-sensitive phenotype.

ABSTRACT

Formation of the multi-subunit oxygen-evolving photosystem II (PSII) complex involves a number of auxiliary protein factors. In this study we compared the localization and possible function of two homologous PSII assembly factors, Psb28-1 and Psb28-2, from the cyanobacterium *Synechocystis* sp. PCC 6803. We demonstrate that FLAG-tagged Psb28-2 is present in both the monomeric PSII core complex and a PSII core complex lacking the inner antenna CP43 (RC47), whereas Psb28-1 preferentially binds to RC47. When cells are exposed to increased irradiance, both tagged Psb28 proteins additionally associate with oligomeric forms of PSII and with PSII-PSI supercomplexes composed of trimeric photosystem I (PSI) and two PSII monomers as deduced from electron microscopy. The presence of the Psb27 accessory protein in these complexes suggests the involvement of PSI in PSII biogenesis, possibly by photoprotecting PSII through energy spillover. Under standard cultivation conditions, the distribution of PSII complexes is similar to wild-type and each of the single *psb28* null mutants except for loss of RC47 in the absence of Psb28-1. In comparison with the wild type, growth of mutants lacking Psb28-1 and Psb27, but not Psb28-2, was retarded under high-light conditions and, especially, intermittent high-light-dark conditions, emphasizing the physiological importance of PSII assembly factors for light acclimation.

INTRODUCTION

The photosystem II (PSII) complex is the light-driven water-plastoquinone oxidoreductase of oxygenic photosynthesis, responsible for splitting water into molecular oxygen and releasing protons and electrons for the generation of the ATP and NADPH needed for the fixation of carbon dioxide in cyanobacteria, algae and plants. The most active form of PSII is a dimer whose structure from thermophilic cyanobacteria is now known to a resolution of 1.9 Å (Umena et al., 2011). The PSII monomer features 17 transmembrane protein subunits, three peripheral proteins and about 80 cofactors (Guskov et al., 2009). The transmembrane reaction center (RCII) subunits D1 and D2 are essential for the binding of cofactors involved in primary charge separation and subsequent electron transfer (Diner et al., 2001). The chlorophyll-containing CP47 and CP43 inner antenna complexes deliver energy from the outer antennae to the reaction center are located on either side of the D1-D2 heterodimer. CP43 also has a role with D1 in binding the Mn_4CaO_5 cluster involved in water splitting (Ferreira et al., 2004).

Assembly of PSII is thought to be a stepwise process (Komenda et al., 2004) proceeding through several intermediate complexes. Initially, the large pigment proteins form pre-complexes (or modules) with small transmembrane polypeptides, pigments, and possibly other cofactors (Komenda et al., 2012b). First the D1 and D2 modules form a reaction center intermediate complex (RCII) to which the CP47 module is attached to form a core complex lacking CP43 (termed RC47). Subsequent attachment of the CP43 module leads to the formation of a PSII monomeric core complex (RCC(1)) with assembly completed by dimerization to form RCC(2) (reviewed in Nixon et al., 2010). Light-driven assembly of the Mn_4CaO_5 cluster and attachment of the lumenal extrinsic subunits is thought to occur after formation of RCC(1) (Nixon et al., 2010). Correct and efficient assembly of PSII is controlled by a number of auxiliary protein factors that are absent from the final functional PSII complex. Some of these, such as the Psb28 proteins (Pfam: PF03912), are highly conserved and are found both in cyanobacteria and chloroplasts.

The genome of the cyanobacterium *Synechocystis* sp. PCC 6803 (hereafter *Synechocystis* 6803) codes for two Psb28 homologs: Psb28-1 (encoded by gene *sll1398*) and Psb28-2 (encoded by gene *slr1739*) (Boehm et al., 2012). Psb28-1 (also named Psb13 and Ycf79) was first identified as a component of a His-tagged PSII preparation isolated from *Synechocystis* 6803 (Kashino et al., 2002) and, subsequently, shown to be a hydrophilic protein peripherally attached to the membrane (Dobáková et al., 2009). The absence of transmembrane structural motifs was later confirmed by the determination of the solution structure of His-tagged Psb28-1 by NMR (PDB: 2KVO; Yang et al., 2011). Psb28-1 in *Synechocystis* 6803 most probably exists as a dimer (Bialek et al., 2013) and has been detected in the RC47 complex (Boehm et al., 2012; Dobáková et al., 2009; Sakata et al., 2013) in the vicinity of the PsbH subunit (Dobáková et al., 2009).

The phenotype of *psb28-1* null mutants of *Synechocystis* 6803 is controversial. The knockout mutant constructed by Dobáková et al. (2009) exhibited slower autotrophic growth, accelerated turnover of the D1 subunit, decreased synthesis of the CP47 inner antenna and a lower cellular level of chlorophyll (Chl) in comparison with wild-type (WT). In contrast, the phenotype of the null mutant described by Sakata et al. (2013) was much milder showing just growth retardation under increased temperature, especially when combined with inactivation of the *dgdA* gene causing a defect in the biosynthesis of digalactosyldiacylglycerol.

The genomes of *Synechocystis* 6803 and some other cyanobacteria contain another *psb28* gene designated *psb28-2*. A knock-out mutant of *Synechocystis* 6803 lacking Psb28-2 behaves

like WT and deletion of the *psb28-2* gene in the Psb28-1-less strain does not show an additional effect, indicating that Psb28-2 is not able to substitute for Psb28-1 (Sakata et al., 2013). The structure of Psb28-2 is thought to be similar to that of Psb28-1 (Mabbitt et al., 2014) except that it likely exists as a monomer (Bialek et al., 2013), due to the lack of several amino acid residues putatively involved in dimerization of Psb28 (Mabbitt et al., 2014). Psb28-2 like Psb28-1 has been detected in RC47 complexes (Boehm et al., 2012).

The physiological importance of Psb28 proteins in PSII assembly and function in *Synechocystis* 6803 remains unknown. Here we show that, under increased irradiance, both proteins together with Psb27, a lumenal accessory protein associated with non-oxygen-evolving PSII core complexes (Nowaczyk et al., 2006), become components of PSII-PSI supercomplexes, the formation of which may be an important step in PSII biogenesis especially under high irradiance. Consistent with this, we show that growth of both the Psb27 and Psb28-1 mutants is affected under conditions of continuous and especially intermittent high light.

RESULTS

Differences in the Association of Psb28 Proteins with PSII

Previous work has shown that both Psb28-1 and Psb28-2 are able to bind to the RC47 complex (Bialek et al., 2013; Boehm et al., 2012; Dobáková et al., 2009). However, the weak Psb28-2 signal detected by immunoblotting in this earlier work prevented a complete analysis of the binding of Psb28-2 to other types of PSII complexes. To address this problem, we used commercial FLAG-tag specific antibodies to detect expression of a Psb28-2 derivative containing a 3xFLAG tag fused to the N-terminus (FLAG-Psb28-2) (Boehm et al., 2012). Two-dimensional (2D) gel electrophoresis of solubilized thylakoids isolated from this strain confirmed the presence of the protein not only in RC47 but also at similar levels in the monomeric PSII core complex (RCC(1)) (Figure 1). Additional probing of the same blot with an antibody against Psb28-1 detected Psb28-1 just in RC47 in agreement with earlier work (Dobáková et al., 2009). The apparent masses of the RC47 complexes containing Psb28-1 and FLAG-Psb28-2 in RC47 were slightly different, suggesting that the two Psb28 proteins might not bind to the same complex. The position of unassembled Psb28-1 in the native gel was also in agreement with its postulated dimeric structure, whereas unassembled FLAG-Psb28-2 migrated as a monomer.

FLAG-Psb28-2-containing complexes immunopurified under mild solubilization conditions were also examined by 2D gel electrophoresis. In the first dimension, we used clear-native (CN) PAGE, which enables sensitive identification of PSII complexes directly in the gel due to the emission of Chl fluorescence. This analysis confirmed the association of FLAG-Psb28-2 with RC47, but unlike a previous study (Boehm et al., 2012) (see also Supplemental Figure 1), we observed a monomeric PSII core complex RCC(1) in the pull-down experiment (Figure 2, left panel), possibly because the use of a milder MES buffer containing Mg^{2+} and Ca^{2+} ions stabilized binding of CP43 within the isolated RCC(1) complex during purification. Immunoblotting showed that RCC(1) complexes isolated using FLAG-Psb28-2 contained another PSII assembly factor, Psb27 (Figure 2). Both the RC47 and RCC(1) complexes were present in two versions: a larger one containing FLAG-Psb28-2 and a smaller one lacking FLAG-Psb28-2 as judged from the relative migration of the FLAG-tagged protein band (Figure 2, complexes with asterisks). This suggests that a sub-population of FLAG-tagged Psb28-2 is released from PSII complexes during native PAGE and migrates in the region of unassembled proteins. This is even better documented in Supplemental Figure 1 when the 2D gel analysis was performed using FLAG-tagged Psb28-2 isolated by the previously described method (Boehm et al., 2012).

Although the amount of SYPRO-stained FLAG-Psb28-2 in Figure 2 seemed to be sub-stoichiometric in comparison with the pulled-down larger PSII proteins, comparison of the staining obtained with SYPRO orange, used in this study due to its compatibility with immunoblotting, and with Coomassie blue (CBB) (Supplemental Figure 1) showed that the reason is the lower stainability of the tagged Psb28-2 and other smaller proteins (e.g., PsbE) by SYPRO stain. Indeed, comparison of the approximate intensity ratio of the FLAG-Psb28-2 and CP47 in the SYPRO-stained and CBB-stained gels showed a much higher value with CBB staining (Supplemental Figure 1).

To exclude the effect of the position of the FLAG tag on the binding specificity of the Psb28 proteins, we analyzed membranes of two other strains expressing either N-terminally tagged Psb28-1 or C-terminally tagged Psb28-2 (FLAG-Psb28-1 and Psb28-2-FLAG, respectively) from their native promoters (Supplemental Figure 2). Membrane protein analysis confirmed that the position of the tag did not affect the binding specificity of each of the Psb28 proteins to PSII since FLAG-Psb28-1 was found in RC47 and Psb28-2-FLAG in both RC47 and

RCC(1) (Supplemental Figure 2). In addition, RC47 and RCC(1) were both pulled down by Psb28-2-FLAG (Supplemental Figure 3).

Both FLAG-Tagged Psb28 Proteins Associate with Large PSII-PSI Supercomplexes under Increased Irradiance

We found that exposure of cells to increased irradiance led to an altered composition of the resulting pull-down preparations. FLAG-Psb28-2 isolated from more illuminated cultures contained a higher proportion of dimeric PSII core complexes and, in addition, a non-fluorescent large Chl-protein complex visible at the edge of the CN gel (Figure 2, right panel). The 2D gel showed that the latter complex contained all four large PSII Chl-binding proteins but its pigmentation was clearly higher than that of PSII core complexes. The absorption spectrum of the band showing a maximum at about 677 nm and a main 77 K fluorescence band peaking at 722 nm pointed to the presence of the photosystem I (PSI) complex (Figure 3, right panel). This was further confirmed by mass spectrometry analysis, which showed the presence of the PsaA, PsaF, and PsaL subunits of PSI (Table 1). The presence of PSI in the complex was also confirmed by immunodetection of the PsaD protein; the weaker signals detected in smaller complexes most probably reflect the presence of PSI trimeric, dimeric, and monomeric complexes (Figure 2 and Supplemental Figure 2D blots). Therefore, we ascribe the large complex to a supercomplex of PSII and PSI (RCCS, Figure 2, right panel). In agreement with previously published data, the supercomplex also contained Psb27 (Komenda et al., 2012a), a lumenal accessory protein associated with non-oxygen-evolving PSII core complexes (Nowaczyk et al., 2006), which suggests a role for the supercomplex in PSII assembly/repair. A similar pattern of PSII complexes was also obtained when we affinity purified C-terminally tagged Psb28-2 (Psb28-2-FLAG) from cells grown under standard and high irradiance (Supplemental Figure 3). The complexes again contained Psb27.

We further tested whether FLAG-tagged Psb28-1 also co-isolated with RCCS under increased irradiance. Psb28-1-FLAG co-purified with RC47, a very small amount of RCC(1) and RCC(1)-RC47 complex, when isolation was performed from cells grown under standard conditions (Figure 4, left panel). Here again the seemingly low level of the pulled down Psb28-1-FLAG was related to the weaker staining of the protein by SYPRO orange (Supplemental Figure 4). When isolated from cells exposed to high irradiance, the preparation additionally contained a significant amount of the PSII-PSI supercomplex (Figure 4, right panel). The

presence of PSI was again confirmed by identification of both PsaD in the complex by immunoblotting (Figure 4 and 2D blots) and PsaE in the pull-down by mass spectrometry (Supplemental Table 1). We never identified Psb28-2 in Psb28-1-FLAG pull-down, confirming their independent binding (not shown).

To further characterize the PSII-PSI supercomplex, we subjected the Psb28-1-FLAG preparation to single-particle analysis. Due to the low amount of supercomplexes in the preparation (Figure 5A), the resolution of the obtained images was rather limited; nevertheless it was sufficient for the unequivocal identification of PSI trimers in the particles. The shape and size of the additional structures attached to the PSI trimer corresponded well to two monomeric PSII complexes (Figure 5B). Results from single-particle analysis also supported the presence of RCC(1)-RC47 complexes (Figure 5C), which were detected by 2D gel electrophoresis on the basis of a relative decrease in intensity of the CP43 band in the complex compared with RCC(1) complexes (Figure 4).

The PSII-PSI supercomplexes were present in WT cells even under standard light conditions, and their quantity only slightly increased after exposure of the cells to high light (Supplemental Figure 5). These data indicate that these complexes are constitutively present in cells, but after high-light treatment there is an increase in the amount of a specific fraction that binds the Psb28 and Psb27 proteins.

We also tested unspecific binding of RCCS and other PSII complexes to FLAG-affinity resin using solubilized membranes from the control WT strain subjected to high irradiance. No apparent Chl-containing complexes present in the eluate excluded an artifactual binding of RCCS to the affinity resin (Supplemental Figure 5).

Differences in the Profile of PSII Complexes in psb28 Null Mutants

Previous results have suggested that the strain lacking Psb28-1 shows impaired synthesis of CP47 and PSI and accumulates lower levels of Chl in the cell (Dobáková et al., 2009). However, this phenotype was not observed in a second independently constructed *psb28-1* mutant (Sakata et al., 2013). Since this disagreement could be caused by differences in the genetic backgrounds of the two WT strains used to make the mutants, we constructed two new Psb28-1- and Psb28-2-less mutants using a different WT strain. In our original study (Dobáková et al., 2009), we used a WT strain very similar to the glucose-tolerant GT-O2 strain (Morris et

al., 2014), which was subsequently shown to exhibit partial Chl depletion upon autotrophic growth conditions. The new set of mutants was instead constructed in a strain similar to the GT-Kazusa strain (Supplemental Figure 6), which contains a similar content of Chl as the standard motile PCC 6803 strain (Tichý et al., 2016). The resulting *psb28* mutants were found to have a similar cellular Chl content as the control and contained very similar levels of PSI and both monomeric and dimeric PSII core complexes as revealed by CN gel electrophoresis (Figure 6) in agreement with Sakata et al. (2013). This result indicates that the decreased level of Chl in the Psb28-1-less strain seen by Dobáková et al. (2009) was most probably related to the Chl-deficient phenotype of the WT strain originally used for mutant construction.

Nevertheless, when we performed radioactive labeling of proteins in the new strains, the Psb28-1-less mutant still showed lower labeling of CP47 and PSI in comparison with the other two strains (Supplemental Figure 7). Another common feature of the new ΔPsb28-1 strain shared with the one constructed by Dobáková et al. (2009) was the lack of detectable RC47 complex and a lower level of free unassembled CP47, while in the strain lacking Psb28-2, the RC47 complex was clearly visible and was even more abundant than in WT (Figure 6, right panel and quantification table). All three strains show the presence of PSI-PSII supercomplexes under both standard and high-light conditions indicating that the accumulation of PSII supercomplexes is not dependent on the presence of Psb28 proteins.

Loss of Psb28-1 but Not Psb28-2 Impairs Growth in Continuous High Light and Especially Intermittent Light

Under standard illumination conditions, growth of the *psb28-1* and *psb28-2* null mutants on agar plates was indistinguishable to WT (Figure 7, left panels). Under high irradiance, the strain lacking Psb28-1 grew slightly slower than the WT and Psb28-2-less strains but its sensitivity to high light was exacerbated when we used intermittent (5 min dark and 5 min 400 μmol photons m^{-2} s^{-1}) instead of continuous (400 μmol photons m^{-2} s^{-1}) high light (Figure 7, upper right panel). When the *psb28-2* gene was additionally inactivated in the Psb28-1 mutant, the growth of the resulting double mutant was identical to that of the psb28-1 mutant under all tested conditions (not shown). A *psb27* null mutant also grew more slowly under intermittent light in comparison with WT (Figure 7, lower right panel). Finally, we constructed the Psb27/Psb28-1 double mutant, which showed the slowest growth of all the tested strains in high continuous light and did not grow at all in intermittent light.

As the Psb28-1-less strain showed a light-sensitive phenotype, we checked whether it is a light-inducible stress protein like members of the family of high-light-inducible proteins (Hlips, He et al., 2001). While the level of Psb28-1 remained the same after 2 h exposure of WT cells to 500 μmol photons m^{-2} s^{-1}, the content of HliA/B in these cells sharply increased, meaning that pool of Psb28-1 in the cell is stable and the protein is not high-light inducible.

DISCUSSION

Many cyanobacteria, like *Synechocystis* 6803, encode two different Psb28 proteins. Here we confirm that under standard cultivation conditions both Psb28-1 and Psb28-2 associate with the RC47 complex. One difference between the two forms of Psb28 is that Psb28-2 is found at higher levels in the monomeric RCC(1) complex (Figures 1, 2, and 4). When the Psb28 proteins were purified from cells exposed to increased irradiance, oligomeric PSII complexes, small amounts of PSI, and especially PSII-PSI supercomplexes now appeared in the affinity-purified preparations. Interestingly, the Psb27 assembly factor was also present in these complexes in accordance with previous results indicating a close relationship between Psb27 and Psb28 proteins (Kashino et al., 2002; Liu et al., 2011a; Liu et al., 2011b; Nowaczyk et al., 2012). Association of Psb27 with large PSI-PSII complexes has also been demonstrated in previous studies (Komenda et al., 2012a; Liu et al., 2011b). Given that Psb27 is associated with PSII complexes lacking a functional oxygen-evolving complex (Nowaczyk et al., 2006), the complexes containing both Psb27 and Psb28 are therefore likely to be involved in de novo assembly and/or repair of PSII.

Single-particle analysis of preparations isolated using FLAG-tagged Psb28 proteins from high-light exposed cells showed the presence of large particles containing PSI trimer together with two additional densities corresponding in size and shape to two PSII monomers; however, the organization of the two monomers is clearly different from their arrangement in the known dimeric crystal structures, which would suggest binding to trimeric PSI as monomers rather than a dimer (Figure 5). The close association of PSI trimeric complexes with PSII complexes containing the Psb28 and Psb27 assembly factors supports our previous hypothesis that PSI might play a protective role during PSII biogenesis (Komenda et al., 2012a). Indeed this association between PSII and PSI in the supercomplexes resulted in the loss of Chl fluorescence of otherwise highly fluorescent PSII complexes, indicating efficient energy spillover to PSI (Figures 2 and 4). Thus, the formation of PSI-PSII supercomplexes might reflect a light-induced

response of the PSII assembly machinery to protect PSII assembly complexes via efficient PSI-mediated quenching of harmful excitation energy absorbed by these intermediates. Moreover, as we have recently identified trimeric PSI as the main sink for newly synthesized Chl (Kopečná et al., 2012), association of PSII assembly complexes with PSI trimeric complexes may also allow production of PSII assembly modules using Chl released from trimeric PSI.

The crystal structure of Psb28 from *Thermosynechococcus elongatus* suggests that the proximity of the C termini of the two monomers in the dimer does not allow tagging of the molecule without destabilization of the dimer and this was supported by analysis of the strain expressing Psb28-1 with a FLAG tag on the C terminus. Nevertheless, the FLAG-tagged protein was still able to bind to RC47 in cells (Supplemental Figure 2, left) and PSII co-purified with the isolated tagged protein, suggesting that the dimeric structure of the Psb28-1 protein is not needed for binding to PSII (Figure 4).

Binding of Psb28 proteins to PSII is dependent on the presence of PsbH (Bialek et al., 2013; Dobáková et al., 2009); this fact, together with the inhibitory effect of deleting *psb28-1* on synthesis of CP47, led to speculation that Psb28-1 is bound to CP47. However, taking into account the oligomeric structure of native Psb28-1 together with the presence of a long N-terminal helix of PsbH stretching over CP47, it is also possible that Psb28 binds more in the center of PSII than previously envisaged and so prevents binding of CP43 to RC47 thereby allowing accumulation of RC47 in the membrane.

PsbH is also essential for the binding to PSII of HliB (also termed ScpD), a member of the family of high-light-inducible proteins (Hlips) (He et al., 2001) or small chlorophyll-a/b-binding-like proteins (Scps) (Funk and Vermaas, 1999). We show that expression of Hlips is quickly induced upon increase of irradiance, while the Psb28-1 protein is present constitutively in cells and its content does not respond to high light (Figure 8). Although we cannot exclude that all Psb28-1 proteins weakly interact with PSII in the membrane and this interaction is disrupted during native PAGE, there is nevertheless a fraction of Psb28-1 that binds to RC47 more stably and which is identified in the native gels as the component of the complex (Figure 1; Dobáková et al., 2009). Thus, it seems that the Psb28-1 protein is available for binding to PSII before the production of Hlips and that its prompt binding may be important for Psb28-1 function during high/intermittent light stress.

WT-like sensitivity to continuous high light (Figure 7) and the presence of RC47 in the Psb28-2-less strain (Figure 6) on the one hand and similarity between the Psb28-1-less strain and the *psb28-1/psb28-2* double mutant on the other hand (Sakata et al. 2013) suggest that

Psb28-2 is not a redundant Psb28-1 copy with the same function. Instead, we speculate that Psb28-2 may act as an antagonist that prevents formation of RC47 by excluding Psb28-1 from its binding site. That the two Psb28 proteins might play different roles is in line with the upregulation of the *psb28-1* transcript level but downregulation of *psb28-2* in a *Synechocystis* 6803 mutant lacking the PsbO protein (Schriek et al., 2008), which is highly sensitive to photoinhibition and exhibits very fast D1 turnover (Komenda and Barber, 1995). Similarly, the expression profiles of the *psb28-1* and *psb28-2* genes were found to be quite different under a variety of environmental conditions in a very recent transcriptomic study (Hernández-Prieto et al., 2016), again supporting a distinct functional role for each protein.

In the absence of Psb28-1, the RC47 complex is undetectable in cells grown under standard conditions, while in WT cells this complex is detectable. This difference has previously been related to an effect on CP47 synthesis as the *psb28-1*-null mutant contains an increased level of RCII, the assembly complex that immediately precedes RC47 in the PSII assembly pathway (Dobáková et al., 2009). For the newly constructed *psb28-1* mutant described here, there was also reduced synthesis of CP47 (autoradiogram in Supplemental Figure 7). Interestingly, unlike the *Synechocystis* 6803 CP43-less mutant, the CP47-less mutant shows a Chl-deficient phenotype reflecting reduced PSI accumulation (Supplemental Figure 8), and the decreased synthesis of PSI detected in the *psb28*-null mutant could similarly be related to the lower synthesis of CP47 (autoradiogram in Supplemental Figure 7). A specific effect on the synthesis of PSI and CP47 has also been seen in the *Δpor* (Kopečná et al., 2013) and *Δgun4* (Sobotka et al., 2008) mutants disrupted in the PChlide reduction and Mg-chelatase steps, respectively, and in the *ycf54* mutant affected in the function of aerobic cyclase involved in the synthesis of the fifth Chl ring (Hollingshead et al., 2016). Given that newly synthesized Chl in *Synechocystis* 6803 is preferentially incorporated into the PSI trimer (Kopečná et al., 2012) and that this complex is particularly deficient in the CP47-less, *Δpor* and *Δgun4* mutants, Psb28-1 could regulate this main pathway for Chl incorporation. A link between Psb28-1 and the synthesis of Chl-binding proteins is also suggested from analysis of gene transcription during the diurnal cycle of the nitrogen-fixing cyanobacterium *Cyanothece* sp. ATCC 51142. Unlike transcripts for other PSII-associated genes, *psb28* transcripts preferentially accumulate during the dark period when Chl biosynthesis is activated and PSI proteins in particular are synthesized, probably in readiness for the start of the light period (Stöckel et al., 2011).

Previous studies on *psb28* mutants constructed in *Synechocystis* 6803 have led to conflicting results regarding the importance of Psb28-1 for accumulation and assembly of both

photosystems. By constructing new deletion mutants in a WT strain of *Synechocystis* 6803 that is known not to be affected in chlorophyll biosynthesis, we have confirmed that Psb28-1 has very little impact on growth under standard continuous illumination (40 μmol photons m^{-2} s^{-1}). Importantly, we have been able to show here that Psb28-1 and Psb27 are needed for optimal growth especially under intermittent high-light conditions (Figure 7). This phenotype has not been reported before for cyanobacteria. In the case of higher plants, Psb28 is already known to be required for normal growth and pigmentation of rice plants (Jung et al., 2008). The mechanism of Psb28-1 action remains unclear, but it apparently differs from that of Psb27, since the intermittent light condition affected the growth of the Psb27/Psb28-1 double mutant more severely than each of the single mutants (Figure 7).

METHODS

Construction of Mutant Strains

The non-motile, glucose-tolerant strain of *Synechocystis* sp. PCC 6803 (GT-P; Tichý et al., 2016) was used in this study as a WT strain and as a background for the generated deletion mutant strains (ΔPsb28-1, ΔPsb28-2, ΔPsb28-1/ΔPsb28-2, and ΔPsb27/ΔPsb28-1) and FLAG-tagged mutants (Psb28-1-FLAG, FLAG-Psb28-1, Psb28-2-FLAG, and FLAG-Psb28-2).

Deletion Mutant Strains

The psb28-1 knockout vector was constructed in two steps. First, the upstream region of *sll1398* was PCR amplified from WT genomic DNA of *Synechocystis* PCC 6803 with the primer set Sll1398-1F and Sll1398-2R, and the downstream region was amplified with Sll1398-3F and Sll1398-4R. The resulting PCR fragments were then mixed together to serve as the DNA template to perform overlap extension PCR with primer set Sll1398-1F and Sll1398-4R. The joint PCR fragment, which has the entire sll1398 ORF replaced with an EcoRV restriction site, was cloned into pGEM-T Easy vector (Promega). The resulting plasmid, namely pGEMSll1398, was then used as an intermediate vector for insertion of either kanamycin or chloramphenicol cassette via an EcoRV restriction site to create the final transformation vectors termed pSll1398Cam and pSll1398Kan (Supplemental Figure 6). The sequencing confirmed that the orientation of the resistance cassette was the same as the orientation of the gene of interest. The plasmid pSll1398Cam was used for transformation of the WT and ΔPsb27 strain to create deletion mutants ΔPsb28-1 and ΔPsb27/ΔPsb28-1, respectively. The segregation was checked

by PCR. Transformants were selected for Cam^R antibiotic resistance and PCR was used to show integration of the selectable marker and elimination of the WT gene copy.

The psb27 and psb28-2 knockout vector was constructed using an identical approach. The resulting plasmids pGEMSlr1645 and pGEMSlr1739 were then used as intermediate vectors for insertion of gentamicin, kanamycin, or chloramphenicol cassette via EcoRV restriction site to create the final transformation vectors termed pSlr1645Gent, pSlr1739Kan, and pSlr1739Cam. The pSlr1739Cam which has a chloramphenicol resistance cassette, was used for transformation of WT to create a deletion mutant ΔPsb28-2 and the pSlr1739Kan for transformation of the ΔPsb28-1 strain with Cam^R to create a double mutant ΔPsb28-1/ΔPsb28-2. The pSlr1645Gent was used for transformation of WT to create a deletion mutant ΔPsb27. Segregations were again checked by PCR. The transcription orientation of antibiotic cassettes was again along the genes of interest.

FLAG-Tagged Mutant Strains

The constructs Sll1398C'FLAG and Slr1739C'FLAG, designed to place the C-terminally FLAG-tagged *sll1398* and *slr1739* genes under the native promoters, consist of an upstream region, a gene with three repetitions of an eight amino acid FLAG sequence (3 x AspTyrLysAspAspAspAspLys; Sigma-Aldrich) on the C terminus, a zeocine cassette in reversed orientation, and downstream region of the corresponding gene (Supplemental Figure 9, right). The constructs were commercially synthesized and cloned to the pUC57 plasmid by EcoRV (Gene Synthesis Service, GenScript; Supplemental Figure 9, left). The obtained plasmids pUC57Sll1398C'FLAG and pUC57Slr1739C'FLAG were then used to transform the WT cells to yield strains expressing C-terminally FLAG-tagged Psb28-1 and Psb28-2. The complete segregation was checked by PCR (data not shown).

To create N-terminally FLAG-tagged Psb28-1, the pUC57Sll1398C'FLAG plasmid was used to generate pUC57Sll1398N'FLAG vector by replacing sll1398-FLAG with the FLAG-sll1398 sequence using NdeI and AvrII restriction sites. The N-terminally FLAG-tagged Psb28-2 was placed under the petJ promoter in a ΔPsb28-2 background (Boehm et al., 2012).

Cultivation Conditions of Cyanobacterial Strains

The cells used in this study were grown in 100 mL of liquid BG11 medium using 250 mL flasks on an orbital shaker at 29°C under continuous light of 40 µmol photons m^{-2} s^{-1} (normal

light). For (photo)heterotrophic growth conditions, the medium was supplemented with 5 mM glucose.

The cells used for protein purification were grown in 4 L of BG11 medium containing 1 mM glucose using 10L flasks. The culture was air bubbled, stirred, and incubated at 29°C under continuous surface illumination of 120 μmol photons m^{-2} s^{-1} from a light source placed on one side of the flask (creating low-light conditions, due to the big volume of the culture). For high-light cultivation, the cells were grown in 400 mL of liquid BG11 medium using 1 L flasks containing 1 mM glucose and cultivated on an orbital shaker under gradually increasing surface illumination of 20-120 μmol photons m^{-2} s^{-1}. WT cells were always grown under the same conditions as the mutant strains.

Growth Assay on Agar Plates

Cells of *Synechocystis* 6803 strains used for growth assay were cultivated autotrophically in 70 mL of liquid BG11 medium using 250 mL flasks on an orbital shaker at 29°C under continuous light of 40 μmol photons m^{-2} s^{-1} (normal light). After reaching the exponential phase, the cells were diluted to $OD_{750\ nm}$ 0.1, 0.05, and 0.025 and spotted on autotrophic BG11 agar plates containing 10 mM TES buffer. One plate was always incubated at 40 μmol photons m^{-2} s^{-1} for 4 days, and identical plate was incubated under intermittent light conditions (5 min dark and 5 min 400 μmol photons m^{-2} s^{-1}) or continuous high light (400 μmol photons m^{-2} s^{-1}) for 4 days.

Radioactive Labeling

Radioactive pulse labeling of the cells was performed at 500 μmol of photons m^{-2} s^{-1} and 30°C using a mixture of [^{35}S]Met and [^{35}S]Cys (Trans-label, MP Biochemicals) as described previously (Dobáková et al., 2009a).

Protein Analysis

The Chl*a* content of the samples was determined by extraction into methanol and absorption measurements at 666 and 720 nm (Wellburn, 1994).

Membranes were prepared by breaking the cells with zirconia/silica beads in A buffer (25 mM MES/NaOH [pH 6.5], 10 mM $CaCl_2$, 10 mM $MgCl_2$, and 20% glycerol). The broken cells were centrifuged at 20,000 *g* for 20 min and the pelleted thylakoid membranes were then resuspended in half volume of the supernatant, which represents the soluble fraction, in buffer

A. The Chl concentration of 1% (w/v) *n*-dodecyl-β-D-maltoside solubilized membranes was measured by extraction into methanol and absorption measurements at 666 and 720 nm.

Thylakoid membranes corresponding to 4 µg of Chl*a* were solubilized with 1% (w/v) *n*-dodecyl-β-D-maltoside and separated on a 4%–14% (w/v) polyacrylamide CN-PAGE linear gradient gel (Wittig et al., 2007) or a 4%–14% (w/v) polyacrylamide blue-native PAGE linear gradient gel (Komenda et al., 2012a). Chl fluorescence of separated PSII complexes was recorded using an LAS-4000 camera (Fujifilm, Japan). Gel strips from the first dimension were incubated in 25 mM Tris/HCl buffer (pH 7.5) containing 1% DTT (w/v) and 1% SDS (v/v) at room temperature for 30 min and then separated on 12%-20 % (w/v) polyacrylamide SDS-PAGE gel containing 7 M urea, the second dimension. The gels were stained either with CBB or, for immunoblotting, with fluorescence dye SYPRO orange (Sigma-Aldrich), blotted onto PVDF membrane, and subsequently used for immunodetection. Membranes were incubated with specific primary antibodies raised against Psb27 and PsaD (Komenda et al. 2012a), Psb28 (Dobáková et al. 2009), FLAG (Abgent), and HliA/B (Agrisera), and then with secondary antibody horse-radish peroxidase conjugate (Sigma-Aldrich). After incubation with chemiluminescent substrate Luminata Crescendo (Merck, Germany) blots were scanned with an LAS-4000 camera.

Isolation of FLAG-Tagged Proteins

For isolation of FLAG-tagged proteins, membranes were prepared by breaking the cells with zirconia/silica beads in buffer A (25 mM MES/NaOH [pH 6.5], 10 mM $CaCl_2$, 10 mM $MgCl_2$ and 25% glycerol) with protease inhibitor (SIGMAFAST Protease Inhibitor Cocktail Tablets, EDTA-Free, Sigma-Aldrich), separated from the soluble fraction by centrifugation at 60,000 *g* for 20 min; pelleted membranes were resuspended in buffer A and solubilized in 1.5% (w/v) *n*-dodecyl-β-D-maltoside. The supernatant was then loaded onto a column containing 300 µL of anti-FLAG M2 affinity gel (Sigma-Aldrich, USA) pre-equilibrated with A buffer containing 0.04% *n*-dodecyl-β-D-maltoside (A-DDM buffer). To remove any loosely bound contaminants, the column was first washed with 5 mL of buffer A-DDM and then the FLAG-tagged protein was eluted by a 30 min incubation of resin in 200 µL of A-DDM buffer containing 20% glycerol and 150 µL 3xFLAG peptide (Sigma-Aldrich). Resin was removed by centrifugation at 500 *g* for 5 min. The obtained preparations were separated by 2D gel electrophoresis with subsequent western blotting or Coomassie staining.

Spectroscopy Analysis

Chl fluorescence emission spectra at 77K were measured using an Aminco Bowman Series 2 luminescence spectrometer (Spectronic Unicam) and fluorescence spectra were recorded in the range 600-800 nm.

Absorption spectra of whole cells and FLAG-tagged preparations were recorded in the range 350-750 nm using a Shimadzu UV-3000 spectrophotometer.

Transmission Electron Microscopy

Freshly prepared complexes were used for electron microscopy. The specimens were placed on glow-discharged carbon-coated copper grids and negatively stained with 2% uranyl acetate, visualized by a JEOL JEM-2100F transmission electron microscope (JEOL Japan, using 200 kV at 20,000x magnification) and processed by image analysis. Transmission electron microscopy images were recorded with a bottom-mount Gatan CCD Orius SC1000 camera, corresponding to a pixel size of 3.4 Å. Image analyses were carried out using the Spider and Web software package (Frank et al., 1996). The selected projections were rotationally and translationally aligned, and treated by multivariate statistical analysis in combination with a classification procedure (Harauz et al., 1988; Van Heel and Frank, 1981). Classes from each of the subsets were used for refinement of alignments and subsequent classifications. For the final sum, the best of the class members were summed using a cross-correlation coefficient of the alignment procedure as a quality parameter. The projection was overlaid with cyanobacterial X-ray models of PSI (PDB: 1JB0, Jordan et al., 2001) and monomer of PSII core complexes (PDB: 2AXT, Loll et al., 2005).

Protein Identification by Mass Spectrometry

The MS analyses of protein bands excised from the gel or the liquid pull-down preparations of the tagged proteins were done on a NanoAcquity UPLC (Waters) coupled on-line to an ESI Q-ToF Premier mass spectrometer (Waters) as described in (Janouškovec et al., 2013).

FUNDING

We gratefully acknowledge support from the Grant Agency of the Czech Republic (project P501/12/G055), the Czech Academy of Sciences (RVO 60077344 and RVO61388971), the Czech Ministry of Education (projects LO1416 and CZ 1.05/2.1.00/19.0392) and BBSRC (projects BB/L003260/1 and BB/I00937X/1).

AUTHOR CONTRIBUTIONS

M.B. constructed the strains expressing FLAG-tagged Psb28 proteins, performed most of the biochemical experiments, and participated in writing; Z.G. carried out the electron microscopy study; J.Y. constructed the Psb28 deletion mutants, P.K. performed the mass spectrometric analyses; P.J.N. planned the research, evaluated data, and drafted the manuscript; J.K. planned the research, participated in the experimental design and in experiments, evaluated data, and drafted the manuscript.

ACKNOWLEDGMENTS

We thank Eva Prachová and Jiří Šetlík for excellent technical assistance.

No conflict of the interest declared.

REFERENCES

Bialek, W., Wen, S., Michoux, F., Bečková, M., Komenda, J., Murray, J.W., and Nixon, P.J. (2013). Crystal structure of the Psb28 accessory factor of Thermosynechococcus elongatus photosystem II at 2.3 A. Photosynth. Res. 117:375-383.

Boehm, M., Yu, J., Reisinger, V., Bečková, M., Eichacker, L.A., Schlodder, E., Komenda, J., and Nixon, P.J. (2012). Subunit composition of CP43-less photosystem II complexes of Synechocystis sp. PCC 6803: implications for the assembly and repair of photosystem II. Philos. Trans. R. Soc. B Biol. Sci. 367:3444-3454.

Diner, B.A., Schlodder, E., Nixon, P.J., Coleman, W.J., Rappaport, F., Lavergne, J., Vermaas, W.F.J., and Chisholm, D.A. (2001). Site-directed mutations at D1-His198 and D2-His197 of photosystem II in Synechocystis PCC 6803: Sites of primary charge separation and cation and triplet stabilization. Biochemistry 40:9265-9281.

Dobáková, M., Sobotka, R., Tichý, M., and Komenda, J. (2009). Psb28 protein is involved in the biogenesis of the Photosystem II inner antenna CP47 (PsbB) in the cyanobacterium Synechocystis sp. PCC 6803. Plant Physiol. 149:1076-1086.

Ferreira, K.N., Iverson, T.M., Maghlaoui, K., Barber, J., and Iwata, S. (2004). Architecture of the photosynthetic oxygen-evolving center. Science 303:1831-1838.

Frank, J., Radermacher, M., Penczek, P., Zhu, J., Li, Y., Ladjadj, M., and Leith, A. (1996). SPIDER and WEB: processing and visualization of images in 3D electron microscopy and related fields. J. Struct. Biol. 116(1):190-199.

Funk, C., and Vermaas, W. (1999). A cyanobacterial gene family coding for single-helix proteins resembling part of the light-harvesting proteins from higher plants. Biochemistry 38:9397-9404.

Guskov, A., Kern, J., Gabdulkhakov, A., Broser, M., Zouni, A., and Saenger, W. (2009). Cyanobacterial photosystem II at 2.9-A resolution and the role of quinones, lipids, channels and chloride. Nat. Struct. Mol. Biol. 16:334-342.

Harauz, G., Boekema, E., and van Heel, M. (1988). Statistical image analysis of electron micrographs of ribosomal subunits. In: Methods Enzymol.: Academic Press. 35-49.

He, Q., Dolganov, N., Bjorkman, O., and Grossman, A.R. (2001). The high light-inducible polypeptides in Synechocystis PCC6803. Expression and function in high light. J. Biol. Chem. 276:306-314.

Hernández-Prieto, M.A., Semeniuk, T.A., Giner-Lamia, J., and Futschik, M.E. (2016). The Transcriptional Landscape of the Photosynthetic Model Cyanobacterium Synechocystis sp. PCC6803. Sci. Rep. 6:22168.

Hollingshead, S., Kopečná, J., Armstrong, D.R., Bučinská , L., Jackson, P.J., Chen, G.E., Dickman, M.J., Williamson, M.P., Sobotka, R., and Hunter, C.N. (2016). Synthesis of chlorophyll-binding proteins in a fully-segregated Δycf54 strain of the cyanobacterium Synechocystis PCC 6803. Front. Plant. Sci. 7:292.

Janouškovec, J., Sobotka, R., Lai, D.H., Flegontov, P., Koník, P., Komenda, J., Ali, S., Prášil, O., Pain, A., Oborník, M., et al. (2013). Split Photosystem Protein, Linear-Mapping Topology, and Growth of Structural Complexity in the Plastid Genome of Chromera velia. Mol. Biol. Evol. 30:2447-2462.

Jordan, P., Fromme, P., Witt, H.T., Klukas, O., Saenger, W., and Krauss, N. (2001). Three-dimensional structure of cyanobacterial photosystem I at 2.5 A resolution. Nature 411:909-917.

Jung, K.-H., Lee, J., Dardick, C., Seo, Y.-S., Cao, P., Canlas, P., Phetsom, J., Xu, X., Ouyang, S., An, K., et al. (2008). Identification and functional analysis of light-responsive unique genes and gene family members in rice. PLoS Genet. 4:e1000164.

Kashino, Y., Lauber, W.M., Carroll, J.A., Wang, Q.J., Whitmarsh, J., Satoh, K., and Pakrasi, H.B. (2002). Proteomic analysis of a highly active photosystem II preparation from the cyanobacterium Synechocystis sp. PCC 6803 reveals the presence of novel polypeptides. Biochemistry 41:8004-8012.

Komenda, J., and Barber, J. (1995). Comparison of PsbO and PsbH deletion mutants of Synechocystis PCC-6803 indicates that degradation of D1 protein is regulated by the Q(b) site and dependent on protein-synthesis. Biochemistry 34:9625-9631.

Komenda, J., Knoppová, J., Kopečná, J., Sobotka, R., Halada, P., Yu, J.F., Nickelsen, J., Boehm, M., and Nixon, P.J. (2012a). The Psb27 assembly factor binds to the CP43 complex of photosystem II in the cyanobacterium Synechocystis sp. PCC 6803. Plant Physiol. 158:476-486.

Komenda, J., Reisinger, V., Muller, B.C., Dobáková, M., Granvogl, B., and Eichacker, L.A. (2004). Accumulation of the D2 protein is a key regulatory step for assembly of the photosystem II reaction center complex in Synechocystis PCC 6803. J. Biol. Chem. 279:48620-48629.

Komenda, J., Sobotka, R., and Nixon, P.J. (2012b). Assembling and maintaining the Photosystem II complex in chloroplasts and cyanobacteria. Curr. Opin. Plant Biol. 15:245-251.

Kopečná, J., Komenda, J., Bučinská, L., and Sobotka, R. (2012). Long-term acclimation of the cyanobacterium Synechocystis sp. PCC 6803 to high light is accompanied by an enhanced production of chlorophyll that is preferentially channeled to trimeric Photosystem I. Plant Physiol. 160:2239-2250.

Kopečná, J., Sobotka, R., and Komenda, J. (2013). Inhibition of chlorophyll biosynthesis at the protochlorophyllide reduction step results in the parallel depletion of Photosystem I and Photosystem II in the cyanobacterium Synechocystis PCC 6803. Planta 237:497-508.

Liu, H.J., Huang, R.Y.C., Chen, J.W., Gross, M.L., and Pakrasi, H.B. (2011a). Psb27, a transiently associated protein, binds to the chlorophyll binding protein CP43 in photosystem II assembly intermediates. Proc. Natl. Acad. Sci. U.S.A. 108:18536-18541.

Liu, H.J., Roose, J.L., Cameron, J.C., and Pakrasi, H.B. (2011b). A genetically tagged Psb27 protein allows purification of two consecutive photosystem II (PSII) assembly intermediates in Synechocystis 6803, a cyanobacterium. J. Biol. Chem. 286:24865-24871.

Loll, B., Kern, J., Saenger, W., Zouni, A., and Biesiadka, J. (2005). Towards complete cofactor arrangement in the 3.0 angstrom resolution structure of photosystem II. Nature 438:1040-1044.

Mabbitt, P.D., Wilbanks, S.M., and Eaton-Rye, J.J. (2014). Structure and function of the hydrophilic Photosystem II assembly proteins: Psb27, Psb28 and Ycf48. Plant Physiol. Biochem. (Paris) 81:96-107.

Morris, J.N., Crawford, T.S., Jeffs, A., Stockwell, P.A., Eaton-Rye, J.J., and Summerfield, T.C. (2014). Whole genome re-sequencing of two 'wild-type' strains of the model cyanobacterium Synechocystis sp. PCC 6803. N. Z. J. Bot. 52:36-47.

Nixon, P.J., Michoux, F., Yu, J.F., Boehm, M., and Komenda, J. (2010). Recent advances in understanding the assembly and repair of photosystem II. Ann. Bot. (Lond.) 106:1-16.

Nowaczyk, M.M., Hebeler, R., Schlodder, E., Meyer, H.E., Warscheid, B., and Rogner, M. (2006). Psb27, a cyanobacterial lipoprotein, is involved in the repair cycle of photosystem II. Plant Cell 18:3121-3131.

Nowaczyk, M.M., Krause, K., Mieseler, M., Sczibilanski, A., Ikeuchi, M., and Rogner, M. (2012). Deletion of psbJ leads to accumulation of Psb27-Psb28 photosystem II complexes in Thermosynechococcus elongatus. Biochim. Biophys. Acta 1817:1339-1345.

Sakata, S., Mizusawa, N., Kubota-Kawai, H., Sakurai, I., and Wada, H. (2013). Psb28 is involved in recovery of photosystem II at high temperature in Synechocystis sp. PCC 6803. Biochim. Biophys. Acta 1827:50-59.

Schriek, S., Aguirre-von-Wobeser, E., Nodop, A., Becker, A., Ibelings, B.W., Bok, J., Staiger, D., Matthijs, H.C.P., Pistorius, E.K., and Michel, K.P. (2008). Transcript profiling indicates that the absence of PsbO affects the coordination of C and N metabolism in Synechocystis sp. PCC 6803. Physiol. Plant 133:525-543.

Sobotka, R., Duerhring, U., Komenda, J., Peter, E., Gardian, Z., Tichý, M., Grimm, B., and Wilde, A. (2008). Importance of the cyanobacterial GUN4 protein for chlorophyll metabolism and assembly of photosynthetic complexes. J. Biol. Chem. 283:25794-25802.

Stöckel, J., Jacobs, J.M., Elvitigala, T.R., Liberton, M., Welsh, E.A., Polpitiya, A.D., Gritsenko, M.A., Nicora, C.D., Koppenaal, D.W., Smith, R.D., et al. (2011). Diurnal rhythms result in significant changes in the cellular protein complement in the cyanobacterium *Cyanothece* 51142. PLoS ONE 6:e16680.

Tichý, M., Bečková, M., Kopečná, J., Noda, J., Sobotka, R., and Komenda, J. (2016). Strain of Synechocystis PCC 6803 with aberrant assembly of Photosystem II contains tandem duplication of a large chromosomal region. Front. Plant. Sci. 7:648.

Umena, Y., Kawakami, K., Shen, J.R., and Kamiya, N. (2011). Crystal structure of oxygen-evolving photosystem II at a resolution of 1.9 A. Nature 473:55-60.

Van Heel, M., and Frank, J. (1981). Use of Multivariate Statistics in Analyzing the Images of Biological Macromolecules. Ultramicroscopy 6:187-194.

Wellburn, A.R. (1994). The spectral determination of chlorophyll-a and chlorophyll-b, as well as total carotenoids, using various solvents with spectrophotometers of different resolution. J. Plant Physiol. 144:307-313.

Wittig, I., Karas, M., and Schagger, H. (2007). High resolution clear native electrophoresis for in-gel functional assays and fluorescence studies of membrane protein complexes. Mol. Cell. Proteomics 6:1215-1225.

Yang, Y., Ramelot, T.A., Cort, J.R., Wang, D., Ciccosanti, C., Hamilton, K., Nair, R., Rost, B., Acton, T.B., Xiao, R., et al. (2011). Solution NMR structure of photosystem II reaction center protein Psb28 from Synechocystis sp. strain PCC 6803. Proteins Struct. Funct. Bioinformat. 79:340-344.

4.4.1 Figure legend

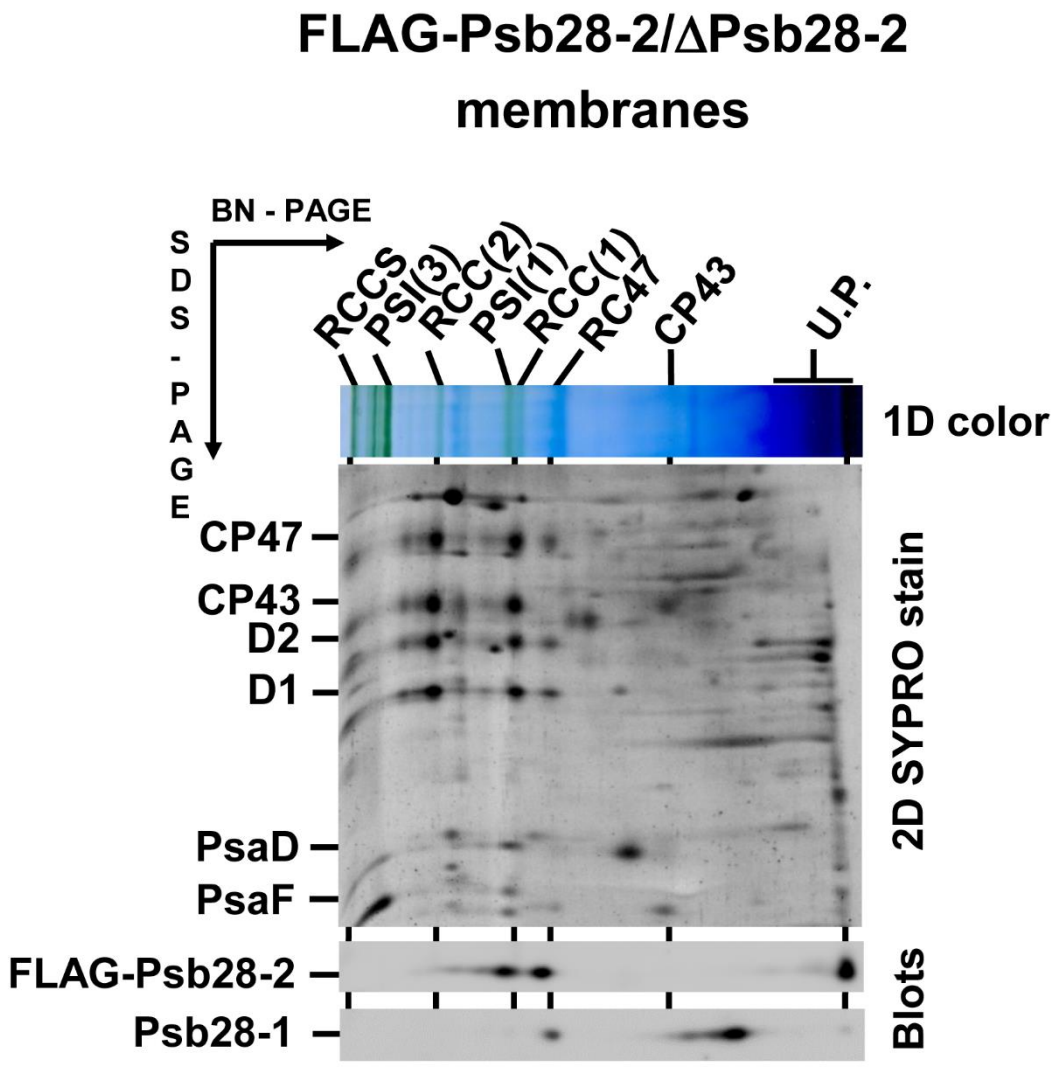

Figure 1.

Figure 1. Two-Dimensional Protein Analysis of a *Synechocystis* 6803 Strain FLAG-Psb28-2/ΔPsb28-2 Expressing the FLAG-Psb28-2 Protein Instead of Psb28-2. Solubilized membranes isolated from the strain corresponding to 4 µg of Chl*a* were analyzed by blue-native PAGE in the first dimension (1D color) and by SDS-PAGE in the second dimension. The gel was stained with SYPRO orange (2D SYPRO stain); proteins were blotted onto PVDF membrane and subsequently probed with specific antibodies (Blots). The designation of complexes: RCCS, supercomplex of PSI trimer and PSII dimer; PSI(3) and PSI(1), trimeric and monomeric photosystem I; RCC(2) and RCC(1), dimeric and monomeric PSII core complexes; RC47, the monomeric PSII core complex lacking CP43; U.P., unassembled proteins.

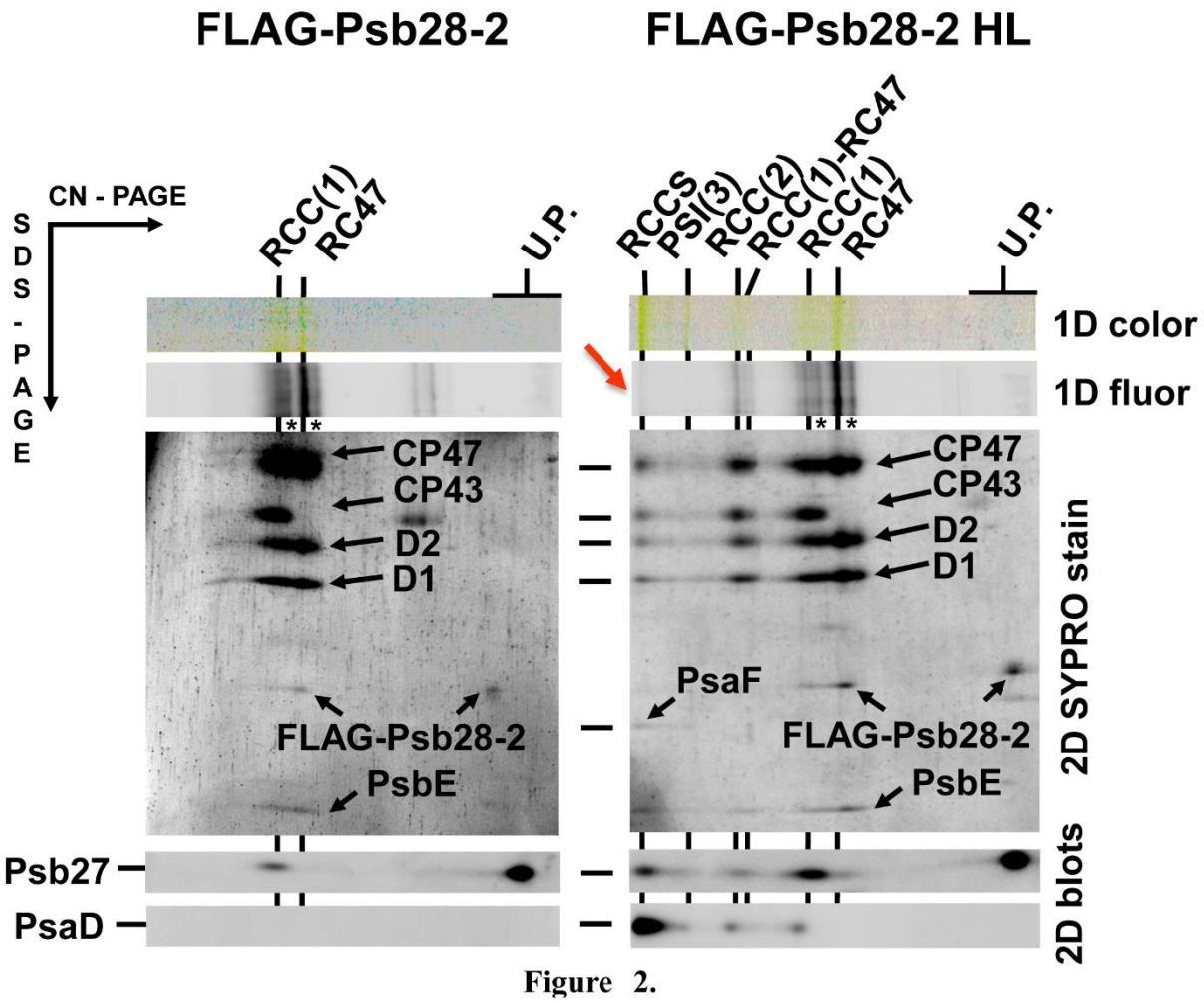

Figure 2.

Figure 2. Two-Dimensional Protein Analysis of N-terminally FLAG-tagged Psb28-2 Preparation (FLAG-Psb28-2) Isolated by Affinity Chromatography from Cells of FLAG-Psb28-2/ΔPsb28-2 Strain Grown Under Low (Left) or High (HL, Right) Irradiance. Preparations were analyzed by CN-PAGE in the first dimension, and the native gel was photographed (1D color) and scanned with an LAS-4000 camera for fluorescence (1D fluor); after SDS-PAGE in the second dimension, the gel was stained with SYPRO orange (2D SYPRO stain), electroblotted to PVDF membrane and probed with the antibody specific for Psb27 and PsaD (2D blots). The designation of complexes as in Figure 1, RCC(1)-RC47 is a PSII dimeric core complex lacking one of the CP43 inner antenna. The red arrow points to the fluorescence quenching in RCCS. Asterisks indicate PSII complexes lacking FLAG-Psb28-2.

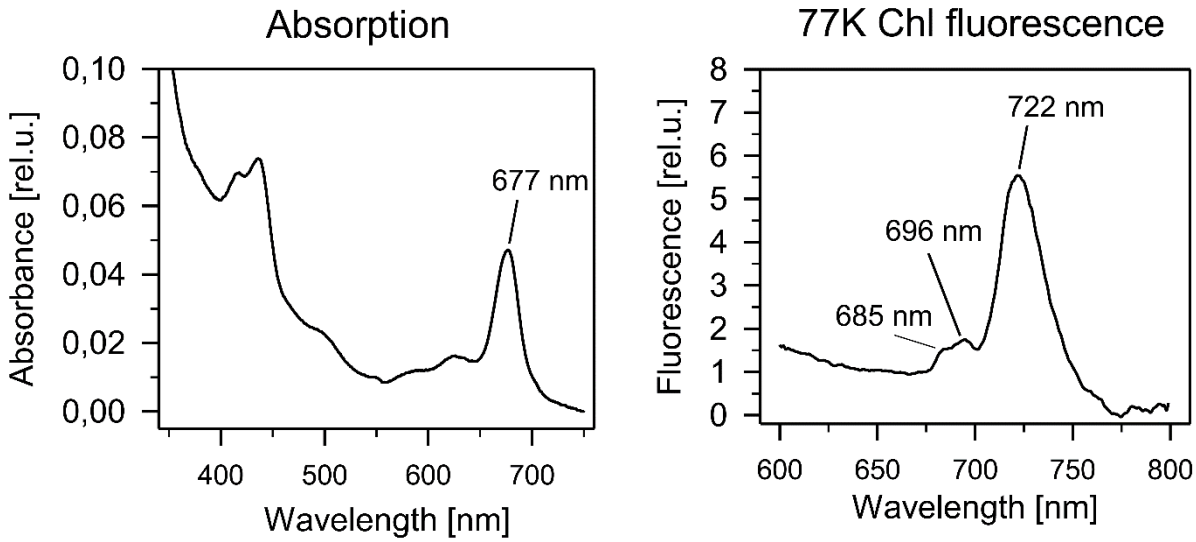

Figure 3.

Figure 3. The Room Temperature Absorption (Left) and 77K Chl Fluorescence (Right) Spectra of the RCCS Band Cut from the CN Gel Shown in Figure 2 (Right). The absorption spectrum was measured using a Shimadzu UV-3000 spectrometer; the fluorescence spectrum was measured using an Aminco Bowman Series 2 luminescence spectrometer.

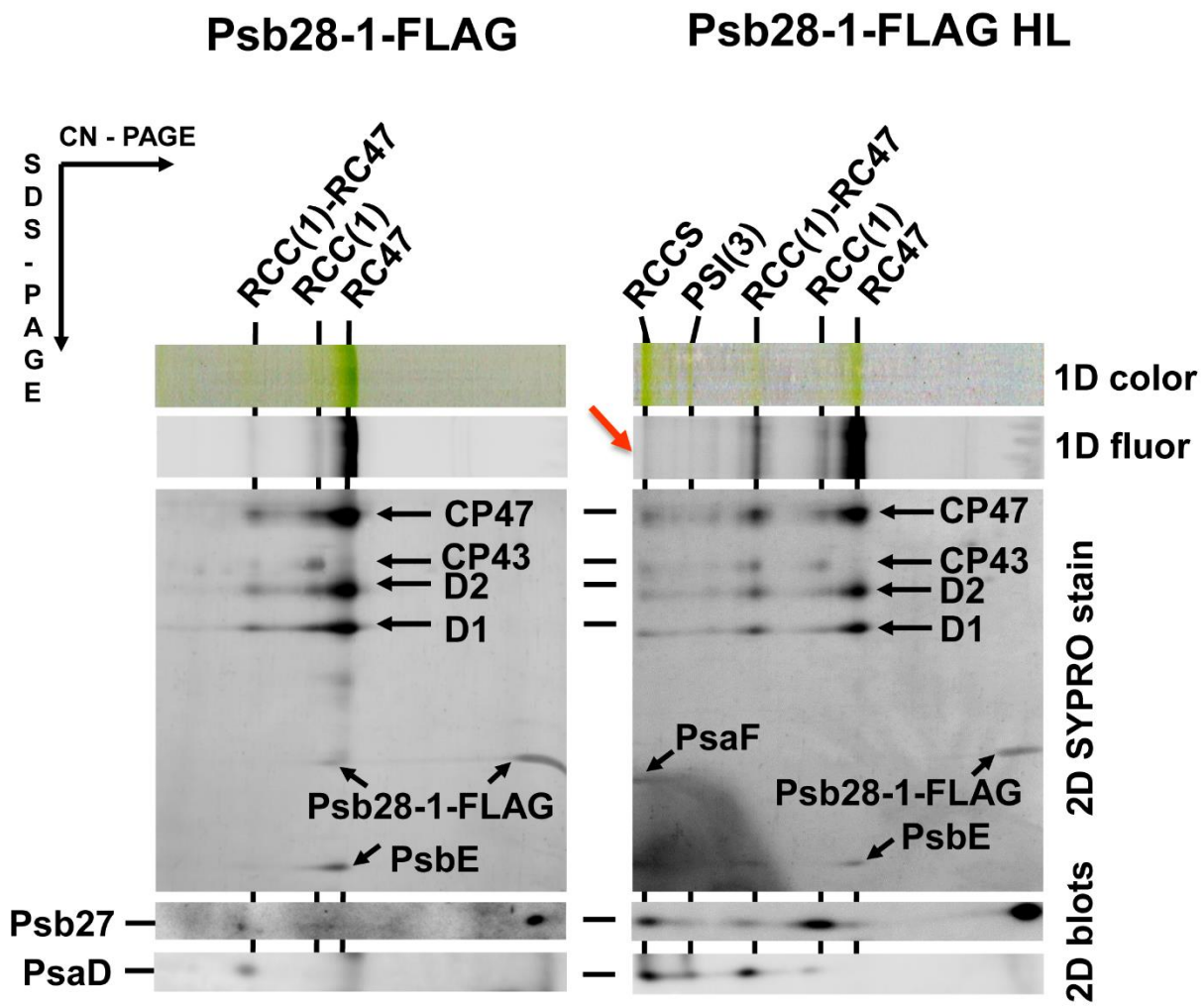

Figure 4.

Figure 4. Two-Dimensional Protein Analysis of FLAG-tagged Psb28-1 Preparation Isolated by Affinity Chromatography from Cells of Psb28-1-FLAG/ΔPsb28-1 Strain Grown Under Low (Left) or High (HL, Right) Irradiance. Preparations were analyzed by CN PAGE in the first dimension, and the native gel was photographed (1D color) and scanned by an LAS-4000 camera for fluorescence (1D fluor); after SDS-PAGE in the second dimension, the gel was stained with SYPRO orange (2D SYPRO stain), electroblotted to PVDF membrane, and probed with the specific antibodies against Psb27 and PsaD (2D blots). The designation of complexes as in Figures 1 and 2. The red arrow points to the fluorescence quenching in RCCS.

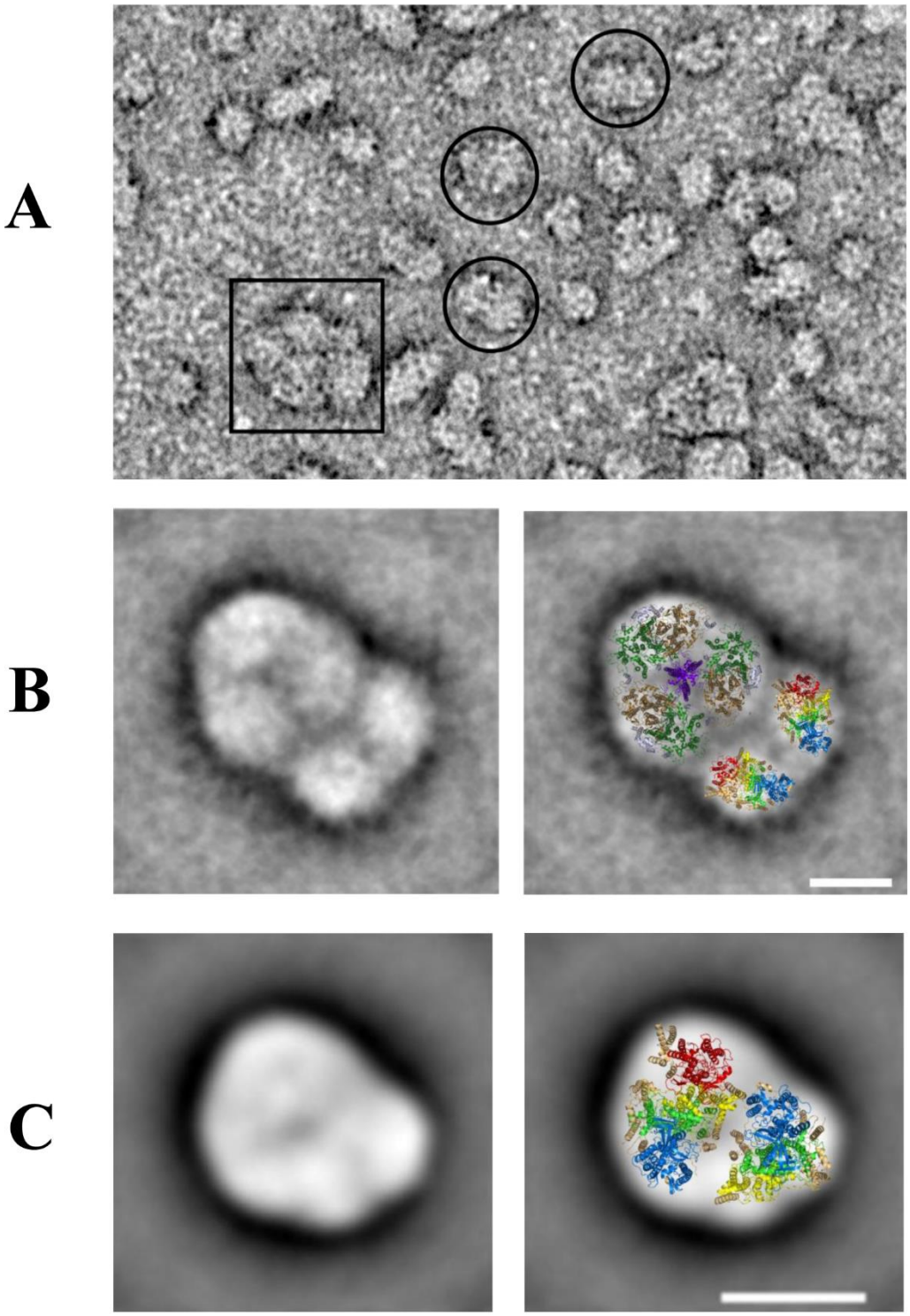

Figure 5.

Figure 5. Electron Microscopic Analysis of Complexes Co-isolated with Psb28-1-FLAG from High-Light Exposed Culture. (A) Electron micrographs of negatively stained complexes. The labeled RCCS and RCC(1)-RC47 particles are in square and circles, respectively. (B) The top view projection map of the RCCS supercomplex containing trimeric

PSI complex and two PSII monomers. The negatively stained particle (left) was obtained by classification of 95 particles. Right: the projection was overlaid with a cyanobacterial X-ray models of the PSI trimer and two PSII core complexes. (C) The negatively stained particles of RCC(1)-RC47 (left) was obtained by classification of 5600 particles. The projection was overlaid with a cyanobacterial X-ray model of the PSII monomer and PSII monomer lacking CP43 and associated proteins (PsbK, PsbZ, and Psb30). Color designation of proteins: PsaA, brown; PsaB, dark green; PsaL, violet; other small PSI subunits, gray; D1, yellow; D2, light green; CP47, blue; CP43, red; small PSII subunits, ochre. The coordinates are taken from the PDB (http://www.rcsb.org/pdb): PSI code, PDB: 1JB0 (Jordan et al. 2001); PSII code, PDB: 2AXT (Loll et al. 2005). The scale bars represent 10 nm.

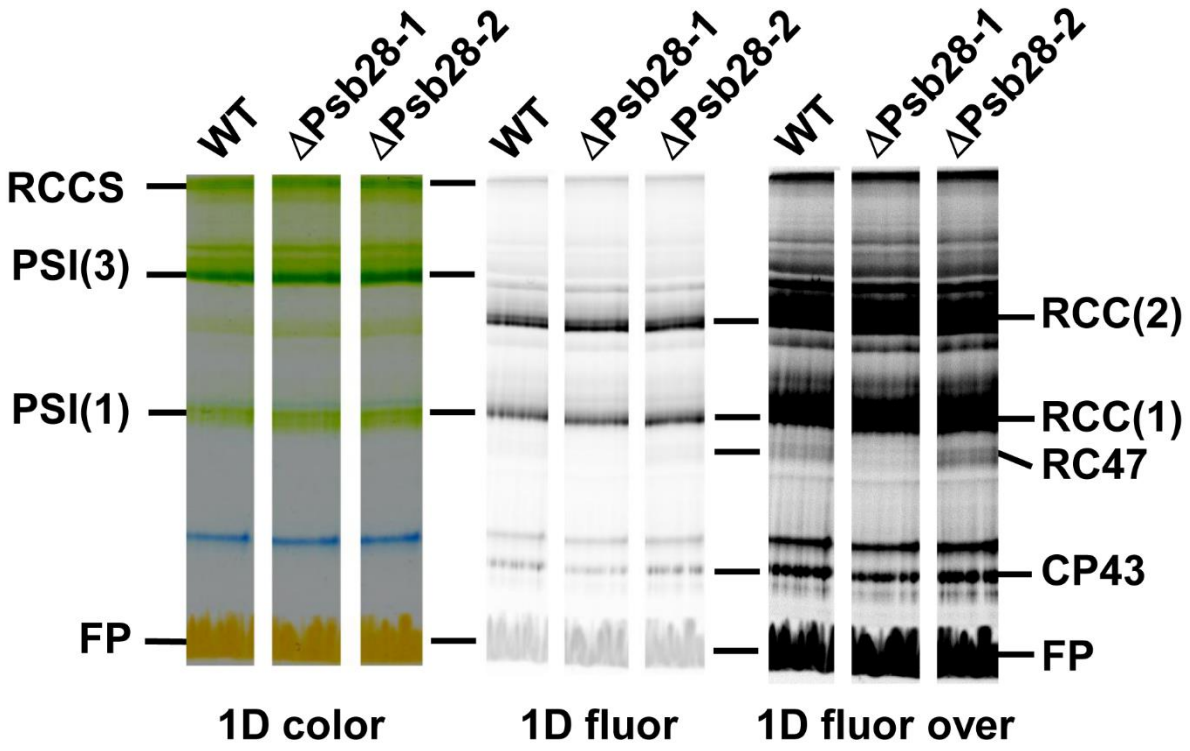

Strain	RC47 band (% of WT)	CP43 band (% of WT)
WT	100	100
ΔPsb28-1	25±6	69±4
ΔPsb28-2	177±17	121±7

Figure 6.

Figure 6. Pigment-Protein Analysis of Membranes Isolated from WT, ΔPsb28-1, and ΔPsb28-2 *Synechocystis* 6803 Strains by CN PAGE. Strains were grown at irradiance of 40 μmol photons m^{-2} s^{-1}. Each sample contained 4 μg of Chl*a* corresponding to the same OD_{750nm}. The native gel was photographed (1D color) and scanned with an LAS-4000 camera for Chl fluorescence before (1D fluor) and after enhancement of the signal (1D fluor over). Signals of RC47 and CP43 in 1D fluor were quantified with ImageQuant software and expressed as % of the WT band intensity. The values represent means of three independent measurements ± SD.

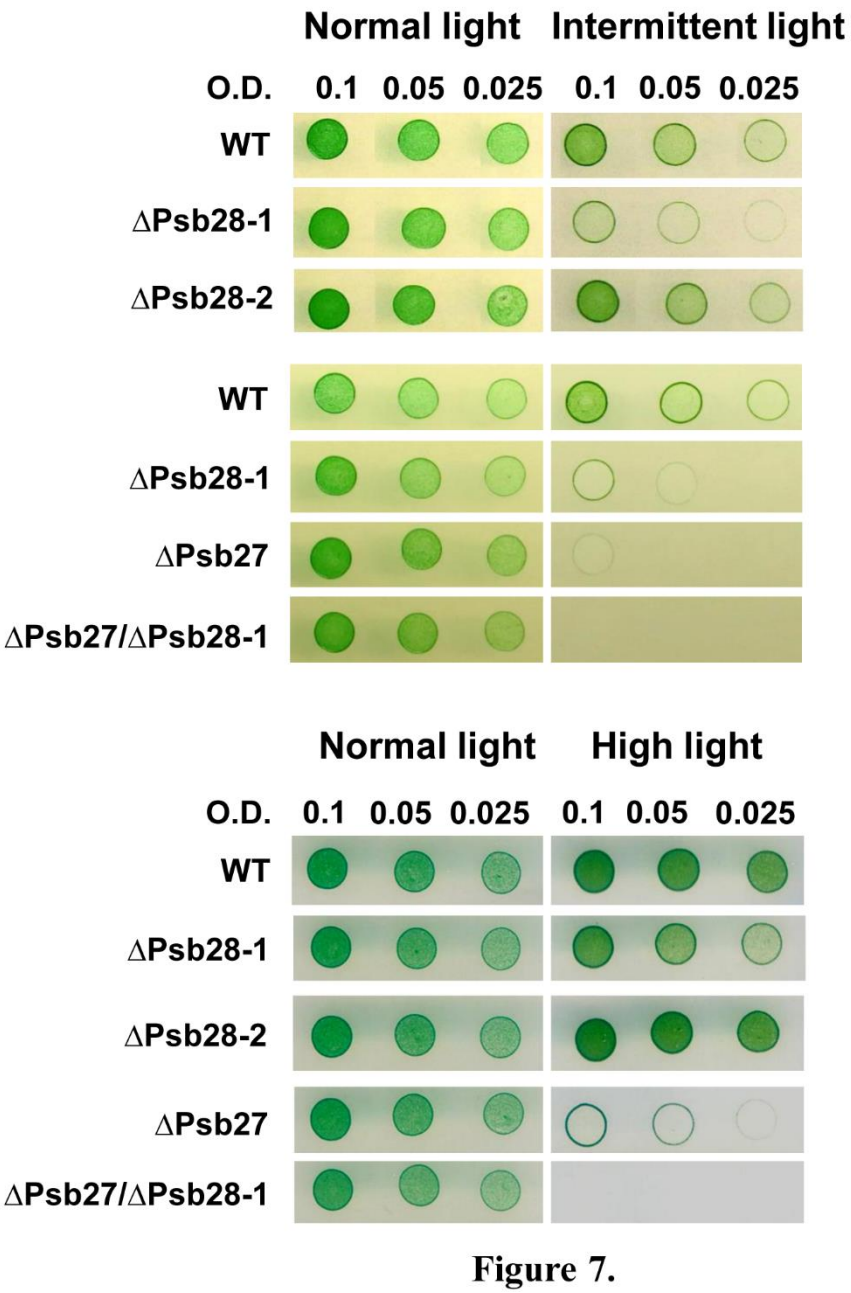

Figure 7.

Figure 7. Growth Assay on Agar Plates of WT, ΔPsb28-1, ΔPsb28-2, ΔPsb27, and ΔPsb27/ΔPsb28-1. Each strain was cultivated autotrophically in liquid BG11 medium at 40 µmol photons m^{2-} s^{-1}. After reaching the exponential phase, the cells were diluted to $OD_{750\ nm}$ 0.1, 0.05, and 0.025 and spotted on autotrophic agar plates. Identical plates were incubated for 4 days either at 40 µmol photons m^{2-} s^{-1} (left) or under intermittent light conditions (5 min dark and 5 min 400 µmol photons m^{2-} s^{-1}, upper right) or at constant high light (400 µmol photons m^{2-} s^{-1}, lower right).

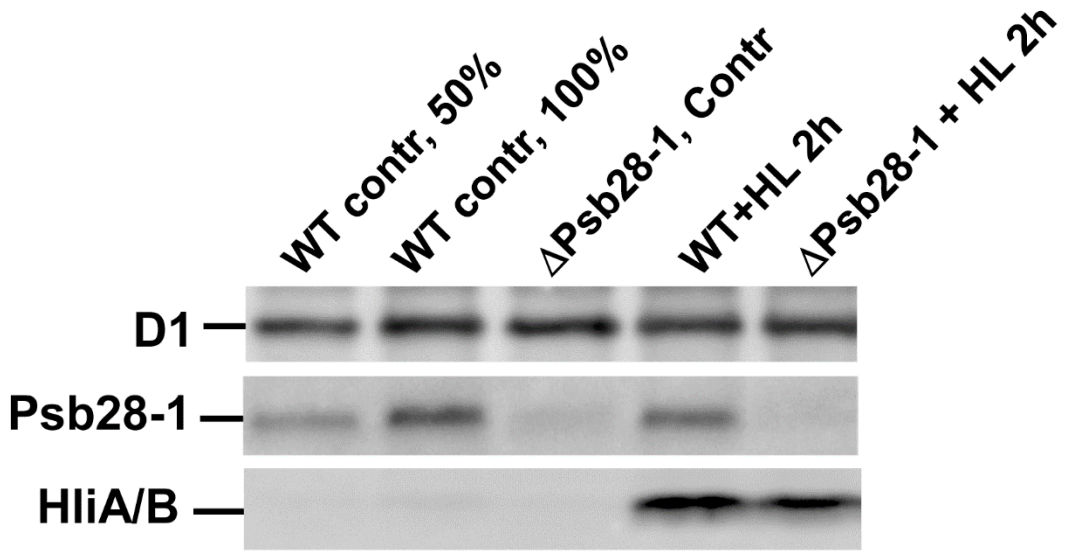

Figure 8.

Figure 8. Protein Analysis of WT and ΔPsb28 Cells Grown under Standard (contr) and High (500 µmol photons m^{-2} s^{-1}) irradiance for 2 h (HL 2h). Membranes isolated from the cells corresponding to 4 µg of Chl*a* (only lane designated WT contr, 50% contained 2 µg of Chl*a*) were separated by SDS-PAGE, and proteins were blotted onto PVDF membrane and subsequently probed with antibody specific to the D1 protein (loading control), Psb28-1, and HliA/B.

Table 1. List of Proteins Identified by Mass Spectrometry in the CN-PAGE-separated PSII-PSI Supercomplex RCCS of the Psb28-2-FLAG Pull-Down (Figure 2) Isolated from High-Light-Treated Cells of the *Synechocystis* Strain Expressing Psb28-2-FLAG. The PLGS score is a statistical measure of peptide assignment accuracy; it is calculated with Protein Lynx Global Server (PLGS 2.2.3) software (Waters).

Protein UniProtKB No.	Size (Da) Length (AA)	Coverage (%)	Detected/theoretical no. of peptides	PLGS score
CP47 P05429	55903 507	5	1/27	208
D1 P14660	39695 360	3	1/14	130
PsaA P29254	82950 751	5	3/34	338
PsaF P29256	18249 165	19	2/11	95
PsaL P37277	16624 157	25	2/6	160

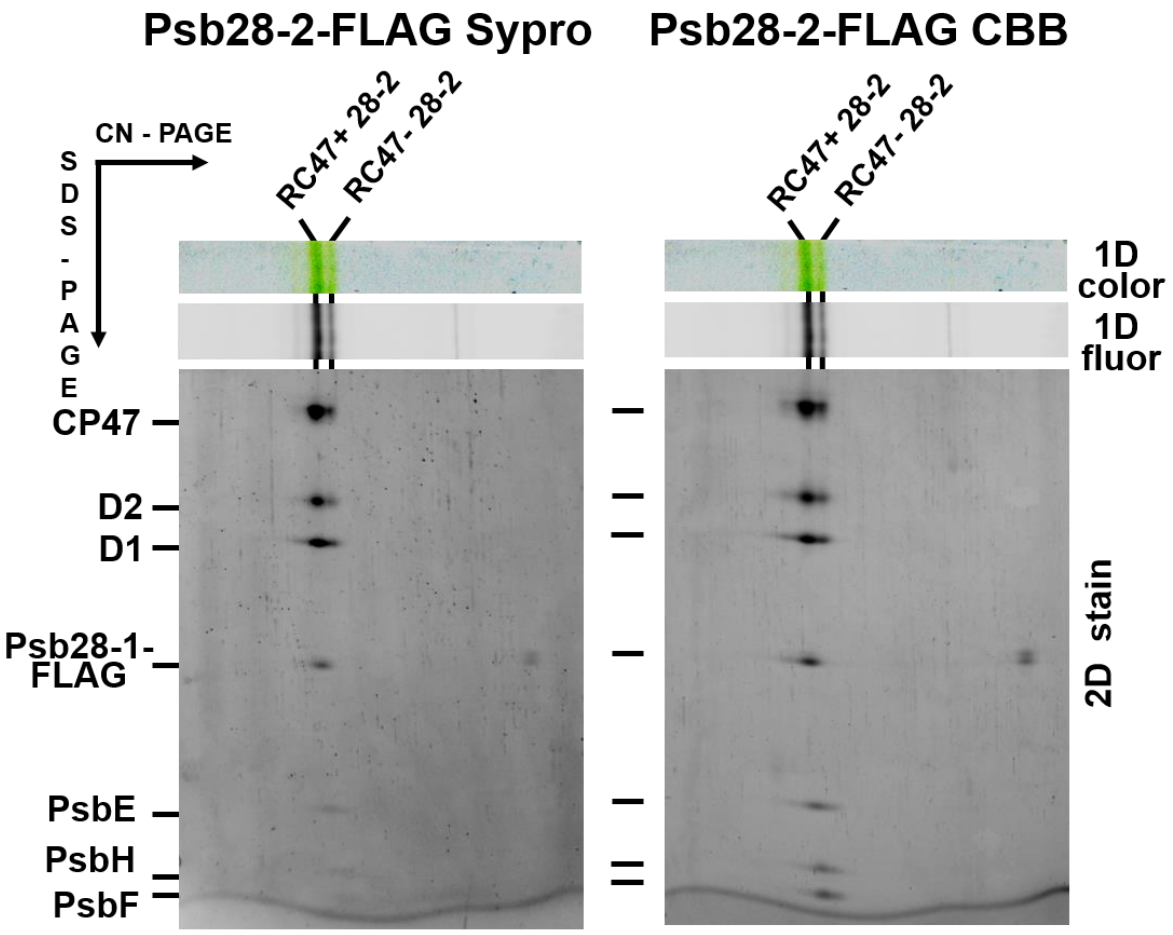

Protein	Protein band intensity/M_w	Protein/CP47 stoichiometry
CP47	917±30	1.00±0.03
D1	807±14	0.88±0.01
Psb28-2	532±58	0.58±0.06
PsbE	287±8	0.31±0.01

Protein	Protein band intensity/M_w	Protein/CP47 stoichiometry
CP47	1646±24	1.00±0.03
D1	1271±60	0.77±0.07
Psb28-2	826±56	0.82±0.08
PsbE	13547±16	0.82±0.02

Figure S1. Two-Dimensional Protein Analysis of C-terminally FLAG-Tagged Psb28-2 Preparation (Psb28-2-FLAG) Isolated by Affinity Ahromatography from Cells of Psb28-2-FLAG/ΔPsb28-2 Strain Grown under Low Irradiance. Preparation was isolated in the phosphate buffer according to Boehm et al. (2012), analyzed by CN PAGE in the first dimension; the native gel was photographed (1D color) and scanned with an LAS 4000 camera for fluorescence (1D fluor); after SDS-PAGE in the second dimension the gel was first stained by SYPRO orange (2D stain) and then by Coomassie Blue (CBB). Signals of CP47, D1, PsbE, and Psb28-2-FLAG in the band of RCC47 containing Psb28-2(RC47+ 28-2) were quantified by

Image Quant software; values were divided by their molecular mass (Band intensity/Mw) and then related to the value obtained for CP47 (Protein/CP47 stoichiometry). The values represent means ± SD of three quantifications of the bands in the gel in the upper panels.

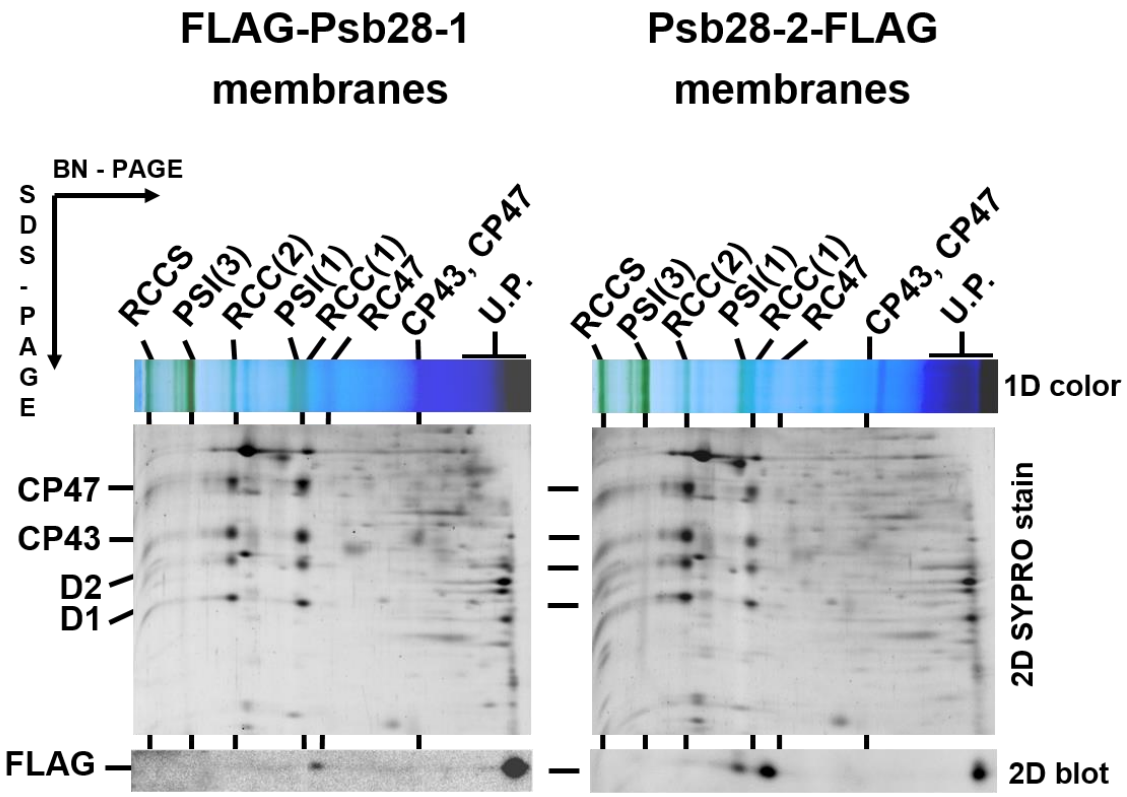

Figure S2. Two-Dimensional Analysis of Membranes from *Synechocystis* Strains Expressing FLAG-Psb28-1 and Psb28-2-FLAG Proteins. Membranes isolated from the cells corresponding to 4 µg of Chl*a* were separated by BN-PAGE, the native gel was photographed (1D color), after SDS-PAGE in the second dimension the gel was stained with SYPRO orange (2D SYPRO stain), proteins were blotted onto PVDF membrane and subsequently probed with antibody specific to FLAG-tag (2D blot). The designation of complexes: RCCS, supercomplex of PSI trimer and PSII dimer; PSI(3) and PSI(1), trimeric and monomeric photosystem I; RCC(2) and RCC(1), dimeric and monomeric PSII core complexes; RC47, the monomeric PSII core complex lacking CP43; U.P., unassembled proteins.

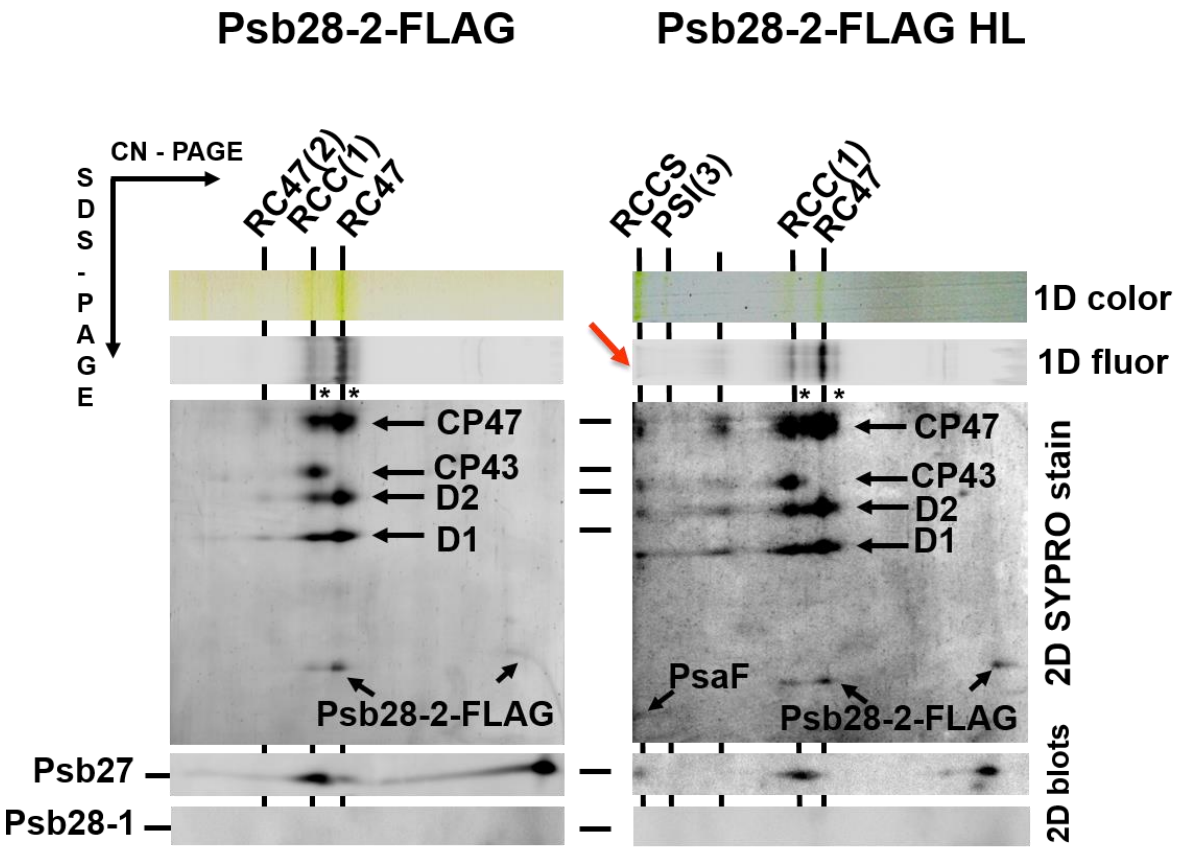

Figure S3. Two-Dimensional Protein Analysis of C-terminally FLAG-Tagged Psb28-2 Preparation (Psb28-2-FLAG) Isolated by Affinity Chromatography from Cells of Psb28-2-FLAG/ΔPsb28-2 Strain Grown under Low (Left) or High (HL, Right) Irradiance. Preparations were analyzed by CN PAGE in the first dimension, the native gel was photographed (1D color) and scanned with an LAS 4000 camera for fluorescence (1D fluor), after SDS-PAGE in the second dimension the gel was stained by SYPRO orange (2D SYPRO stain), electroblotted to PVDF membrane and probed with the antibody specific for Psb27 and Psb28-1 (2D blot). The designation of complexes as in Fig. 1, the red arrow points at the fluorescence quenching in RCCS. Asterisks indicate PSII complexes lacking Psb28-2-FLAG.

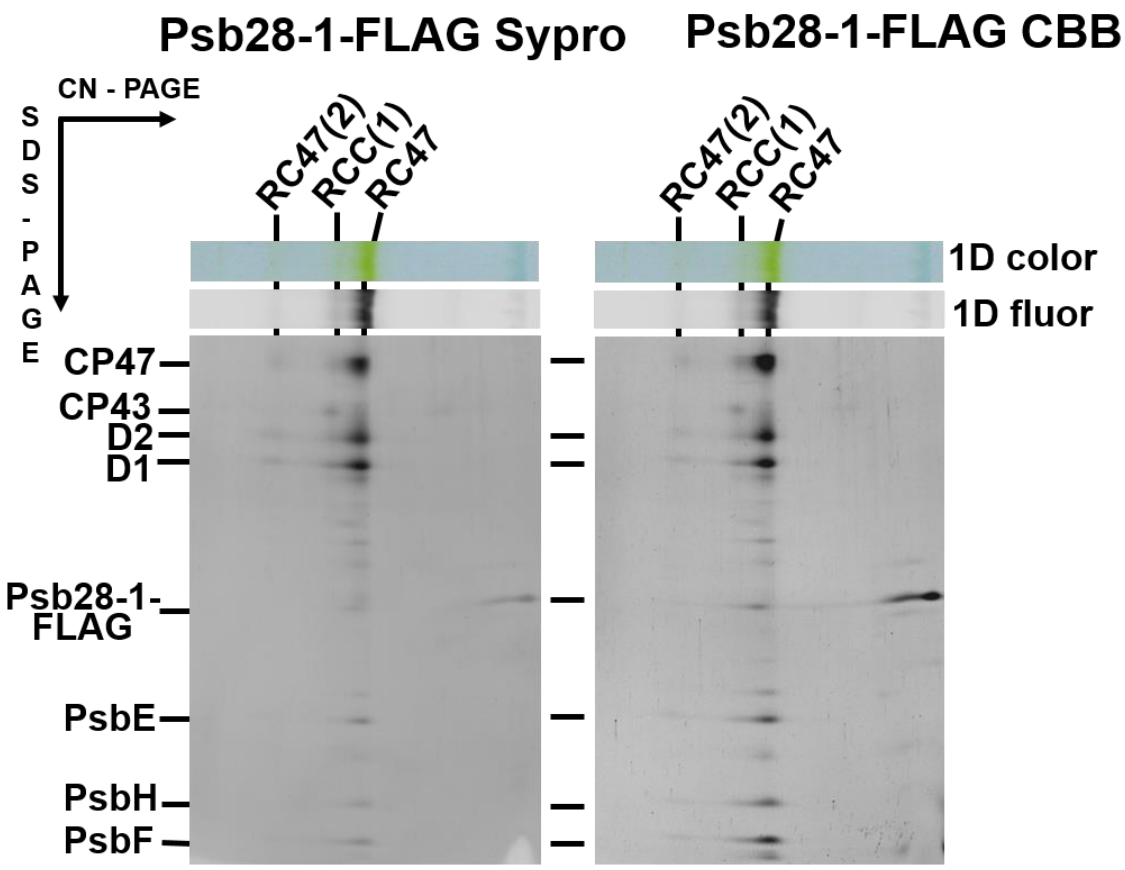

Protein	Protein band intensity/M_w	Protein/CP47 stoichiometry
CP47	3679±151	1.00±0.04
D1	3983±84	1.08±0.02
Psb28-1	2995±178	0.80±0.05
PsbE	1925±158	0.52±0.04

Protein	Protein band intensity/M_w	Protein/CP47 stoichiometry
CP47	2790±24	1.00±0.01
D1	2121±52	0.76±0.02
Psb28-1	6433±263	2.08±0.06
PsbE	3031±306	1.09±0.08

Figure S4. Two-Dimensional Protein Analysis of C-terminally FLAG-Tagged Psb28-1 Preparation (Psb28-1-FLAG) Isolated by Affinity Chromatography from Cells of Psb28-1-FLAG/ΔPsb28-1 Strain Grown under Low Irradiance. Preparation was analyzed by CN PAGE in the first dimension, the native gel was photographed (1D color) and scanned with an LAS 4000 camera for fluorescence (1D fluor), after SDS-PAGE in the second dimension the gel was stained by SYPRO orange (Sypro) and then by Coomassie Blue (CBB) stain. The designation of complexes as in Figure 1). Signals of CP47, D1, PsbE, and Psb28-1-FLAG were quantified by Image Quant software, values were divided by their molecular mass (Band intensity/Mw) and then rela*te*d to the value obtained for CP47 (Protein/CP47 stoichiometry).

The values represent means ± SD of three quantification of the bands in the gel in the upper panels.

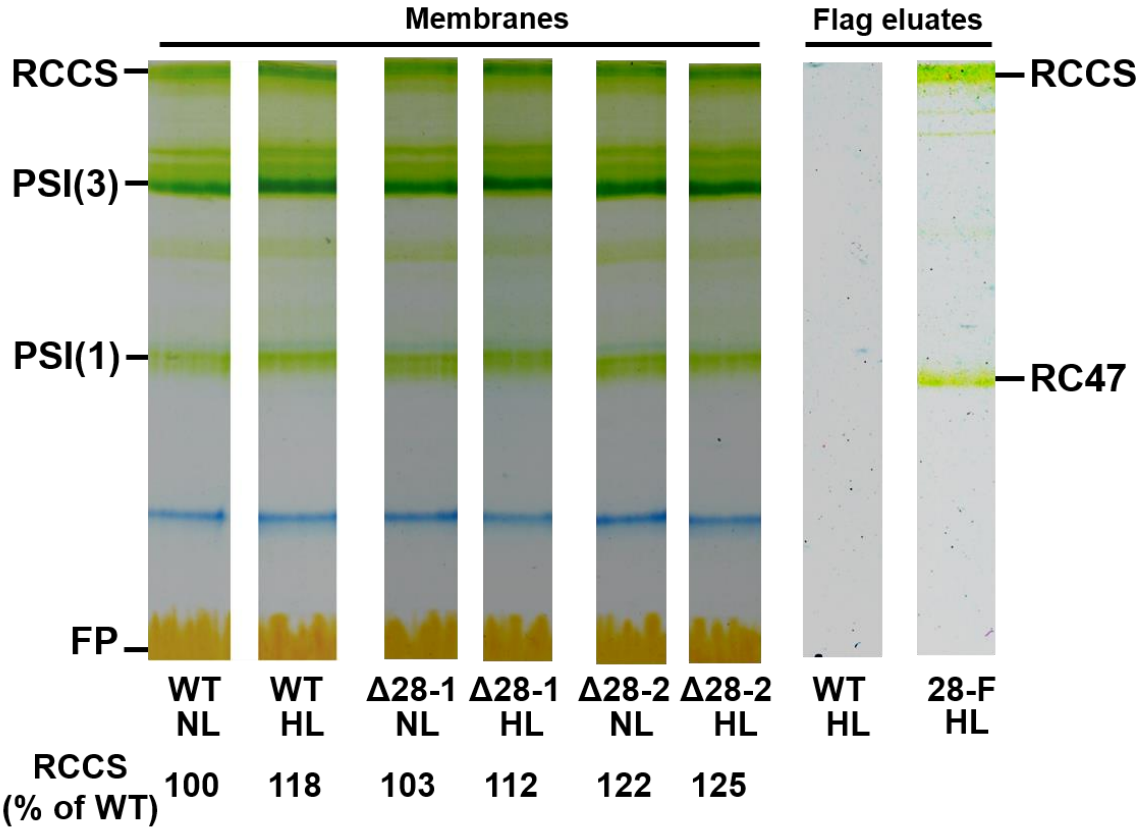

Figure S5. Pigment-Protein Analysis of Membranes and FLAG-Eluates Isolated and FLAG-Eluates Isolated from WT and Psb28-1-FLAG Containing Cells Grown at Standard Irradiance (NL) and Then Treated With High Irradiance for 2 h (HL). WT, ΔPsb28-1 (Δ28-1), ΔPsb28-2 (Δ28-2) and strain expressing Psb28-1-FLAG protein (28-F) were grown initially at irradiance of 40 µmol photons m^{-2} s^{-1} (NL) and then transferred to 500 µmol photons m^{-2} s^{-1} (HL) for 2 h. Cells were used for isolation of membranes and then analyzed or used for purification on FLAG-affinity column. Membranes sample contained 4 µg of Chl*a*, isolation from both strains was performed from the same amount of membranes (0.5 mg Chl). The CN gel was photographed. Bands of RCCS in membranes were quantified by Image Quant software and expressed as % of the WT NL band intensity. The values represent means of three measurements, SD did not exceed 10%.

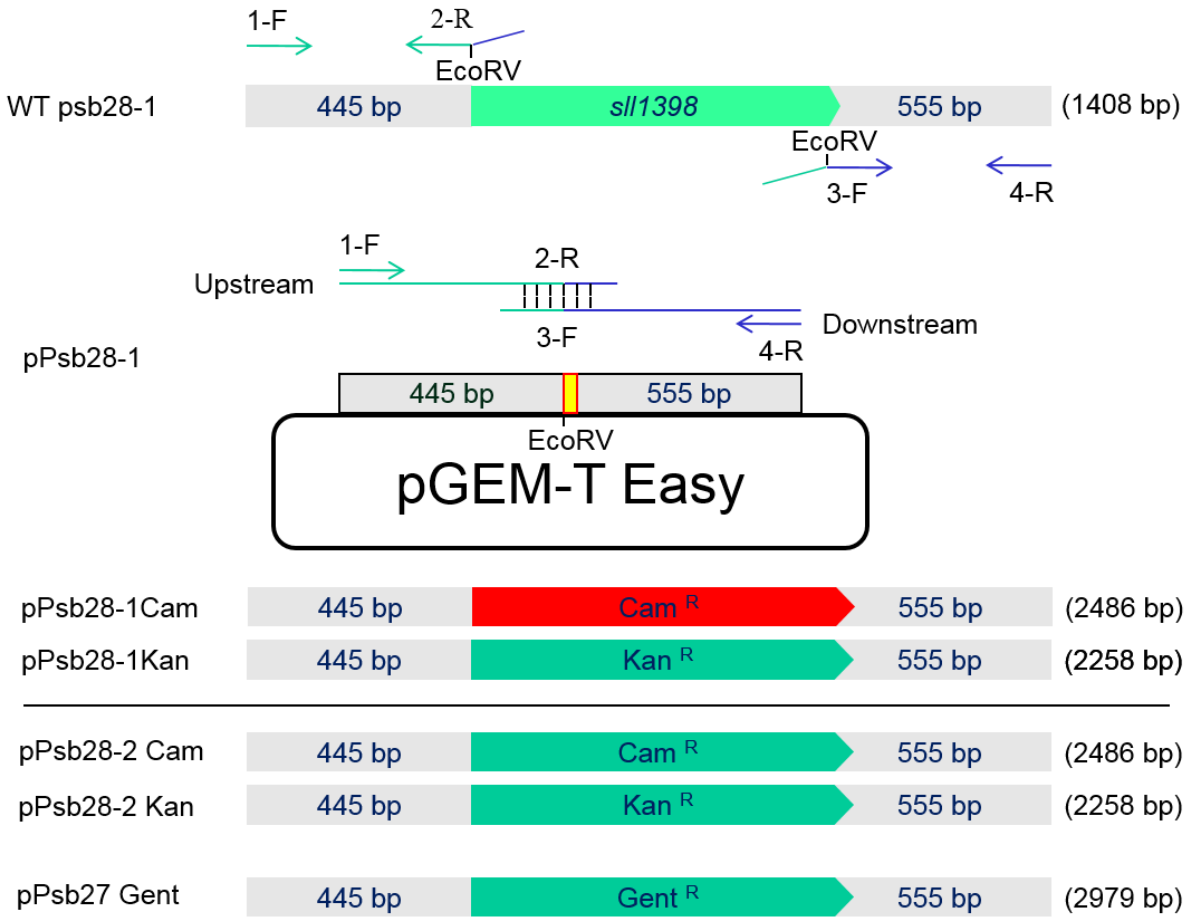

Figure S6. Construction of pPsb28-1Cam, pPsb28-1Kan, pPsb28-2Cam, pPsb28-2Kan and pPsbGent Vectors. Vectors were used for transformation of *Synechocystis* 6803 WT-G strain to generated deletion mutants ΔPsb28-1, ΔPsb28-2, ΔPsb28-1/Δ Psb28-2, ΔPsb27, and ΔPsb27/ΔPsb28-1.

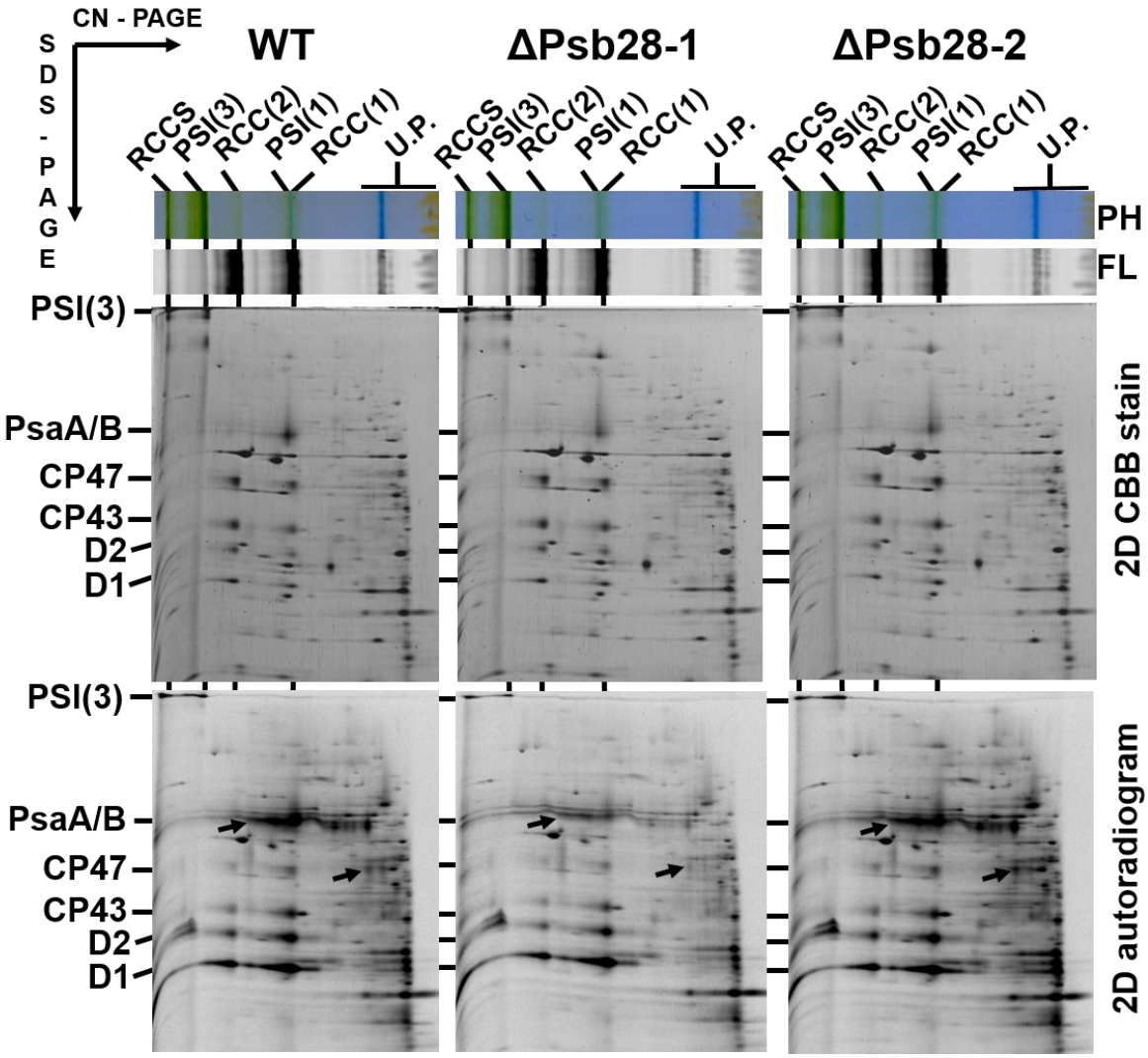

Figure S7. Two-Dimensional Analysis of Radioactively Labeled Membrane Protein Complexes of WT and the Psb28-less Strains. Membranes isolated from radioactively labeled cells were analyzed by 2D CN/SDS-PAGE. The native gel was photographed (PH) and scanned for chlorophyll fluorescence (FL), after SDS-PAGE in the second dimension the gels were stained with Coomassie Blue (2D CBB stain) and exposed to Phosphorimagerplate (2D autoradiogram). Complexes are designated as in Supplementary Figure 2. 5 µg of Chl were loaded for all three strains**.**

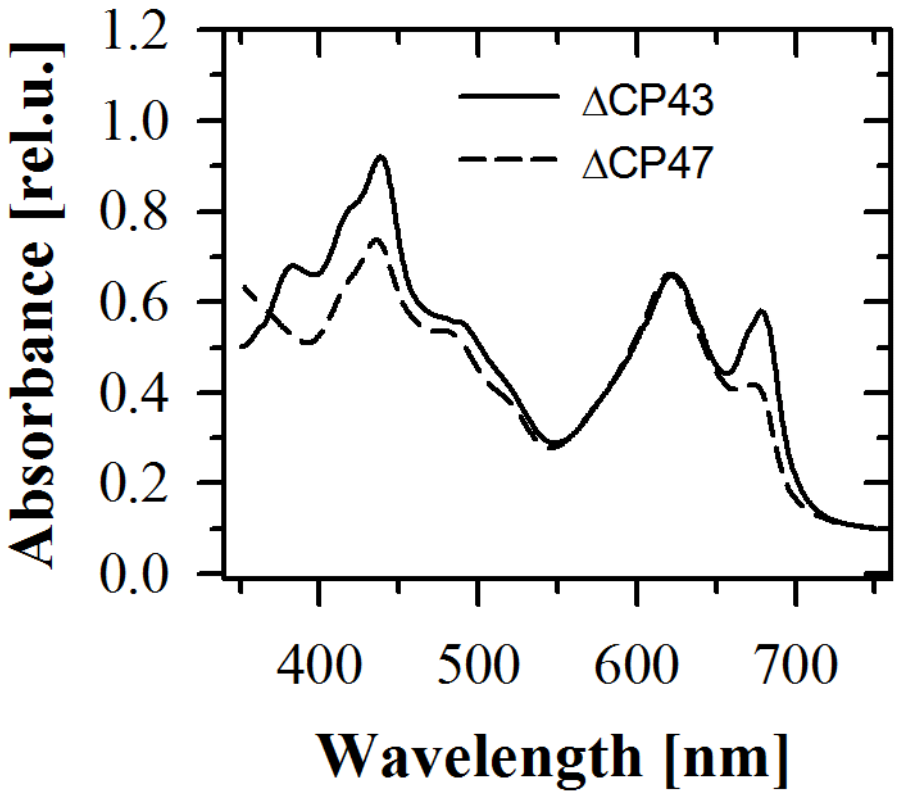

Figure S8. The Whole Cell Absorption Spectra of Mutants Lacking CP43 (ΔCP43) and CP47 (ΔCP47). Cells were cultivated photoheterotrophically at 40 µmol photons m^{2-} s^{1-} and measured while reaching exponential growth phase. Spectra of cells with the same OD_{750nm} = 0.1 are shown.

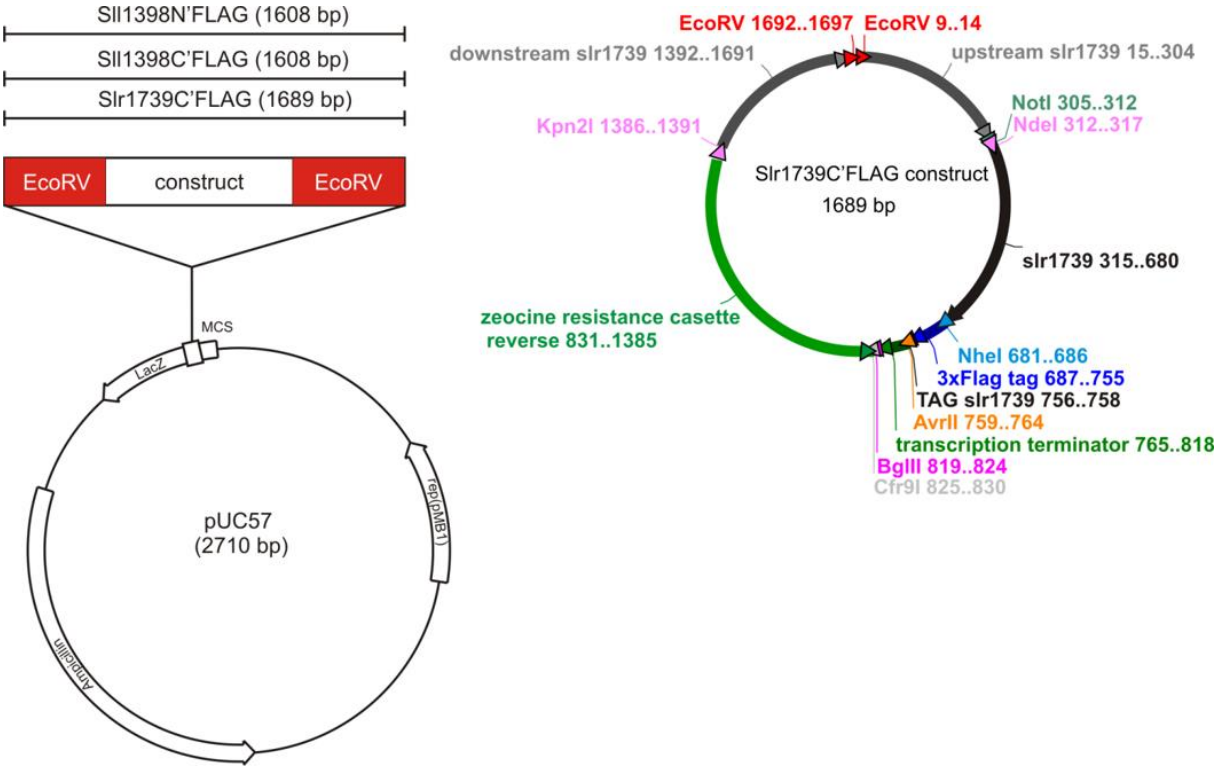

Figure S9. Construction of FLAG-tagged Psb28-1 and Psb28-2. Commercially synthetized construct Slr1739C'FLAG (right) was cloned to a pUC57-Simple vector (GenScript, USA) using an EcoRV restriction site (left). Obtained plasmid was used for transformation of WT *Synechocystis* strain. Construction of Sll1398C'FLAG and Sll1398N'FLAG constructs was identical.

Table S1. List of Proteins Identified in the Psb28-1-FLAG Pull-Down Isolated from High Light Treated Cells of the Synechocystis Strain Expressing Psb28-1-FLAG. The PLGS score is a statistical measure of peptide assignment accuracy; it is calculated with Protein Lynx Global Server (PLGS 2.2.3) software (Waters).

Protein UniProtKB No.	**Size (Da) Length (AA)**	**Coverage (%)**	**Detected/theoretical no. of peptides**	**PLGS score**
CP47 P05429	55903 507	14	6/27	444
CP43 P16033	39695 360	27	8/25	898
D2 P09192	39466 352	20	5/14	799
D1 P14660	39695 360	15	4/14	600
Psb28-1 Q55356	12590 112	20	2/11	153
Psb27 P74367	14786 134	29	4/8	183
PsbE P09190	9442 81	50	3/5	432
PsbF P09191	4929 44	39	1/3	264
PsaE P29256	18249 165	55	2/3	95

5 Conclusions

This PhD thesis significantly extends the knowledge of Psb28 proteins, namely Psb28-1 and Psb28-2, in the cyanobacterium *Synechocystis* sp. PCC 6803. It provides new insights into the localization of the proteins within the thylakoid membrane protein complexes, protein structures and their probable role in the assembly of Photosystem II. The outcome of this research is four publications, one first-author and three co-author publications. The main conclusions are as follows:

- In thylakoid membranes the Psb28-1 protein is preferentially bound in RC47 assembly complex whereas Psb28-2 in the complete monomeric PSII core complex. They are never bound together in one complex and under standard conditions most of the proteins were detected as membrane-associated but outside of the PSII complexes.

- We proposed a different oligomeric state for each of the Psb28 proteins. The Psb28-1 preferentially forms a dimer whereas Psb28-2 is present as a monomer. The crystal structure of Psb28-1 protein from *T. elongatus* confirmed the existence of a dimeric form of Psb28-1 and possible tetramer composed of two dimers. However, dimeric form seems to be more probable.

- We show the heterogeneity in protein composition of the RC47 complex that indicates a possible regulatory function of this assembly sub-complex. It is a harbor for not only Psb28 proteins but also for different HLIPs. Our results lead to the conclusion that Psb28-1 and Psb28-2 may share a similar or overlapping binding site on the RC47 complex with HLIPs and influence their binding affinity.

- Our results confirm the that Psb28-1 is involved in the regulation of the synthesis of CP47 inner antenna which was previously proposed by Dobáková and coworkers (Dobáková et al., 2009). Furthermore, we suggest that the synthesis of PsaA/B subunits of PSI is controlled through the regulation of CP47 synthesis: The CP47 less mutant shows Chl deficiency reflecting reduced PSI accumulation and so the reduced PSI content in Psb28-1 mutant is most probably related to the decreased synthesis of CP47.

- The resequencing of genomes of WT sub-strains used in our laboratory revealed sub-strain specific mutations underlying the phenotype variability of mutant strains depending on the chosen WT sub-strain. Based on these results, we explained the

observed variability in phenotypes of Psb28 deletion strains characterized in previous studies, which were constructed in different WT sub-strains.

- The undetectable level of RC47 complexes in the Psb28-1 single and Psb28-1/Psb28-2 double deletion strain and the higher amount of RC47 complexes in Psb28-2 deletion strain compared to WT raised the working hypothesis that Psb28-1 and Psb28-2 do not have the same function and, instead, they work as antagonists. Psb28-1 bound to RC47 could support synthesis of CP47 and PSI and so promote assembly of Photosystems while Psb28-2 works as an antagonist and prevents binding of Psb28-1 to RC47 inhibiting synthesis of CP47 and PSI.

- Growth assay of Psb28 proteins showed sensitivity of Psb28-1 to high continuous and intermittent light stress conditions that was enhanced in double mutant Psb27/Psb28-1 strain while remained unaffected in the Psb28-2-less mutant. This shows that Psb28-1 and Psb27 are needed for optimal growth, especially under intermittent high light conditions. The mechanism of Psb28-1 action remains unclear but it apparently differs from that of Psb27.

- Our pull-down assays performed with solubilized membranes isolated from high light-exposed cells of the strains expressing FLAG-tagged Psb28 detected interaction of these proteins with unique PSII-PSI supercomplexes consisting of Photosystem I trimer and two Photosystem II monomers. The missing room temperature fluorescence of the supercomplexes indicates a possible photoprotection of PSII by PSI. Since the supercomplexes also contained Psb27 assembly factor, which is likely to be involved in *de novo* assembly or repair of PSII, we conclude that the supercomplexes contain incompletely assembled PSII complexes that are protected by energy spillover to PSI to avoid their unwanted photodamage. Taking into consideration the fact that the PSI trimer was proposed to be a sink of newly synthetized Chl, we speculate that under certain conditions PSI trimer could also be a source of chlorophyll for newly synthesized PSII Chl-binding proteins.

6 References

Anbudurai, P.R., Mor, T.S., Ohad, I., Shestakov, S.V., and Pakrasi, H.B. (1994). The ctpA gene encodes the C-terminal processing protease for the D1 protein of the Photosystem II reaction center complex. Proceedings of the National Academy of Sciences of the United States of America 91:8082-8086.

Armbrust, E.V., Berges, J.A., Bowler, C., Green, B.R., Martinez, D., Putnam, N.H., Zhou, S., Allen, A.E., Apt, K.E., Bechner, M., et al. (2004). The genome of the diatom Thalassiosira Pseudonana: ecology, evolution, and metabolism. Science 306:79-86.

Armbruster, U., Labs, M., Pribil, M., Viola, S., Xu, W., Scharfenberg, M., Hertle, A.P., Rojahn, U., Jensen, P.E., Rappaport, F., et al. (2013). Arabidopsis CURVATURE THYLAKOID1 proteins modify thylakoid architecture by inducing membrane curvature. The Plant Cell 25:2661-2678.

Bialek, W., Wen, S., Michoux, F., Beckova, M., Komenda, J., Murray, J.W., and Nixon, P.J. (2013). Crystal structure of the Psb28 accessory factor of Thermosynechococcus elongatus photosystem II at 2.3 A. Photosynthesis Research 117:375-383.

Boehm, M., Romero, E., Reisinger, V., Yu, J.F., Komenda, J., Eichacker, L.A., Dekker, J.P., and Nixon, P.J. (2011). Investigating the early stages of Photosystem II assembly in *Synechocystis* sp PCC 6803. Isolation of CP47 and CP43 complexes. Journal of Biological Chemistry 286:14812-14819.

Boehm, M., Yu, J., Reisinger, V., Beckova, M., Eichacker, L.A., Schlodder, E., Komenda, J., and Nixon, P.J. (2012). Subunit composition of CP43-less Photosystem II complexes of Synechocystis sp. PCC 6803: implications for the assembly and repair of Photosystem II. Philosophical Transactions of the Royal Society B-Biological Sciences 367:3444-3454.

Boudière, L., Michaud, M., Petroutsos, D., Rébeillé, F., Falconet, D., Bastien, O., Roy, S., Finazzi, G., Rolland, N., Jouhet, J., et al. (2014). Glycerolipids in photosynthesis: Composition, synthesis and trafficking. Biochimica et Biophysica Acta (BBA) - Bioenergetics 1837:470-480.

Bricker, T.M., Roose, J.L., Fagerlund, R.D., Frankel, L.K., and Eaton-Rye, J.J. (2012). The extrinsic proteins of Photosystem II. Biochimica et Biophysica Acta (BBA) - Bioenergetics 1817:121-142.

Daum, B., Nicastro, D., Austin, J., McIntosh, J.R., and Kühlbrandt, W. (2010). Arrangement of photosystem II and ATP synthase in chloroplast membranes of spinach and pea. The Plant Cell 22:1299-1312.

Dobáková, M., Sobotka, R., Tichý, M., and Komenda, J. (2009). Psb28 protein is involved in the biogenesis of the photosystem II inner antenna CP47 (PsbB) in the cyanobacterium *Synechocystis* sp PCC 6803. Plant Physiology 149:1076-1086.

Dobakova, M., Tichy, M., and Komenda, J. (2007). Role of the PsbI protein in photosystem II assembly and repair in the cyanobacterium Synechocystis sp PCC 6803. Plant Physiology 145:1681-1691.

Ermakova-Gerdes, S., and Vermaas, W. (1999). Inactivation of the open reading frame slr0399 in Synechocystis sp PCC 6803 functionally complements mutations near the Q(A) niche of photosystem II - A possible role of slr0399 as a chaperone for quinone binding. Journal of Biological Chemistry 274:30540-30549.

Ferreira, K.N., Iverson, T.M., Maghlaoui, K., Barber, J., and Iwata, S. (2004). Architecture of the photosynthetic oxygen-evolving center. Science 303:1831-1838.

Fristedt, R., Willig, A., Granath, P., Crèvecoeur, M., Rochaix, J.D., and Vener, A.V. (2009). Phosphorylation of Photosystem II controls functional macroscopic folding of photosynthetic membranes in Arabidopsis. The Plant Cell 21:3950-3964.

Garcia-Cerdan, J.G., Kovacs, L., Toth, T., Kereiche, S., Aseeva, E., Boekema, E.J., Mamedov, F., Funk, C., and Schroder, W.P. (2011). The PsbW protein stabilizes the supramolecular organization of photosystem II in higher plants. Plant Journal 65:368-381.

Gounaris, K., and Barber, J. (1983). Monogalactosyldiacylglycerol: The most abundant polar lipid in nature. Trends in Biochemical Sciences 8:378-381.

Grasse, N., Mamedov, F., Becker, K., Styring, S., Rogner, M., and Nowaczyk, M.M. (2011). Role of novel dimeric Photosystem II (PSII)-Psb27 protein complex in PSII repair. Journal of Biological Chemistry 286:29548-29555.

Guskov, A., Kern, J., Gabdulkhakov, A., Broser, M., Zouni, A., and Saenger, W. (2009). Cyanobacterial photosystem II at 2.9-A resolution and the role of quinones, lipids, channels and chloride. Nature Structural & Molecular Biology 16:334-342.

Hagio, M., Sakurai, I., Sato, S., Kato, T., Tabata, S., and Wada, H. (2002). Phosphatidylglycerol is essential for the development of thylakoid membranes in Arabidopsis thaliana. Plant and Cell Physiology 43:1456-1464.

Hernandez-Prieto, M.A., and Futschik, M.E. (2012). CyanoEXpress: A web database for exploration and visualisation of the integrated transcriptome of cyanobacterium Synechocystis sp. PCC6803. Bioinformation 8:634-638.

Hernández-Prieto, M.A., Semeniuk, T.A., Giner-Lamia, J., and Futschik, M.E. (2016). The transcriptional landscape of the photosynthetic model cyanobacterium Synechocystis sp. PCC6803. Scientific Reports 6:22168.

Chen, H., Zhang, D., Guo, J., Wu, H., Jin, M., Lu, Q., Lu, C., and Zhang, L. (2006). A Psb27 homologue in Arabidopsis thaliana is required for efficient repair of photodamaged Photosystem II. Plant Molecular Biology 61:567-575.

Ifuku, K. (2015). Localization and functional characterization of the extrinsic subunits of photosystem II: an update. Bioscience, Biotechnology, And Biochemistry 79:1223-1231.

Irrgang, K.D., Shi, L.X., Funk, C., and Schroder, W.P. (1995). A nuclear-encoded subunit of the Photosystem II reaction center. Journal of Biological Chemistry 270:17588-17593.

Jiroutová, K., Kořený, L., Bowler, C., and Oborník, M. (2010). A gene in the process of endosymbiotic transfer. PLoS ONE 5:e13234.

Jung, K.-H., Lee, J., Dardick, C., Seo, Y.-S., Cao, P., Canlas, P., Phetsom, J., Xu, X., Ouyang, S., An, K., et al. (2008). Identification and functional analysis of light-responsive unique genes and gene family members in rice. PLoS Genetics 4:e1000164.

Kaneko, T., Sato, S., Kotani, H., Tanaka, A., Asamizu, E., Nakamura, Y., Miyajima, N., Hirosawa, M., Sugiura, M., Sasamoto, S., et al. (1996). Sequence analysis of the genome of the unicellular cyanobacterium Synechocystis sp. strain PCC6803. II. Sequence determination of the entire genome and assignment of potential protein-coding regions. DNA Research 3:109-136.

Kanesaki, Y., Shiwa, Y., Tajima, N., Suzuki, M., Watanabe, S., Sato, N., Ikeuchi, M., and Yoshikawa, H. (2012). Identification of substrain-specific mutations by massively parallel whole-genome resequencing of Synechocystis sp. PCC 6803. DNA Research 19:67-79.

Kashino, Y., Lauber, W.M., Carroll, J.A., Wang, Q.J., Whitmarsh, J., Satoh, K., and Pakrasi, H.B. (2002). Proteomic analysis of a highly active photosystem II preparation from the cyanobacterium Synechocystis sp. PCC 6803 reveals the presence of novel polypeptides. Biochemistry 41:8004-8012.

Kelley, L.A., and Sternberg, M.J.E. (2009). Protein structure prediction on the Web: a case study using the Phyre server. Nature Protocols 4:363-371.

Knoppová, J., Sobotka, R., Tichý, M., Yu, J., Konik, P., Halada, P., Nixon, P.J., and Komenda, J. (2014). Discovery of a chlorophyll binding protein complex involved in the early steps of Photosystem II assembly in Synechocystis. The Plant Cell 26:1200-1212.

Knoppová, J., Yu, J., Konik, P., Nixon, P.J., and Komenda, J. (2016). CyanoP Is involved in the early steps of photosystem two assembly in the cyanobacterium Synechocystis sp. PCC 6803. Plant and Cell Physiology doi: 10.1093/pcp/pcw115.

Komenda, J., Barker, M., Kuvikova, S., de Vries, R., Mullineaux, C.W., Tichy, M., and Nixon, P.J. (2006). The FtsH protease slr0228 is important for quality control of photosystem II in the thylakoid membrane of Synechocystis sp PCC 6803. Journal of Biological Chemistry 281:1145-1151.

Komenda, J., Knoppova, J., Kopecna, J., Sobotka, R., Halada, P., Yu, J.F., Nickelsen, J., Boehm, M., and Nixon, P.J. (2012a). The Psb27 assembly factor binds to the CP43 complex of photosystem II in the cyanobacterium Synechocystis sp. PCC 6803. Plant Physiology 158:476-486.

Komenda, J., Kuvikova, S., Granvogl, B., Eichacker, L.A., Diner, B.A., and Nixon, P.J. (2007a). Cleavage after residue Ala352 in the C-terminal extension is an early step in the maturation of the D1 subunit of photosystem II in Synechocystis PCC 6803. Biochimica Et Biophysica Acta-Bioenergetics 1767:829-837.

Komenda, J., Nickelsen, J., Tichy, M., Prasil, O., Eichacker, L.A., and Nixon, P.J. (2008). The cyanobacterial homologue of HCF136/YCF48 is a component of an early Photosystem II assembly complex and is important for both the efficient assembly and repair of Photosystem II in Synechocystis sp PCC 6803. Journal of Biological Chemistry 283:22390-22399.

Komenda, J., Reisinger, V., Muller, B.C., Dobakova, M., Granvogl, B., and Eichacker, L.A. (2004). Accumulation of the D2 protein is a key regulatory step for assembly of the photosystem II reaction center complex in Synechocystis PCC 6803. Journal of Biological Chemistry 279:48620-48629.

Komenda, J., Sobotka, R., and Nixon, P.J. (2012b). Assembling and maintaining the Photosystem II complex in chloroplasts and cyanobacteria. Current opinion in plant biology 15:245-251.

Komenda, J. and Sobotka, R. (2016). Cyanobacterial high-light-inducible proteins - Protectors of chlorophyll-protein synthesis and assembly. Biochimica et Biophysica Acta 1857:288-295.

Komenda, J., Tichy, M., and Eichacker, L.A. (2005). The PsbH protein is associated with the inner antenna CP47 and facilitates D1 processing and incorporation into PSII in the cyanobacterium Synechocystis PCC 6803. Plant and Cell Physiology 46:1477-1483.

Komenda, J., Tichý, M., Prášil, O., Knoppová, J., Kuviková, S., de Vries, R., and Nixon, P.J. (2007b). The exposed N-terminal tail of the D1 subunit is required for rapid D1 degradation during photosystem II repair in Synechocystis sp PCC 6803. Plant Cell 19:2839-2854.

Krynická, V., Shao, S., Nixon, P.J., and Komenda, J. (2015). Accessibility controls selective degradation of photosystem II subunits by FtsH protease. Nature Plants 1:15168.

Liu, H., Huang, R.C., Chen, J., Gross, M.L., and Pakrasi, H.B. (2011a). Psb27, a transiently associated protein, binds to the chlorophyll binding protein CP43 in photosystem II assembly intermediates. Proceedings of the National Academy of Sciences 108:18536-18541.

Liu, H., Roose, J.L., Cameron, J.C., and Pakrasi, H.B. (2011b). A genetically tagged Psb27 protein allows purification of two consecutive Photosystem II (PSII) assembly intermediates in Synechocystis 6803, a cyanobacterium. Journal of Biological Chemistry 286:24865-24871.

Liu, H., Zhang, H., Weisz, D.A., Vidavsky, I., Gross, M.L., and Pakrasi, H.B. (2014). MS-based cross-linking analysis reveals the location of the PsbQ protein in cyanobacterial photosystem II. Proceedings of the National Academy of Sciences 111:4638-4643.

Lorkovic, Z.J., Schroder, W.P., Pakrasi, H.B., Irrgang, K.D., Herrmann, R.G., and Oelmuller, R. (1995). Molecular characterization of PsbW, a nuclear-encoded component of the Photosystem II reaction center complex in spinach. Proceedings of the National Academy of Sciences of the United States of America 92:8930-8934.

Lu, Y. (2016). Identification and roles of Photosystem II assembly, stability, and repair factors in Arabidopsis. Frontiers in Plant Science 7 (FEB2016), [168]. doi: 10.3389/fpls.2016.00168.

Mabbitt, P.D., Wilbanks, S.M., and Eaton-Rye, J.J. (2014). Structure and function of the hydrophilic Photosystem II assembly proteins: Psb27, Psb28 and Ycf48. Plant Physiology and Biochemistry (Paris) 81:96-107.

Margulis, L. (1967). Genetic and evolutionary consequences of symbiosys. Experimental Parasitology 39 (2): 277-349.

Martin, W., and Herrmann, R.G. (1998). Gene transfer from organelles to the nucleus: How much, what Happens, and why? Plant Physiology 118:9-17.

Meurer, J., Plucken, H., Kowallik, K.V., and Westhoff, P. (1998). A nuclear-encoded protein of prokaryotic origin is essential for the stability of photosystem II in Arabidopsis thaliana. Embo Journal 17:5286-5297.

Mizusawa, N., and Wada, H. (2012). The role of lipids in photosystem II. Biochimica et Biophysica Acta (BBA) - Bioenergetics 1817:194-208.

Moore, J. (2011). The Psb28 proteins of oxygenic photosynthesis (Thesis, Master of Science). University of Otago. Retrieved from http://hdl.handle.net/10523/2073.

Morris, J.N., Crawford, T.S., Jeffs, A., Stockwell, P.A., Eaton-Rye, J.J., and Summerfield, T.C. (2014). Whole genome re-sequencing of two 'wild-type' strains of the model cyanobacterium Synechocystis sp. PCC 6803. New Zealand Journal of Botany 52:36-47.

Mullineaux, C.W. (2008). Phycobilisome-reaction centre interaction in cyanobacteria. Photosynthesis Research 95:175-182.

Nagarajan, A., and Burnap, R.L. (2014). Parallel expression of alternate forms of psbA2 gene provides evidence for the existence of a targeted D1 repair mechanism in Synechocystis sp. PCC 6803. Biochimica et Biophysica Acta (BBA) - Bioenergetics 1837:1417-1426.

Nanba, O., and Satoh, K. (1987). Isolation of a photosystem II reaction center consisting of D-1 and D-2 polypeptides and cytochrome b-559. Proceedings of the National Academy of Sciences of the United States of America 84:109-112.

Nevo, R., Charuvi, D., Shimoni, E., Schwarz, R., Kaplan, A., Ohad, I., and Reich, Z. (2007). Thylakoid membrane perforations and connectivity enable intracellular traffic in cyanobacteria. The EMBO Journal 26:1467-1473.

Nickelsen, J., and Rengstl, B. (2013). Photosystem II assembly: from cyanobacteria to plants. Annul Review of Plant Biology 64:609-635.

Nickelsen, J., Rengstl, B., Stengel, A., Schottkowski, M., Soll, J., and Ankele, E. (2011). Biogenesis of the cyanobacterial thylakoid membrane system – an update. FEMS Microbiology Letters 315:1-5.

Nixon, P.J., Michoux, F., Yu, J.F., Boehm, M., and Komenda, J. (2010). Recent advances in understanding the assembly and repair of photosystem II. Annals of Botany (London) 106:1-16.

Nixon, P.J., Trost, J.T., and Diner, B.A. (1992). Role of the carboxy terminus of polypeptide-1 in the assembly of a functional water-oxidizing manganese cluster in Photsystem-II of the cyanobacterium Synechocystis sp. PCC 6803 - assembly requires a free carboxyl group at C-terminal position 344. Biochemistry 31:10859-10871.

Nowaczyk, M.M., Hebeler, R., Schlodder, E., Meyer, H.E., Warscheid, B., and Rogner, M. (2006). Psb27, a cyanobacterial lipoprotein, is involved in the repair cycle of photosystem II. Plant Cell 18:3121-3131.

Oudot-Le Secq, M.P., Grimwood, J., Shapiro, H., Armbrust, E.V., Bowler, C., and Green, B.R. (2007). Chloroplast genomes of the diatoms Phaeodactylum tricornutum and Thalassiosira pseudonana: comparison with other plastid genomes of the red lineage. Molecular Genetics and Genomics 277:427-439.

Pagliano, C., Saracco, G., and Barber, J. (2013). Structural, functional and auxiliary proteins of photosystem II. Photosynthesis Research 116:167-188.

Peschek, G.A., Obinger, C., and Paumann, M. (2004). The respiratory chain of blue-green algae (cyanobacteria). Physiologia Plantarum 120:358-369.

Pisareva, T., Kwon, J., Oh, J., Kim, S., Ge, C.R., Wieslander, A., Choi, J.S., and Norling, B. (2011). Model for membrane organization and protein sorting in the cyanobacterium *Synechocystis* sp PCC 6803 inferred from proteomics and multivariate sequence analyses. Journal of Proteome Research 10:3617-3631.

Plucken, H., Muller, B., Grohmann, D., Westhoff, P., and Eichacker, L.A. (2002). The HCF136 protein is essential for assembly of the photosystem II reaction center in Arabidopsis thaliana. FEBS Letters 532:85-90.

Pribil, M., Labs, M., and Leister, D. (2014). Structure and dynamics of thylakoids in land plants. Journal of Experimental Botany 65:1955-1972.

Promnares, K., Komenda, J., Bumba, L., Nebesarova, J., Vacha, F., and Tichy, M. (2006). Cyanobacterial small chlorophyll-binding protein ScpD (HliB) is located on the periphery

of photosystem II in the vicinity of PsbH and CP47 subunits. Journal of Biological Chemistry 281:32705-32713.

Rast, A., Heinz, S., and Nickelsen, J. (2015). Biogenesis of thylakoid membranes. Biochimica et Biophysica Acta (BBA) - Bioenergetics 1847:821-830.

Rast, A., Rengstl, B., Heinz, S., Klingl, A., and Nickelsen, J. (2016). The role of Slr0151, a tetratricopeptide repeat protein from Synechocystis sp. PCC 6803, during Photosystem II assembly and repair. Frontiers in Plant Science 7:605. doi: 10.3389/fpls.2016.00605.

Rengstl, B., Knoppová, J., Komenda, J., and Nickelsen, J. (2013). Characterization of a Synechocystis double mutant lacking the photosystem II assembly factors YCF48 and Sll0933. Planta 237:471-480.

Rengstl, B., Oster, U., Stengel, A., and Nickelsen, J. (2011). An intermediate membrane subfraction in cyanobacteria is involved in an assembly network for photosystem II biogenesis. Journal of Biological Chemistry 286(24): 21944-21951.

Roose, J.L., and Pakrasi, H.B. (2008). The Psb27 protein facilitates manganese cluster assembly in photosystem II. Journal of Biological Chemistry 283:4044-4050.

Roose, J.L., Wegener, K.M., and Pakrasi, H.B. (2007). The extrinsic proteins of photosystem II. Photosynthesis Research 92:369-387.

Sakata, S., Mizusawa, N., Kubota-Kawai, H., Sakurai, I., and Wada, H. (2013). Psb28 is involved in recovery of photosystem II at high temperature in Synechocystis sp. PCC 6803. Biochimica Et Biophysica Acta-Bioenergetics 1827:50-59.

Sakurai, I., Mizusawa, N., Wada, H., and Sato, N. (2007). Digalactosyldiacylglycerol is required for stabilization of the oxygen-evolving complex in Photosystem II. Plant Physiology 145:1361-1370.

Selão, T.T., Zhang, L., Knoppová, J., Komenda, J., and Norling, B. (2016). Photosystem II assembly steps take place in the thylakoid membrane of the cyanobacterium Synechocystis sp. PCC 6803. Plant and Cell Physiology 57:95-104.

Shi, L.X., Hall, M., Funk, C., and Schroder, W.P. (2012). Photosystem II, a growing complex: Updates on newly discovered components and low molecular mass proteins. Biochimica Et Biophysica Acta-Bioenergetics 1817:13-25.

Shi, L.X., Lorković, Z.J., Oelmüller, R., and Schröder, W.P. (2000). The low molecular mass PsbW protein is involved in the stabilization of the dimeric Photosystem II complex in Arabidopsis thaliana. Journal of Biological Chemistry 275:37945-37950.

Shi, L.X., and Schröder, W.P. (2004). The low molecular mass subunits of the photosynthetic supracomplex, photosystem II. Biochimica et Biophysica Acta (BBA) - Bioenergetics 1608:75-96.

Schottkowski, M., Gkalympoudis, S., Tzekova, N., Stelljes, C., Schunemann, D., Ankele, E., and Nickelsen, J. (2009). Interaction of the periplasmic PratA factor and the PsbA (D1)

protein during biogenesis of Photosystem II in *Synechocystis* sp PCC 6803. Journal of Biological Chemistry 284:1813-1819.

Stengel, A., Gugel, I.L., Hilger, D., Rengstl, B., Jung, H., and Nickelsen, J. (2012). Initial steps of photosystem II de novo assembly and preloading with manganese take place in biogenesis centers in Synechocystis. Plant Cell 24:660-675.

Suga, M., Akita, F., Hirata, K., Ueno, G., Murakami, H., Nakajima, Y., Shimizu, T., Yamashita, K., Yamamoto, M., Ago, H., et al. (2015). Native structure of photosystem II at 1.95 A resolution viewed by femtosecond X-ray pulses. Nature 517:99-103.

Thangaraj, B., Ryan, C.M., Souda, P., Krause, K., Faull, K.F., Weber, A.P.M., Fromme, P., and Whitelegge, J.P. (2010). Data-directed top-down Fourier-transform mass spectrometry of a large integral membrane protein complex: photosystem II from Galdieria sulphuraria. Proteomics 10:3644-3656.

Thidholm, E., Lindstrom, V., Tissier, C., Robinson, C., Schroder, W.P., and Funk, C. (2002). Novel approach reveals localisation and assembly pathway of the PsbS and PsbW proteins into the photosystem II dimer. FEBS Letters 513:217-222.

Umena, Y., Kawakami, K., Shen, J.R., and Kamiya, N. (2011). Crystal structure of oxygen-evolving photosystem II at a resolution of 1.9 A. Nature 473:55-60.

Uniacke, J., and Zerges, W. (2007). Photosystem II assembly and repair are differentially localized in Chlamydomonas. The Plant Cell 19:3640-3654.

Van Amerongen, H., and Croce, R. (2013). Light harvesting in photosystem II. Photosynthesis Research 116:251-263.

van de Meene, A.M.L., Hohmann-Marriott, M.F., Vermaas, W.F.J., and Roberson, R.W. (2006). The three-dimensional structure of the cyanobacterium *Synechocystis* sp PCC 6803. Archives of Microbiology 184:259-270.

Vermaas, W.F.J. (1994). Molecular-genetic approaches to study photosynthetic and respiratory electron transport in thylakoids from cyanobacteria. Biochimica et Biophysica Acta (BBA) - Bioenergetics 1187:181-186.

Watanabe, M., and Ikeuchi, M. (2013). Phycobilisome: architecture of a light-harvesting supercomplex. Photosynthesis Research 116:265-276.

Wei, L., Guo, J., Ouyang, M., Sun, X., Ma, J., Chi, W., Lu, C., and Zhang, L. (2010). LPA19, a Psb27 homolog in Arabidopsis thaliana, facilitates D1 protein precursor processing during PSII biogenesis. Journal of Biological Chemistry 285:21391-21398.

Wei, X., Su, X., Cao, P., Liu, X., Chang, W., Li, M., Zhang, X., and Liu, Z. (2016). Structure of spinach photosystem II–LHCII supercomplex at 3.2 Å resolution. Nature 534:69-74.

Williams, J.G.K. (1988). Construction of specific mutations in Photosystem-II photosynthetic reaction center by genetic-engineering methods in Synechocystis-6803. Methods in Enzymology 167:766-778.

Yang, H., Liao, L., Bo, T., Zhao, L., Sun, X., Lu, X., Norling, B., and Huang, F. (2014). Slr0151 in Synechocystis sp. PCC 6803 is required for efficient repair of Photosystem II under high-light condition. Journal of Integrative Plant Biology 56:1136-1150.

Yang, Y., Ramelot, T.A., Cort, J.R., Wang, D., Ciccosanti, C., Hamilton, K., Nair, R., Rost, B., Acton, T.B., Xiao, R., et al. (2011). Solution NMR structure of photosystem II reaction center protein Psb28 from Synechocystis sp. strain PCC 6803. Proteins Structure Function and Bioinformatics 79:340-344.

Yao, D., Kieselbach, T., Komenda, J., Promnares, K., Prieto, M.A.H., Tichy, M., Vermaas, W.F.J., and Funk, C. (2007). Localization of the small CAB-like proteins in photosystem II. Journal of Biological Chemistry 282:267-276.

Zak, E., Norling, B., Maitra, R., Huang, F., Andersson, B., and Pakrasi, H.B. (2001). The initial steps of biogenesis of cyanobacterial photosystems occur in plasma membranes. Proceedings of the National Academy of Sciences of the United States of America 98:13443-13448.

Zang, X., Liu, B., Liu, S., Arunakumara, K.K.I.U., and Zhang, X. (2007). Optimum conditions for transformation of Synechocystis sp. PCC 6803. Journal of Microbiology 45(3):241-245.